SYNTHESIS AND CHARACTERIZATION OF EARLY AND LATE TRANSITION METALLOCALIX[5]ARENE COMPLEXES

by

Bernat Abeit Martinez-Ortega

Bachelor of Science, 2004
Universidad Autónoma del Estado de Hidalgo
Pachuca de Soto, Hidalgo, México

Submitted to the Graduate Faculty of the
College of Science and Engineering
Texas Christian University
in partial fulfillment of the requirements
for the degree of

Doctor of Philosophy

December 2010

SYNTHESIS AND CHARACTERIZATION OF EARLY AND LATE TRANSITION METALLOCALIX[5]ARENE COMPLEXES

by

Bernat Abeit Martinez-Ortega

Dissertation approved

Mary S. Hanna

Major Professor

Robert A. Nielson

For the College of Science and Engineering

Copyright by

Bernat Abeit Martinez-Ortega

2010

This Dissertation is dedicated with love to:

Leslie Azul

Carlos Bernat and Oscar Abeit

My loved ones

AKNOWLEDGEMENTS

I thank God for all the blessings in my life especially the joy of my children and a wonderful wife.

I would like to express my deepest gratitude to my advisor Professor Tracy A. Hanna. Thank you for all the encouragement, guidance and invaluable advice during this doctorate period. Thank you for giving me the opportunity to belong to your research group, and for all the knowledge that I received from you. Without your kind guidance this journey could have been very difficult.

I would like to thank Adriana Luqueño Reyes for sharing these last six years of her life with me during the good and hard times. You were an essential part of my life during this period. Thanks for cheering me up and for your kindness. I could not have gone this far without you.

I am very grateful to all the professors from the Chemistry Department, especially Professor David Minter for all his support and interest in my scientific career. Thanks a lot for all your advice and guidance in the NMR field. I also thank the members of my committee: Professor Bob Neilson and Professor Sergei Dzyuba for their time, advice, and continuous support.

Thanks to Dr. Hanna's group members and the Chemistry Department at TCU for their help and the good moments that we shared.

I would like to thank my father Elias Martinez Guillen and my brother and sisters to whom I also dedicate this work. Thank you for all the support, love, patience, and for all the shared efforts in order to achieve all of my goals. Thanks for all your motivation that kept me going and reaching for more.

Thanks to my younger brother Dr. Daniel Mendoza Espinosa for his friendship and for giving me priceless assistance during this entire doctorate period. I wish you the best always.

Also I would like to thank to Lina Bernal, Dr. Kimberly Brien and Lauren Howell for being with me and cheering me up in the hardest moments during this time.

"Dory: Just keep swimming…" Finding Nemo (2003)

TABLE OF CONTENTS

Acknowledgements ii

List of Figures ix

List of Tables xv

List of Schemes xviii

List of Equations xx

CHAPTER 1

BACKGROUND AND PURPOSE 1

1.1 Calixarenes 1

1.1.1 Introduction 1

1.2 Nomenclature 2

1.3 Functionalized calixarenes 4

1.4 Structural characteristics of calixarenes 5

1.5 Metallocalixarenes 8

1.6 Bimetallic calixarene complexes 12

CHAPTER 2

ALKALI METAL CALIXARENES 17

2.1 Introduction 17

2.2 Results and discussion 21

2.2.1 Synthesis of para-*tert*-butylcalix[5]arene mono- and dianions 21

2.2.2 NMR spectroscopy 22

2.2.3 Conformational studies 24

2.2.3.1 Inversion energies 25

2.2.4 Crystal structures of the calixanions 26

2.2.4.1 Metal-oxygen versus metal-carbon (π-cation) interactions 30

2.2.4.2 Core structures 31

2.3 Experimental section.....33

2.3.1 General information 33

2.3.2 Preparation of compounds 34

2.3.2.1 General procedure for mono- and dianion synthesis 34

2.3.3 Solubility and air-sensitivity of calixanions 36

2.3.4 VT-NMR studies.....36

2.3.5 General X-ray crystal structure information 36

2.4 Conclusions.....38

CHAPTER 3

CALIX[5]ARENE TITANIUM(IV) COMPLEXES 39

3.1 Introduction.....39

3.2 Results and discussion 41

3.2.1 Reactivity of the calix[5]arene dianion, compounds **3.1** and **3.2**.....41

3.2.2 Synthesis of compounds **3.3** and **3.4**.....46

3.3 Crystal and molecular structures.....48

3.4 NMR spectroscopy.....53

3.4.1 Spectral data of compounds **3.1** and **3.2** 53

3.4.2 Spectral data of compounds **3.3** and **3.4** 57

3.5 Experimental section.....59

3.5.1 General information.....59

3.5.2 Synthesis of complexes.....60

3.5.3 General X-ray information.....64

2.4 Conclusions.....66

CHAPTER 4

CALIX[5]ARENE MOLYBDENUM(VI) COMPLEXES.....67

4.1 Introduction.....67

4.2 Results and discussion 68

4.2.1 Synthesis of dioxomolybdenum(VI) calixarene complex from MoO_2Cl_2.....68

4.2.1.1 Mechanism of formation of complex **4.1**.....71

4.2.2 Synthesis of dioxomolybdenum(VI) calixarene complex from MoO_2Cl_2(bipy).....72

4.2.2.1 Synthetic approach using acetonitrile (CH_3CN).....72

4.2.2.2 Synthetic approach using mixture of hexanes and acetonitrile

(in a 7:2 ratio).....76

4.2.3 Synthesis of dioxomolybdenum(VI) calixarene complexes from $MoO_2(acac)_2$.....82

4.2.3.1 ^{1}H NMR and infrared spectroscopies and EDX analysis.....92

4.2.3.2 Crystal and molecular structure of complex [**4.5a**]$_2\cdot 2C_5H_8O_2$ 98

4.3 Experimental Section.....102

4.3.1 General Information.....102

4.3.2 Synthesis of complexes.....102

4.4 General X-ray crystal structure information 112

4.5 Conclusions 114

CHAPTER 5

CALIXARENE PALLADIUM(II) COMPLEXES 115

5.1 Introduction 115

5.2. Results and discussion 118

5.2.1 Synthesis of **^{t}BuC5(H)$_5$** palladium complexes 118

5.2.1.1 First approach using [Pd(CH_3CN)$_2$Cl$_2$] 118

5.2.1.2 Second approach using [Pd(bipy)Cl$_2$] generated *in situ* 119

5.2.1.2.1 Synthesis of palladium precursors [Pd(L)Cl$_2$] 122

5.2.1.3 Proposed mechanism for the formation of palladium calix[5]arene complexes 124

5.2.2 Synthesis of **^{t}BuC4(H)$_4$**, **HC4(H)$_4$** and **^{t}BuC6(H)$_6$** palladium complexes 125

5.3 Spectral data 128

5.3.1 Spectral data for palladium calix[5]arene complexes 128

5.3.2 Spectral data for palladium calix[4,6]arene complexes 136

5.4 Crystal structures 141

5.4.1 Crystal structures of by-products [Pd(bipy){**^{t}BuC5(H)$_3$**}]·4CH_3CN (**5.1**·4CH_3CN) and [Pd((4-Me)$_2$bipy){**^{t}BuC5(H)$_3$**}]·4CH_3CN (**5.2**·4CH_3CN) 146

5.5 Experimental Section 149

5.5.1 General information 149

5.5.1.1 Preparation of compounds 150

5.5.1.1.1 General procedure for the synthesis of [Pd(L)Cl_2] (L = bipy, tmeda, (4-Me)$_2$bipy, 1,10-phen, dpa).....150

5.5.1.1.2 Synthesis of [Pd(L){M·^{t}**BuC5(H)$_2$**}] (L = bipy, (4-Me)$_2$bipy, 1,10-phen, dpa) complexes.....151

5.5.1.1.3 General synthesis of [Pd(L){^{t}**BuC4(H)$_2$**}] (L = bipy, (4-Me)$_2$bipy, 1,10-phen, dpa, tmeda) complexes 163

5.5.1.1.4 Synthesis of [Pd(L){**HC4(H)$_2$**}] (L = bipy, (4-Me)$_2$bipy, 1,10-phen) complexes 167

5.5.1.1.5 Synthesis of [Pd((4-Me)$_2$bipy){Cs·^{t}**BuC6(H)$_3$**}] complex **5.7**....169

5.5.2 General X-ray crystal structure information 171

5.6 Conclusions.....174

CHAPTER 6

HETEROBIMETALLIC PALLADIUM(II)/TITANIUM(IV) AND PALLADIUM(II)/MOLYBDENUM(VI) COMPLEXES.....175

6.1 Introduction.....175

6.2 Results and discussion 177

6.2.1 Synthesis of palladium(II)/titanium(IV) complexes 177

6.2.1.1 NMR spectroscopy.....179

6.2.1.2 Crystal and molecular structures.....185

6.2.2 Synthesis of palladium(II)/molybdenum(IV) complexes 194

6.2.2.1 Spectroscopy analysis 196

6.2.2.1.1. Conformational analysis and symmetry.....202

6.3 Experimental Section 205

6.3.1 General Information 205

6.3.2 Synthesis of complexes 206

6.3.2.1 General procedure for the synthesis of Ti[(L)Pd{M·^{t}**BuC5**}]$_2$ (L = bipy, (4-Me)$_2$bipy, 1,10-phen, M = Rb, Cs) (**6.1-6.6**) 206

6.3.2.2 General procedure for the synthesis of [MoO$_2$(acac){M·^{t}**BuC5(H)**}Pd(L)] (L = bipy, (4-Me)$_2$bipy, 1,10-phen, M = Rb, Cs) (**6.7-6.12**) 211

6.4 General X-ray crystal structure information 217

6.5 Conclusions 219

References 220

VITA

ABSTRACT

LIST OF FIGURES

Figure 1.1 Potential metal binding sites in a calix[4]arene ligand (Q = coordinating group) 4

Figure 1.2 The four limiting and ideal conformations of a *p-tert*-butylcalix[4]arene 6

Figure 1.3 ^{1}H NMR spectra in *$CDCl_3$ at room temperature of calix[n]arenes (n = 4, 5, 6, 8).....7

Figure 1.4 Examples of coordination types I-VI found in calix[4]arene containing two metal centers 12

Figure 2.1 X-ray structures of [Rb·^{t}**BuC4(H)$_3$**]·$4C_4H_8O$ (**A**) and [Rb_2·**HC6(H)$_4$**]·$3H_2O$·$2(CH_3)_2CO$ (**B**), showing cone and 1,2,3-alternate conformations, respectively 19

Figure 2.2 ^{1}H NMR spectra of ^{t}**BuC5(H)$_5$** and alkali metal salts of mono- and dianions at room temperature in $CDCl_3$ 23

Figure 2.3 Crystal structures of monoanions M·^{t}**BuC5(H)$_4$**·C_4H_8O (M = Rb or Cs). Thermal ellipsoids are shown at 50% probability; hydrogen atoms are omitted for clarity 27

Figure 2.4 Crystal structures of dianions. a) Rb_2·^{t}**BuC5(H)$_3$**·$4C_4H_8O$·$2H_2O$ and b) Cs_2·^{t}**BuC5(H)$_3$**·$4C_4H_8O$·$4H_2O$. Thermal ellipsoids are shown at 50% probability; hydrogen atoms are omitted for clarity 28

Figure 2.5 Crystal structures of coordination sphere of **a)** [Rb(2)] and **b)** [Cs(2)] showing the coordination numbers 7 and 8 respectively. Thermal ellipsoids are shown at 50% probability 32

Figure 3.1 X-ray structures of a) dimeric K_2·^{t}**BuC5(H)$_3$**·4DMSO and b) dimeric Rb_2·^{t}**BuC5(H)$_3$**·2THF·H_2O. Thermal ellipsoids are shown at 50% probability; hydrogen atoms and non-coordinated DMSO molecules are omitted for clarity 41

Figure 3.2 Line drawing (left) and X-ray structure (right) of the dimeric structure of **3.1**. Thermal ellipsoids are shown at 50% probability. Hydrogen atoms and some DMSO crystallization molecules have been omitted for clarity. The second part of the molecule is drawn in wireframe style for clarity 44

Figure 3.3 Line drawing (left) and X-ray structure (right) of compound **3.2**. Thermal ellipsoids are shown at 50% probability, and crystallization molecules and hydrogen atoms are not shown for clarity 45

Figure 3.4 Proposed structure of compound **3.4** 48

Figure 3.5 X-ray structures of a) [{MeOH·K·^{t}**BuC5(H)**}-μ-O-[Ti(acac)]$_2${THF·K·^{t}**BuC5(H)$_3$**}] and b) [(-TiCp-μ-O-TiCp-μ-O-)$_2${^{t}**BuC4**}] reported by Lamb et al. 49

Figure 3.6 X-ray structure of compound **3.1** a) asymmetric unit, b) titanium oxygen core. Thermal ellipsoids are shown at 50% probability. Crystallization molecules and hydrogen atoms are omitted for clarity 51

Figure 3.7 Segments of the crystal structure of complex **3.1**·6DMSO. Conformations observed a) around Ti(1), a boat chair conformation in two fused metallocycles, b) around Ti(2), a boat chair conformation. c) An ideal boat chair conformation 52

Figure 3.8 X-ray structure of compound **3.2**·2C_6H_6. a) Side view showing the μ-oxo bridge and b) boat chair conformation around Ti(1) and Ti(2). Thermal ellipsoids are shown at 50% probability; hydrogen atoms and non-coordinating molecules are omitted for clarity 53

Figure 3.9 Idealized conformations of calix[5]arenes 54

Figure 3.10 ^{1}H NMR spectra of compounds **3.1** and **3.2** in $^{*}C_6D_6$. §DMSO, *s* = ether and *i* = impurity. Each box highlights an interesting chemical shift observed for the methylene protons 54

Figure 3.11 X-ray structure of compound **3.1** showing selected M···H (1A-7A) and O···H (1B-2B) distances with thermal ellipsoids at the 50% probability level. H atoms and *tert*-butyl groups are omitted for clarity.....55

Figure 3.12 ^{1}H NMR spectra of compound **3.3** and **3.4** in $^{*}CDCl_3$. §residual THF solvent and *s* = pentane 58

Figure 4.1 ^{1}H NMR spectrum of complex **4.1** in *$CDCl_3$. §Residual hexane 70

Figure 4.2 EDX spectrum of the blue solid (**4.1** and calix[5]arene) demonstrating that just Mo is contained in the sample 70

Figure 4.3 IR spectrum of MoO_2Cl_2(bipy) recorded in a KBr pellet.....73

Figure 4.4 ^{1}H NMR spectrum of compound [MoO_2(bipy){K·^{t}**BuC5(H)$_2$**}] **4.2** in *$CDCl_3$. § = bipy aromatic protons and *S* = CH_3CN 74

Figure 4.5 Proposed structure for compound **4.2** based on its spectroscopic characterization 75

Figure 4.6 EDX spectrum of the pale brown solid (**4.2** and calix[5]arene) demonstrating that Mo and K are contained in the sample 76

Figure 4.7 ^{1}H NMR spectrum of compound [MoO_2{K·^{t}**BuC5(H)$_2$**}] **4.3** in *CDCl3. $^{\S}CH_3CN$ residual solvent 77

Figure 4.8 Proposed structure for compound **4.2** on the basis of its spectroscopic characterization 78

Figure 4.9 X-ray structure of the dimeric structure of **4.4a**. A ball and stick drawing is used for clarity. Non-coordinating acetonitrile molecules and hydrogen atoms have been omitted for clarity 84

Figure 4.10 X-ray structure of the dimeric structure of **4.4b** displaying the atom connectivity. Ball and stick drawing is used for clarity. Hydrogen atoms have been omitted for clarity 85

Figure 4.11 ORTEP drawing of the partial X-ray structure of compound **4.4a** showing the geometries around Mo(1) and Mo(2) centers 86

Figure 4.12 X-ray structure of the asymmetric unit of **4.4a**. The ball and stick and ORTEP drawing styles (50% probability ellipsoids) are used for clarity. Non-coordinating acetonitrile molecules, *tert*-butyl groups and hydrogen atoms have been omitted for clarity 89

Figure 4.13 ^{1}H NMR spectrum of compound **4.5a** in *$CDCl_3$. § = Cs_2·^{t}**BuC5(H)$_3$**, + = Hacac, S = THF 90

Figure 4.14 Molecular structure of compound **4.5a** 92

Figure 4.15 ^{1}H NMR spectrum of pure compound **4.5a** in *$CDCl_3$ 93

Figure 4.16 ^{1}H NMR spectrum of compound **4.5b** in *$CDCl_3$. § Hacac 94

Figure 4.17 ^{1}H NMR spectrum of compound **4.5c** in *$CDCl_3$. § Hacac 95

Figure 4.18 X-ray structure of [**4.5a**]$_2$·$2C_5H_8O_2$. ORTEP drawing (50% probability ellipsoids) and ball and stick drawing styles are used for clarity. Hydrogen atoms have been omitted for clarity 98

Figure 4.19 X-ray structure of the **a)** geometry around Mo(1) and of the **b)** top view of compound [**4.5a**]$_2$·$2C_5H_8O_2$. ORTEP drawing (50% probability ellipsoids) and ball and stick drawing styles are used for clarity. Half of the molecule and hydrogen atoms have been omitted for clarity 101

Figure 5.1 Structural drawing of Rh(II) calix[4]arene complexes 116

Figure 5.2 ^{1}H NMR spectra of [Pd(bipy){K·^{t}**BuC5(H)$_2$**}] **5.1b**, [Pd(bipy){Rb·^{t}**BuC5(H)$_2$**}] **5.1c**, and [Pd(bipy){Cs·^{t}**BuC5(H)$_2$**}] **5.1d** in *$CDCl_3$. The arrow highlights the methylene Pd···H interaction....129

Figure 5.3 ^{1}H NMR spectra of [Pd((4-Me_2)bipy){Na·^{t}**BuC5(H)$_2$**}] **5.2a**, [Pd((4-Me_2)bipy){K·^{t}**BuC5(H)$_2$**}] **5.2b**, [Pd((4-Me_2)bipy){Rb·^{t}**BuC5(H)$_2$**}] **5.2c**, and [Pd((4-Me_2)bipy) {Cs·^{t}**BuC5(H)$_2$**}] **5.2d** in *$CDCl_3$. The arrow highlights the methylene Pd···H interaction 130

Figure 5.4 ^{1}H NMR spectra of [Pd(phen){Na·^{t}**BuC5(H)$_2$**}] **5.3a**, [Pd(phen){K·^{t}**BuC5(H)$_2$**}] **5.3b**, [Pd(phen){Rb·^{t}**BuC5(H)$_2$**}] **5.3c**, and [Pd(phen){Cs·^{t}**BuC5(H)$_2$**}] **5.3d** in *$CDCl_3$. §Residual solvent impurity (acetone). The arrow highlights the methylene Pd···H interaction....131

Figure 5.5 ^{1}H NMR spectra of [Pd(dpa){Na·^{t}**BuC5(H)$_2$**}] **5.4a**, [Pd(dpa){K·^{t}**BuC5(H)$_2$**}] **5.4b**, [Pd(dpa){Rb·^{t}**BuC5(H)$_2$**}] **5.4c**, and [Pd(dpa){Cs·^{t}**BuC5(H)$_2$**}] **5.4d** in *$CDCl_3$. *i* = Impurities. $^§H_2O$. The arrow highlights the methylene Pd···H interaction 132

Figure 5.6 X-ray structure of compound **3.1** showing the boat-chair conformation. Thermal ellipsoids are shown at 50% probability. Molecules of crystallization and hydrogen atoms are omitted for clarity. Part of the molecule is drawn in wireframe style for clarity 133

Figure 5.7 Line drawing of [Mo(PMe_3)$_3$(H)$_2${^{t}**BuC4(H)$_2$**}] complex. Agostic interaction is highlighted....135

Figure 5.8 ^{1}H NMR spectra of complexes **5.5a-5.5e** and ^{t}**BuC4(H)$_4$** in *$CDCl_3$. The arrow highlights the methylene Pd···H interaction 137

Figure 5.9 ^{1}H NMR spectra of complexes **5.6a-5.6c** and ^{t}**BuC4(H)$_4$** in *DMSO-d_6. $^§H_2O$. The arrow highlights the methylene Pd···H interactions....138

Figure 5.10 ^{1}H NMR spectrum of [Pd((4-Me)$_2$bipy))){Cs·^{t}**BuC6(H)$_3$**}] **5.7** complex in *$CDCl_3$. $^§H_2O$. The arrow highlights the methylene Pd···H interactions 139

Figure 5.11 ORTEP diagram of compound a) **5.1d**·2DMSO and b) eight-membered cycle. Thermal ellipsoids at the 50% probability level. H atoms and non-coordinating solvent are omitted for clarity....141

Figure 5.12 ORTEP diagrams of compounds a) **5.5a**·5C_6H_6, b) **5.5b**·5.5C_6H_6, c) **5.5e**·3CH_3CN and d) **5.6b**·2CH_3CN with thermal ellipsoids at the 50% probability level. H atoms and non-coordinating solvent are omitted for clarity 142

Figure 5.13 ORTEP diagram of compound **5.7**·7.5C_6H_6·H_2O with thermal ellipsoids at the 50% probability level. Some H atoms and non-coordinating solvent are omitted for clarity 143

Figure 5.14 Line drawings of compounds **5.1** and **5.2** 146

Figure 5.15 ORTEP diagram of compound a) **5.1**·4CH_3CN and b) **5.2**·4CH_3CN with thermal ellipsoids at the 50% probability level. Some H atoms and non-coordinating solvent are omitted for clarity 147

Figure 6.1 ^{1}H NMR spectra of complexes **6.1** to **6.6** in $CDCl_3$. *Residual solvent C_6H_6. ¥Impurities 180

Figure 6.2 Comparison between ^{1}H NMR spectra of complexes **5.1c** and **6.1** in *$CDCl_3$ 181

Figure 6.3 ^{1}H NMR spectra of expansions in the N-heterocyclic aromatic areas of complexes **5.1c** and **6.1** in $CDCl_3$. The arrows depict the movement of the proton signals 182

Figure 6.4 ^{1}H NMR spectra of expansions of the aromatic (Ar-H) and methylene (Ar-CH_2-Ar) areas of complexes **5.1c** and **6.1** in $CDCl_3$. The arrows depict the movement of the proton signals 183

Figure 6.5 X-ray structure of complex **6.1**. Ellipsoids shown at 50% probability. The second part of the molecule is shown as wireframe model for clarity. Most H atoms and benzene crystallization molecules are not shown for clarity 185

Figure 6.6 X-ray structure of complex **6.1**: a) front view, b) top view, c) side view and d) bottom view. Ellipsoids are shown at 50% probability. Crystallization molecules, H atoms and the second calix[5]arene ligand are not shown for clarity 187

Figure 6.7 Approximate ideal conformations[11111111111] observed in: a) **5.1d** boat-boat conformation and b) **6.1** boat-chair conformation. Only partial structures of compound **5.1d** and **6.1** are shown for clarity 188

Figure 6.8 Calculated geometries for the model of an 8-membered palladium-containing heterocycle. a) BB conformation and b) side view of BB conformation, c) BC conformation and d) side view of BC conformation 189

Figure 6.9 X- ray structure of **6.1** showing the interactions **a)** between D···bipyB' and D'···bipyA and **b)** between the aromatic rings C···C' and E···E' of the calix[5]arene ligands 191

Figure 6.10 View of the crystal packing in complex **6.1** 192

Figure 6.11 View of the crystal π-π stacking showing the parallel displacement and a close-up of the intermolecular π-π stacking with selected distances 193

Figure 6.12 Proposed molecular structure for compounds **6.7 – 6.12** 195

Figure 6.13 ^{1}H NMR spectra of complexes **6.10 – 6.12** in *$CDCl_3$. The arrow highlights the methylene Pd···H interaction proton. § = impurities or residual solvent 199

Figure 6.14 Proposed restricted rotation of the pyridyl rings in phen 202

Figure 6.15 ^{1}H NMR spectra displaying the variation in the chemical shift behavior from **^{t}BuC5(H)$_5$** to [MoO_2(acac){**Cs·^{t}BuC5(H)**}Pd(bipy)] **6.10**, from the OH to the Ar-CH_2-Ar regions 202

Figure 6.16 ^{1}H NMR spectra of the *tert*-butyl area displaying the variation in the chemical shift behavior from **^{t}BuC5(H)$_5$** to [MoO_2(acac){**Cs·^{t}BuC5(H)**}Pd(bipy)] **6.10**. *Impurity 203

Figure 6.17 Conformation and symmetry adopted by the calix[5]arene ligand in **^{t}BuC5(H)$_5$**, Cs_2·**^{t}BuC5(H)$_3$ 2.2b**, [Pd(bipy){Cs·**^{t}BuC5(H)$_2$**}] **5.1d** and [MoO_2(acac){Cs·**^{t}BuC5(H)**}Pd(bipy)] **6.10**. * Proposed structure 204

LIST OF TABLES

Table 1.1 ^{1}H NMR resonances for -O*H*, Ar-*H*, Ar-CH_2-Ar, and C(CH_3)$_3$ in calixarenes at room temperature in $CDCl_3$. 8

Table 1.2 Bimetallic calix[4-8]arene complexes found in the literature. 14

Table 2.1 ^{1}H NMR data of **^{t}BuC5(H)$_5$** mono- and dianions at room temperature in $CDCl_3$ (δ in ppm). 24

Table 2.2 Coalescence temperatures at 300 MHz and free energies of activation for the conformational inversion of M·**^{t}BuC5(H)$_4$** and M_2·**^{t}BuC5(H)$_3$** (M = Rb, Cs) anions ($\Delta G^{\ddagger} = 4.58T_c(10.32 + \log T_c/k_c)/1000$). 25

Table 2.3 Selected M-O and M-C distances of alkali metal salts of calixanions. 29

Table 2.4 Crystallographic data and summary of the data collection and structure refinement of compounds M·**^{t}BuC5(H)$_4$** (M = Rb **2.1a**, Cs **2.2a**) and M_2·**^{t}BuC5(H)$_3$** (M = Rb **2.1b**, Cs **2.2b**) 37

Table 3.1 Selected bond distances (Å) and angles (°) for complexes **3.1**·6DMSO and **3.2**·2C_6H_6 50

Table 3.2 Crystallographic data for complexes **3.1**·6DMSO and **3.2**·2C_6H_6. 65

Table 4.1 IR and qualitative data found in compounds **4.1 – 4.3**. 79

Table 4.2 ^{1}H NMR (δ ppm, $CDCl_3$) data found for compounds **4.1 – 4.3**. 80

Table 4.3 Selected bond lengths (Å) and angles (º) of complex [**4.4a**]$_2$·8CH_3CN 87

Table 4.4 Selected *d*(centroid-Rb(1)), *d*(centroid-Rb(2)) and *d*(centroid-centroid) distances (Å), centroid-O-Rb(1), centroid-O-Rb(2), centroid-Rb(2)-centroid and centroid-C(11/99)-centroid angles (º) in compound **4.4a** 88

Table 4.5 ^{1}H NMR chemical shifts (ppm) of compounds **4.5a** to **4.5c** in $CDCl_3$ 96

Table 4.6 Principal Infrared frequencies (cm^{-1}) of compounds **4.1**, **4.2**, **4.3** and **4.5a-c** in KBr pellets 97

Table 4.7 Selected bond lengths (Å) and angles (º) of complex [**4.5a**]$_2$·2$C_5H_8O_2$ 99

Table 4.8 Selected *d*(centroid-Cs(2)), *d*(centroid E-centroid C) distances (Å) and centroid-O-Cs(2), centroid A-C(44)-centroid B angles (º) in compound [**4.5a**]$_2$·2$C_5H_8O_2$. 99

Table 4.9 Crystallographic data for complexes [**4.4a**]$_2$·8CH_3CN and **4.5a**·2$C_5H_8O_2$·C_5H_{12}. 113

Table 5.1 Yields for complexes containing coordinating N-heterocyclic ligands. 123

Table 5.2 Summary of yields of **RC4(H)$_4$** (R = ^{t}Bu, H) and **^{t}BuC6(H)$_6$** palladium complexes. 128

Table 5.3 ^{1}H NMR chemical shifts in ppm for complexes **5.1a-d**, **5.2a-d**, **5.3a-d** and **5.4a-d** in $CDCl_3$. 134

Table 5.4 ^{1}H NMR chemical shifts in ppm for palladium calix[4,6]arene complexes **5.5a-5.5e** and **5.7**. 140

Table 5.5 Selected bond lengths (Å) and angles (º) of complexes **5.1d**·2DMSO, **5.5a**·5C_6H_6, **5.5b**·5.5C_6H_6, **5.5e**·3CH_3CN, **5.6**·2CH_3CN and **5.7**·7.5C_6H_6·H_2O. 144

Table 5.6 Pd···H interactions (Å) of complexes **5.1d**·2DMSO, **5.5a**·5C_6H_6, **5.5b**·5.5C_6H_6, **5.5e**·3CH_3CN, **5.6**·2CH_3CN and **5.7**·7.5C_6H_6·H_2O. 145

Table 5.7 Overview of characteristic bond distances for palladium alkoxide and aryloxide compounds. 145

Table 5.8 Selected bond lengths (Å) and angles (º) of complexes **5.1**·4CH_3CN and **5.2**·4CH_3CN 148

Table 5.9 Crystallographic data and summary of data collection and structure refinement of complexes **5.1d**·2DMSO, **5.5a**·5C_6H_6, **5.5b**·6C_6H_6, **5.5e**·3CH_3CN, **5.6**·4CH_3CN and **5.7**·8C_6H_6·H_2O. 172

Table 5.10 Crystallographic data and summary of data collection and structure refinement of complexes **5.1**·4CH_3CN and **5.2**·4CH_3CN. 173

Table 6.1 Comparative ^{1}H NMR data for compounds **5.1c** and **6.1** in $CDCl_3$. Highlighted values refer to the major changes found between compounds. 181

Table 6.2 Common ppm ranges found in literature for the Ar-*H*, Ar-C*H*$_2$-Ar and ^{t}Bu resonances in metallocalix[5]arenes in $CDCl_3$. 184

Table 6.3 Selected bond distances (Å) and angles (^{o}) for complex **6.1**. 186

Table 6.4 Selected bond distances and angles for calculated BB and BC conformations, and values found experimentally. 190

Table 6.5 Principal Infrared frequencies (cm^{-1}) of compounds **6.7** to **6.12** in KBr pellets, with comparative values from literature. 197

Table 6.6 Chemical shifts (ppm) of compounds **6.7** to **6.12** in $CDCl_3$. 198

Table 6.7 Comparative chemical shifts (ppm) of the aromatic, methylene and *tert*-butyl area of compounds **6.7** to **6.12** with starting material and normal values found in literature..200

Table 6.8 Crystallographic data for complex Ti[(bipy)Pd{Rb·^{t}**BuC5**}]$_2$·C_6H_6 **6.1**·C_6H_6.....218

LIST OF SCHEMES

Scheme 1.1 Simplified syntheses and representation of the calix[n]arene ligands. 1

Scheme 1.2 The first transition metal calixarene complexes prepared by Power and co-workers. 9

Scheme 1.3 M-C bond functionalities on an oxo surface modeled by ^{t}**BuC4(H)$_4$**. 11

Scheme 1.4 Synthesis of the first heterobimetallic calix[4]arene complex. 15

Scheme 1.5 Bimetallic calix[4]arene complex that showed catalytic activity. 16

Scheme 2.1 Synthesis of [MoO{**HC4**}] and [MoO{^{t}**BuC4**}] metallocalixarenes. 19

Scheme 2.2 Synthesis of the heterobimetallic Ti/K calix[5]arene complex. 20

Scheme 2.3 Synthesis of *para-tert*-butylcalix[5]arene anions. 22

Scheme 3.1 ^{t}**BuC5(PNMe$_2$)(H)$_3$** and ^{t}**BuC5(H)$_5$** titanium(IV) complexes found in literature.....40

Scheme 3.2 Proposed products **3a** to **3d** for reaction **A** according to suggested pathways 1-4. ...42

Scheme 3.3 Synthesis of compound [(TiCpCl)$_2${^{t}**BuC5(H)$_3$**}] **3.3**. 47

Scheme 3.4 Proposed structure of compounds **3e** or **3d** by using $CpTiCl_3$ with dry $Cs_2\cdot$^{t}**BuC5(H)$_3$**. 47

Scheme 4.1 Synthesis of dioxomolybdenum(VI) calix[4]arene complexes. 67

Scheme 4.2 Synthesis of $(MoO_2)^{2+}$-containing calix[5]arene complexes **4.1 – 4.3**. 81

Scheme 4.3 Synthesis of compounds **4.4a** and **4.4b**. 83

Scheme 5.1 Synthesis of a monometallic late transition metal calixarene complex with a metal-O coordination mode. 117

Scheme 5.2. Synthesis of N-ligated bis(aryloxo)palladium(II) complex. 120

Scheme 5.3 Preparation of heterobimetallic palladium(II)-M(I) (M = Na, K, Rb, Cs) calix[5]arene complexes **5.1a-d**. 121

Scheme 5.4 Proposed mechanism for the formation of [Pd(bipy){Cs·^{t}**BuC5(H)$_2$**}] **5.1d**. 124

Scheme 5.5 Preparation of complexes **5.5a** to **5.5e** and **5.6a** to **5.6c**. 126

Scheme 6.1 Preparation of monometallic bismuth or antimony and heterobimetallic Mo/M (M = Bi, Sb) calix[5]arene complexes. 175

LIST OF EQUATIONS

Equation 4.1 69

Equation 4.2 71

Equation 4.3 71

Equation 4.4 72

Equation 4.5 73

Equation 4.6 90

Equation 4.7 91

Equation 5.1 119

Equation 5.2 122

Equation 5.3 127

Equation 6.1 177

Equation 6.2 194

CHAPTER 1

BACKGROUND AND PURPOSE

1.1 Calixarenes

1.1.1 Introduction

The macrocyclic compounds built from phenol units linked by methylene bridges were first called “calixarenes” by Gutsche.[2] The name is derived from the Greek *calix* meaning “vase” or “chalice”, and *arene*, describing the repeating aryl units in the macrocyclic array.

Despite their relatively early discovery, calixarenes have received much attention only in recent years. Adolf von Bayer was the first to report the reaction of phenols with aldehydes in the presence of acid.[3-5] The products were described as complex, difficult to characterize, and in some cases, "kettartige" or "cement-like" substances. From these beginnings, and after a century of research into the nature of the products and optimal conditions for their preparation, Gutsche and coworkers developed inexpensive and convenient one-pot syntheses of the calix[n]arenes (n = 4, 6, 8) from the condensation of phenol with formaldehyde as shown in Scheme 1.1.[6-8]

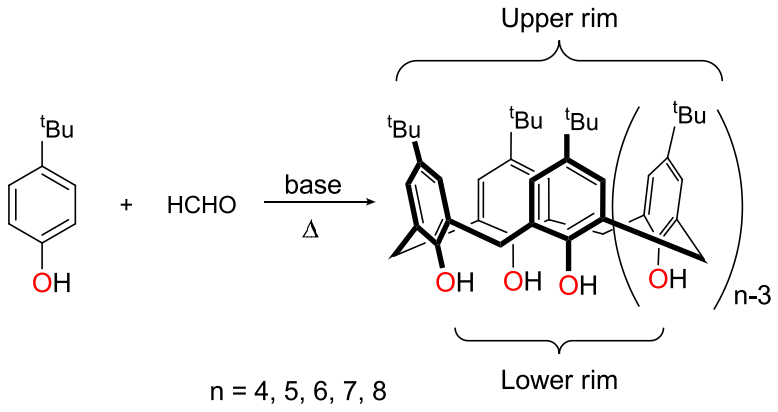

Scheme 1.1 Simplified syntheses and representation of the calix[n]arene ligands.

1.2 Nomenclature

Due to the complexity of the full names of various metallated calixarenes, in this work we will introduce a new systematic shorthand for describing calixarene coordination compounds. We developed this method in order to convey the important aspects of the structure in minimal space. For example, the *p-tert*-butylcalix[4]arene ligand is represented by **^{t}BuC4(H)$_4$**. In this nomenclature some important aspects should be taken into account:

Ligand:

1. **C4** describes the ring size; in this example, calix[4]arene.
2. The notation to the left of **C4** describes the *para* substituent on the upper rim. If all *para* substituents are the same, the subscript is omitted. If there are nonequivalent *para* substituents, parentheses ( ) and subscripts are used to describe the number of each group. For example; **AC4(H)$_4$**. The notation **A** is used to describe the allyl group. Here the allyl group is present in the *para* position of each aromatic ring. The compound **(A)$_2$(^{t}Bu)$_2$C4(H)$_4$** has two *para* ^{t}Bu groups and two *para* allyl groups.
3. The notation to the right of **C4** describes the substituent attached to the lower rim. When the label **H** is used, it should be understood as OH. However, if there is a functional group attached to the oxygen atom, e.g. –Me, the notation would be written as **OMe**. All groups are enclosed between parentheses.

Coordination Complex:

4. When the calixarene ligand forms a transition metal-containing complex, the transition metal is identified first by its chemical symbol followed by any coordinating ligands, while the calixarene ligand is placed between braces { }, following rules 1-3. If the metal is directly attached to the oxygen atoms, fewer hydrogen atoms are attached to the lower rim (e.g. [TiCp{^{t}**BuC4(H)$_2$**}]). The metallocalixarene complex overall is enclosed in square brackets [ ]. If the metal is an alkali metal, braces and the square brackets are omitted and a middle dot · is used instead. For example, [WCl_2{^{t}**BuC4**}] and Rb·^{t}**BuC4(H)$_3$**. The first name describes that the tungsten atom is directly attached to the four oxygen atoms of the lower rim and therefore the **(H)$_4$** are omitted. In the second example one rubidium atom is in the calixarene complex, therefore **(H)$_3$** is used. If coordinating solvent molecules are present in the molecule the square brackets are followed by a dot, the number of solvent molecules, and finally the solvent. For example, four molecules of THF were found in the rubidium salt, therefore the formula is written as [Rb·^{t}**BuC4(H)$_3$**]·4THF.
5. If the transition metal-containing calixarene complex additionally contains an alkali metal, then the alkali metal is considered as a part of the ligand environment and is enclosed in the braces as well, e.g. the compound [Ti(acac){K·^{t}**BuC4**}]·H_2O·MeOH.

1.3 Functionalized calixarenes

Starting with the simple calixarenes, research groups around the world have developed methods for contouring their shapes and placing a variety of functional groups on the rim of the cavity. Both the wider (upper) and narrower (lower) rims can be easily modified by the addition of coordinating pendant arms, providing them with new properties that increase their selectivity and affinity toward specific ions or metal centers. These modifications (e.g. ether, ester, amide, carboxylic acid groups)[9-14] have been of great interest in the supramolecular and coordination[15-21] chemistry of calixarene derivatives, allowing the production of new metal-containing calixarene compounds.

The conformational flexibility, presence of a cavity and ability to simultaneously coordinate numerous metal centers make calixarene derivatives into an excellent set of coordinating ligands able to bind metals in various positions,[15-18,22-24] as illustrated in Figure 1.1.

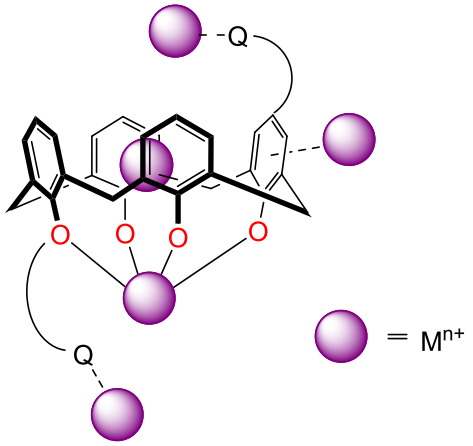

Figure 1.1 Potential metal binding sites in a calix[4]arene ligand (Q = coordinating group).[15-18,22-24]

Remarkable applications of calixarene derivatives have been discovered, including their use as enzyme mimics, in host-guest chemistry, for selective ion transport, as platforms for shape-selective catalysts, and as molecular sensors.[12,25-28]

1.4 Structural characteristics of calixarenes

The basic structure of a calixarene consists of repeating phenolic units linked by methylene groups to form a distinct cone-shaped cavity.

The spatial orientation of each phenolic unit leads to a conformation that is a function of reaction conditions, the number of phenols linked together, their degree of substitution, and the nature of the linkage between phenols. Rotation of the methylene linkers forms variable conformations in substituted calixarenes. For example, *p-tert*-butylcalix[4]arene can assume the cone, partial cone, 1,2-alternate, or 1,3-alternate conformation.[29] Figure 1.2 illustrates each conformation. By convention, when all phenolic rings are pointed up, this signifies the cone. When one or two are pointed down, this signifies a partial cone arrangement.

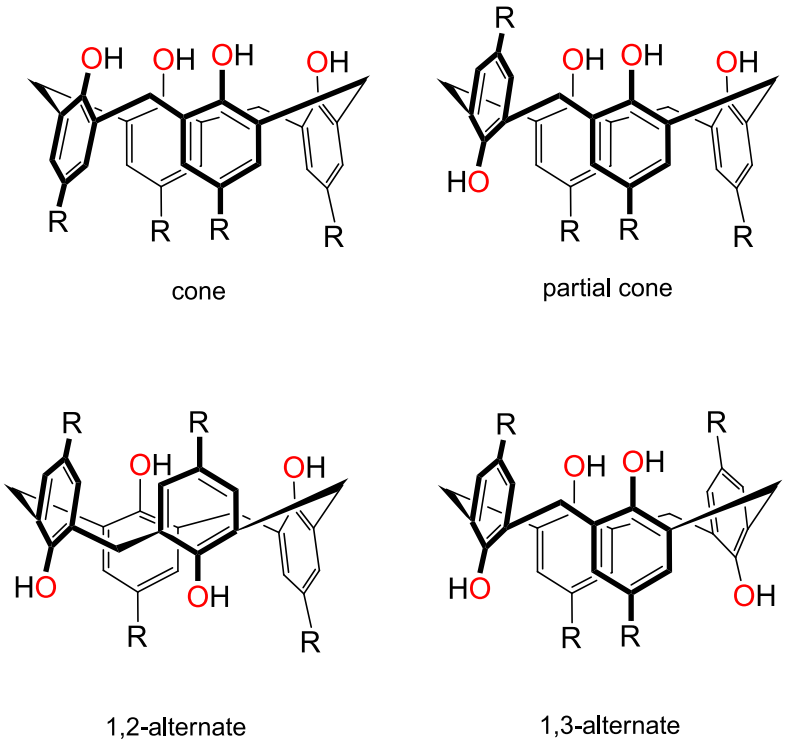

Figure 1.2 The four limiting and ideal conformations of a *p-tert*-butylcalix[4]arene.

One especially convenient aspect of working with calixarenes is their characteristic and simple proton nuclear magnetic resonance (^{1}H NMR) spectra, which reveal the geometry and symmetry of calixarene products. For example, the resonances of *p-tert*-butylcalix[n]arenes (n = 4, 5, 6, 8) from the aromatic protons, the *tert*-butyl protons, and the hydroxyl protons are singlets. The number of peaks can be related to the symmetry of the calixarene ring.

The methylene region is generally the most useful aspect of the spectrum. The resonances in the 4.5-3.5 ppm region in the ^{1}H NMR spectra provide a very distinct pattern for conformational analysis, because the methylene bridge protons are affected most by conformational changes. In the cone conformation, neither proton is positioned inside the cavity. This results in a splitting pattern consisting of a pair of doublets, one occurring around 3.2 ppm

and the other at 4.9 ppm. The CH_2 protons appear as a pair of doublets at room temperature for *p-tert*-butylcalix[4]arene (**^{t}BuC4(H)$_4$**) and *p-tert*-butylcalix[8]arene (**^{t}BuC8(H)$_8$**), and as a broad signal for *p-tert*-butylcalix[5]arene (**^{t}BuC5(H)$_5$**) and *p-tert*-butylcalix[6]arene (**^{t}BuC6(H)$_6$**).

^{1}H NMR studies of several calixarenes in solution showed that they mainly exist in the cone conformation, but they are conformationally mobile at room temperature. The flexibility of calixarenes can be reduced by derivatization of the upper and lower rims with bulky groups that inhibit rotation.[30] A singlet arising from the OH groups varies in position (8.5-10.5 ppm) with the size of the calixarene (Figure 1.3).

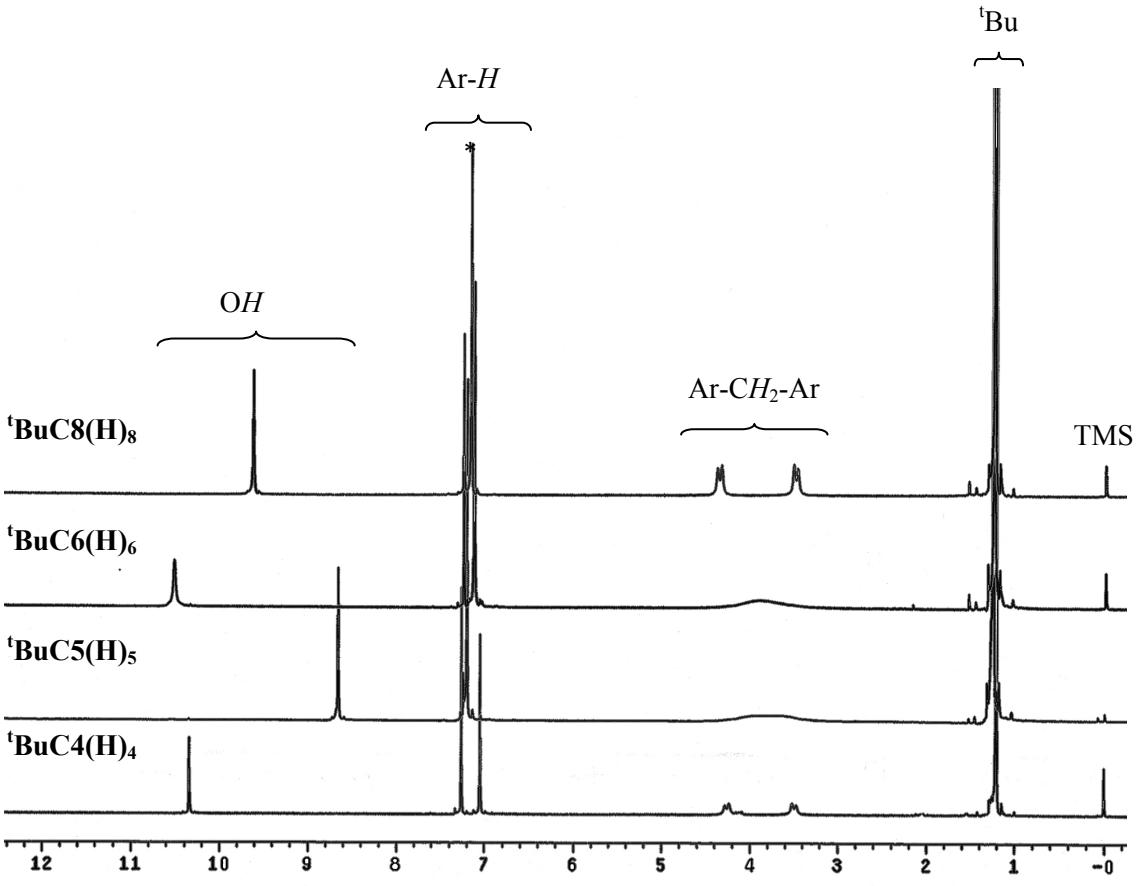

Figure 1.3 ^{1}H NMR spectra in *$CDCl_3$ at room temperature of calix[n]arenes (n = 4, 5, 6, 8).

For the parent calixarenes listed in Table 1.1 the δ_{OH} value is taken to be a measure of the strength of intramolecular hydrogen bonding: the greater the value the stronger is the hydrogen bond. Thus, intramolecular hydrogen bonding is particularly strong in calix[4]- and -[6]arenes, slightly less so in calix[8]arene, and still less so in calix[5]arene.[29]

Table 1.1 ^{1}H NMR resonances for -O*H*, Ar-*H*, Ar-CH_2-Ar, and C(CH_3)$_3$ in calixarenes at room temperature in $CDCl_3$.

	O*H*	Ar-*H*	Ar-CH_2-Ar	C(CH_3)$_3$
^{t}BuC4(H)$_4$	10.34	7.05	d, 4.25, 3.49	1.21
^{t}BuC5(H)$_5$	8.66	7.20	b, 3.80	1.25
^{t}BuC6(H)$_6$	10.53	7.14	b, 4.00	1.25
^{t}BuC8(H)$_8$	9.64	7.17	d, 4.36, 3.48	1.25

1.5 Metallocalixarenes

In 1985 Power et al. reported[31] the synthesis of the earliest metallocalixarene complexes. The complexes [Ti{**^{t}BuC4**}]$_2$, [(H$_3$N)Fe{**^{t}BuC4(SiMe$_3$)**}]$_2$ and Co[Co{**^{t}BuC4(SiMe$_3$)**}]$_2$·THF were obtained when parent **^{t}BuC4(H)$_4$** was allowed to react with the corresponding metal amide (Scheme 1.2). All products were characterized by X-ray crystallography.

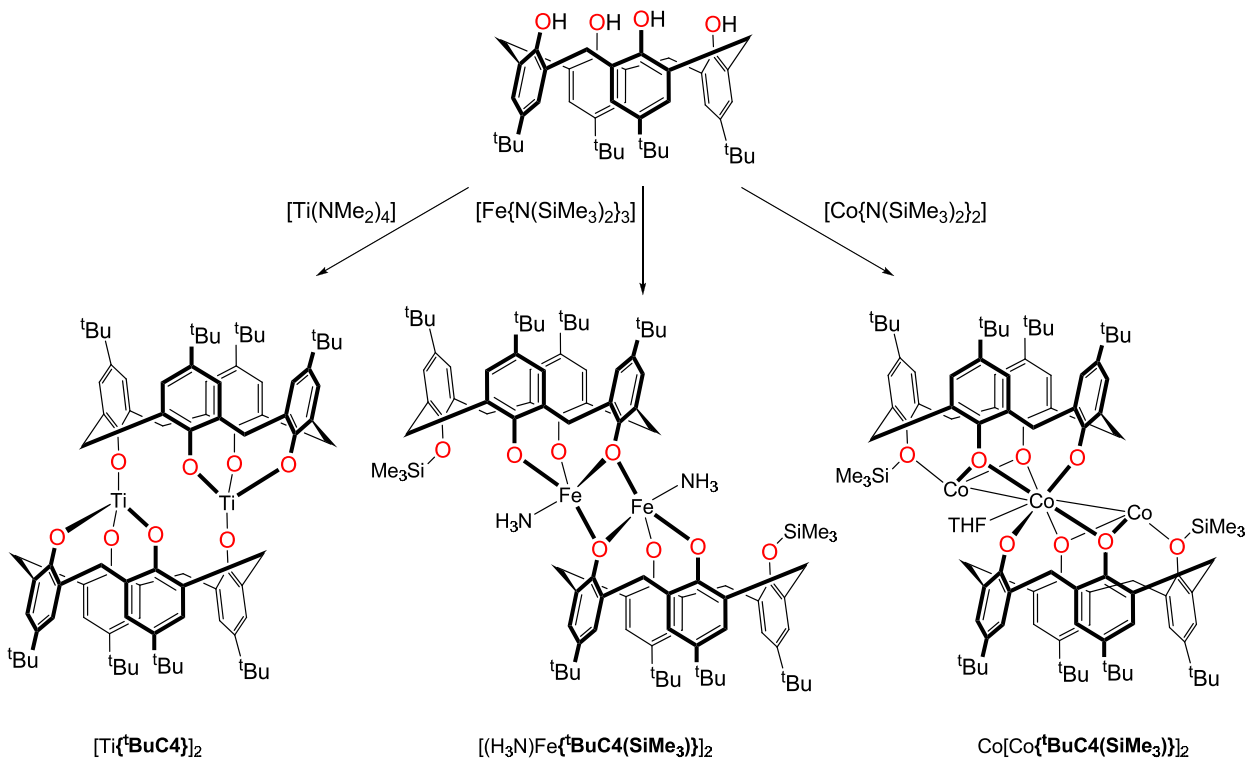

Scheme 1.2 The first transition metal calixarene complexes prepared by Power and coworkers.[31]

After these first examples other transition metal calixarene compounds were described[32-36] and opened a new field in coordination chemistry. The majority of calixarene coordination chemistry reported in the literature has been developed with the calix[n]arenes (n = 4, 6 or 8) because of their ready availability on a multigram scale.[16,19,22] In contrast to the even-numbered calixarenes, the chemistry of the odd-numbered rings, such as calix[n]arene (n = 5 or 7), is relatively unexplored due to their difficult synthesis and isolation.[23]

Floriani recognized that for the calix[4]arene ligand system, the four oxygen donors preorganized in a quasi-planar geometry offer an ideal opportunity for modeling oxo surfaces and heterogeneous catalysts.[16,37] Floriani and others found that calix[*n*]arenes are capable of acting as ancillary ligands for the metal-containing components of a catalyst, allowing the

resulting metal-calixarene compounds to be used for a variety of transformations.[11] Floriani et al. prepared a series of lower rim coordinated Mo^{VI}, W^{VI}, Zr^{IV}, Ta^{V}, and V^{IV} complexes and found that the reactivity of these compounds is similar to that occurring on metal oxide surfaces.[38-45]

For example, an elegant series of experiments performed by Floriani's group using a tungsten(VI)-containing calix[4]arene complex (**A**, Scheme 1.3) allowed the formation of the M-C bonded compounds **B**-**H**.[36,39,46-47] The η^2-olefin complexes **B** and **H** were formed by the reduction of **A** below -20 ^{o}C in the presence of an excess of ethylene or propylene. The η^2-cyclohexene complex **D** was obtained by an analogous procedure. Compound **D** showed high thermal lability of the coordinated olefin. The η^2-*trans*-stilbene complex **F**, the diphenyl acetylene complex **G**, and the η^2-norbonene derivative **E** were obtained when compound **D** was further heated in toluene in the presence of a slight excess of the appropriate olefin. Compound **C** was produced when a catalytic amount of Na metal (10%) was added.[36,39,46-47]

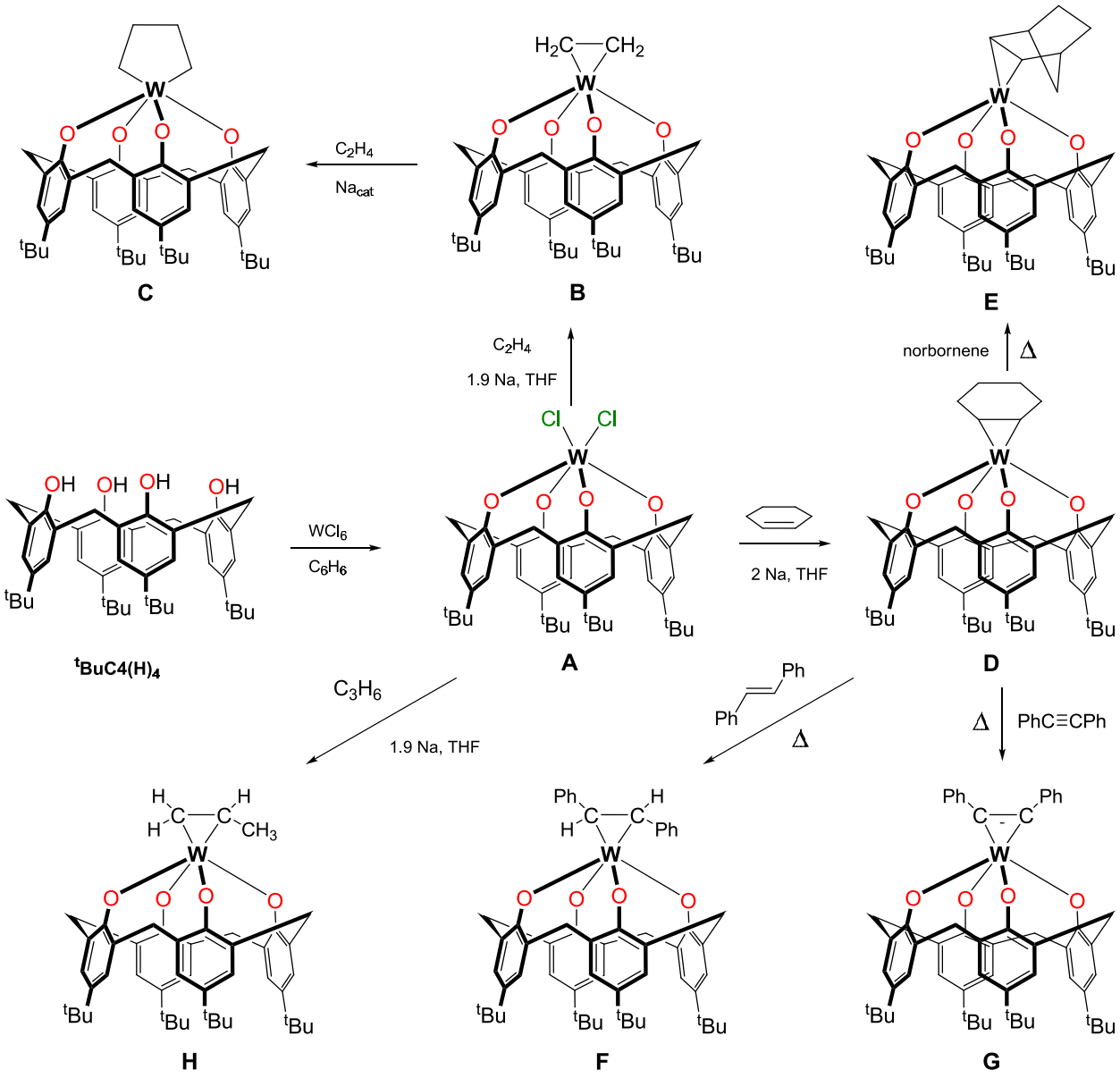

Scheme 1.3 M-C bond functionalities on an oxo surface modeled by **^{t}BuC4(H)$_4$**.[36,39,46-47]

While many studies in calixarene chemistry have focused on the reactivity and synthesis of mono metallocalixarene derivatives, there are few reports of selective synthesis and reactivity of heterobimetallic complexes with the metals attached directly to the lower rim.

1.6 Bimetallic calixarene chemistry

Most of the bimetallic calixarene complexes described in literature contain M and M' functionalities, in which either M = M' or M ≠ M' (M, M' = transition, alkali, or main group metal). These complexes may be grouped depending on where the metal centers are localized and the calixarene coordination mode. The structures of bimetallocalixarenes can be described by six categories. The coordination modes are illustrated with calix[4]arene in Figure 1.4 while a summary of bimetallic calixarene complexes found in literature are presented in Table 1.2.

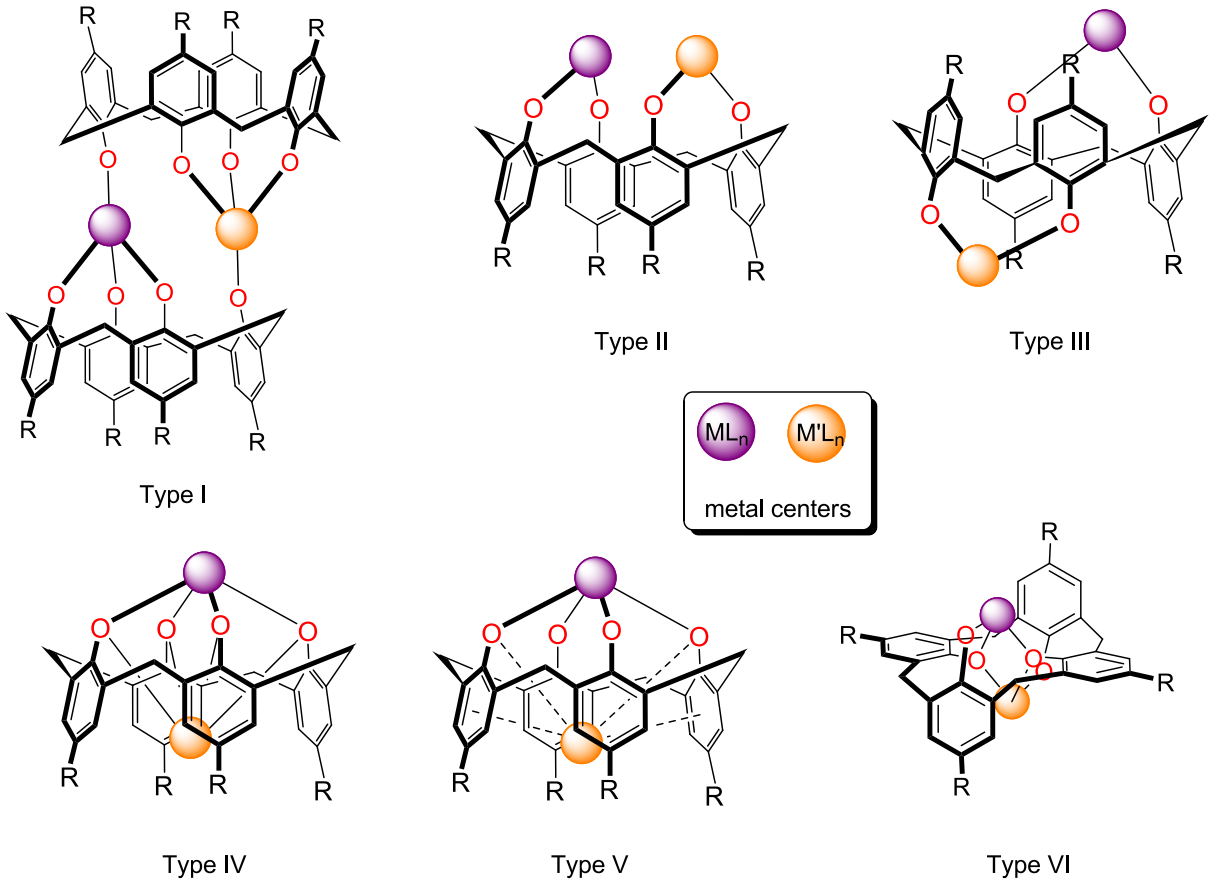

Figure 1.4 Examples of coordination types I-VI found in calix[4]arene containing two metal centers.[31-33,35,38,43-44,48-95]

Type I: The metal centers are sandwiched by two calixarenes. Both calixarene ligands contribute to the coordination spheres of the metals involved. The calixarenes adopt a cone conformation.

Type II: In contrast to Type I only one calixarene moiety serves as support for both metals. The metal centers are found in the lower rim while the calixarene adopts a cone conformation. The coordination sphere of the metal is completed with external ligands.

Type III: 1,2-coordination from the calixarene is observed towards the metallic centers, and the calixarene adopts a 1,2-alternate conformation so that the metals are on opposite sides of the ring system.

Type IV: Both metal centers interact with the lower rim, but one of the metal centers is located in the cavity of the calixarene. An important feature of this coordination type is that neither metal participates in π-interactions with the calixarene cavity. The calixarene may be in a cone conformation or a 1,3-flattened cone conformation.

Type V: Similar to Type IV, but one of the metal centers is stabilized in the cavity of the calixarene by π-interactions with the aryl moieties. The other metal center is localized on the lower rim and its coordination sphere is completed by external ligands. Generally the metal that is localized in the cavity is an alkali metal.

Type VI: This coordination mode shows a 1,3-alternate flattened cone conformation. This coordination mode is commonly observed for main group elements.

l

Table 1.2 Bimetallic calix[4-8]arene complexes found in the literature.

Research Group	Type	Elements	Ref
calix[4]arene			
Power et al.	**I**	M = M' = Ti, Fe, Co	31
Lippard et al.	**II**	M = M' = Mo	48
Limberg et al.	**II**	M = M' = V	49
Weinert et al.	**VI**	M = M' = Ge	50
Ishii et al.	**IV**	M = Re; M' = Pd	51
Raston et al.	**V**	M = Ti; M' = K, Cs	52-53
	IV, VI	M = M' = Zn	54
Gottfriedsen et al.	**VI**	M = M' = Be	55
Vigalok et al.	**IV, VI**	M = M' = Zn	56-57
Hanna et al.	**VI**	M = M' = Bi, Sb	58
Redshaw et al.	**I**	M = M' = Mo	59
Lattman et al.	**II, III**	M = M' = As	60
Atwood et al.	**VI**	M = M' = Al, Ga	61
Floriani et al.	**I**	M = M' = Nb	35,62
	II, IV	M = Nb; M' = Na	63
	V, II	M = W; M' = Na, K	64
	V, II	M = Nb; M' = Na	62-63,65
	I	M = M' = Nb, Ta	65
	V	M = Nb, Ta; M' = Li, Na, K	65
	I	M = M' = V	43-44
	I	M = M' = W	66-67
	I	M = M' = Mo	38
calix[4]arene			
Clegg et al.	**I**	M = M' = Ti	68
Cowley et al.	**IV, VI**	M = M' = Sn	69
Ladipo et al.	**III**	M = Ti; M' = Si	70-73
Anwander et al.	**I**	M = M' = Y	74
Cotton et al.	**I**	M = M' = Ti	75
thiacalix[4]arene			
Morohashi et al.	**III**	M = M' = Pd	76
Hidai et al.	**II**	M = Ti M' = Mo	77
	II, III	M = M' = Ir, Rh	78
Parkin et al.	**III**	M = M' = W	79
		M = M' = Mo	
		M = W; M' = Mo	
Liao et al.	**I**	M = Mn M' = Gd	80

Research Group	Type	Elements	Ref
calix[5]arene			
Raston et al.	**V**	M = Ti; M' = K	81
Lattman et al.	**II**	M = P; M' = W	82
	I, II	M = P; M' = W, Zr, Ti	83
Ephritikhine et al.	**I, III**	M = M' = U	84
Hanna et al.	**I**	M = M' = Bi	85
	III	M = M' = Bi, Sb	85
	III	M = Bi; M' = Si	86
Leverd et al.	**I**	M = M' = U	87
calix[6]arene			
Atwood et al.	**III**	M = M' = Ti	32
Limberg et al.	**II**	M = M' = V	49
Ephritikhine et al.	**III**	M = M' = U	88
Redshaw et al.	**II**	M = M' = Mo, W	59
Leverd et al.	**III**	M = M' = La, Sm, Yb	89
Raston et al.	**III**	M = M' = Ti	90
	V	M = Ti; M' = Ba	91-92
		M = Ti; M' = Sr	
		M = Zr; M' = Ba	
Hanna et al.	**I, III**	M = M' = Bi	93
	III	M = M' = Sb	93
calix[7]arene			
Hanna et al.	**I**	M = M' = Bi	93
calix[8]arene			
Pedersen et al.	**II**	M = M' = Ti	33
Gibson et al.	**III**	M = M' = Mo	94
Redshaw et al.	**II, III**	M = M' = W	95
Hanna et al.	**I, II**	M = M' = Bi	58,93

Although most bimetallic calixarene complexes in the literature are homometallic, there is one example of a heterobimetallic complex containing two different transition metals. The synthesis and characterization of the first such heterobimetallic (Re-Pd) calixarene complex was reported by Ishii et al.[51] Ishii used a stepwise synthesis starting with the isolation of a mononuclear Re-containing calix[4]arene, then allowed it to react with an allylpalladium complex (Scheme 1.4). Overall, the calixarene ligand adopts a pseudo cone conformation. The molecular structure of the complex was confirmed by X-ray crystallography.[51]

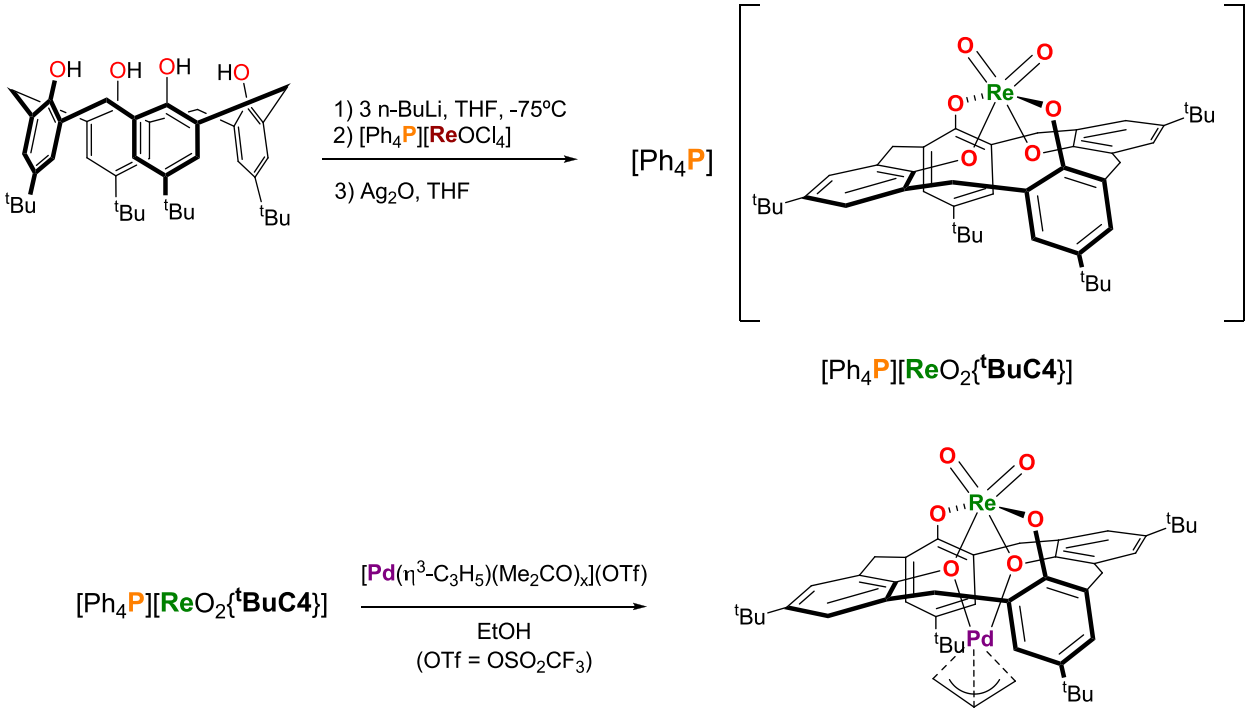

Scheme 1.4 Synthesis of the first heterobimetallic calix[4]arene complex.[51]

One interesting complex of Type III containing two zinc centers showed catalytic activity in the ring-opening polymerization of L-lactide (Scheme 1.5). Polymers with high molecular weight and a low degree of polydispersity were obtained.[96]

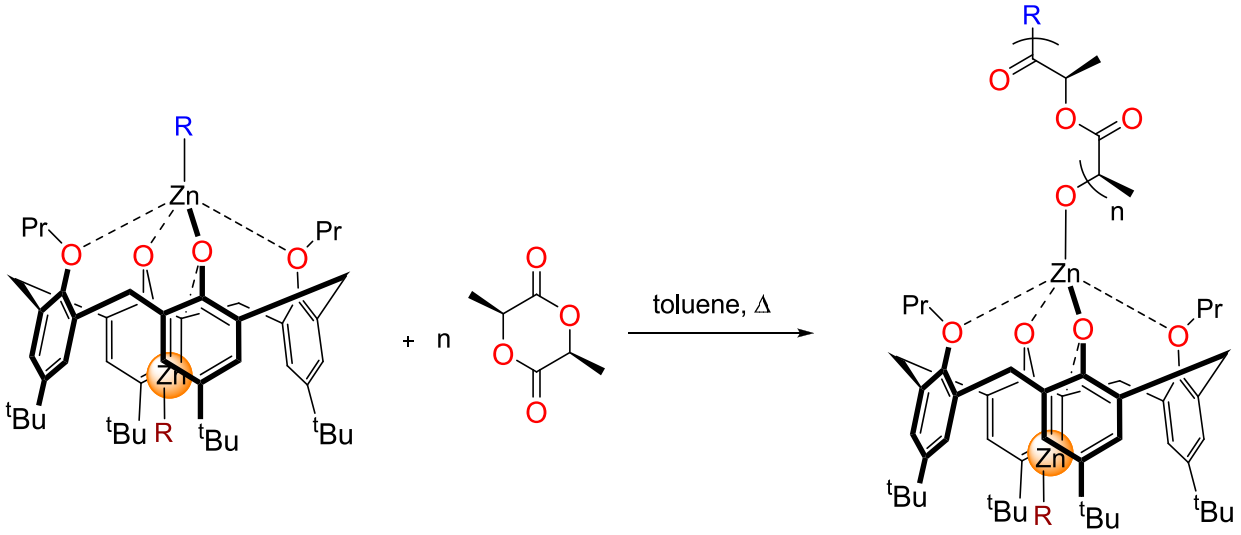

Scheme 1.5 Bimetallic calix[4]arene complex that showed catalytic activity.[96]

Motivated by the interesting properties of metallocalixarenes, we decided to explore their coordination chemistry. The present dissertation work is focused on the design of monometallic calix[5]arene complexes that can be used as precursors for the synthesis of new heterobimetallic calix[5]arene complexes. Ideally the compounds should contain free OH groups on the ligand and/or labile terminal groups to facilitate the addition of the second transition metal to the same calixarene framework. We took advantage of the large cavity size of the calix[5]arene as supportive ligand for our bimetallic complexes.

We synthesized and used calix[5]anions (Chapter 2) as metal precursors to obtain the first monometallic Ti^{IV} (Chapter 3), Mo^{VI}(Chapter 4), and Pd^{II} (Chapter 5) calix[5]arene complexes containing free OH groups.

Finally, as part of our studies on the reactivity of the monometallic Pd^{II} calixarene complexes, we prepared the first two classes of M/Pd^{II} ($M = Ti^{IV}$), Mo^{VI}) heterobimetallic complexes supported by calixarene ligands (Chapter 6).

CHAPTER 2

ALKALI METAL CALIXARENES

2.1 Introduction

As noted in Chapter 1, calixarenes are macrocyclic compounds prepared by the base-induced condensation of certain *para*-substituted phenols with formaldehyde (Scheme 1.1).[2] Nowadays, the easy one-step preparations of *p-tert*-butylcalix[4]arene[6] (**^{t}BuC4(H)$_4$**), *p-tert*-butylcalix[6]arene[7] (**^{t}BuC6(H)$_6$**), and *p-tert*-butylcalix[8]arene[8] (**^{t}BuC8(H)$_8$**), make these compounds extremely attractive for structural, conformational, and host-guest studies. Two interesting features make the calixarene unique to study; the cyclic framework and the oxygen donor atoms. The cyclic framework makes a pocket or cavity that allows the inclusion of charged or neutral guest molecules.[9,15,25,27,97-102]

The functionalization of either the upper rim or of the OH groups from the lower rim provides sites for the attachment of other functional groups, facilitating the use of calixarenes in supramolecular chemistry.[25] The hard acid character of the lower rim makes calixarenes attractive as ligands for binding high-valent transition metal ions and modeling oxo surfaces.[16,23,37]

Deprotonated calixarene derivatives, “calixanions”, have attracted interest in a number of fields. Calixanions have been utilized in organic chemistry, for example, as precursors for the synthesis of new host molecules by the addition of functional groups.[14] Certain isolated calixanions have been shown to have interesting layered solid state structures similar to organic clays.[103-104] The discovery that the parent calixarenes effect the transport of alkali metal ions in

water/organic solvent/water membrane systems has led to a particular interest in mono-deprotonated calixanions.[105-106]

As a result of the easy synthesis and availability in multigram scale, considerable attention has been focused on the chemistry of even membered calix[n]arenes (n = 4, 6, 8).[16,19,22] More recently, due to improvements in their syntheses, significant progress has also been made in the odd membered calix[n]arenes (n = 5, 7, 9).[11,23]

In 2003 our group described the synthesis of a large series of mono- and dianionic calix[4,6,8]arene alkali metal salts,[107-108] observing that the size and the nature of the alkali metal and the kind of base used, have a very important role in the conformation and the characteristics of the resulting calixanions. Solid state structures were obtained for the monoanionic species Li·**HC4(H)$_3$**, Na·**HC4(H)$_3$**, Rb·**HC4(H)$_3$**, Rb·^{t}**BuC4(H)$_3$**, Cs·**HC4(H)$_3$**, which all exhibited the cone conformation. The dianionic species M_2·**HC6(H)$_4$** (M = K, Rb, Cs) contained calixarenes in a flattened 1,2,3-alternate conformation (Figure 2.1).

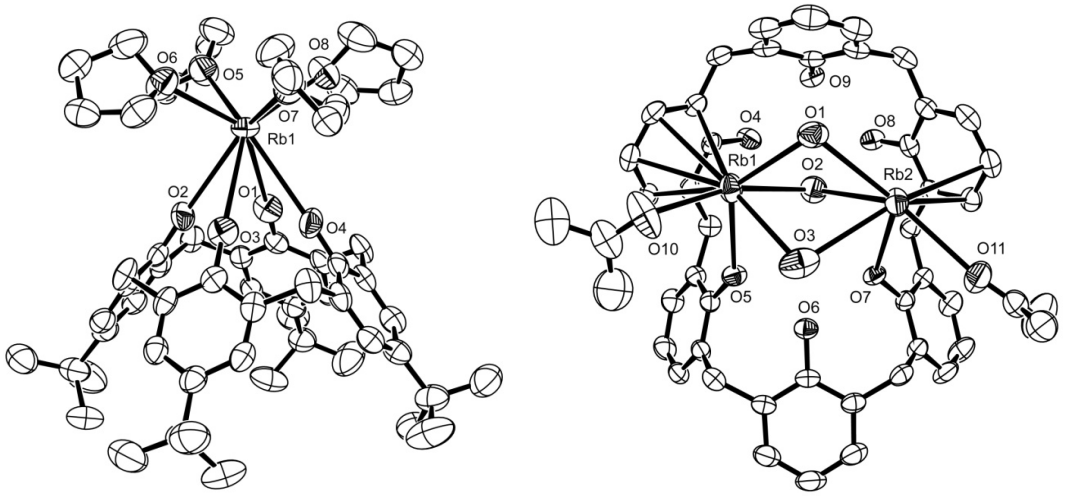

(A) **(B)**

Figure 2.1 X-ray structures of [Rb·^{t}**BuC4(H)$_3$**]·4C_4H_8O (**A**) and [Rb_2·**HC6(H)$_4$**]·3H_2O·2$(CH_3)_2CO$ (**B**), showing cone and 1,2,3-alternate conformations, respectively.[107]

Our group demonstrated the utility of calixanions as an entry into both main-group (the first antimony calixarene[109]) and transition metal calixarene complexes[110] that were inaccessible using the traditional parent calixarene as precursor (e.g. Scheme 2.1).

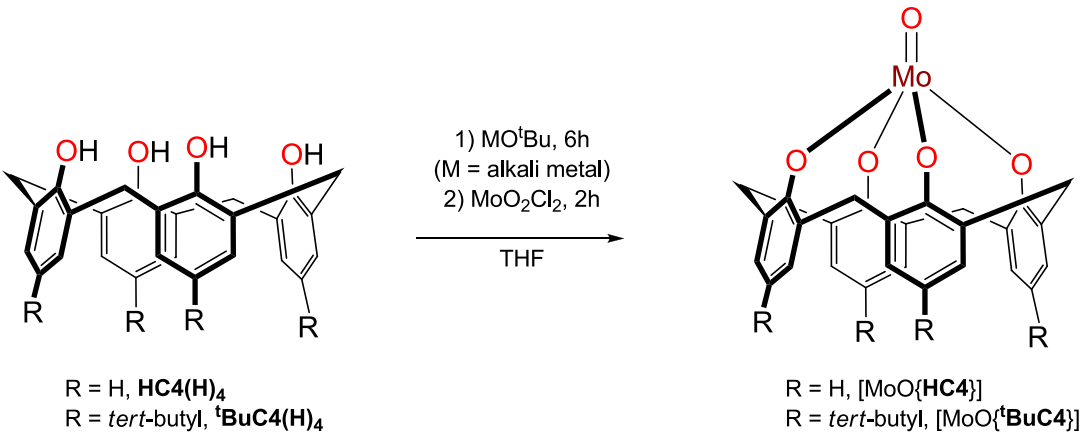

Scheme 2.1 Synthesis of [MoO{**HC4**}] and [MoO{^{t}**BuC4**}] metallocalixarenes.[110]

Unlike the even-numbered calix[n]arenes (n = 4, 6, 8), information about the chemistry of *p-tert*-butylcalix[5]arene (**^{t}BuC5(H)$_5$**) is very limited. Early work on **^{t}BuC5(H)$_5$** calixanion chemistry started with the functionalization of the lower rim. Gustche and coworkers reacted **^{t}BuC5(H)$_5$** and $KHCO_3$ in a 1:1 ratio to generate the precursor for lower rim monosubstituted derivatives. They used an excess of K_2CO_3 to produce the pentaanion, followed by addition of the alkylating agent to yield the desired substituted calixarene. No isolation or characterization of the monoanion or pentanion salt was performed.[30,111]

Et_3N has also been employed in order to deprotonate the **^{t}BuC5(H)$_5$**, and further reaction with lanthanide(III) ions led to the formation of calix[5]arene lanthanide(III) complexes.[112]

An unsymmetrical dimeric 1:1 K/Ti complex was isolated in a one-pot reaction by the reaction of **^{t}BuC5(H)$_5$** with potassium followed by $Ti(acac)_2(O^iPr)_2$.[81] The solid state structure showed a central Ti-O-Ti core with an encapsulated K^+ ion on each calix[5]arene unit (Scheme 2.2).

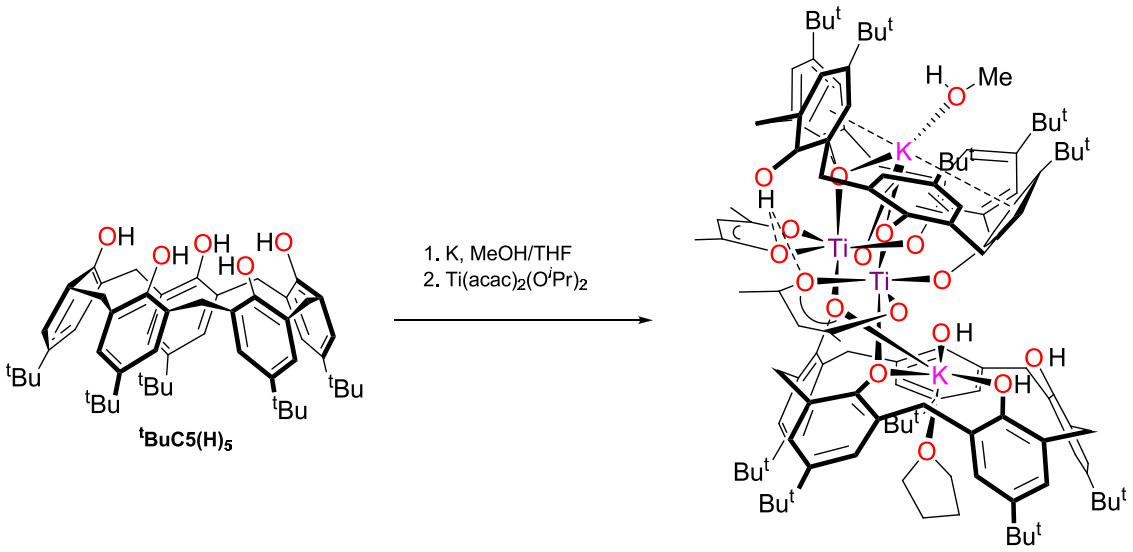

Scheme 2.2 Synthesis of the heterobimetallic Ti/K calix[5]arene complex.[81]

It is apparent that isolation, study, and full characterization of the anionic salts of **^{t}BuC5(H)$_5$** is lacking. In most of the cases where **^{t}BuC5(H)$_5$** anion was prepared the level of deprotonation and conformation of the parent calix[n]arene remains unclear. We believe that if a controlled metallation of **^{t}BuC5(H)$_5$** can be achieved, the affinity of the calixanion precursors to specific metal centers will be greatly enhanced. Therefore, in this chapter we describe the syntheses and characterization of the alkali metal salts of **^{t}BuC5** mono- and dianions derived from Rb and Cs ions.* The effects of the alkali metal on the calixarene ring will be discussed. *The synthesis of calix[5]anions were performed in collaboration with Dr. Daniel Mendoza-Espinosa, but in this chapter I will describe the work that I performed during this collaboration.[113]

2.2 Results and discussion

2.2.1 Synthesis of para-tert-butylcalix[5]arene mono- and dianions

The syntheses of **^{t}BuC5(H)$_5$** mono- and dianions provided product in good yields (81-86%). Base was added to **^{t}BuC5(H)$_5$** in a MeOH/benzene (1:3) mixture and the mixture was heated to reflux overnight, according to Scheme 2.3. When **^{t}BuC5(H)$_5$** was treated with MOH (M = Rb, Cs) in a 1:1 molar ratio or with M_2CO_3 (M = Rb, Cs) in a 1:0.5 molar ratio, the resulting salts were the monoanionic species M·**^{t}BuC5(H)$_4$** (M = Rb **2.1a**, Cs **2.1b**). Similarly, treatment of **^{t}BuC5(H)$_5$** with MOH (M = Rb, Cs) in a 1:2 molar ratio or with M_2CO_3 (M = Rb, Cs) in a 1:1 molar ratio, produced the dianionic species M_2·**^{t}BuC5(H)$_3$** (M = Rb **2.2a**, Cs **2.2b**). These results are similar to those obtained for the mono- and dicalix[6]anions previously reported by our group.[107]

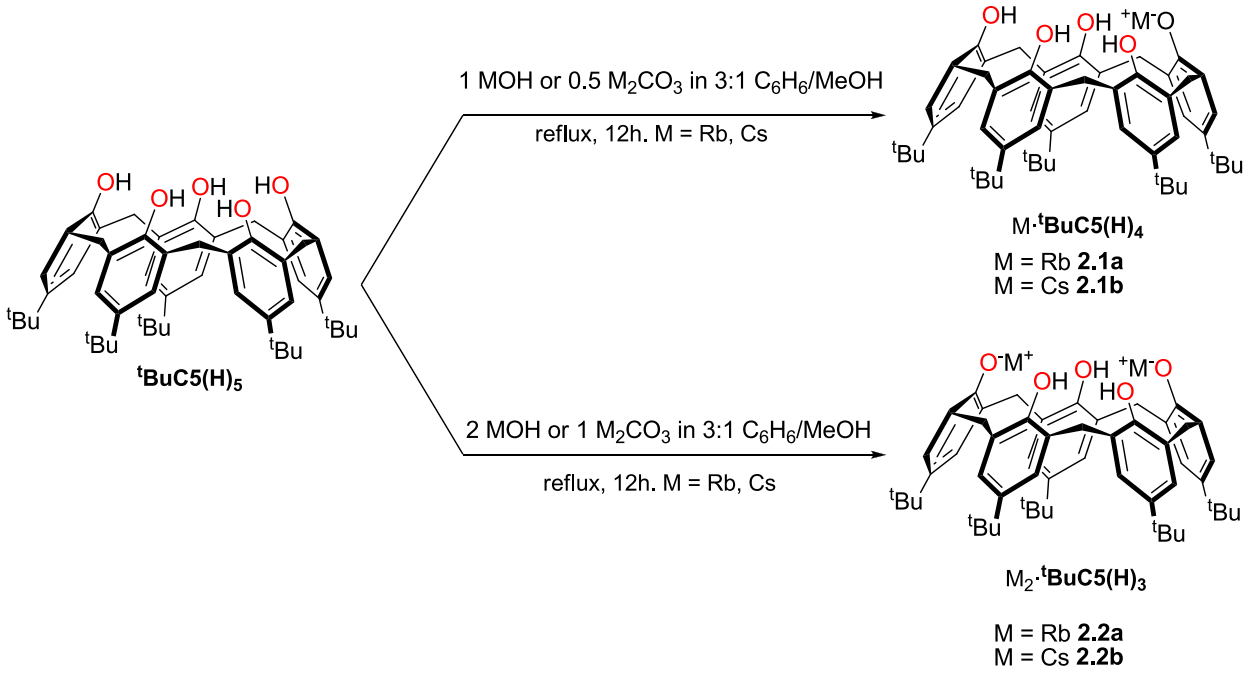

Scheme 2.3 Synthesis of *para-tert*-butylcalix[5]arene anions.

All of these **^{t}BuC5(H)$_5$** salts are air-stable, but their crystals readily lose solvent molecules to become a white powder. Crude **^{t}BuC5(H)$_5$** mono- or dianion salts were initially obtained as light yellow or off-white powders but suitable X-ray quality crystals were obtained by pentane diffusion into a concentrated solution of THF.

2.2.2 NMR spectroscopy

The NMR spectral patterns of calixarenes provide a useful measure of conformational identity, and the temperature dependence of the methylene proton signals allows an assessment of the rates of conformational inversion. In the room temperature ^{1}H NMR spectra, the **^{t}BuC5(H)$_5$** mono- and dianions all show single sharp signals for the aromatic protons around 7.12–6.97 ppm, and for the *tert*-butyl groups at 1.23–1.18 ppm. The simplicity of the ^{1}H NMR

patterns for the Rb or Cs mono- and dianions suggests a cone conformation (Figure 2.2). The ^{1}H NMR data is summarized in Table 2.1.

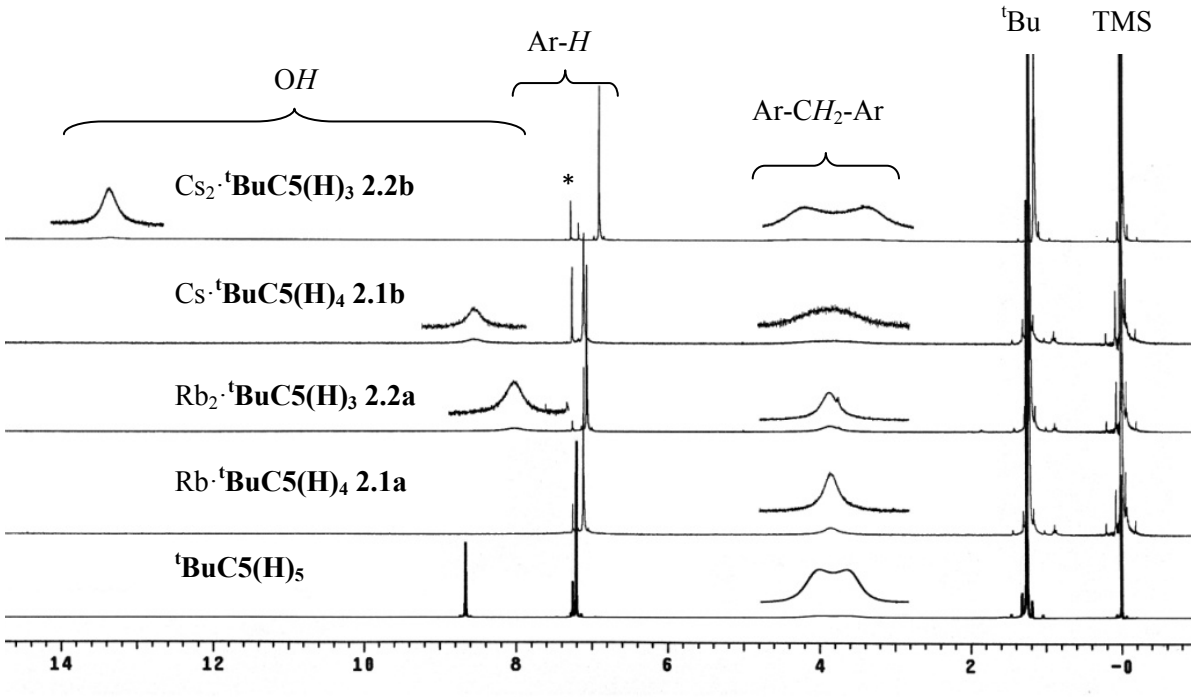

Figure 2.2 ^{1}H NMR spectra of ^{t}**BuC5(H)$_5$** and alkali metal salts of mono- and dianions at room temperature in $CDCl_3$.

The hydroxyl group in Rb·^{t}**BuC5(H)$_3$ 2.1a** is too broad to see at room temperature, while for Rb$_2$·^{t}**BuC5(H)$_3$ 2.2a** the OH peak is a broad signal localized at 8.03 ppm. The OH resonance for Cs·^{t}**BuC5(H)$_4$ 2.1b** is observed at 8.75 ppm and for Cs$_2$·^{t}**BuC5(H)$_3$ 2.2b** at 13.49 ppm. The downfield shift from 8.66 to 13.49 ppm for Cs$_2$·^{t}**BuC5(H)$_3$ 2.2b** could be attributed to the increased strength of H-bonding between the remaining OH and phenolate groups;[9] presumably the larger cation enforces proximity of the lower rim oxygens.

Table 2.1 ^{1}H NMR data of **^{t}BuC5(H)$_5$** mono- and dianions at room temperature in $CDCl_3$ (δ in ppm).

Compound	O*H*	Ar-*H*	Ar-CH_2-Ar	C(CH_3)
^{t}Bu^{t}C5(H)$_5$	8.66 (s)	7.21 (s)	3.94 (b), 3.69 (b)	1.26 (s)
Rb·**^{t}BuC5(H)$_4$ 2.1a**	Not seen	7.12 (s)	3.86 (b)	1.23 (s)
Cs·**^{t}BuC5(H)$_4$ 2.2a**	8.75 (b)	7.10 (s)	4.21 (b), 3.46 (b)	1.22 (s)
Rb_2·**^{t}BuC5(H)$_3$ 2.1b**	8.03 (b)	7.07 (s)	3.86 (b)	1.20 (s)
Cs_2·**^{t}BuC5(H)$_3$ 2.2b**	13.49 (b)	6.97 (s)	4.24 (b), 3.48 (b)	1.18 (s)

^{13}C NMR spectra of all the mono and dianionic salts show four peaks for the aromatic carbons, one peak for the methylene groups and two peaks for *tert*-butyl groups. In the ^{13}C NMR spectra the signals at about 34 ppm are assigned to the Ar-CH_2-Ar groups. The simplicity of the ^{1}H NMR, and the single methylene peak in the ^{13}C NMR spectra for the mono and dianionic salts, are typical of cone structures in the solution state, consistent with the solid state structures (*vide infra*).[30]

2.2.3 Conformational studies

^{t}BuC5(H)$_5$ resembles **^{t}BuC4(H)$_4$** in having four basic conformations (cone, partial cone, 1,2 -alternate, 1,3 -alternate). However, because of the wider dimension of its annulus, **^{t}BuC5(H)$_5$** is more prone to conformational interconversion.[30] Temperature-dependent ^{1}H NMR studies for the four salts were carried out, their coalescence temperatures were obtained, and the energies for conformational interconversion $\Delta G^{\ddagger}$ were calculated (Table 2.2).

Table 2.2 Coalescence temperatures at 300 MHz and free energies of activation for the conformational inversion of M·^{t}**BuC5(H)$_4$** and M_2·^{t}**BuC5(H)$_3$** (M = Rb, Cs) anions ($\Delta G^{\ddagger}$ = $4.58T_c(10.32 + \log T_c/k_c)/1000$).[114-117]

Compound	T_c K	Δν (±15) Hz	$\Delta G^{\ddagger}$ (± 0.4) kcal mol^{-1}
^{t}**BuC5(H)$_5$**[30]	271		13.2
Rb·^{t}**BuC5(H)$_4$ 2.1a**	280	255	12.8
Cs·^{t}**BuC5(H)$_4$ 2.2a**	301	182	14.1
Rb_2·^{t}**BuC5(H)$_3$ 2.1b**	278	297	12.7
Cs_2·^{t}**BuC5(H)$_3$ 2.2b**	300	339	13.6

Note: ^{1}H NMR experiments were performed in $CDCl_3$.

2.2.3.1 Inversion energies

The room-temperature ^{1}H NMR spectrum of ^{t}**BuC5(H)$_5$** exhibits two broad peaks for the methylene groups that bridge the arene units (Ar-CH_2-Ar groups), indicating that the two types of protons of the cone conformer are exchanging environments fairly slowly on the NMR time scale (see Figure 2.2). The ^{1}H NMR spectra of the Rb·^{t}**BuC5(H)$_4$ 2.1a** and Rb_2·^{t}**BuC5(H)$_3$ 2.2a** salts give a broad peak at 3.86 ppm, showing that inversion is more rapid than in the parent molecule. In Rb·^{t}**BuC5(H)$_4$ 2.1a** and Rb_2·^{t}**BuC5(H)$_3$ 2.2a** the coalescence temperatures are higher and the energies for conformational interconversion $\Delta G^{\ddagger}$ are slightly lower (12.8 (± 0.4) and 12.7 (± 0.4) kcal mol^{-1}, respectively) than that of parent ^{t}**BuC5(H)$_5$** (13.2 ± 0.4 kcal mol^{-1}) (Table 2.2). For Cs·^{t}**BuC5(H)$_4$ 2.1b** and Cs_2·^{t}**BuC5(H)$_3$ 2.2b** the ^{1}H NMR spectra exhibit two broad peaks in the methylene area around 4.24 and 3.46 ppm, indicating that the two types of

protons are exchanging environments slowly on the NMR time scale. The coalescence temperatures and the energies of conformational interconversion ($\Delta G^{\ddagger}$ = 14.1 (± 0.4) and 13.6 (± 0.4) kcal mol^{-1}, respectively) for the cesium salts are higher.

These results suggest that Cs salts have a more rigid structure than the parent **^{t}BuC5(H)$_5$** and Rb salts. All of the energy differences are rather small, though, and other factors can influence the ^{1}H NMR pattern of the salts. Water or residual traces of solvent lead to changes in the methylene area, probably due to their interactions either with the cation or phenol groups of the calixarene.

2.2.4 Crystal structures of the calixanions

The solid state structures are consistent with the ^{1}H NMR patterns, and confirm the cone-like conformation adopted by the **^{t}BuC5(H)$_5$**. The X-ray structures of M·**^{t}BuC5(H)$_4$** and M_2·**^{t}BuC5(H)$_3$** (M = Rb or Cs) are shown in Figures 2.3 and 2.4, respectively.

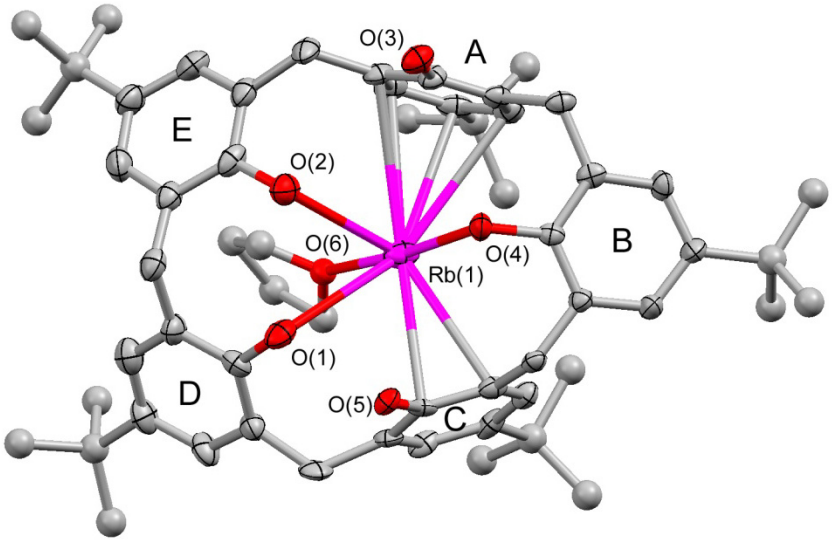

a)

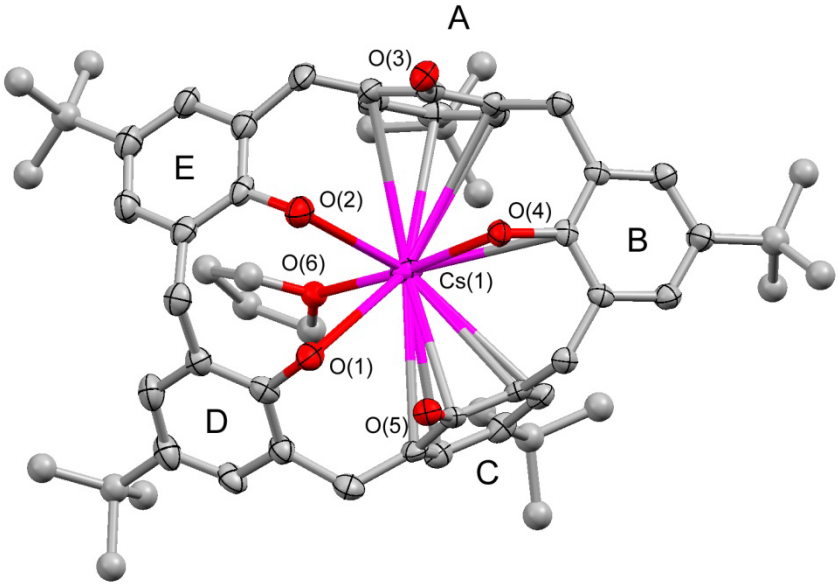

b)

Figure 2.3 Crystal structures of monoanions M·^{t}**BuC5(H)$_4$**·C_4H_8O (M = Rb or Cs). Thermal ellipsoids are shown at 50% probability; hydrogen atoms are omitted for clarity.

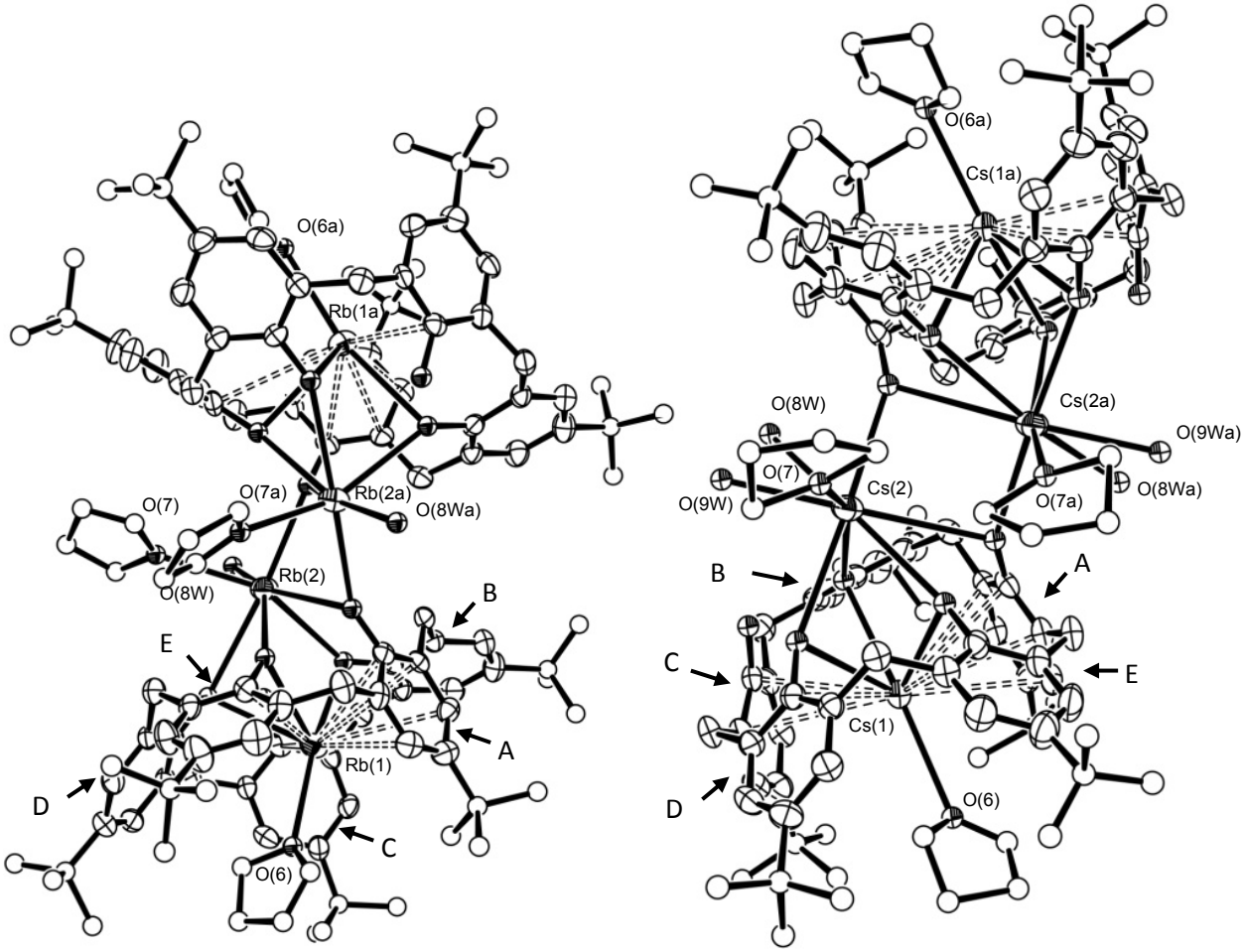

a) **b)**

Figure 2.4 Crystal structures of dianions. a) $Rb_2 \cdot$ **^{t}BuC5(H)$_3$**$\cdot 4C_4H_8O \cdot 2H_2O$ and b) $Cs_2 \cdot$ **^{t}BuC5(H)$_3$**$\cdot 4C_4H_8O \cdot 4H_2O$. Thermal ellipsoids are shown at 50% probability; hydrogen atoms are omitted for clarity.

The strong π-cation interaction between M^+ and the phenyl rings A and C is the major conformation-determining feature, comparable to our previous report.[107] Bond distances fall within normal ranges, as can be seen in Table 2.3.

Table 2.3 Selected M-O and M-C distances of alkali metal salts of calixanions

Compound	M-O (OAr)/Å	M-O (solvate)/Å	M-C/Å[a]	ref
Rb *salts*				
-Monoanions				
Rb·**HC4(H)$_3$**·C_4H_8O	2.943(3)	2.7770(17)	3.349(3)-3.579(3)	107
Rb·^{t}**BuC4(H)$_3$**·$4C_4H_8O$	3.124(2)	2.796(2)	Not observed	107
Rb·^{t}**BuC5(H)$_4$**·C_4H_8O	2.872(6)-3.242(7)	2.920(8)	3.263(9)-3.495(9)	b
-Dianions				
Rb_2·^{t}**BuC5(H)$_3$**·$2C_4H_8O$ ·H_2O	2.820(3)-3.294(3)	2.615(14)-2.975(5)	3.329(4)-3.503(5)	b, c
Rb_2·^{t}**BuC6(H)$_4$**·$2(CH_3)_2CO$	2.986(2)-2.999(3)	2.835(4)-3.095(4)	3.304(4)-3.731(4)	107
Cs *salts*				
-Monoanions				
Cs·**HC4(H)$_3$**·$(CH_3)_2CO$	3.100(3)	2.959(3)	3.599(3)-3.840(3)	107
Cs·**HC4(H)$_3$**·pyridine	3.169(12)-3.704(16)		3.53(1)-4.17(1)	118
Cs·**HC4(H)$_3$**·H_2O	3.065(5)-3.673(5)	2.97(3)	3.530(7)	118
Cs·^{t}**BuC4(H)$_3$**·CH_3CN	~4.0		3.545(3)-3.961(3)	119
Cs·^{t}**BuC5(H)$_4$**·C_4H_8O	3.015(4)-3.352(4)	3.063(5)	3.368(5)-3.604(6)	b
Cs·**HC6(H)$_4$**·$(CH_3)_2CO$	3.073(12)-3.535(15)	2.99(2)	3.416(15)-3.886(16)	107
-Dianions				
Cs_2·^{t}**BuC5(H)$_3$**·$2C_4H_8O$·$2H_2O$	3.081(3)-3.455(3)	2.873(11)-3.084(8)	3.454(4)-3.607(4)	b, c
Cs_2·**HC6(H)$_4$**·$2(CH_3)_2CO$	2.975(12)-3.000(8)	2.853(10)-3.093(9)	3.301(13)-3.728(13)	107

[a] Distances for cation-π arene interactions. [b] This work. [c] Asymmetric unit.

2.2.4.1 Metal-oxygen versus metal-carbon (π-cation) interactions

The **^{t}BuC5(H)$_5$** calixanions allow us to examine the relative affinities of each metal for interaction with the phenolic oxygens in the calixarene lower rim versus π-cation interactions with the arene rings within the cavity. A combination of these effects determines the following structure types:

a) *Discrete monomeric units*. M·**^{t}BuC5(H)$_4$**·C_4H_8O (M = Rb or Cs) (Figure 2.3) exhibits a monomeric structure with coordination of the alkali metal M (M = Rb, Cs) to three phenolic oxygens in the calixarene ring and one molecule of THF. The conformation of the calixarene ring can be described as flattened cone due to the M-C π interactions. The crystal structures are consistent with the ^{1}H NMR patterns observed in solution. In these complexes the presence of bulky *tert*-butyl groups blocks the formation of polymeric structures.[118]

b) *Discrete dimeric units*. The Rb_2·**^{t}BuC5(H)$_3$**·$4C_4H_8O$·$2H_2O$ (**2.2a**·$4C_4H_8O$·$2H_2O$) and Cs_2·**^{t}BuC5(H)$_3$**·$4C_4H_8O$·$4H_2O$ (**2.2b**·$4C_4H_8O$·$4H_2O$) dimers (Figure 2.4) contain a C_2 symmetry element located at the center of the metallocycle and between the THF molecules coordinated to the alkali metal (Figure 2.3). The structure shows π-cation interaction as observed in the monoanion, resulting in the flattened cone conformation of the **^{t}BuC5(H)$_5$**.

2.2.4.2 Core structures

In molecules of M·^{t}**BuC5(H)$_4$** (M = Rb or Cs) containing one mono-deprotonated ^{t}**BuC5(H)$_5$**, the metal atom M does not appear to closely interact with the oxygen atoms of the calixarene; the metal-solvate distances (2.920(8) – 3.063(5) Å) are similar to the M-O calixarene distances (2.872(6) – 3.352(4) Å). M·^{t}**BuC5(H)$_4$** holds the metal within the calixarene cup. Like other calixarene inclusion complexes,[27,81,119] the metal center is coordinated to four O donors; one THF, one phenolate, and two phenol groups from the calixarene. The aromatic rings **A** and **C** of the calixarene interact with the metal center with typical M-C bond distances (3.263(9) to 3.604(6) Å) comparable to 3.65 Å (avg) M-C distances observed in similar compounds.[107,119]

The dimeric molecules of M_2·^{t}**BuC5(H)$_3$** (M = Rb or Cs, Figure 2.4) comprise two doubly deprotonated ^{t}**BuC5** dianions fused at the lower rim by two bridging M cations [M(2) and M(2a)]. Each bridging Rb cation [Rb(2) and Rb(2a)] is coordinated to seven O donors. These are a coordinated water molecule (O(8W)), one THF molecule (O(7)), four phenol groups from one calixarene moiety (O(1), O(2), O(4) and O(5)), and finally one phenol of the second calixarene moiety (O(5a)). The Cs cations [Cs(2) and Cs(2a)] are similar but have an extra molecule of water resulting in a coordination number of 8 (Figure 2.5).

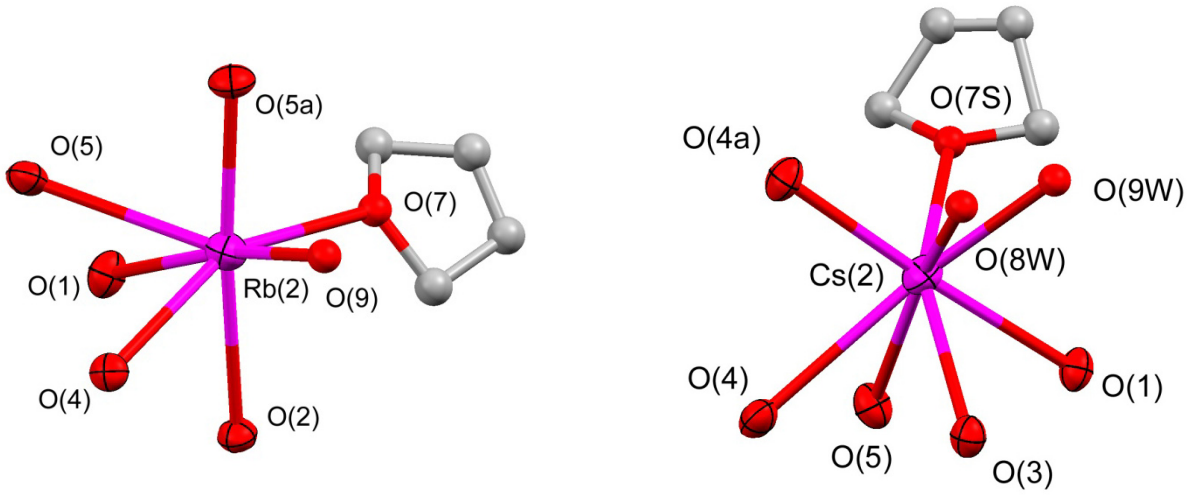

a) **b)**

Figure 2.5 Crystal structures of coordination sphere of **a)** [Rb(2)] and **b)** [Cs(2)] showing the coordination numbers 7 and 8 respectively. Thermal ellipsoids are shown at 50% probability.

The M(1) and M(1a) cations of each $M_2 \cdot$**^{t}BuC5(H)$_3$** molecule (M = Rb or Cs) are found inside the calixarene cavity due again to strong π interactions with the aromatic rings **A** and **C**. The M-C distances range from 3.329(4) to 3.607(4) Å. As in the monocalix[5]anions, the metal cation inside the cavity is coordinated to four O-donors, three of them coming from the calixarene and the remaining one from a THF molecule. The polyhapto coordination of the metal with two of the aromatic rings imposes the flattened conformations of the calixarenes.

2.3 Experimental section

2.3.1 General information

All manipulations were carried out in air. Benzene was dried by refluxing over Naº/benzophenone ketyl and stored over 4 Å molecular sieves. Methanol was passed through a column of activated 4 Å molecular sieves, kept over 4 Å molecular sieves for 15 days, and then the solvent was distilled and stored over 4 Å molecular sieves. The melting points of all compounds were taken in capillary tubes on a Mel-Temp apparatus (Laboratory Devices, Cambridge, MA) using a 500 ºC thermometer. A melting temperature proceeded by ">" sign indicates that the compound starts to decompose at that temperature. ^{1}H NMR and ^{13}C NMR spectra were recorded at room temperature on a Varian XL-300 spectrometer at 300 and 75 MHz respectively. Microanalyses were performed by Atlantic Microlab, Inc, Norcross, GA. IR and UV/Vis spectra were obtained with an infinity Gold™ FTIR spectrometer and Agilent 8453 spectrophotometer, respectively. All X-ray diffraction experiments were performed in a Bruker SMART 1000 CCD detector at 223 K using Mo Kα radiation. **^{t}BuC5(H)$_5$** was synthesized according to the procedure of Gutsche *et al.*[120] RbOH, CsOH, Rb_2CO_3 and Cs_2CO_3 were purchased from Aldrich and were used as received.

2.3.2 Preparation of compounds

2.3.2.1 General procedure for mono- and dianion synthesis

All the Rb and Cs mono- and dianion salts were prepared following a general procedure. The procedure can be used in a **^{t}BuC5(H)$_5$**:0.5M_2CO_3 molar ratio (M = Rb, Cs) to produce monocalixanion, or in a **^{t}BuC5(H)$_5$**:2MOH molar ratio (M = Rb, Cs) for dicalixanion.

To a solution of 0.250 mmol **^{t}BuC5(H)$_5$** (0.202 g) and 0.250 mmol of MOH (M = Rb, Cs) or M_2CO_3 (M = Rb, Cs) in 25 mL of dry benzene was added 5 mL of dry methanol. A Dean Stark condenser was connected to the flask and the mixture was stirred under a flow of nitrogen gas. After 12 hrs of reflux all volatiles were removed under reduced pressure. The crude product was obtained by diffusion of pentane into a concentrated THF solution to obtain colorless crystals suitable for X-ray analysis.

Rb·**^{t}BuC5(H)$_4$** (**2.1a**): White solid (0.198 g, 86% yield). Mp: >205 ^oC. ^1H NMR ($CDCl_3$) δ (ppm) = 1.23 (s, 45H, C(C*H*$_3$)$_3$), 3.86 (b, 10H, Ar-C*H*$_2$-Ar), 7.12 (s, 10H, Ar-*H*) (O*H* peaks were not observed at room temperature). $^{13}C\{^1H\}$ NMR ($CDCl_3$) δ (ppm) = 31.5 (C(*C*H$_3$)$_3$), 32.4 (*C*(CH$_3$)$_3$), 33.9 (Ar-*C*H$_2$-Ar), 125.6 (C_{Ar}-H), 128.2 (C_{Ar}-CH$_2$), 142.0 (C_{Ar}- C(CH$_3$)$_3$), 150.6 (C_{Ar}-OH). FTIR (KBr, cm^{-1}): 3426s (OH), 3309sh, 2960s, 2906m, 2868m, 1610w, 1483s, 1363m, 1294m, 1260m, 1204s, 1101m, 1020m, 878m, 803m. UV/vis (THF) λ_{max}/nm (ε/$dm^3mol^{-1}cm^{-1}$): 286 (4.218 x 10^4), 240 (1.271 x 10^3). $C_{55}H_{69}O_5Rb{\cdot}C_4H_8O$ (976.1): calcd C 73.21, H 8.03; found C 72.94, H 8.06.

Cs·**^{t}BuC5(H)$_4$** (**2.1b**): White solid (0.202 g, 86% yield). Mp: >225 ^oC. ^1H NMR ($CDCl_3$) δ (ppm) = 1.22 (s, 45H, C(C*H*$_3$)$_3$), 3.46 (b, 5H, Ar-C*H*$_2$-Ar), 4.21 (b, 5H, Ar-C*H*$_2$-Ar), 7.10 (s,

10H, Ar-*H*), 8.75 (b, 4H, O*H*). $^{13}C\{^1H\}$ NMR ($CDCl_3$) δ (ppm) = 31.6 ($C(CH_3)_3$), 32.3 ($C(CH_3)_3$), 33.8 ($ArCH_2Ar$), 125.6 (C_{Ar}-H), 128.2 (C_{Ar}-CH_2), 141.9 (C_{Ar}- $C(CH_3)_3$), 151.1 (C_{Ar}-OH). FTIR (KBr, cm^{-1}): 3409s (OH), 2960s, 2904m, 2866m, 1612w, 1483s, 1363m, 1292m, 1257m, 1205s, 1118w, 1018w, 879w, 818w. UV/vis (THF) λ_{max}/nm (ε/$dm^3mol^{-1}cm^{-1}$): 285 (1.966 x 10^4), 241 (1.190 x 10^4). $C_{55}H_{69}O_5Cs$ (942.4): calcd C 69.58, H 7.89; found C 69.23, H 7.90.

Rb_2·**^{t}BuC5(H)$_3$** (**2.2a**): White solid (0.203 g, 83% yield). Mp: >235 °C. ^1H NMR ($CDCl_3$) δ (ppm) = 1.20 (s, 45H, $C(CH_3)_3$), 3.86 (b, 10H, Ar-CH_2-Ar), 7.07 (s, 10H, Ar-*H*), 8.03 (b, 3H, O*H*). $^{13}C\{^1H\}$ ($CDCl_3$) δ (ppm) = 31.6 ($C(CH_3)_3$), 33.1 ($C(CH_3)_3$), 33.8 (Ar-CH_2-Ar), 125.5 (C_{Ar}-H), 128.8 (C_{Ar}-CH_2), 140.7 (C_{Ar}- $C(CH_3)_3$), 152.6 (C_{Ar}-OH). FTIR (KBr, cm^{-1}): 3434s (OH), 2960s, 2908m, 2870m, 1633m, 1481s, 1362m, 1295m, 1261w, 1203m, 1107m, 1022m, 883w, 803m. UV/vis (THF) λ_{max}/nm (ε/$dm^3mol^{-1}cm^{-1}$): 287 (2.167 x 10^4), 241 (1.817 x 10^4). $C_{55}H_{68}O_5Rb·C_4H_8O·H_2O$ (1069.5): calcd C 66.20, H 7.35; found C 65.85, H 7.32.

Cs_2·**^{t}BuC5(H)$_3$** (**2.2b**): White solid (0.215 g, 81% yield). Mp: >260 °C. ^1H NMR ($CDCl_3$) δ (ppm) = 1.18 (s, 45H, $C(CH_3)_3$), 3.48 (b, 5H, Ar-CH_2-Ar), 4.24 (b, 5H, Ar-CH_2-Ar), 6.97 (s, 10H, Ar-*H*), 13.49 (b, 3H, O*H*). $^{13}C\{^1H\}$ NMR ($CDCl_3$) δ (ppm) = 31.0 ($C(CH_3)_3$), 33.2 ($C(CH_3)_3$), 33.8 (Ar-CH_2-Ar), 125.4 (C_{Ar}-H), 128.9 (C_{Ar}-CH_2), 139.9 (C_{Ar}- $C(CH_3)_3$), 153.9 (C_{Ar}-OH). FTIR (KBr, cm^{-1}): 3437s (OH), 2960s, 2908m, 2870m, 1633m, 1480s, 1362m, 1296m, 1261w, 1206m, 1099m, 1022m, 879w, 801m. UV/vis (THF) λ_{max}/nm (ε/$dm^3mol^{-1}cm^{-1}$): 287 (1.766 x 10^4), 242 (1.885 x 10^4). $C_{55}H_{68}O_5Cs_2·C_4H_8O$ (1146.4): calcd C 61.76, H 6.68; found C 61.95, H 6.97.

2.3.3 Solubility and air-sensitivity of calixanions

All calixarene salts are very soluble in chloroform and dimethylsulfoxide but less soluble in benzene or toluene. The mono- and dianionic salts are air stable, so it is easy to purify them by recrystallization. Their crystals lose coordinating solvent molecules to become a powder. Partial decomposition of metal salts was noted within one month of air exposure, as judged by the increased amounts of parent calixarene (established by ^{1}H NMR).

2.3.4 VT-NMR studies

Temperature-dependent ^{1}H NMR spectra were recorded on a Varian XL-300 spectrometer at 300 MHz, with liquid nitrogen as coolant. The rate constants (k_c in s^{-1}) for conformational interconversion at the coalescence temperature were calculated from the equation $k_c = 2.22(\Delta\nu^2 + 6J^2_{AB})^{1/2}$.[114-117] The free energy barrier to conformational interconversion in kcal·mol^{-1} was calculated from the equation $\Delta G^{\ddagger} = 4.58T_c(10.32 + \log T_c/k_c)/1000$.[114-117] Assuming an accuracy of ±5 ^{o}C for the value of T_c, an accuracy of ±15 Hz for the value of $\Delta\nu$, and an accuracy of ±2 Hz for the value of J_{AB}, it is estimated that the values should be accurate to ±0.4 kcal·mol^{-1}. The value of $\Delta\nu$ was taken as the difference in Hz between the frequencies of methylene doublets undergoing coalescence (observed at a sufficiently low temperature that peaks are sharp).[114-117]

2.3.5 General X-ray crystal structure information

Data for **^{t}BuC5** monoanions and dianions were collected on a Bruker Smart 1000 CCD area detector under a 223 K nitrogen stream. The crystals used in the experiments were coated with Paratone-N oil. Crystallographic data are summarized in Table 2.4. All structures were

solved by direct methods and subsequent difference Fourier syntheses and refined by full-matrix least-squares methods against F^2.[121] The crystal structures of this chapter were solved in collaboration with Dr. Mauricio Quiroz-Guzmán, Dr. Daniel Mendoza-Espinosa and Professor Rheingold.

Table 2.4 Crystallographic data and summary of the data collection and structure refinement of compounds M·^{t}**BuC5(H)$_4$** (M = Rb **2.1a**, Cs **2.2a**) and M_2·^{t}**BuC5(H)$_3$** (M = Rb **2.1b**, Cs **2.2b**)

	2.1a·C_4H_8O	**2.1b**·C_4H_8O	**2.2a**·$4C_4H_8O$·$2H_2O$	**2.2b**·$4C_4H_8O$·$4H_2O$
Empirical Formula	$C_{59}H_{77}O_6Rb$	$C_{59}H_{77}O_6Cs$·C_4H_8O	$C_{126}H_{172}O_{16}Rb_4$	$C_{126}H_{176}O_{18}Cs_4$
FW	966.67	1015.12	2276.45	2496.20
cryst syst	Monoclinic	Monoclinic	Monoclinic	Monoclinic
space group	*P*21/c	*P*21/c	C2/c	C2/c
T, K	223(2)	223(2)	213(2)	223(2)
a, Å	16.657(2)	16.6321(10)	38.854(2)	39.5795(16)
b, Å	21.062(3)	21.3979(13)	16.1785(9)	16.0732(6)
c, Å	19.198(2)	19.1894(11)	21.4390(12)	21.5063(9)
α, deg	90	90	90	90
β, deg	108.944(2)	108.70(10)	91.0460(10)	91.1230(10)
γ, deg	90	90	90	90
V, Å^3	6370.8(13)	6468.6(7)	13474.2(13)	13679.0(9)
Z, Z´	4	4	4	4
$d_{calcd,}$ g·cm^{-3}	1.008	1.042	1.122	1.212
μ, mm^{-1}	0.818	0.612	1.498	1.113
Refl collected	43091	74471	22368	50002
T_{min}/T_{max}	0.857	0.89	0.765	0.853
N measd [R_{int}]	11209 [0.1749]	15551 [0.0779]	13404 [0.0559]	16071 [0.0634]
R (*I*> *2*sigma*(I))*	0.1032	0.0846	0.0595	0.0521
R_w (*I*> *2*sigma*(I))*	0.3101	0.2481	0.1439	0.1568
GOF	0.959	1.094	0.927	0.804

2.4 Conclusions

We have reported the high-yield synthesis and complete characterization for a series of *p-tert*-butylcalix[5]arene mono- and dianions. The synthesis consists of the simple addition of base to the parent calixarene and reflux under a dry flow of nitrogen. NMR and X-ray structural studies show that the complexes with rubidium and cesium are in their flattened cone conformation due to their M-C π-arene interactions.

We have illustrated the structural types of rubidium and cesium metal salts of *p-tert*-butylcalix[5]arene in the solid state. These include monomeric and dimeric units. Bulky *tert*-butyl groups in the upper rim of the **^{t}BuC5(H)$_5$** appear to block polymer formation in the solid state. Alkali metal atoms were found to bind the calixarene ring in the *endo* and *exo* positions. Alkali metal cation-π interactions can be observed for rubidium and cesium cations, and these interactions become progressively more important as the size of the alkali metal increases.

CHAPTER 3

CALIX[5]ARENE TITANIUM(IV) COMPLEXES

3.1 Introduction

Calixarenes have found numerous applications in many fields, including catalysis[17] and complexation of cations for sensing and nuclear waste remediation.[122] Recently, interest has focused on the synthesis of metallocalixarenes due to their potential for modeling heterogeneous oxygen-rich surfaces.[16,37]

Most of the calixarene coordination chemistry has focused on complexes containing d (M-calixarene) and f-block (Ln-calixarene) metals (M = Y, Ti, Zr, V, Nb, Ta, Cr, Mo, W, Fe, Co, and Ln = La, Pr, Nd, Sm, Yb),[18-20,23,89,123] compared with the number of main group-containing calixarene complexes (E-calixarene; E = B, Al, Ga, Si, Sn, Ge, P, As, Sb, Bi, Zn).[50,54,58,60-61,69,74,83,85,93,109,124-141] The synthesis of these calixarene complexes has been done using metal amides, metal alkoxides or metal chlorides with either parent or ether-substituted calix[n]arenes (n = 4, 6, 8) as precursors.[31,33,35,41,43-45,50,54,60-62,69,74,82,123-125,127-131,133-136,139,142-148]

Our group, on the other hand, is taking advantage of calixarene salts. We have described the synthesis and characterization of a large series of mono-, di-, tri-, and pentaanionic alkali metal calixarene salts,[107-108,113] and used them as starting materials for the successful synthesis of the first bismuth(III) and antimony(III) calix[4]arene complexes.[109] Recently, our group published general procedures for the preparation of bismuth **RC4(H)$_4$** (R = H, ^{t}Bu, allyl) complexes[58] and transition metallocalixarenes[85,110] that were inaccessible using the traditional parent calixarene as precursor.

We are currently interested in forming partially metallated calixarenes. We will determine the three-dimensional structure adopted by the calixarene ligand when it is coordinated to the transition metal, and later use the metallocalixarene as starting material for further reactions.

The ability to selectively prepare complexes containing just one metal center, with free OH groups available for further reactivity, is critical for the rational design of bimetallic species.

Only two examples of titanium(IV)-containing calix[5]arene complexes have been reported in literature. Both Lamb *et al.*[81] and Lattman *et al.*[83] started from the parent **^{t}BuC5(H)$_5$**, but Lattman first prepared a phosphorus-containing *p-tert*-butylcalix[5]arene (**^{t}BuC5(PNMe$_2$)(H)$_3$**), then added titanium (Scheme 3.1).

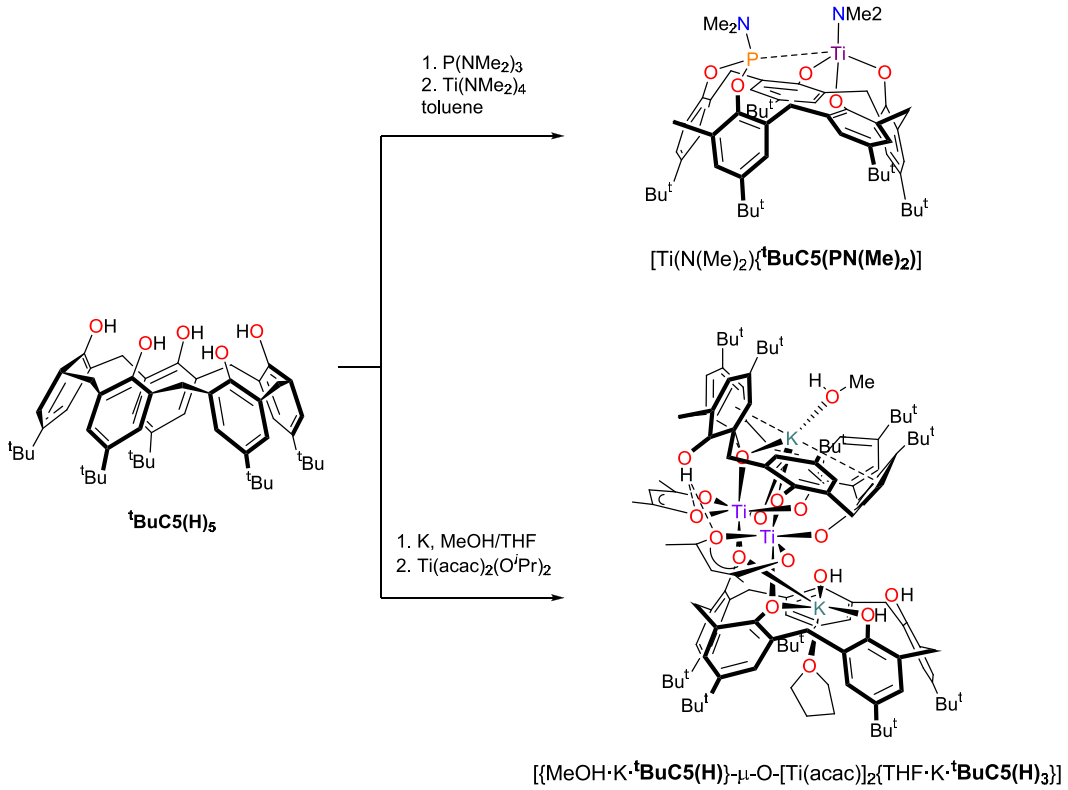

Scheme 3.1 ^{t}BuC5(PNMe$_2$)(H)$_3$ and **^{t}BuC5(H)$_5$** titanium(IV) complexes found in literature.[81,83]

In this chapter, we describe the synthesis and characterization of novel titanium(IV) calix[5]arene complexes. Our synthetic approach uses isolated calixanions and the corresponding chlorotitanium derivatives.

3.2 Results and discussion

*3.2.1 Reactivity of the calix[5]arene dianion, compounds **3.1** and **3.2***

In the X-ray structures of the calix[5]arene dianions $M_2 \cdot$**^{t}BuC5(H)$_3$** (M = K, Rb, Cs) we observed an interesting feature. In $K_2 \cdot$**^{t}BuC5(H)$_3$** we observed that the two potassium ions are localized in the lower rim of the calix[5]arene while in $M_2 \cdot$**^{t}BuC5(H)$_3$** (M = Rb, Cs), one M^+ (M = Rb, Cs) ion is observed in the cavity of the calixarene (*endo*) and the second alkali ion lies on the lower rim of the calix[5]arene, *exo*- to the cavity (Figure 3.1).[113]

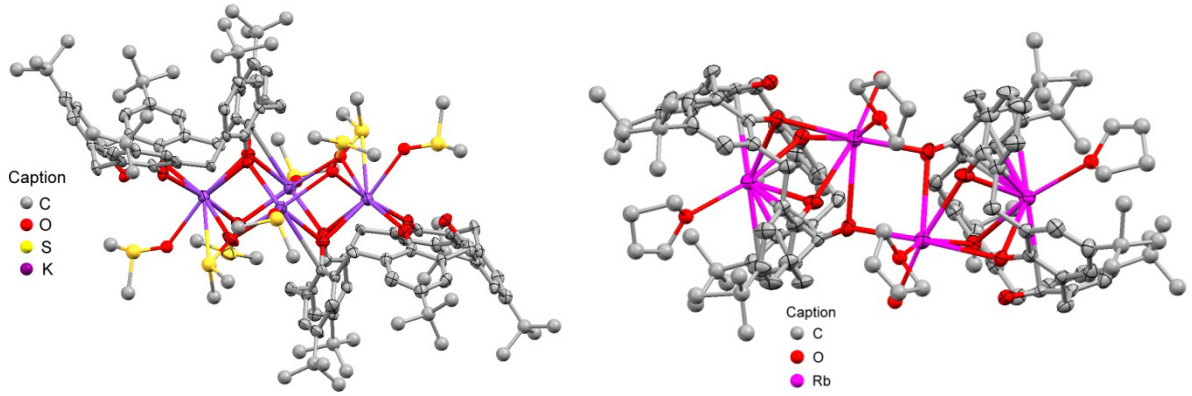

a) **b)**

Figure 3.1 X-ray structures of a) dimeric $K_2 \cdot$**^{t}BuC5(H)$_3$**$\cdot$4DMSO and b) dimeric $Rb_2 \cdot$**^{t}BuC5(H)$_3$**$\cdot$2THF$\cdot H_2O$. Thermal ellipsoids are shown at 50% probability; hydrogen atoms and non-coordinated DMSO molecules are omitted for clarity.[113]

From this solid state observation, we became interested in the reactivity of the calix[5]arene dianion with the larger Rb^+ and Cs^+ ions. We hypothesize two possible scenarios for the reactivity of the cation found inside of the calix[5]arene cavity. First, the cation found inside the cavity might be displaced in a salt elimination reaction, i.e., be easily removed from the cavity using chloride-containing metal derivatives in order to produce a bimetallic calix[5]arene complex. Alternatively, the cation availability may be reduced by the π-interactions between the ion and the aryl part of the calix[5]arene, resulting in low reactivity for that ion. The ion located in the lower rim may therefore have greater reactivity.

In order to distinguish between these two possibilities, we initially reacted Cp_2TiCl_2 with $Cs_2{\cdot}^t$**BuC5(H)$_3$** in a 1:1 ratio in THF at room temperature (reaction **A**) for 12 hrs. From reaction **A**, we suggested the formation of one of compounds **3a** to **3d** (according to the pathways **1-4**, Scheme 3.2). We chose the Cp_2TiCl_2 reactant as starting material in order to avoid dimeric titanium bridged complexes,[31,68] which would not be useful for our purposes.

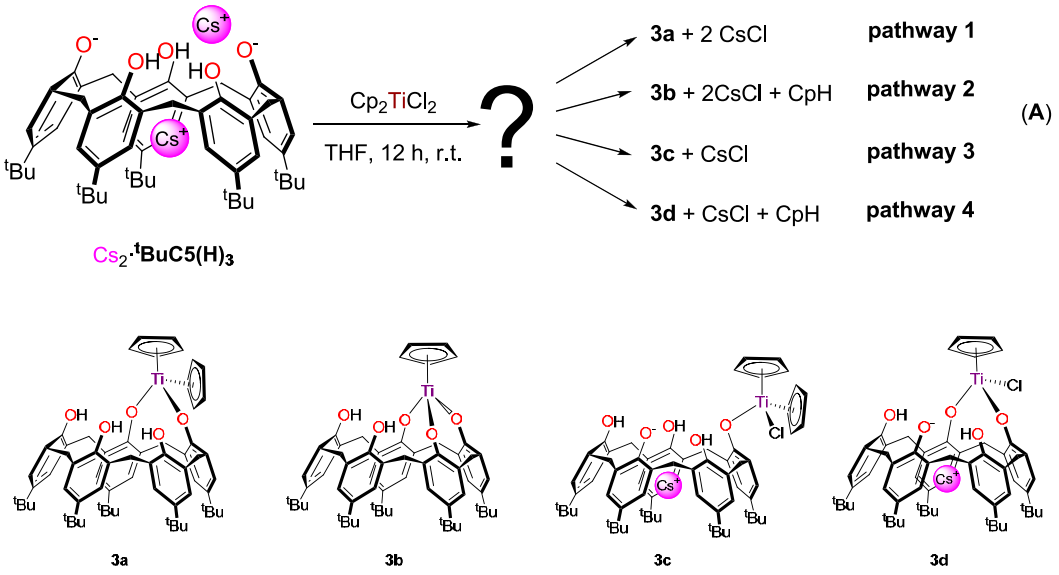

Scheme 3.2 Proposed products **3a** to **3d** for reaction **A** according to suggested pathways 1-4.

In pathways **1** and **2** we suggest the displacement of both Cs^+ ions. Displacement of the two chlorines would give the proposed structure **3a**, while the formation of **3b** might occur from the cleavage and reaction of one of the cyclopentadienyl (Cp) ligands with one available proton of the lower rim of the calix[5]arene. Cleavage of the Cp and binding to the lower rim has been previously observed in the formation of [CpTi{^{t}**BuC6(H)$_3$**}] and [(CpTi)$_2${^{t}**BuC6**}] complexes.[90]

In pathways **3** and **4** we propose that Cs^+ ion localized in the lower rim is the only reactive one. Chlorine displacement would produce compound **3c**, and the formation of **3d** would occur upon cleavage and further reactivity of one of the Cp ligands.

Reaction **A** was performed and the crude product was analyzed. After 12 hrs of reaction time, the solvent was removed by high vacuum and an orange-red solid was obtained. The ^{1}H NMR spectrum of the product in C_6D_6 showed a complex mixture of compounds in which a major compound was the parent ^{t}**BuC5(H)$_5$**.

In order to isolate a single titanium-containing calix[5]arene compound from the reaction mixture, we induced its separation by crystallization. After one week, a small amount of orange and colorless crystals were obtained. The crystals were carefully separated with the aid of a microscope in order to get one small orange crystal suitable for single crystal X-ray diffraction analysis. The X-ray structure for that crystal is labeled as **3.1**, and shown in Figure 3.2.

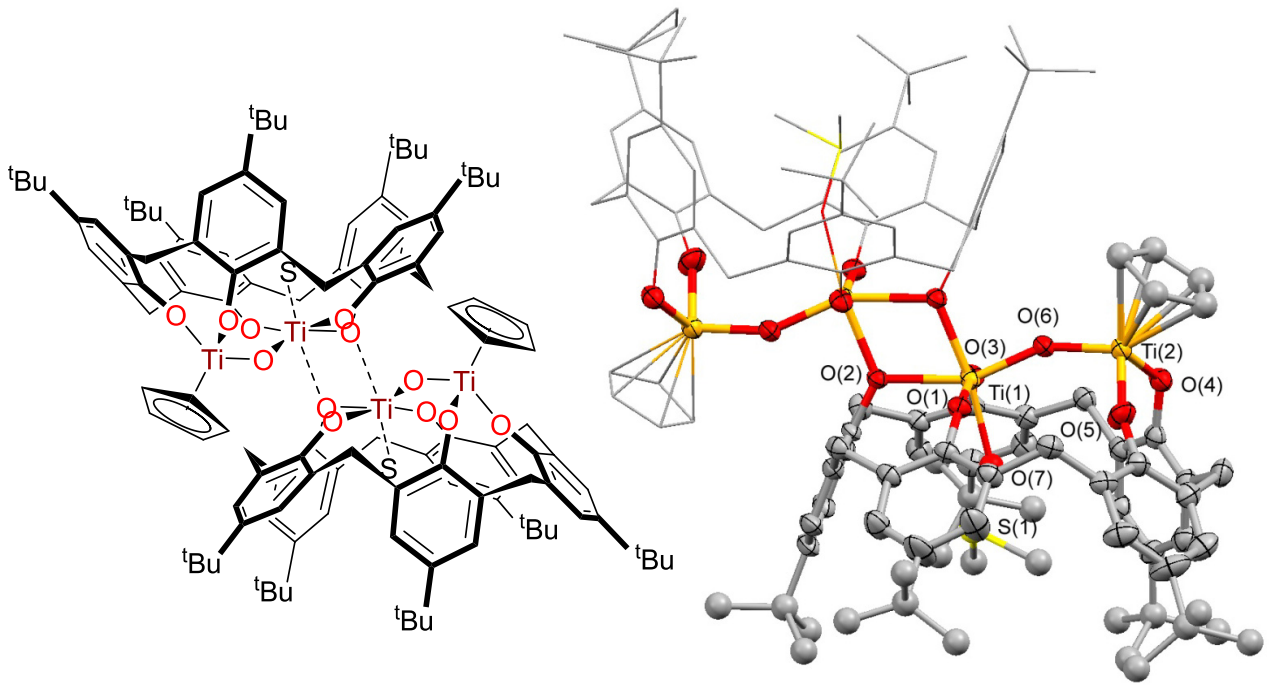

Figure 3.2 Line drawing (left) and X-ray structure (right) of the dimeric structure of **3.1**. Thermal ellipsoids are shown at 50% probability. Hydrogen atoms and some DMSO crystallization molecules have been omitted for clarity. The second part of the molecule is drawn in wireframe style for clarity.

The structure of compound **3.1** does not match any of those proposed (**3a-d**) for reaction **A**. Nevertheless, the structure of compound **3.1** contains two titanium atoms per calix[5]arene ring. One of the titanium atoms still contains a Cp ligand while the second is coordinated entirely to oxygen atoms. The two titanium atoms are bridged by an oxygen atom O(6). The presence of the titanium atom and a Cp ligand suggests that one of the proposed pathways proposed may be followed in order to produce a precursor to compound **3.1**. The structure of compound **3.1** also provides an answer about the reactivity of the calix[5]arene dianion; both Cs^+ ions were displaced from the calix[5]arene ligand.

Our next approach was using the same 1:1 ratio of reactants (Cp_2TiCl_2:Cs_2·**^{t}BuC5(H)$_3$**), but we changed the reaction temperature from room temperature to 85 ^oC. Unfortunately, the ^1H NMR spectrum displayed a different complex pattern, with **^{t}BuC5(H)$_5$** as the major observable compound. Crystallization resulted in a small amount of red crystals, **3.2**. The crystal structure of compound **3.2** (Figure 3.3) matched neither that of compound **3.1** nor any of the proposed structures **3a-d**.

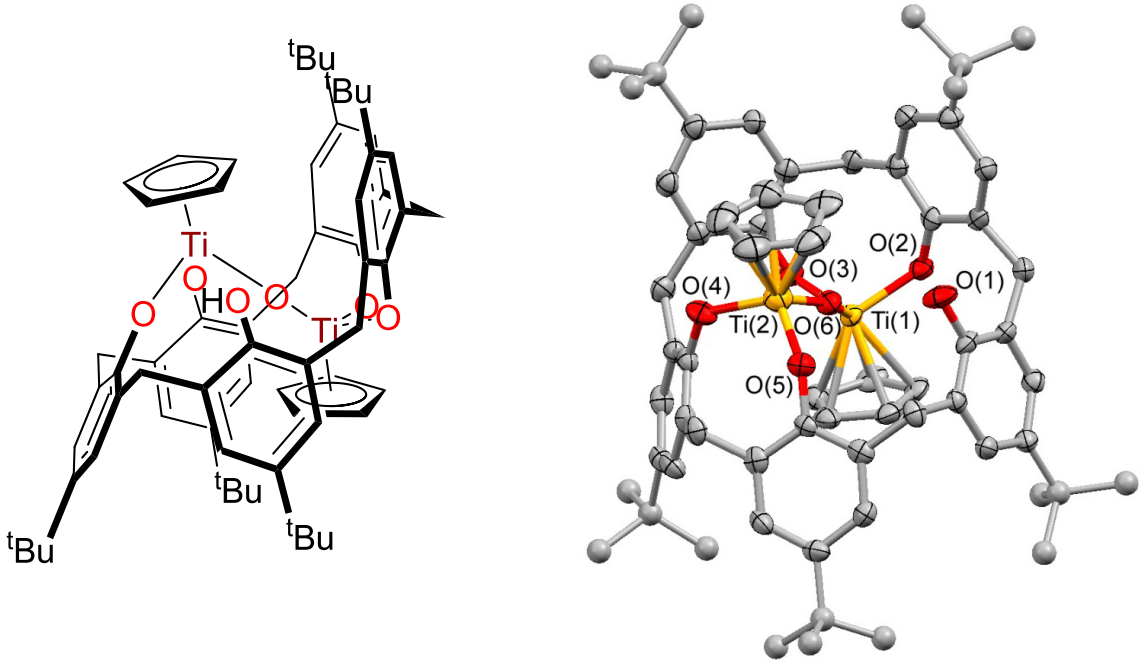

Figure 3.3 Line drawing (left) and X-ray structure (right) of compound **3.2**. Thermal ellipsoids are shown at 50% probability, and crystallization molecules and hydrogen atoms are not shown for clarity.

From the X-ray structures of compounds **3.1** and **3.2**, an interesting feature is evident: in both cases two titanium atoms (Ti(1) and Ti(2)) are connected by a μ-oxo bridge O(6). It is likely that the oxo bridge comes from adventitious water.[81,149] In our reaction conditions, it was not possible to reproduce these results, probably because the water content in the $Cs_2 \cdot$**^{t}BuC5(H)$_3$** salt varies from one batch to another. Compounds **3.1** and **3.2** may be the products of hydrolysis of the actual products obtained from reaction **A**. In order to avoid interference from adventitious water, we decided to dry the $Cs_2 \cdot$**^{t}BuC5(H)$_3$** salt by placing it in the oven at 100 ^oC for at least 12 hrs.

*3.2.2 Synthesis of compounds **3.3** and **3.4***

Dry $Cs_2 \cdot$**^{t}BuC5(H)$_3$** starting material produced good results. When dry $Cs_2 \cdot$**^{t}BuC5(H)$_3$** salt was reacted in a 1:1.15 molar ratio with Cp_2TiCl_2, we obtained a new bimetallic complex [$(TiCpCl)_2${**^{t}BuC5(H)$_3$**}] **3.3** in 77% yield (Scheme 3.3). The structure of compound **3.3** is proposed on the basis of its spectroscopic and analytical data and the presence of the Cl was supported by using Energy Dispersive X-ray analysis (EDX).

Attempts to increase the yield of complex **3.3** by increasing the equivalents of Cp_2TiCl_2 were unsuccessful, yielding a complex mixture of compounds. Similar results were obtained using the sodium, potassium or rubidium dianionic salts.[113]

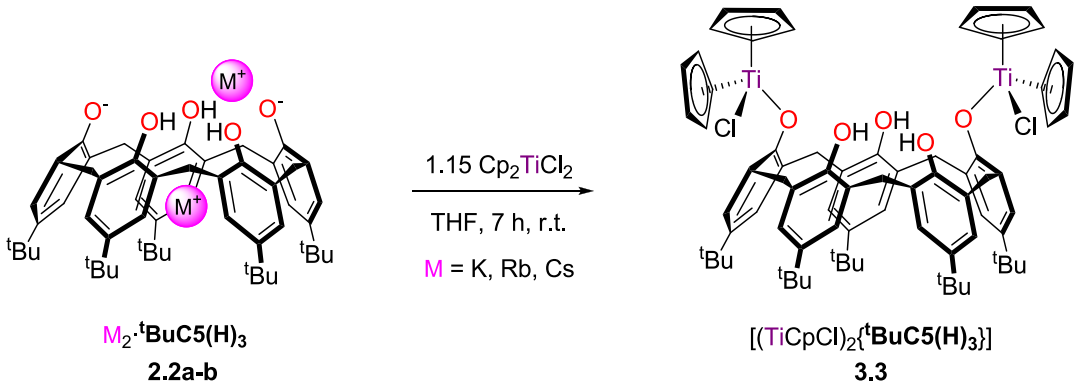

Scheme 3.3 Synthesis of compound [(TiCpCl)$_2${^{t}**BuC5(H)$_3$**}] **3.3**.

In a second approach, we hypothesized that $CpTiCl_3$ might give the monometallic species **3e** by removal of two Cs^+ ions by chlorides, or **3d** by removal of a H^+ with the third chloride, as depicted in Scheme 3.4.

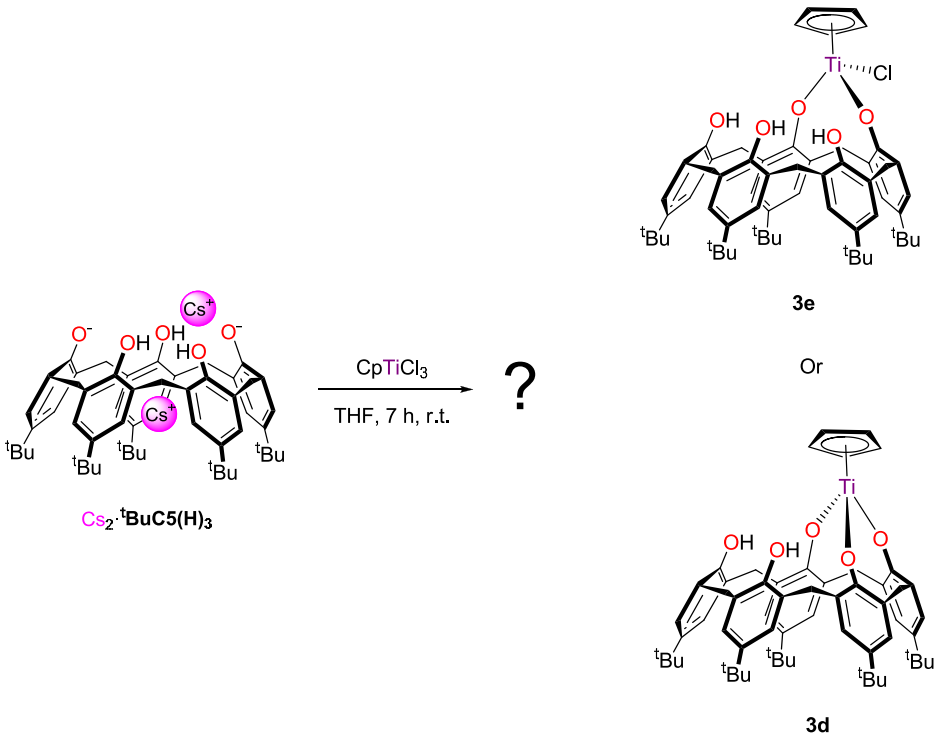

Scheme 3.4 Proposed structure of compounds **3e** or **3d** by using $CpTiCl_3$ with dry $Cs_2\cdot$**^{t}BuC5(H)$_3$**.

Again the proposed result was not obtained. A mixture of products was observed by ^{1}H NMR spectroscopy. One of them (**3.4**) was isolated by successive hexane and pentane washing cycles.

The molecular structure of compound **3.4** is proposed (Figure 3.4) on the basis of its spectroscopic characterization, since attempts to obtain crystals suitable for X-ray analysis were unsuccessful. A similar result was obtained when we used the sodium, potassium or rubidium dianionic salts.

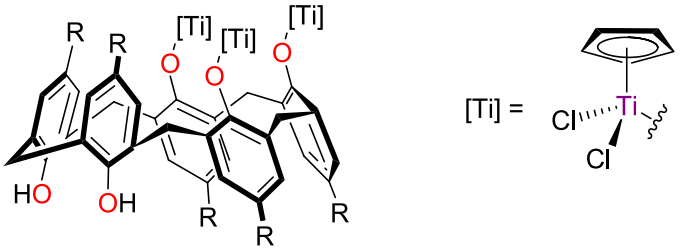

Figure 3.4 Proposed structure of compound **3.4**.

3.3 Crystal and molecular structures

Compounds **3.1**·6DMSO and **3.2**·$2C_6H_6$ are shown in Figures 3.2 and 3.3, respectively, and selected bond distances and angles are listed in Table 3.1. Complexes **3.1**·6DMSO and **3.2**·$2C_6H_6$ both have a Ti(1)-(μ-O)-Ti(2) core with an oxygen bridging two titanium atoms, similar to [{MeOH·K·^{t}**BuC5(H)**}-μ-O-[Ti(acac)]$_2${THF·K·^{t}**BuC5(H)$_3$**}] and [(-TiCp-μ-O-TiCp-μ-O-)$_2${^{t}**BuC4**}] reported by Lamb et al. (Figure 3.5).[81,149] The Ti(1)-(μ-O)-Ti(2) angles of 152.85(12)^{o} in **3.1** and 157.7(3)^{o} in **3.2** are close to the 151.5(2)^{o} found in a known titanium compound [{MeOH·K·^{t}**BuC5(H)**}-μ-O-[Ti(acac)]$_2${THF·K·^{t}**BuC5(H)$_3$**}],[81] but are larger than that found in [(-TiCp-μ-O-TiCp-μ-O-)$_2${^{t}**BuC4**}] (139.55(9)^{o}).[149]

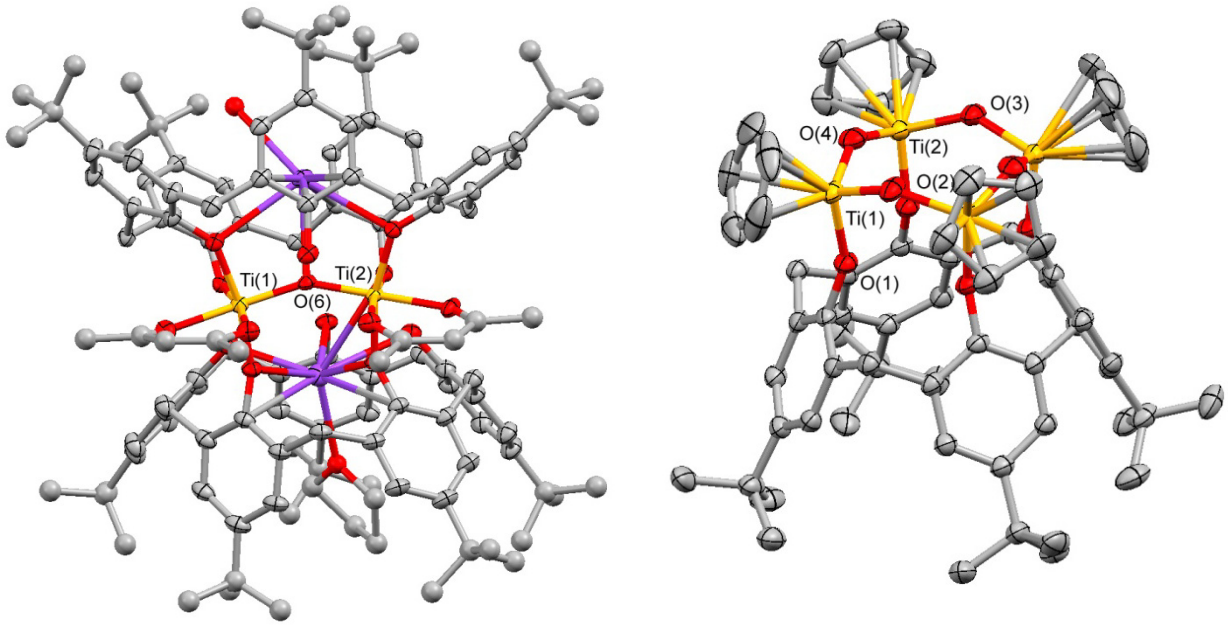

a) **b)**

Figure 3.5 X-ray structures of a) [{MeOH·K·^{t}**BuC5(H)**}-μ-O-[Ti(acac)]$_2${THF·K·^{t}**BuC5(H)$_3$**}] and b) [(-TiCp-μ-O-TiCp-μ-O-)$_2${^{t}**BuC4**}] reported by Lamb et al. [81,149]

In complexes **3.1**·6DMSO and **3.2**·2C_6H_6, the Ti-(μ-O) bond lengths range from 1.791(5) to 1.845(5) Å. In **3.1**·6DMSO, solvent coordination does not affect the Ti-(μ-O) distances. All of the Ti-O octahedral distances (1.966 Å avg.) and the Ti-O tetrahedral distances (1.838 Å avg.) are close to those reported in literature; octahedral average = 1.947 Å[52-53,81,91-92] and tetrahedral average = 1.854 Å.[90]

Table 3.1 Selected bond distances (Å) and angles (°) for complexes **3.1**·6DMSO and **3.2**·$2C_6H_6$.

	3.1·6DMSO	**3.2**·$2C_6H_6$	
Ti(1)-O(6)	1.8396(19)	1.791(5)	
Ti(1)-O(3)	1.8790(19)	1.855(5)	
Ti(1)-O(1)	1.9021(19)	-	
Ti(1)-O(2a)	2.0158(18)	-	
Ti(1)-O(7)	2.048(2)	-	
Ti(1)-O(2)	2.1121(18)	1.882(5)	
Ti(2)-O(4)	1.874(2)	1.898(5)	
Ti(2)-O(5)	1.784(2)	1.821(5)	
Ti(2)-O(6)	1.7916(19)	1.845(5)	
Ti(1)-O(6)-Ti(2)	152.85(12)	Ti(1)-O(6)-Ti(2)	157.7(3)
O(6)-Ti(1)-O(3)	93.45(8)	O(6)-Ti(1)-O(3)	99.8(2)
O(6)-Ti(1)-O(1)	98.63(9)	O(6)-Ti(1)-O(2)	101.3(2)
O(3)-Ti(1)-O(1)	162.28(8)	O(3)-Ti(1)-O(2)	107.7(2)
O(6)-Ti(1)-O(2a)	87.23(8)	O(5)-Ti(2)-O(6)	99.9(2)
O(3)-Ti(1)-O(2a)	97.28(8)	O(5)-Ti(2)-O(4)	108.9(2)
O(1)-Ti(1)-O(2a)	96.20(8)	O(6)-Ti(2)-O(4)	102.5(2)
O(6)-Ti(1)-O(7)	101.42(9)		
O(3)-Ti(1)-O(7)	80.46(9)		
O(1)-Ti(1)-O(7)	84.47(9)		
O(2a)-Ti(1)-O(7)	171.15(9)		
O(6)-Ti(1)-O(2)	155.33(8)		
O(3)-Ti(1)-O(2)	85.38(8)		
O(1)-Ti(1)-O(2)	88.92(8)		
O(2a)-Ti(1)-O(2)	68.55(8)		
O(7)-Ti(1)-O(2)	102.67(8)		
O(5)-Ti(2)-O(6)	99.16(10)		
O(5)-Ti(2)-O(4)	97.25(10)		
O(6)-Ti(2)-O(4)	107.79(9)		

In compound **3.1**·6DMSO there are two oxo-bridged titaniums, one octahedral (Ti(1)) and one tetrahedrally coordinated (Ti(2)), the Ti(1)-O(6)-Ti(2) angle being 152.85(12)^{o} (Figure 3.6a). The Ti(1) atom serves as a bridge between two calix[5]arenes to form the dimeric species. Three oxygen atoms O(1-3) from the calix[5]arene bind in a meridional fashion to the Ti(1), and the octahedral coordination is completed by an oxo bridge O(6), a DMSO molecule, and O(2a) from the second molecule of calix[5]arene. The Ti(1) center displays a distorted octahedral geometry (Figure 3.6b).

The remaining two oxygen atoms O(4-5) bind to the second Ti(2) atom. The tetrahedral geometry of the Ti(2) is completed by the Cp ligand and the oxo bridge O(6) (Figure 3.6b). The coordination of the two titanium atoms results in a cone conformation of the calix[5]arene with a resulting C_s symmetry, consistent with the NMR data (Section 3.3).

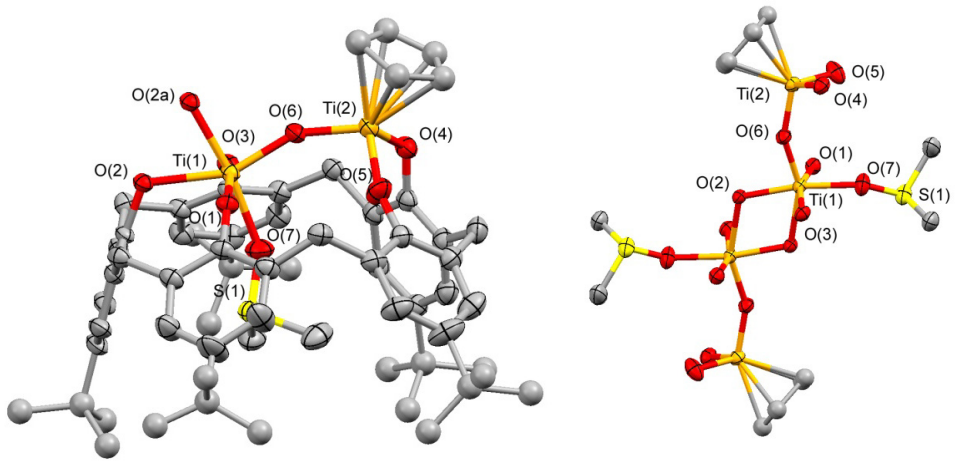

a) **b)**

Figure 3.6 X-ray structure of compound **3.1** a) asymmetric unit, b) titanium oxygen core. Thermal ellipsoids are shown at 50% probability. Crystallization molecules and hydrogen atoms are omitted for clarity.

Figure 3.7 illustrates the eight-membered metallocycles in compound **3.1**·6DMSO. Two fused cycles can be observed around the Ti(1) atom, while around Ti(2) there is just one. The conformation may be described as being close to a boat-chair conformation.[1]

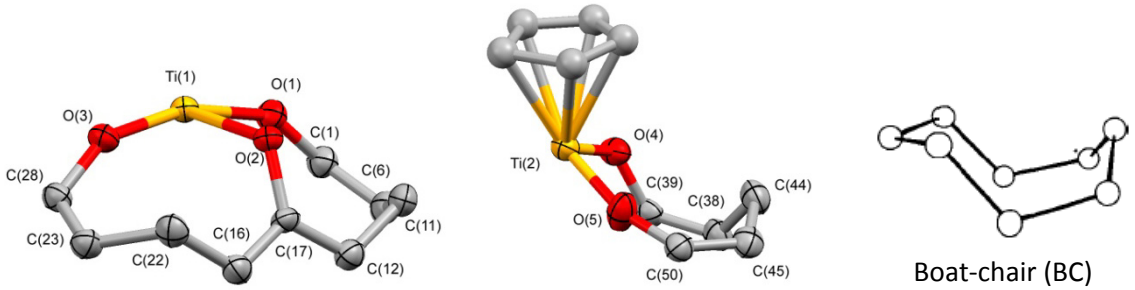

a) **b)** **c)**

Figure 3.7 Segments of the crystal structure of complex **3.1**·6DMSO. Conformations observed a) around Ti(1), a boat chair conformation in two fused metallocycles, b) around Ti(2), a boat chair conformation. c) An ideal boat chair conformation.[1]

Complex **3.2**·$2C_6H_6$ crystallizes in the space group *P*-1, with two molecules of benzene. There are two oxo-bridged tetrahedrally coordinated titanium atoms Ti(1) and Ti(2), and the Ti(1)-O(6)-Ti(2) angle is 157.7(3)^o (Figure 3.8a). Each titanium atom is a member of an eight-membered metallocycle (Figure 3.8b). The coordination of the two titanium atoms results in a 1,2-alternate conformation of the calix[5]arene with a resulting C_s symmetry, consistent with the ^{1}H NMR spectrum (Section 3.3).

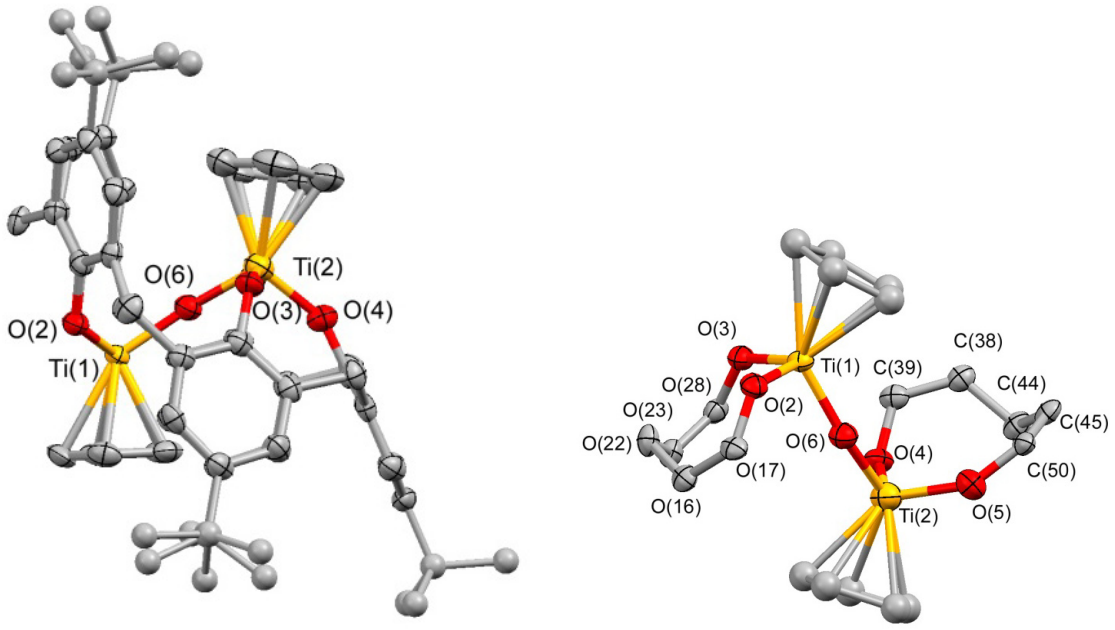

a) **b)**

Figure 3.8 X-ray structure of compound **3.2**·$2C_6H_6$. a) Side view showing the μ-oxo bridge and b) boat chair conformation around Ti(1) and Ti(2). Thermal ellipsoids are shown at 50% probability; hydrogen atoms and non-coordinating molecules are omitted for clarity.

3.4 NMR spectroscopy

*3.4.1 Spectral data of compounds **3.1** and **3.2***

^{1}H NMR spectroscopy is an important tool for the conformational analysis of calix[n]arenes (n = 4, 5).[30] These two ligands show four limiting up/down conformations (Figure 3.9) that can be designated as cone, partial cone, 1,2-alternate and 1,3-alternate, though in calix[5]arene the conformational assignments are less accurate due to the larger cavity size and flexibility as compared to calix[4]arene.

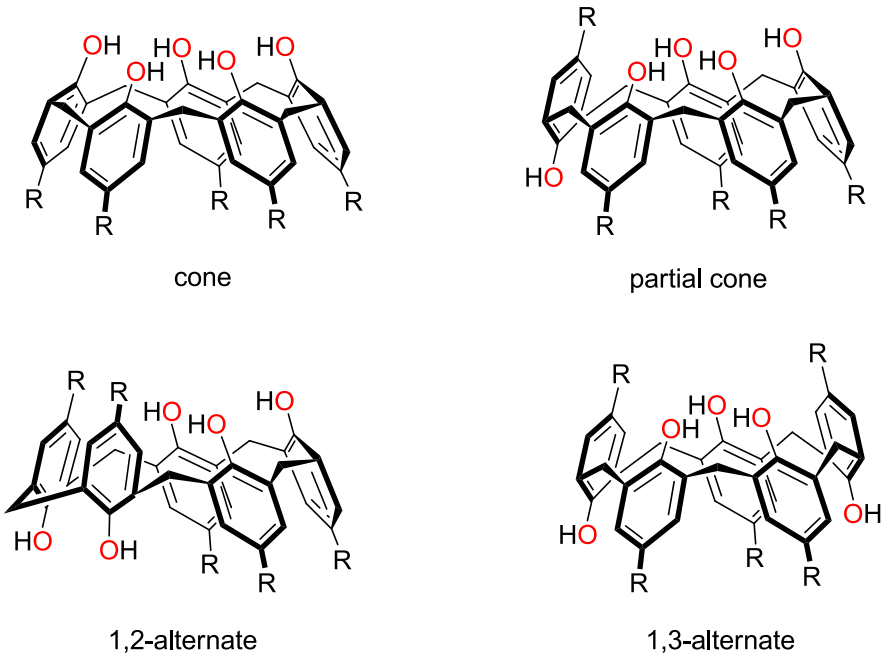

Figure 3.9 Idealized conformations of calix[5]arenes.

The two bimetallic complexes **3.1**·6DMSO and **3.2**·$2C_6H_6$ display very different behavior in solution. The ^{1}H NMR spectrum of complex **3.1** shows three pairs of methylene doublets (2:2:1 ratio), five signals for the Ar-*H* protons (1:1:1:1:1 ratio), and three signals for the ^{t}Bu groups (1:2:2 ratio) (Figure 3.10). In contrast, the ^{1}H NMR spectrum for complex **3.2** shows two pairs of doublets and a singlet for the methylene groups, integrating for two protons each, and three singlets for the ^{t}Bu groups (Figure 3.10). Both spectra are clear indications of C_s symmetry.[30] Complex **3.1** does not show an OH signal because all oxygen atoms are saturated (coordinated to the titanium centers), but **3.2** shows a sharp singlet for the OH group at 5.75 ppm about 3.16 ppm upfield from the OH for **^{t}BuC5(H)$_5$** (8.91 ppm). Similar upfield chemical shifts for the OH groups were found in the compounds **^{t}BuC5(H)(SiMe$_2$)$_2$** (5.66 ppm) and **^{t}BuC5(H)(Si(MePh))$_2$** (5.35 ppm) reported by Lattman et al.[130]

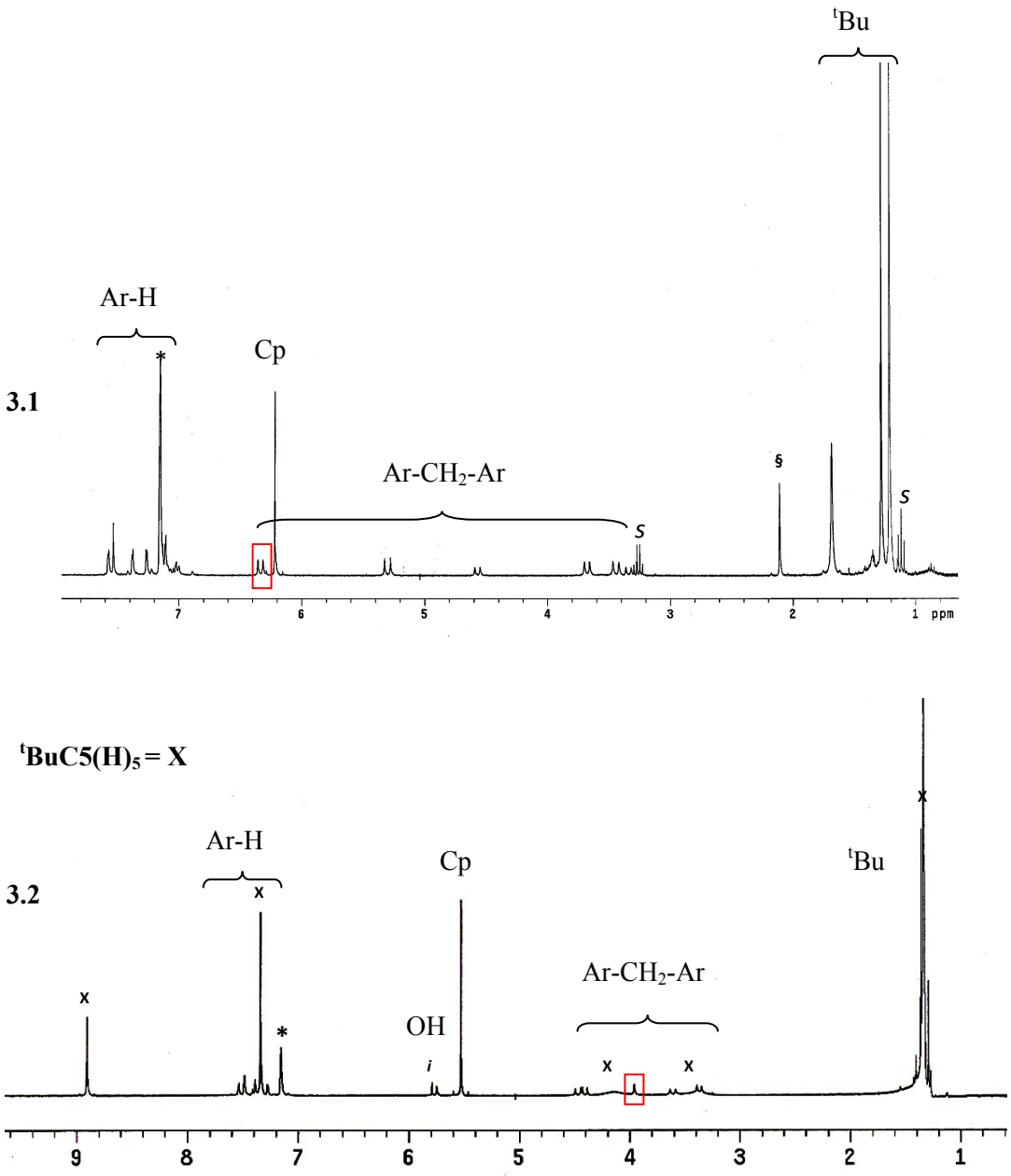

Figure 3.10 ^{1}H NMR spectra of compounds **3.1** and **3.2** in $^{*}C_6D_6$. §DMSO, *s* = ether and *i* = impurity. Each box highlights an interesting chemical shift observed for the methylene protons.

The resonances for the Cp ligands in **3.1** and **3.2** are observed at 6.22 (*exo* Cp) and 5.53 (*endo* Cp) ppm, respectively. The chemical shifts for the Cp ligands are close to the values observed in [CpTi{^{t}**BuC6(H)$_3$**}] (5.38 ppm, *endo* Cp) and [(CpTi)$_2${^{t}**BuC6**}] (6.07 ppm, *exo* Cp) complexes.[90] The upfield shift of the Cp in compound **3.2** indicates increased shielding due to the Cp ligand being located between two aromatic rings (see Figure 3.8a).

One of the methylene protons in compound **3.1** is observed very downfield at 6.34 ppm. A downfield chemical shift is common when a late transition M···H interaction is observed, e.g. [PtCl$_2${^{t}**BuC4**(OCH$_2$PPh$_2$)$_4$}Au(PPh$_3$)$_2$}], and [PtCl$_2${^{t}**BuC4(H)$_2$(OCH$_2$PPh$_2$)$_2$**}] (2.61 – 2.67 Å, δ = 7.35 and 7.34 ppm (in CDCl$_3$), respectively).[150] A similar downfield shift was also seen in the metallocalixarene compounds when a boat-boat conformation was observed in the eight-membered ring. Compound [Pt(dppp){^{t}**BuC4(H)$_2$**}] (dppp = diphenylphosphinopropane) has a *d*(M···H) of 2.25 Å (δ = 6.50 ppm in CDCl$_3$) and *d*(M···H) = 2.24 Å (δ = 7.10 in CDCl$_3$) was observed for compound [Rh(cod){^{t}**BuC4(H)$_2$**·η^6-Rh(cod)}] (cod = 1,5-cyclooctadiene).[151-152]

The conformation observed in **3.1** is boat-chair with Ti···H distances ranging from 3.070 to 3.760 Å (distances *d*(M···H) 1A-7A, Figure 3.11), indicating that an M···H interaction is not responsible for the downfield chemical shift. Close observation of the X-ray structure of compound **3.1** reveals two close O···H interactions of 2.353 Å (1B) and 2.393 Å (2B) (Figure 3.11), that are within the van der Waals radii of 2.61 Å (for O-H).[153-154] This interaction may be responsible for the downfield chemical shift.

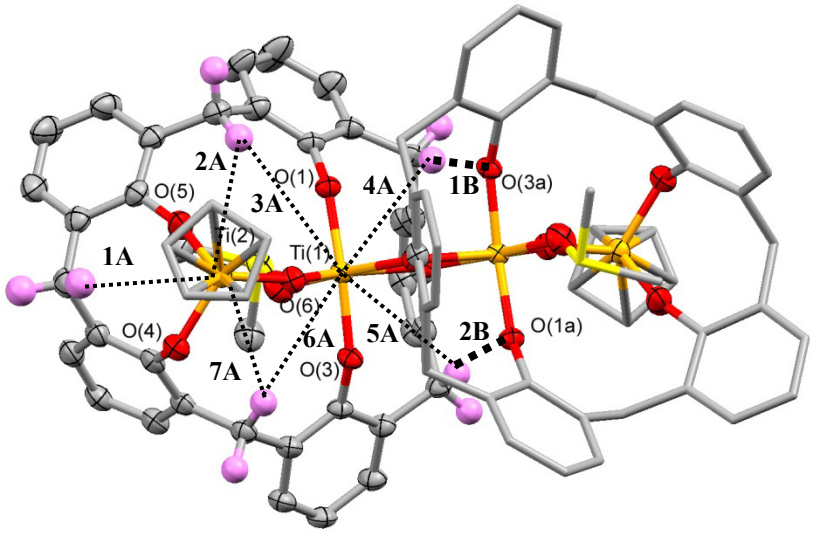

M···H distances (Å)	
1A	3.070
2A	3.368
3A	3.760
4A	3.508
5A	3.601
6A	3.444
7A	3.207
1B	2.353
2B	2.393

Figure 3.11 X-ray structure of compound **3.1** showing selected M···H (1A-7A) and O···H (1B-2B) distances with thermal ellipsoids at the 50% probability level. H atoms and *tert*-butyl groups are omitted for clarity.

*3.4.2 Spectral data of compounds **3.3** and **3.4***

The ^{1}H NMR spectra of bimetallic titanium complexes **3.3** and **3.4** are shown in Figure 3.12. Complex **3.3** gives ten signals for the Ar-H protons (7.32-6.82 ppm, three overlapped), five pairs of doublets for methylene groups from 4.75 to 3.16 ppm (^{2}J = 14.3 to 13.5 Hz), and five singlets for the ^{t}Bu protons (1.42-1.03 ppm). Four resonances for the four different Cp ligands are observed at 6.89, 6.62, 6.34 and 6.26 ppm. This ^{1}H NMR pattern is indicative of a C_1 symmetry.[30]

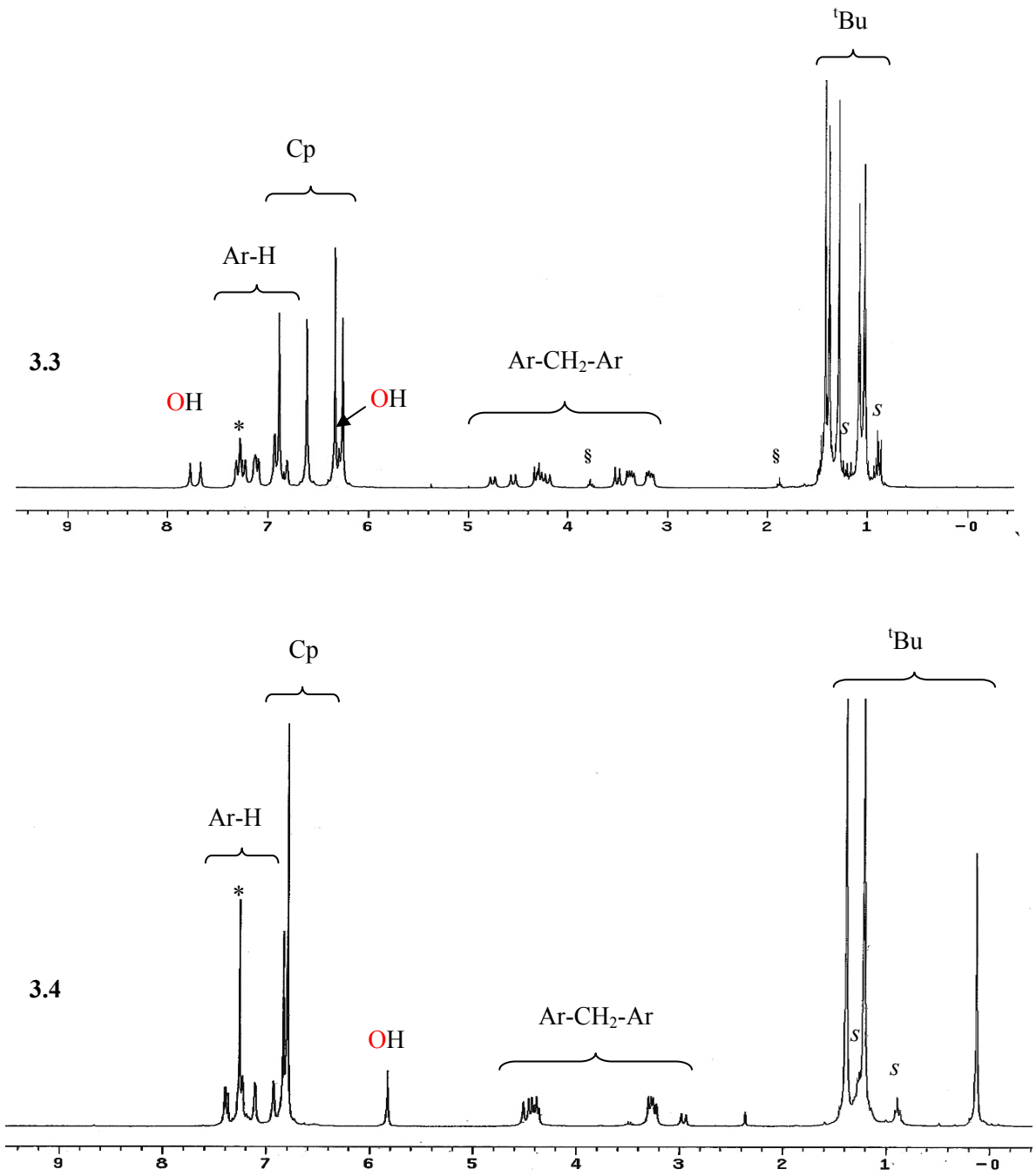

Figure 3.12 ^{1}H NMR spectra of compound **3.3** and **3.4** in $^{*}CDCl_3$. §residual THF solvent and *s* = pentane.

The spectrum of complex **3.4** is consistent with C_s symmetry. Complex **3.4** shows five resonances for the Ar-*H* protons from 7.40 to 6.81 ppm, and six doublets from 4.48 to 2.96 ppm (^2J = 15.4 to 13.5 Hz) are found for the methylene bridging groups, Ar-CH_2-Ar. The Cp protons are found at 6.79 and 6.83 ppm. In the upfield region three singlets are observed for the ^{t}Bu groups (1.38 to 0.12 ppm, 2:2:1 ratio). One of the ^{t}Bu groups is unusually upfield, at 0.12 ppm. The increased shielding for this ^{t}Bu group may be due either to a position above an aromatic ring, or an interaction with the Cp ligand.

The OH resonances are upfield from the normal values for calixarene OH groups. In compound **3.3** we have assigned peaks at 7.78, 7.67 and 6.30 ppm to the free OH groups, while in compound **3.4** the peak at 5.82 ppm is assigned to an OH resonance. We attribute the upfield shift to shielding by CpTi moieties attached to the lower rim, similar to the effect observed in phosphorus-based calix[5]arene ligands described by Lattman et al.[138]

3.5 Experimental section

3.5.1 General information

Unless otherwise noted, all manipulations were carried out in a dry nitrogen-filled glove box. $M_2 \cdot$**^{t}BuC5(H)$_3$** (M = Na, K, Rb, Cs) were prepared as previously described.[113] Cp_2TiCl_2 and $CpTiCl_3$ were purchased from Strem Chemicals and were used as received. The melting point of compound **3.3** was taken in capillary tube on a Mel-Temp apparatus (Laboratory Devices, Cambridge, MA). A temperature proceeded by a “>” sign indicates that the compound starts to decompose at that temperature. ^{1}H NMR and ^{13}C NMR spectra were recorded on a Varian XL-300 spectrometer at 300 and 75 MHz, respectively. Deuterated chloroform ($CDCl_3$) and benzene (C_6D_6) were dried over CaH_2. $CDCl_3$ was referenced to 7.26 ppm and 77.2 ppm for ^{1}H and ^{13}C

NMR, respectively. Microanalyses were performed by Atlantic Microlab, Inc, Norcross, GA. IR and UV/Vis spectra were obtained with an Infinity Gold™ FTIR spectrometer and Agilent 8453 spectrophotometer, respectively. All solvents were anhydrous and were stored over 4 Å molecular sieves for at least one day before use.

3.5.2 Synthesis of complexes

[(CpTi-μ-O-Ti){^{t}**BuC5**}]$_2$ (**3.1**): Cp_2TiCl_2 (0.0133 g, 53.4 μmol) in 3 mL of THF was added dropwise to a colorless solution of Cs_2·^{t}**BuC5(H)$_3$** (0.0539 g, 50.1 μmol) in 5 mL of THF, immediately yielding an orange solution. The reaction mixture was stirred for 24 hrs at room temperature, and then the solvent was removed under vacuum. To the residue was added ~1.5 mL of toluene and 5 drops of DMSO for crystallization. Crystals (~10 mg) suitable for X-ray analysis were obtained after one week at room temperature. Additional characterization of the crystals was performed by ^{1}H NMR spectroscopy. ^{1}H NMR (C_6D_6) δ (ppm): 7.58 (d, 4H, *J* = 2.0 Hz, Ar-*H*), 7.54 (s, 3H,* Ar-*H*), 7.38 (d, 5H,* *J* = 2.5 Hz, Ar-*H*), 7.26 (d, 4H, *J* = 3.2 Hz, Ar-*H*), 7.11 (d, 10H,* *J* = 2.2 Hz, Ar-*H*), 6.34 (d, 5H,* *J* = 12.4 Hz, Ar-CH_2-Ar), 6.22 (s, 8H,* Cp-*H*), 5.30 (d, 5H,* *J* = 14.3 Hz, Ar-CH_2-Ar), 4.57 (d, 4H,* *J* = 12.9 Hz, Ar-CH_2-Ar), 3.68 (d, 5H,* *J* = 12.4 Hz, Ar-CH_2-Ar), 3.44 (d, 5H,* *J* = 15.1 Hz, Ar-CH_2-Ar), 3.34 (d, 4H,* *J* = 12.9 Hz, Ar-CH_2-Ar), 2.11 (s, 6H, CH_3, DMSO), 1.69 (s, 17H,* ^{t}Bu), 1.28 (s, 26H,* ^{t}Bu), 1.22 (s, 35H,* ^{t}Bu). *The integral values reported for the compound are not consistent with the values required. This disagreement in values could be due to overlapping with solvents and impurities. Insufficient product was obtained for further analysis.

[$(CpTi)_2$**^{t}BuC5(H)**] (**3.2**): Solutions of Cp_2TiCl_2 (0.0231 g, 92.8 μmol) and $Cs_2\cdot$**^{t}BuC5(H)$_3$** (0.0983 g, 91.4 μmol) in 4 and 6 mL of THF, respectively, were placed in a solvent bomb and allowed to heat in an isotemp oil bath at 85 ^oC for 12 hrs. The reaction solution turned orange. The solvent was removed under vacuum and to the residue was added ~1.5 mL of benzene and a few drops of DMSO. A small amount (<10 mg) of crystals suitable for X-ray analysis was obtained after one week at room temperature. Additional characterization of the crystals was performed by ^1H NMR spectroscopy. ^1H NMR (C_6D_6) δ (ppm): 8.91 (s, OH,§ Cx_5), 7.54 (d, 2H, *J* = 2.5 Hz, Ar-*H*), 7.49 (d, 3H,* *J* = 2.5 Hz, Ar-*H*), 7.39 (s, 2H, Ar-H), 7.34 (s, 11H,* Ar-H, Cx_5), 7.28 (d, 2H, *J* = 2.5 Hz, Ar-*H*), 5.75 (s, 1H, OH), 5.53 (s, 5H,* Cp-*H*), 4.47 (d, 2H, *J* = 14.6 Hz, Ar-C*H*$_2$-Ar), 4.40 (d, 2H, *J* = 13.2 Hz, Ar-C*H*$_2$-Ar), 4.15 (br, 5H,* Ar-C*H*$_2$-Ar, Cx_5), 3.96 (s, 2H, Ar-C*H*$_2$-Ar), 3.61 (d, 2H, *J* = 14.6 Hz, Ar-C*H*$_2$-Ar), 3.39 (br, 4H,* Ar-C*H*$_2$-Ar, Cx_5), 3.37 (d, 2H, *J* = 12.9 Hz, Ar-C*H*$_2$-Ar), 1.36 (s, 18H,* ^{t}Bu), 1.34 (s, 116H,* ^{t}Bu Cx_5), 1.33 (s, 18H, ^{t}Bu), 1.29 (s, 9H, ^{t}Bu). § Integral value not recorded. *The integral values reported for the compound are not consistent with the values required. This disagreement in values could be due to overlapping with solvent and impurities. Insufficient product was obtained for further analysis.

[$(Cp_2TiCl)_2${**^{t}BuC5(H)$_3$**}] (**3.3**): Note: the salts $M_2\cdot$**^{t}BuC5(H)$_3$** (M = K, Rb, Cs) were left in the oven for 12 hrs before use (100 ^oC). A solution of Cp_2TiCl_2 (0.0429 g, 0.172 mmol) in THF (4 mL) was added dropwise to a solution of $K_2\cdot$**^{t}BuC5(H)$_3$** (0.133 g, 0.150 mmol) in THF (5 mL). After the complete addition of the solution of Cp_2TiCl_2, 4 mL of hexane was added to the reaction mixture. The resulting orange red solution was stirred for 7 h. At the end of this time an orange-yellow suspension was obtained. The suspension was centrifuged for 30 min. The

supernatant was discarded and the solid was stirred with 5 mL of pentane. The reaction mixture was centrifuged again, and the solid was recovered and vacuum dried to give an orange-yellow solid (0.0825 g, 0.0667 mmol, 77% yield). Compound [$(Cp_2TiCl)_2\{^t$**BuC5(H)$_3$**$\}$] **3.3** can also be obtained by the reaction of rubidium or cesium dianionic salts.[113] For Rb, $Rb_2\cdot^t$**BuC5(H)$_3$** (0.147 g, 0.150 mmol) and Cp_2TiCl_2 (0.0432 g, 0.173 mmol) yielded 72% (0.0771 g, 0.0624 mmol). For Cs, $Cs_2\cdot^t$**BuC5(H)$_3$** (0.162 g, 0.151 mmol) and Cp_2TiCl_2 (0.0431 g, 0.173 mmol) yielded 72% (0.0773 g, 0.0625 mmol). Mp > 255 ^oC. ^1H NMR ($CDCl_3$) δ (ppm): 7.78 (s, 1H, O*H*), 7.67 (s, 1H, O*H*), 7.32 (s, 1H, Ar-*H*), 7.28 (s, 2H, Ar-*H*), 7.23 (d, 1H, *J* = 1.9 Hz, Ar-*H*), 7.13 (s, 2H, Ar-*H*), 7.10 (d, 1H, *J* = 1.9 Hz, Ar-*H*), 6.94 (d, 2H, *J* = 1.9 Hz, Ar-*H*), 6.89 (s, 5H, Cp-*H*), 6.82 (s, 1H, Ar-*H*), 6.62 (s, 5H, Cp-*H*), 6.34 (s, 5H, Cp-*H*), 6.30 (s, 1H, O*H*), 6.26 (s, 5H, Cp-*H*), 4.75 (d, 1H, *J* = 14.3 Hz, Ar-CH_2-Ar), 4.55 (d, 1H, *J* = 14.0 Hz, Ar-CH_2-Ar), 4.31 (d, 1H, *J* = 13.8 Hz, Ar-CH_2-Ar), 4.28 (d, 1H, *J* = 13.5 Hz, Ar-CH_2-Ar), 4.20 (d, 1H, *J* = 13.5 Hz, Ar-CH_2-Ar), 3.50 (d, 1H, *J* = 14.0 Hz, Ar-CH_2-Ar), 3.38 (d, 1H, *J* = 14.3 Hz, Ar-CH_2-Ar), 3.36 (d, 1H, *J* = 14.0 Hz, Ar-CH_2-Ar), 3.18 (d, 1H, *J* = 13.8 Hz, Ar-CH_2-Ar), 3.16 (d, 1H, *J* = 13.5 Hz, Ar-CH_2-Ar), 1.42 (s, 9H, ^{t}Bu), 1.38 (s, 9H, ^{t}Bu), 1.28 (s, 9H, ^{t}Bu), 1.08 (s, 9H, ^{t}Bu), 1.03 (s, 9H, ^{t}Bu). $^{13}C\{^1H\}$ NMR $CDCl_3$ δ (ppm): 164.7, 164.1, 150.7, 150.6, 148.6, 143.3, 143.1, 142.9, 142.1, 141.0, 128.1, 127.9, 127.7, 127.2, 126.9, 126.1, 126.0, 125.9, 125.7, 125.6, 125.4, 125.0, 124.3, 124.1 (aromatic carbons), 119.8, 119.3, 118.7, 118.3 (aromatic from Cp), 34.1, 34.0 ($C(CH_3)_3$), 33.3, 32.9 (Ar-CH_2-Ar), 32.0, 31.9, 31.7, 31.4 ($C(CH_3)_3$), 30.2, 28.7 (Ar-CH_2-Ar). FTIR (KBr, cm^{-1}): 3448s (OH), 3116m, 2959vs, 2904s, 2868s, 1602w, 1484vs, 1453vs, 1393m, 1362m, 1296s, 1247s, 1200s, 1126s, 1017m, 916w, 876m, 820s, 766m, 753m, 548w. UV/vis ($CHCl_3$) $\lambda_{max/nm}$ ($\varepsilon/dm^3\ mol^{-1}\ cm^{-1}$): 254 ($3.83 \times 10^4$), 277 ($2.62 \times 10^4$), 288 ($2.20 \times 10^4$), 325 ($1.30 \times 10^4$). Elemental analysis for $C_{75}H_{88}Cl_2O_5Ti_2$ (1236.14): calcd C 72.87, H 7.18; found C 72.65, H 7.36.

3.4: A solution of $CpTiCl_3$ (0.0379 g, 0.173 mmol) in THF (4 mL) was added dropwise to a solution of $K_2 \cdot$**^{t}BuC5(H)$_3$** (0.133 g, 0.150 mmol) in THF (5 mL). After the complete addition of the solution of $CpTiCl_3$, ~1.0 g of 4 Å molecular sieves was added to the reaction mixture. The reaction mixture was stirred for 7 h. At the end of this time an orange milky suspension was obtained. The suspension was centrifuged for 30 min in order to remove the molecular sieves. The supernatant was transferred to another 20 mL vial. The solvent was removed by high vacuum resulting in a yellow-orange solid. This crude product was a mixture of titanium(IV) calix[5]arene complex and parent **^{t}BuC5(H)$_5$** (determined by ^{1}H NMR spectroscopy). To the crude product was added 6.0 mL of hexanes. A yellow solid was recovered after centrifugation. The orange solution (supernatant) was discarded. The yellow solid was washed with pentane (3 x 2 mL), and the supernatant removed by centrifugation and discarded each time. The remaining solid was transferred as a suspension in pentane to another vial. Removal of the solvent under vacuum led to a yellow solid (0.0228 g, 0.0168 mmol, 29% based on proposed structure). ^{1}H NMR ($CDCl_3$) δ (ppm) = 7.40 (d, 2H, *J* = 1.7 Hz, Ar-*H*), 7.23 (s, 2H, Ar-*H*), 7.11 (d, 2H, *J* = 2.2 Hz, Ar-*H*), 6.93 (d, 2H, *J* = 1.9 Hz, Ar-*H*), 6.83 (s, 5H, Cp-*H*), 6.81 (s, 2H, Ar-*H*), 6.79 (s, 10H, Cp-*H*), 5.82 (s, 2H, O*H*), 4.48 (d, 2H, *J* = 15.4 Hz, Ar-CH_2-Ar), 4.40 (d, 2H, *J* = 13.5 Hz, Ar-CH_2-Ar), 4.38 (d, 1H, *J* = 13.5 Hz, Ar-CH_2-Ar), 3.28 (d, 2H, *J* = 13.5 Hz, Ar-CH_2-Ar), 3.25 (d, 2H, *J* = 15.4 Hz, Ar-CH_2-Ar), 2.96 (d, 1H, *J* = 13.8 Hz, Ar-CH_2-Ar), 1.38 (s, 18H, ^{t}Bu), 1.21 (s, 18H, ^{t}Bu), 0.12 (s, 9H, ^{t}Bu). ^{13}C{^{1}H} NMR ($CDCl_3$) δ (ppm) = 164.3, 162.4, 161.7, 146.8, 144.1, 141.8, 133.6, 130.5, 129.8, 127.7, 126.8, 126.1, 125.7, 125.0, 124.9, 122.6 (aromatic carbons), 121.0, 116.4 (aromatic Cp), 35.3, 34.4 (Ar-*C*H_2-Ar), 34.0, 33.7, 32.4 (*C*(CH_3)$_3$), 31.9, 31.8, 30.3 (C(*C*H_3)$_3$). Note that IR, mp, EA, and UV/vis still need to be obtained.

3.5.3 General X-ray information

X-ray data for **3.1**·6DMSO and **3.2**·$2C_6H_6$ were collected on a SMART Bruker 1000 CCD detector diffractometer at low temperature using Mo Kα radiation. The crystallographic data and some details of the data collection and refinement of the structures are given in Table 3.2. Absorption corrections in all cases were applied by SADABS.[155] All structures were solved by direct methods and subsequent difference Fourier syntheses and refined by full matrix least-squares methods against F^2 (SHELX-97).[121] Disorder for some *tert*-butyl groups was due to a 2-fold axis, and was modeled using partial occupancies (PART instruction).[121] Some other disordered molecules and solvents were refined using a combination of restraints on the distances while keeping the disordered parts similar (use of the SADI and SAME instructions).[121] All non-hydrogen atoms were refined with anisotropic displacement coefficients, except atoms of disordered fragments, which were refined with isotropic thermal parameters. The H atoms in structures were taken in calculated positions. Corrections of the X-ray data for **3.1**·6DMSO with the program SQUEEZE[156] (158 electron cell) were close to the required value (168 electron cell). The programs Mercury[157] and PovRay[158] were used to generate the X-ray structural diagrams pictured in this chapter. The structures of this Chapter were solved in collaboration with Dr. Daniel Mendoza-Espinosa.

Table 3.2 Crystallographic data for complexes **3.1**·6DMSO and **3.2**·$2C_6H_6$

	3.1·6DMSO	**3.2**·$2C_6H_6$
Formula	$C_{132}H_{176}O_{18}S_6Ti_4$	$C_{77}H_{88}O_6Ti_2$
FW	2434.69	1205.21
cryst syst	Monoclinic	Triclinic
space group	P 21/c	P-1
T, K	223(2)	223(2)
a, Å	12.9283(16)	9.898(6)
b, Å	20.923(3)	17.591(10)
c, Å	25.380(3)	19.745(11)
α, deg	90	73.506(10)
β, deg	104.836(5)	84.321(10)
γ, deg	90	86.940(10)
V, A^3	6636.4(15)	3279(3)
Z	2	2
d_{calcd}, $g \cdot cm^{-3}$	1.140	1.221
μ, mm^{-1}	0.351	0.296
refl collected	45449	18820
T_{min} / T_{max}	0.980	0.963
N_{measd}	15410	9343
[R_{int}]	[0.1333]	[0.0449]
R [I>2sigma(I)]	0.0764	0.1058
R (all data)	0.0906	0.1470
R_w [I>2sigma(I)]	0.2352	0.2830
R_w (all data)	0.2517	0.3159
GOF	1.123	1.076

3.6 Conclusions

Two new compounds (**3.3** and **3.4**) containing titanium(IV) have been characterized by NMR, UV/vis, and FTIR spectroscopies, while for two others (**3.1** and **3.2**) just ^{1}H NMR spectra and X-ray structures were obtained.

Complexes **3.1** and **3.2** are homo-bimetallic complexes with 1:2 calix[5]arene/metal ratios. In the case of complex **3.1** a dimeric structure with calixarene in the cone conformation was obtained while in compound **3.2** a monomeric structure with a 1,2-alternate conformation was obtained. Compound **3.3** contained two metals per calixarene ligand and no alkali metal ion. In the case of compound **3.4** titanium is present but its ratio has not yet been determined. The calix[5]arene ligand in compound **3.3** produces an unsymmetrical ^{1}H NMR pattern due to C_1 symmetry, while compounds **3.1**, **3.2** and **3.4** have C_s symmetry.

CHAPTER 4

CALIX[5]ARENE MOLYBDENUM(VI) COMPLEXES

4.1 Introduction

The chemistry of dioxomolybdenum(VI) (MoO_2^{2+}) complexes is of importance especially in industrial[159] and biochemical catalysis.[160] Metallocalixarene complexes are of interest as models of heterogeneous metal oxide catalyst surfaces,[16] centers capable of supporting organometallic transformations,[37-39,44,47,66,161] and as building blocks for supramolecular structures.[162-164] However, few MoO_2^{2+}-containing calixarene derivatives have been reported.[110,165] [MoO_2{^{t}**BuC4(OMe)$_2$**}] was the first such complex, reported by Radius,[165]and a series of [MoO_2{M_2·**RC4**}] (M = Li, K, Rb; R = H, ^{t}Bu) complexes were later reported by our group.[110] The complexes were prepared by addition of MoO_2Cl_2 to the calixanions (Scheme 4.1).

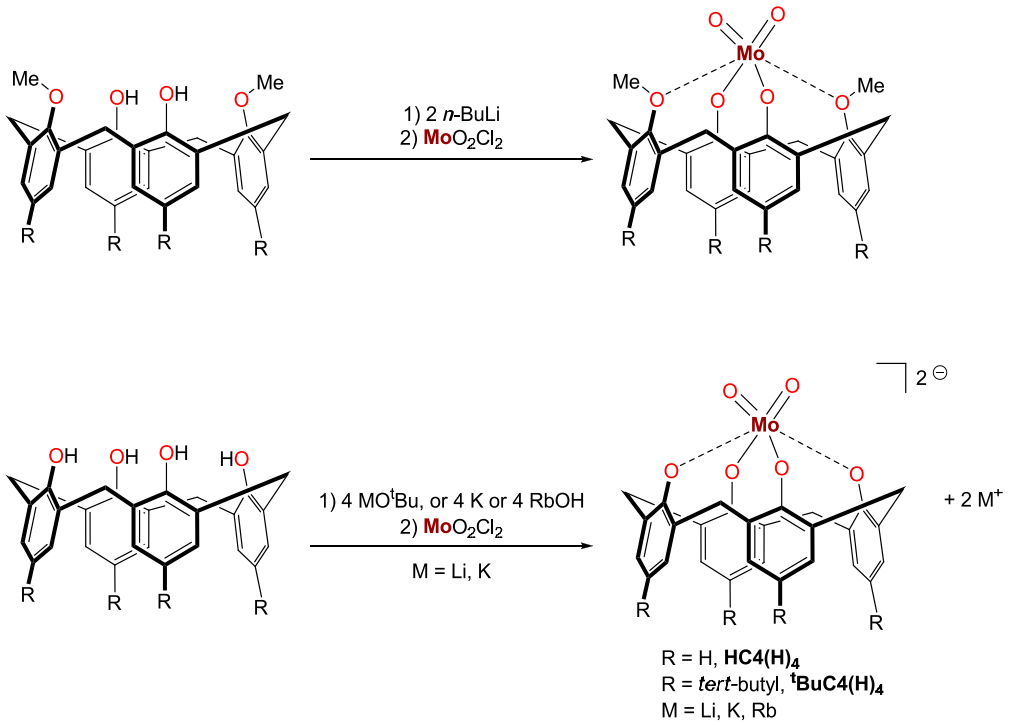

Scheme 4.1 Synthesis of dioxomolybdenum(VI) calix[4]arene complexes.[110,165]

It seems that the synthesis of a MoO_2^{2+}-containing calixarene compound is still a challenge. In this chapter we describe the synthesis and characterization of MoO_2^{2+}-calix[5]arene complexes, achieved by the use of doubly deprotonated calix[5]anions as precursors and with three different starting materials; dichlorodioxomolybdenum(VI) (MoO_2Cl_2), dioxodichloro-2,2'-bipyridylmolybdenum(VI) (MoO_2Cl_2(bipy)) and bis(acetylacetonato)dioxomolybdenum(VI) ($MoO_2(acac)_2$). We describe the reactivity of each reactant toward the calix[5]arene dianions.

4.2 Results and discussion

4.2.1 Synthesis of dioxomolybdenum(VI) calixarene complex from MoO_2Cl_2

For the preparation of MoO_2^{2+}-containing calix[5]arene compounds we decided to follow a strategy previously used in our group.[110] The reaction of MoO_2Cl_2 and $M_2\cdot$**^{t}BuC5(H)$_3$** (M = Na, K, Rb, Cs) in a 1:1 ratio in anhydrous acetonitrile at room temperature for 12 hrs produced a blue solid containing [MoO_2{**^{t}BuC5(H)$_3$**}] **4.1** and **^{t}BuC5(H)$_5$** in an approximate 2:1 ratio (Equation 4.1). More **^{t}BuC5(H)$_5$** is produced when we do not use dry **^{t}BuC5(H)$_5$** or $M_2\cdot$**^{t}BuC5(H)$_3$** (M = Rb, Cs). It is known that adventitious water present in starting calix[4]arene[60] or calix[5]arene[84] ligands can result in hydrolysis or oxidation (e.g. U^{IV} to U^{V})[84] products. So we decided that parent **^{t}BuC5(H)$_5$** or $M_2\cdot$**^{t}BuC5(H)$_3$** (M = Rb, Cs) should be dried at least 12 hrs in an oven at 100 ^oC.

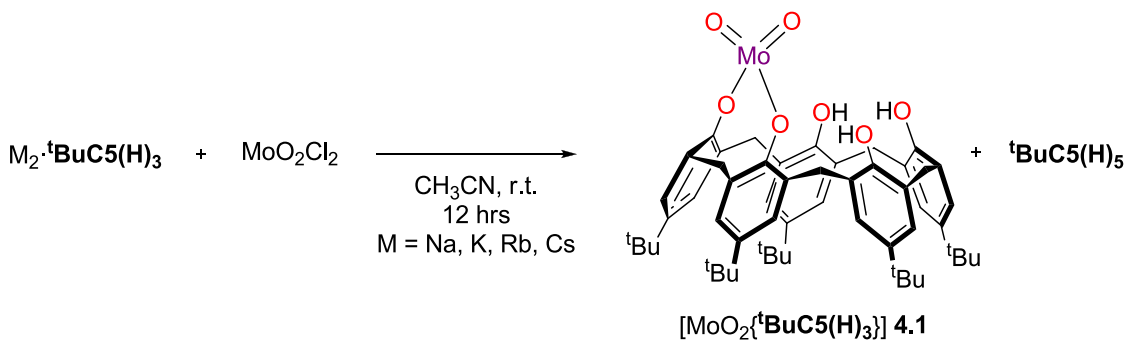

(4.1)

Attempts to separate the mixture of compounds were unsuccessful due to similar solubility in common organic solvents. Complex **4.1** is air sensitive, but thermally stable in the solid form (up to four months under an inert atmosphere). Compound **4.1** slowly decomposes to parent **^{t}BuC5(H)$_5$** after three days in solution. The molecular structure of compound **4.1** is proposed based on its spectroscopic characterization, since attempts to obtain crystals suitable for X-ray studies were unsuccessful.

The ^{1}H NMR spectrum of complex **4.1** shows a characteristic pattern for C_s symmetry of the calix[5]arene ligand.[30] The ^{1}H NMR spectrum shows two singlets at 9.03 and 8.27 ppm in a 1:2 ratio, assigned as free OH groups in complex **4.1**. The singlet at 8.66 ppm belongs to the OH group of parent calix[5]arene. In the aromatic region between 7.24 - 7.05 ppm there are four doublets for the aromatic protons Ar-*H* with a ^4J = 2.5 Hz and one signal (singlet) is overlapped with a signal from the parent calix[5]arene aromatic protons resulting in an overall singlet. In the methylene area (Ar-CH_2-Ar) between 3 and 5 ppm, three pairs of doublets are observed in a 2:2:1 ratio, while a broad signal at ~3.76 ppm is characteristic of the parent calix[5]arene methylene protons. Three singlets in a 1:2:2 ratio (1.26, 1.24, 1.22 ppm) are assigned to the *tert*-butyl groups in complex **4.1**, whereas the singlet at 1.25 ppm belongs to the ^{t}Bu group of the parent calix[5]arene (Figure 4.1).

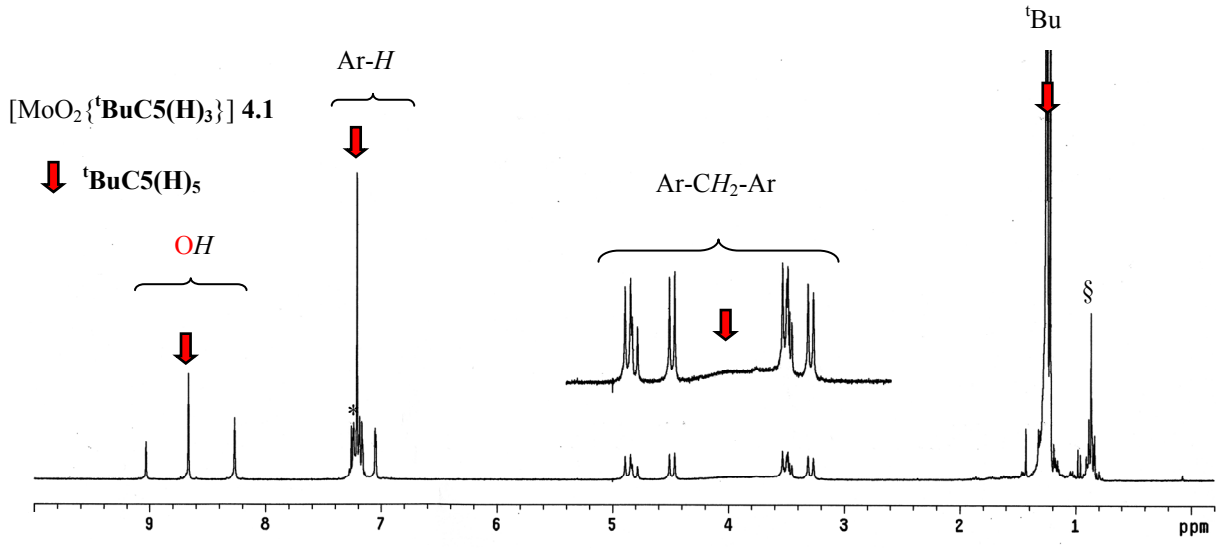

Figure 4.1 ^{1}H NMR spectrum of complex **4.1** in *$CDCl_3$. §Residual hexane.

We performed a qualitative analysis using Energy Dispersive X-ray spectroscopy analysis (EDX), in order to determine what metal(s) were in the blue solid. The EDX analysis showed just Mo; no traces of alkali metals were observed (Figure 4.2).

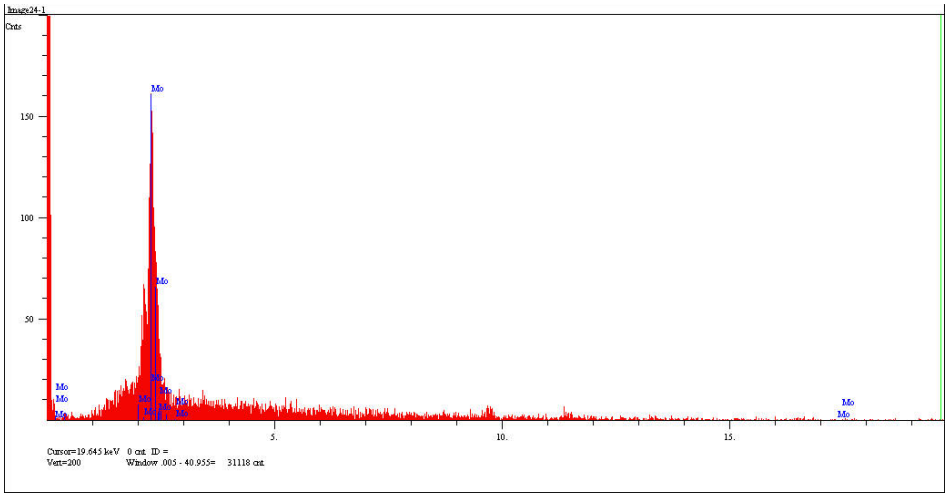

Figure 4.2 EDX spectrum of the blue solid (**4.1** and calix[5]arene) demonstrating that just Mo is contained in the sample.

In order to determine if **4.1** is a mono- or dioxomolybdenum complex, an IR experiment was performed. Two bands at 918 and 885 cm^{-1} fall in the normal range for *cis*-dioxo symmetric and asymmetric M=O stretching vibrations (970-800 cm^{-1}).[166] Based on this data, we propose that **4.1** contains a MoO_2^{2+} moiety, [MoO_2{^{t}**BuC5(H)$_3$**}] (Equation 4.1).

*4.2.1.1 Mechanism of formation of complex **4.1***

In the synthesis of compound **4.1** we could expect a direct metathesis reaction with salt elimination (Equation 4.2).

$$M_2\cdot{}^t\mathbf{BuC5(H)_3} \xrightarrow[\text{M = Na, K, Rb Cs}]{MoO_2Cl_2} [MoO_2\{{}^t\mathbf{BuC5(H)_3}\}] + 2\ MCl \qquad (4.2)$$

However, in this proposed reaction the formation of ^{t}**BuC5(H)$_5$** is not predicted. Experimentally, we found that when $Cs_2\cdot{}^t$**BuC5(H)$_5$** and MoO_2Cl_2 were combined, both compound **4.1** and a considerable amount of ^{t}**BuC5(H)$_5$** were formed. On the other hand, when we placed the $Cs_2\cdot{}^t$**BuC5(H)$_5$** salt in the oven for at least 12 hrs at 100 ^oC the ratio of compound **4.1** increased with respect to the parent ^{t}**BuC5(H)$_5$**.

Parent ^{t}**BuC5(H)$_5$** is probably produced from a source of H^+ in the reaction mixture. One source of H^+ would be hydrolyzed MoO_2Cl_2. The hydrolysis of MoO_2Cl_2 leads to the formation of MoO_3 and two equivalents of HCl (Equation 4.3).[167-168]

$$MoO_2Cl_2 + H_2O \longrightarrow MoO_3 + 2\ HCl \qquad (4.3)$$

The HCl formed from the reaction of MoO_2Cl_2 with traces of water may react with the calixanion resulting in the formation of the parent ^{t}**BuC5(H)$_5$** and MCl (M = Na, K, Rb, Cs).

4.2.2 Synthesis of dioxomolybdenum(VI) calixarene complex from MoO_2Cl_2(bipy)

4.2.2.1 Synthetic approach using acetonitrile (CH_3CN)

In order to avoid the formation of the parent calix[5]arene we employed a different approach. We hypothesized that an external coordinating ligand might deter the hydrolysis of MoO_2Cl_2. The ligand 2,2'-bipyridine (bipy) is suitable for our purpose. Despite the synthesis reported for the isolation of MoO_2Cl_2(bipy)[169-171] and its reported reactivity towards different substrates,[159] we developed an easier and higher-yielding synthetic route. The addition of bipy to a solution of MoO_2Cl_2 in acetonitrile at room temperature (Equation 4.4) caused MoO_2Cl_2(bipy) to precipitate from the reaction mixture as a white solid. The product was purified by filtration and successive acetonitrile washing cycles.

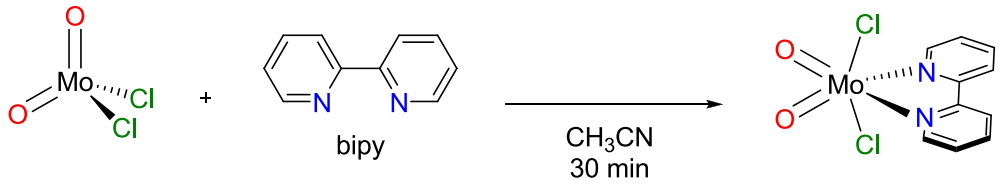

(4.4)

MoO_2Cl_2(bipy) was obtained in 87% yield as a white solid, and the identity was confirmed by IR spectroscopy (Figure 4.3). No vibrational modes for the ν(N≡C) at 2311 and 2286 cm^{-1} were observed from $MoO_2Cl_2(CH_3CN)_2$.[172] However, MoO_2Cl_2(bipy) displayed the absorptions corresponding to the bipy ligand (1600, 1573, 1496, 1475, 1443, 1318, 1155, 1102, 776, 734 and 636 cm^{-1}), and the two characteristic symmetric and asymmetric vibrations for ν(Mo=O) were observed at 936, 905 cm^{-1}, similar to those reported in the literature (936, 906 cm^{-1}).[169,173]

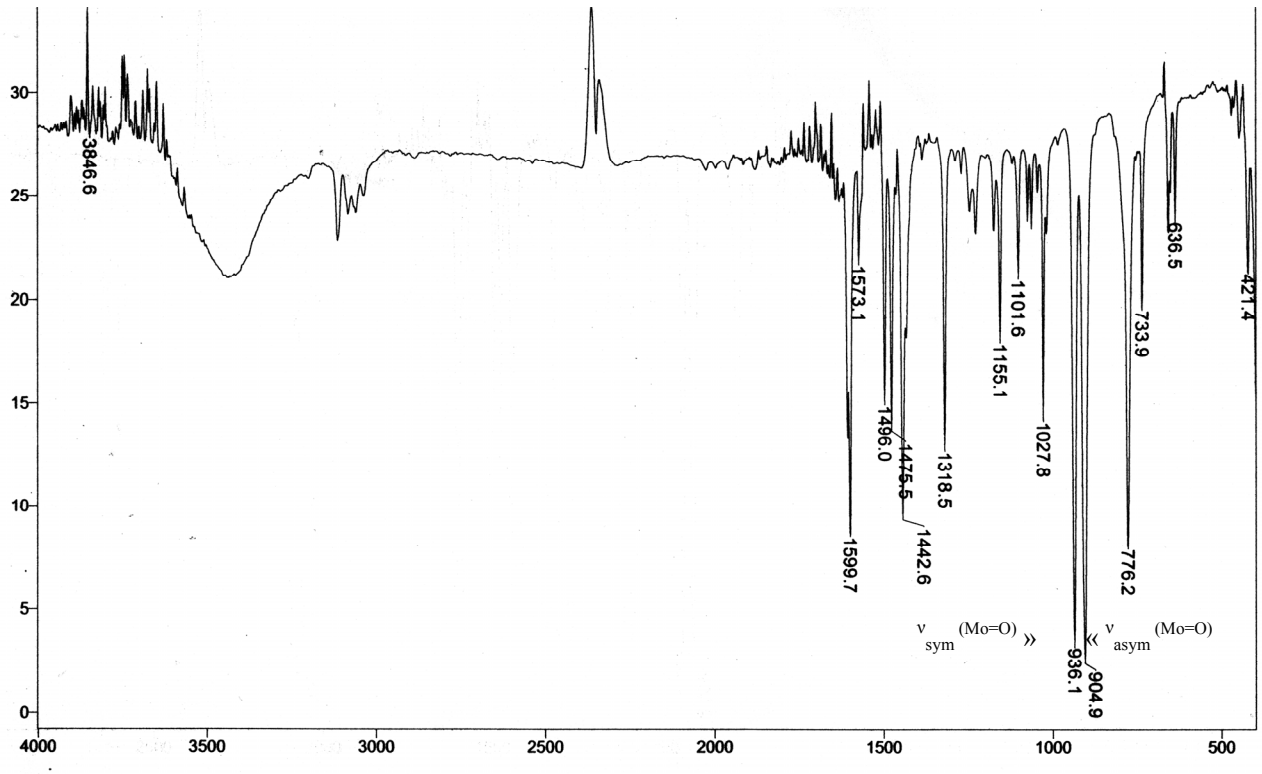

Figure 4.3 IR spectrum of MoO_2Cl_2(bipy) recorded in a KBr pellet.

Once we isolated and characterized the MoO_2Cl_2(bipy) complex, we reacted it with $M_2 \cdot {}^{t}$**BuC5(H)$_3$** (M = Na, K, Rb, Cs) in a 1:1 ratio in acetonitrile at room temperature for 12 hrs (Equation 4.5).

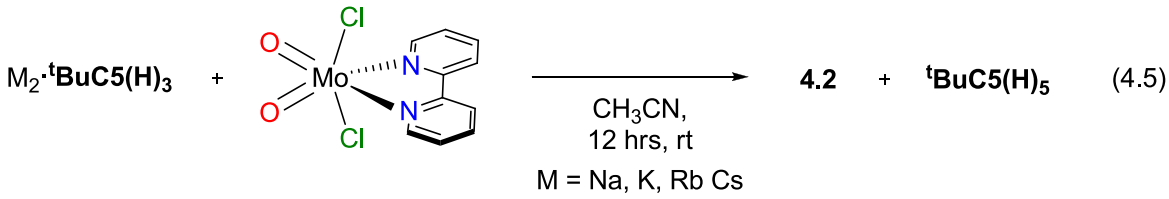

After workup we isolated a pale brown solid. The ^{1}H NMR spectrum showed a different pattern from that described for compound **4.1** (Figure 4.4). In the area around ~9.6-7.2 ppm we

observed signals for the aromatic protons from the bipy ligand. In the range from ~6.5-8.0 ppm we observed nine signals (some overlapped) for the aromatic protons Ar-*H*, corresponding to the calix[5]arene ligand. In the methylene area (Ar-CH_2-Ar), eight well-defined doublets and two broad signals were observed in the range of ~4.8-1.9 ppm. Finally, five resonances were assigned to the *tert*-butyl groups (in a 1:1:1:1:1 ratio). Unfortunately, the product **4.2** contained traces of calix[5]arene.

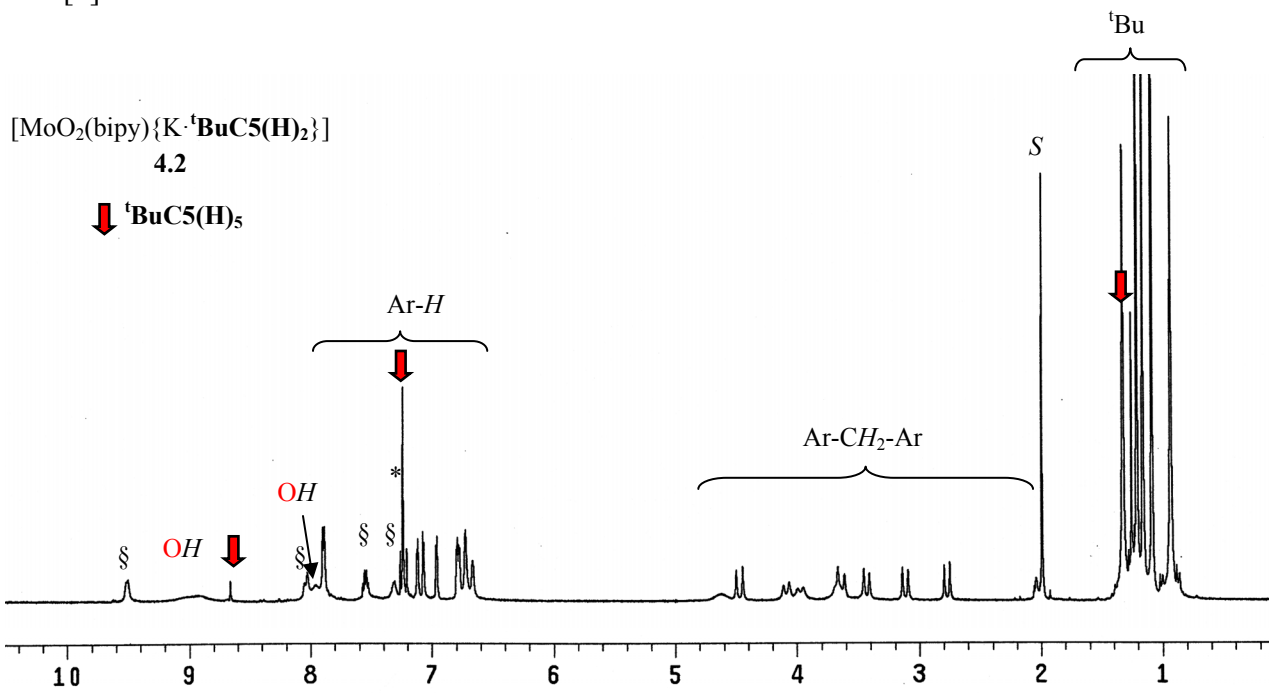

Figure 4.4 ^{1}H NMR spectrum of compound [MoO_2(bipy){K·^{t}**BuC5(H)$_2$**}] **4.2** in *$CDCl_3$. § = bipy aromatic protons and *S* = CH_3CN.

Two interesting observations can be made from the ^{1}H NMR spectrum of compound **4.2**. First, the two broad signals for the methylene protons at 4.61 and 3.67 ppm suggest that these protons are in conformational equilibrium at room temperature. Second, the upfield methylene resonance at 2.02 ppm indicates that there is a high degree of shielding for one methylene proton. This shielding can be caused by an aromatic ring where the proton is positioned above the

aromatic ring.[83] The overall ^{1}H NMR pattern suggests that the metallocalix[5]arene has C_1 symmetry.[30]

Attempts to remove the traces of parent calix[5]arene from compound **4.2** were unsuccessful. Complex **4.2** is air stable, but in solution it decomposes to the parent calix[5]arene. This process is almost instantaneous in the presence of water. The compound can be stored in the solid state in an inert atmosphere with no apparent decomposition.

The molecular structure of compound **4.2** was proposed based on its spectroscopic characterization, since attempts to obtain crystals suitable for X-ray analysis were unsuccessful (Figure 4.5).

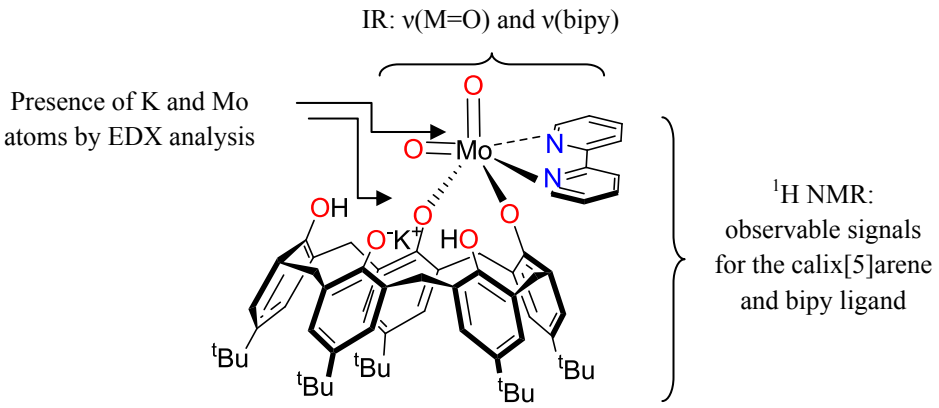

Figure 4.5 Proposed structure for compound **4.2** based on its spectroscopic characterization.

In the ^{1}H NMR spectrum we observed the protons for the bipy ligand, suggesting that the bipy ligand is contained in the molecular structure of **4.2**. Using IR spectroscopy we observed the characteristic frequencies for the symmetric and asymmetric vibrations ν(M=O) at 907 and 886 cm^{-1}, and for the bipy ligand (1602, 1494, 1160, 1107, 1028 and 765 cm^{-1}). Qualitative

analysis performed by EDX established the presence of both K and Mo atoms in the sample, but not the presence of Cl (Figure 4.6).

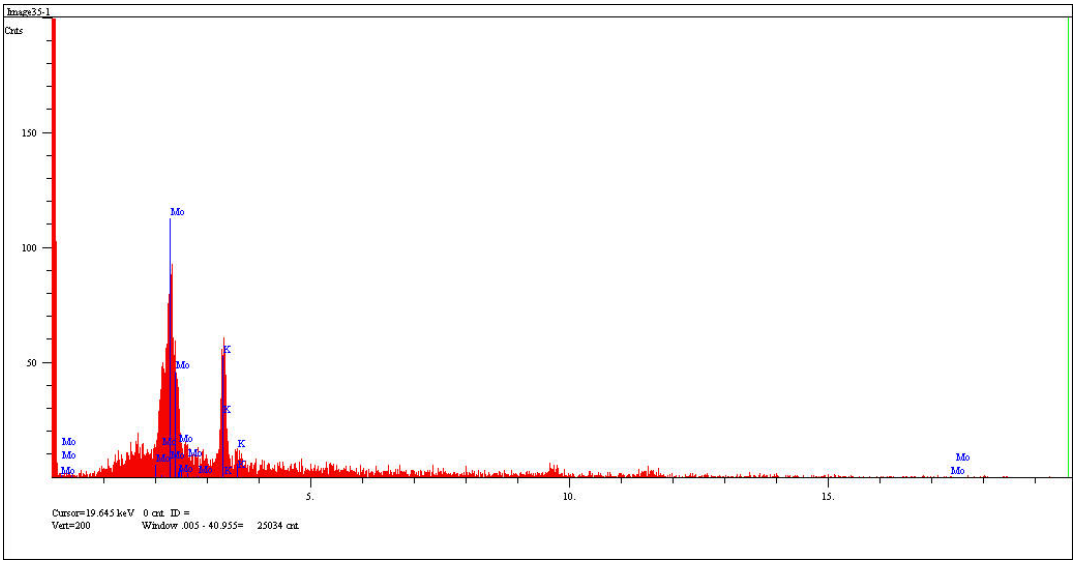

Figure 4.6 EDX spectrum of the pale brown solid (**4.2** and calix[5]arene) demonstrating that Mo and K are contained in the sample.

4.2.2.2 Synthetic approach using mixture of hexanes and acetonitrile (in a 7:2 ratio)

In Sections 4.2.1 and 4.2.2.1 we ended up with different compounds. Compound **4.2** shows totally different spectroscopic data in comparison to compound **4.1**. Attempts to isolate pure compounds or crystals were not successful. In both complexes parent calix[5]arene was present. Presumably moisture is causing the decomposition either the calix[5]arene salt or the product **4.1** or **4.2**, resulting in the formation of parent calix[5]arene.

From Chapter 3 we discovered that successive hexane washing cycles removed parent calix[5]arene from the reaction mixtures, leaving a single compound. However, the same method

was unsuccessful for complex **4.2**. Rather, an increase in the amount of calix[5]arene was observed.

Using a different approach for the synthesis of $(MoO_2)^{2+}$-containing calix[5]arene complexes we decided to use a mixture of solvents. It is well known that acetonitrile and hexane are not miscible solvents.[174] We hypothesized that an excess of hexane would remove any calix[5]arene formed during the reaction, and the molybdenum complex **4.2** could remain in the acetonitrile phase. We therefore ran a reaction between MoO_2Cl_2(bipy) and $K_2\cdot$**^{t}BuC5(H)$_3$** (in a 1:1 ratio) in a mixture of hexane and acetonitrile (in a 7:2 ratio) at room temperature for 12 hrs. At the end of the reaction time and after workup a yellow solid was recovered. Its ^{1}H NMR spectrum is shown in Figure 4.5.

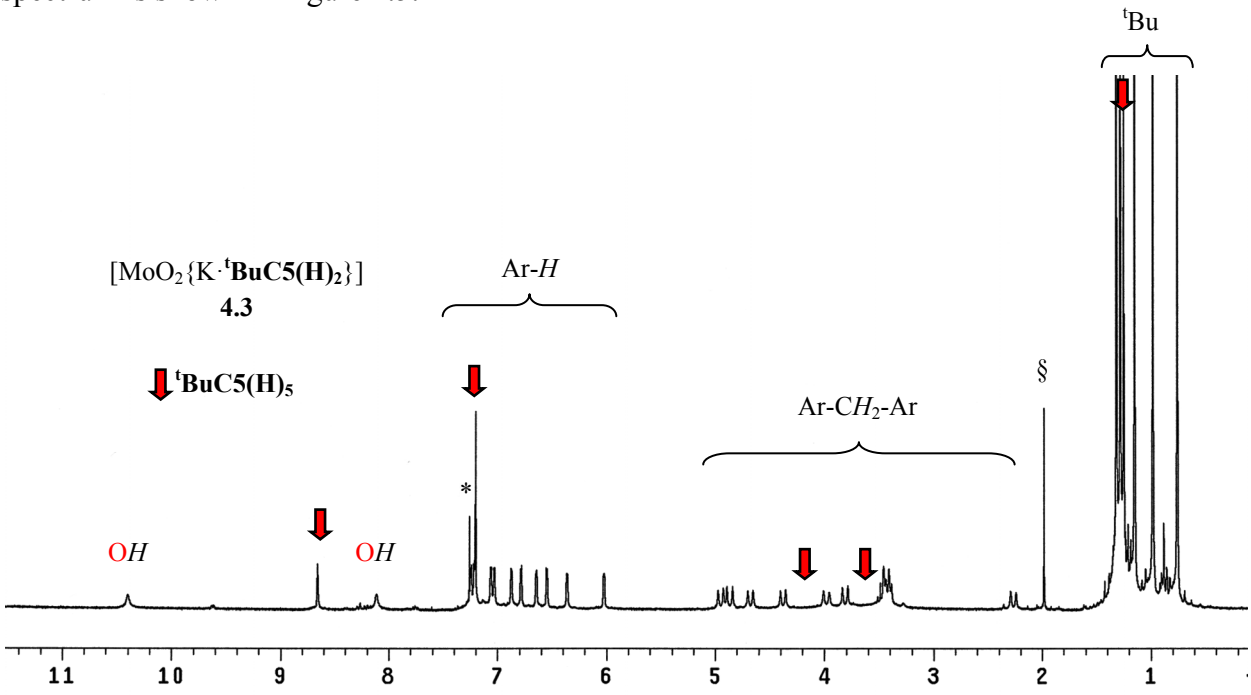

Figure 4.7 ^{1}H NMR spectrum of compound [MoO_2{K·^{t}**BuC5(H)$_2$**}] **4.3** in *$CDCl_3$. §CH_3CN residual solvent.

The ^{1}H NMR pattern for compound **4.3** is totally different from that found for compounds **4.1** and **4.2**. One main difference between **4.2** and **4.3** is the absence of the bipy ligand aromatic resonances for **4.3**.

The ^{1}H NMR spectrum of compound **4.3** shows five resonances for the *tert*-butyl groups and nine doublets (due to the ^{2}J geminal coupling) are found for the methylene bridging groups Ar-CH_2-Ar. In the aromatic region ten doublets for the aromatic protons Ar-*H* (7.25 – 6.04 ppm, ^{4}J = 2.2 Hz) are observed. Finally, two different OH groups are seen at 10.41 and 8.14 ppm in a 1:1 ratio. Overall, the symmetry of compound **4.3** is best described as C_1.[30]

Attempts to separate compound **4.3** from the parent calix[5]arene were unsuccessful. Complex **4.3** is stable in the solid state in an inert atmosphere with no decomposition, but in solution compound **4.3** decomposes slowly to the parent calix[5]arene. The molecular structure of the compound **4.3** was proposed based on its spectroscopic characterization, since attempts to obtain crystals suitable for X-ray analysis were unsuccessful (Figure 4.8).

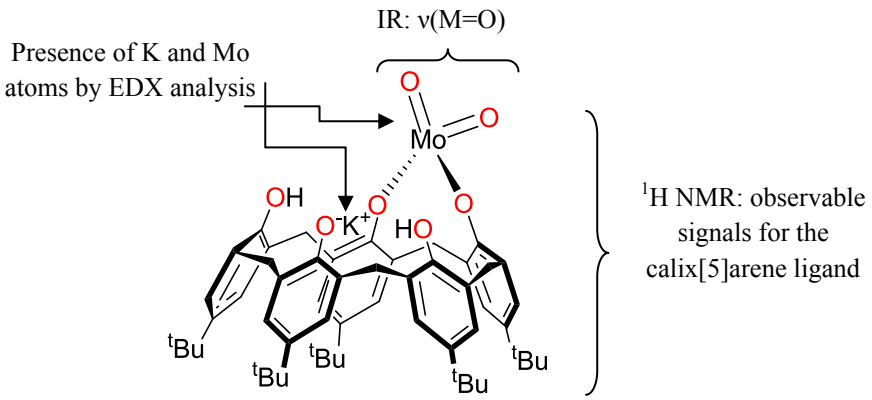

Figure 4.8 Proposed structure for compound **4.2** on the basis of its spectroscopic characterization.

In the IR spectrum we observed the frequencies for the ν(M=O) vibrations at 914 and 883 cm^{-1}, and no bipy absorbance. Qualitative analysis performed by EDX established the presence of both K and Mo atoms in the sample.

One interesting fact is that whenever we used MoO_2Cl_2 or MoO_2Cl_2(bipy) we ended up with a mixture of a MoO_2 calix[5]arene complex (**4.1-3**) in mixture with parent calix[5]arene. Each compound was different, but at this point we are unable to isolate them in pure form, due to their slow decomposition in solution and reactivity towards moisture.

A summary of the IR and ^{1}H NMR data for compounds **4.1-3** is presented in Tables 4.1 and 4.2. In Scheme 4.2 we show the synthetic pathway for each compound.

Table 4.1 IR and qualitative data found for compounds **4.1 – 4.3**.

IR (cm^{-1}) ν(M=O)	918, 885	907, 886	914, 883
Symmetry	C_s	C_1	C_1
Aspect	blue solid	pale brown solid	yellow solid
EDX	Mo	Mo, K	Mo, K

Table 4.2 ^{1}H NMR (δ ppm, $CDCl_3$) data found for compounds **4.1 – 4.3**.

^{1}H NMR	**4.1**	**4.2**[a]	**4.3**[a,§]
-O*H*	9.03 (s, 1H) 8.66 (s, 2.5H, Cx5) 8.27 (s, 2H)	8.93 (br, 1H) 7.95 (br, 1H)	10.41 (s, 1H) 8.14 (s, 1H)
Bipy	-	9.50 (b, 1H*) 8.04 (b, 1H*) 7.55 (dd, 1H*, 4.4, 4.7 Hz) 7.30 (br, 1H*)	-
Ar-*H*	7.24 (d, 2H, *J* = 2.5 Hz) 7.21 (s, 7H, overlapped withCx5) 7.19 (d, 2H, *J* = 2.5 Hz) 7.16 (d, 2H, *J* = 2.2 Hz) 7.05 (d, 2H, *J* = 2.5 Hz)	7.90 (s, 1H) 7.89 (s, 1H) 7.12 (d, 1H, *J* = 2.5 Hz) 7.07 (d, 1H, *J* = 2.5 Hz) 6.96 (d, 1H, *J* = 2.2 Hz) 6.80 (d, 1H, *J* = 2.2 Hz) 6.78 (d, 1H, *J* = 1.9 Hz) 6.73 (s, 2H) 6.67 (s, 1H)	7.25 (d, 1H, *J* = 2.2 Hz) 7.23 (d, 1H, *J* = 3.0 Hz) 7.07 (d, 1H, *J* = 2.2 Hz) 7.04 (d, 1H, *J* = 1.9 Hz) 6.89 (d, 1H, *J* = 2.2 Hz) 6.80 (d, 1H, *J* = 2.5 Hz) 6.66 (d, 1H, *J* = 2.2 Hz) 6.56 (d, 1H, *J* = 2.5 Hz) 6.38 (d, 1H, *J* = 2.2 Hz) 6.04 (d, 1H, *J* = 1.9 Hz)
Ar-CH_2-Ar	4.87 (d, 2H, *J* = 14.0 Hz) 4.81 (d, 1H, *J* = 14.3 Hz) 4.48 (d, 2H, *J* = 13.8 Hz) 3.76 (br, 5H, Cx5) 3.51 (d, 2H, *J* = 13.8 Hz) 3.48 (d, 1H, *J* = 14.3 Hz) 3.29 (d, 2H, *J* = 14.3 Hz)	4.61 (br, 1H) 4.47 (d, 1H, *J* = 16.0 Hz) 4.09 (d, 1H, *J* = 13.8 Hz) 3.97 (d, 1H, *J* = 13.8 Hz) 3.67 (br, 1H) 3.64 (d, 1H, *J* = 16.8 Hz) 3.43 (d, 1H, *J* = 13.8 Hz) 3.12 (d, 1H, *J* = 14.0 Hz) 2.77 (d, 1H, *J* = 13.8 Hz) 2.02 (d, 1H, *J* = 14.6 Hz)	4.96 (d, 1H, *J* = 14.3 Hz) 4.88 (d, 1H, *J* = 15.4 Hz) 4.69 (d, 1H, *J* = 14.6 Hz) 4.39 (d, 1H, *J* = 14.0 Hz) 3.99 (d, 1H, *J* = 15.4 Hz) 3.82 (d, 1H, *J* = 14.6 Hz) 3.45 (d, 2H, *J* = 14.6 Hz) 3.42 (d, 1H, *J* = 14.9 Hz) 2.28 (d, 1H, *J* = 14.9 Hz)
^{t}Bu	1.26 (s, 9H) 1.25 (s, 22.5H, Cx5) 1.24 (s, 18H) 1.22 (s, 18H)	1.32 (s, 9H) 1.21 (s, 9H) 1.16 (s, 9H) 1.09 (s, 9H) 0.93 (s, 10H*)	1.33 (s, 9H) 1.29 (s, 9H) 1.16 (s, 9H) 0.99 (s, 9H) 0.77 (s, 9H)

[a]Chemical shifts for calix[5]arene are omitted. *The integral values reported for the compound are not consistent with the values required. This disagreement in values could be due to overlapping with solvent or impurities. [§]The integral values were not recorded and are fixed to the expected values based on the proposed molecular formula.

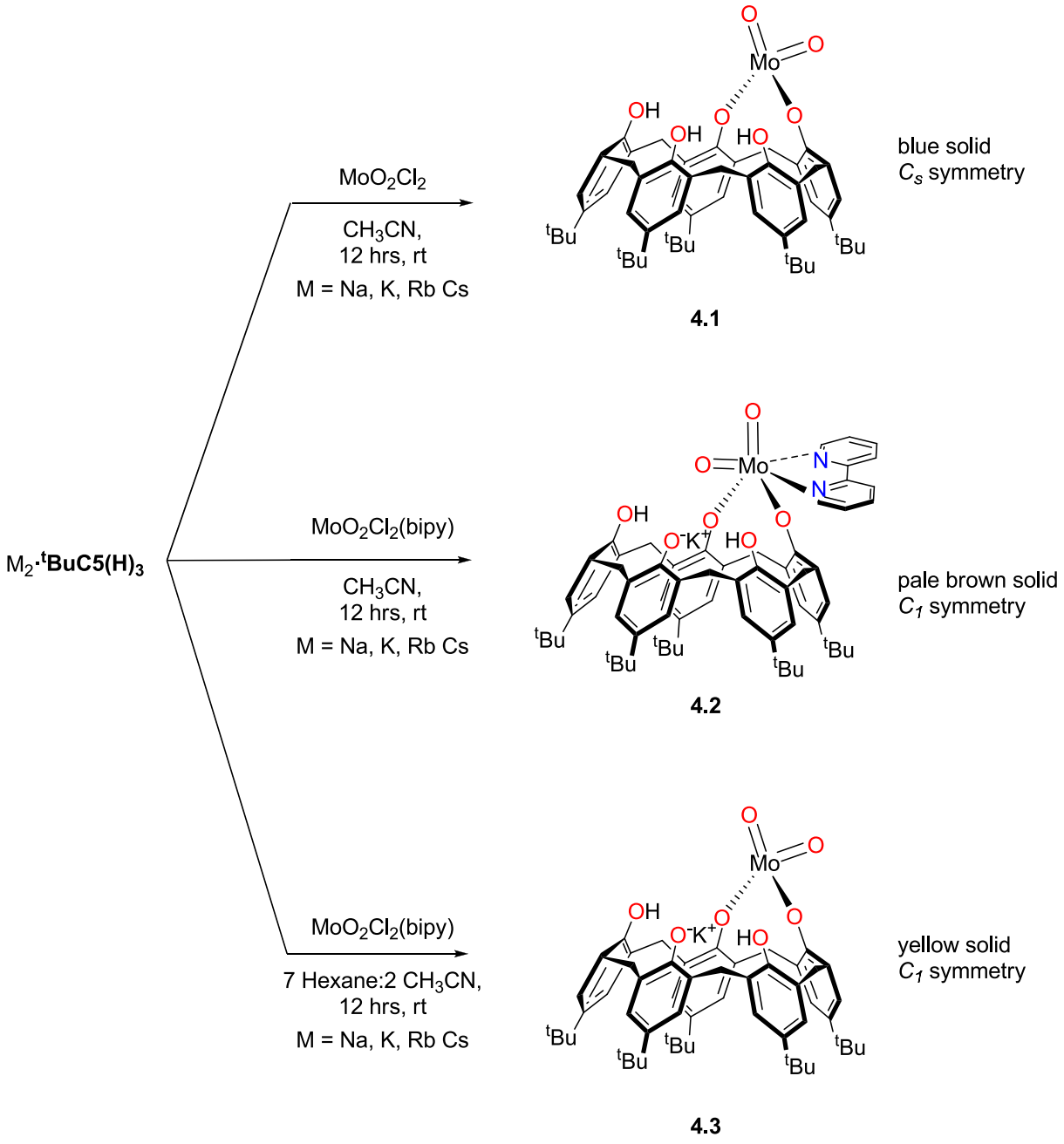

Scheme 4.2 Synthesis of $(MoO_2)^{2+}$-containing calix[5]arene complexes **4.1 – 4.3**.

4.2.3 Synthesis of dioxomolybdenum(VI) calixarene complexes from $MoO_2(acac)_2$

As described above, when we used MoO_2Cl_2 or MoO_2Cl_2(bipy) as precursors we ended up with a mixture of $(MoO_2)^{2+}$-containing calix[5]arene complexes and parent calix[5]arene. We decide to use a different source of $(MoO_2)^{2+}$, bis(acetylacetonato)dioxomolybdenum(VI) ($MoO_2(acac)_2$).

We screened an initial reaction with parent calix[5]arene (**^{t}BuC5(H)$_5$**). The reaction was followed by ^{1}H NMR spectroscopy and no new product was observed in different solvents or at either room or refluxing temperature. This lack of reactivity is consistent with the pK_a of acetylacetone (Hacac) (pK_a = 9.0, in water)[175] compared with the pK_a of **^{t}BuC5(H)$_5$** (pK_{a1} = 11.5 ± 0.7, pK_{a2} = 15.4 ± 1.0, in CH_3CN).[112] However, when $MoO_2(acac)_2$ was reacted with **^{t}BuC5(H)$_5$** and M_2CO_3 (M = Rb, Cs) in acetonitrile at 85 ^oC, two new compounds did form; **4.4a** and **4.4b.**

The synthesis of compounds **4.4a** and **4.4b** is illustrated in Scheme 4.3. Compounds **4.4a** or **4.4b** were each obtained as a small amount of red crystals (~10 mg) on the wall of the reaction vessel and at the bottom was found unreacted starting material. The crystals were carefully separated, and X-ray single crystal diffraction studies (**4.4a** and **4.4b**, respectively) were performed in collaboration with Dr. Daniel Mendoza-Espinosa.

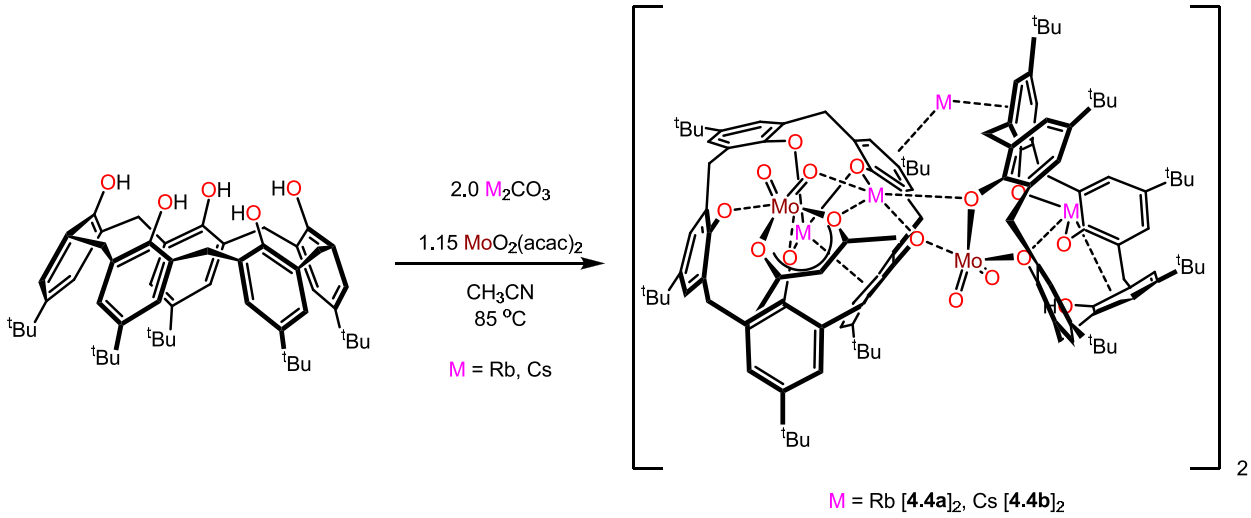

Scheme 4.3 Synthesis of compounds **4.4a** and **4.4b**.

The overall structure of complexes [**4.4a**]$_2$ and [**4.4b**]$_2$ is dimeric. Figures 4.9 and 4.10 illustrate the X-ray structures of [**4.4a**]$_2$ and [**4.4b**]$_2$ and selected bond lengths and angles for complex [**4.4a**]$_2$ are listed in Table 4.3. Compound **4.4b** is isostructural with **4.4a** as was demonstrated by X-ray studies.

In general the crystal structures of complexes [**4.4a**]$_2$ and [**4.4b**]$_2$ display very similar features. The X-ray structure of complex [**4.4b**]$_2$ could not be well refined due to poor quality of the crystal, but the atom connectivity is clear and allows its comparison with complex [**4.4a**]$_2$. The asymmetric units of compounds **4.4a** or **4.4b** each contain two molybdenum atoms, four alkali metals M (M = Rb **4.4a**, Cs **4.4b**) and two calixarene ligands. One of the MoO_2 moieties still contains an acac ligand, while the second is coordinated completely to both calix[5]arene ligands. Two of the alkali metal cations M(1,2) (M = Rb **4.4a**, Cs **4.4b**) are *endo* in calix[5]arene cavities, coordinated to the oxygen atoms, a solvent molecule, and to the arene rings through π-cation interactions. The third alkali metal M(3) (M = Rb **4.4a**, Cs **4.4b**) is *exo*, and connected to

the lower rim of the calix[5]arene. The final alkali metal M(4) (M = Rb **4.4a**, Cs **4.4b**) is *exo*, displaying interactions with solvent and π-cation interactions bridging the outside of two adjacent calix[5]arene rings. The alkali metal interactions observed in compound **4.4a** and **4.4b** are similar to those described in MoO_2 calix[4]arene alkali metal-containing complexes reported by our group.[110]

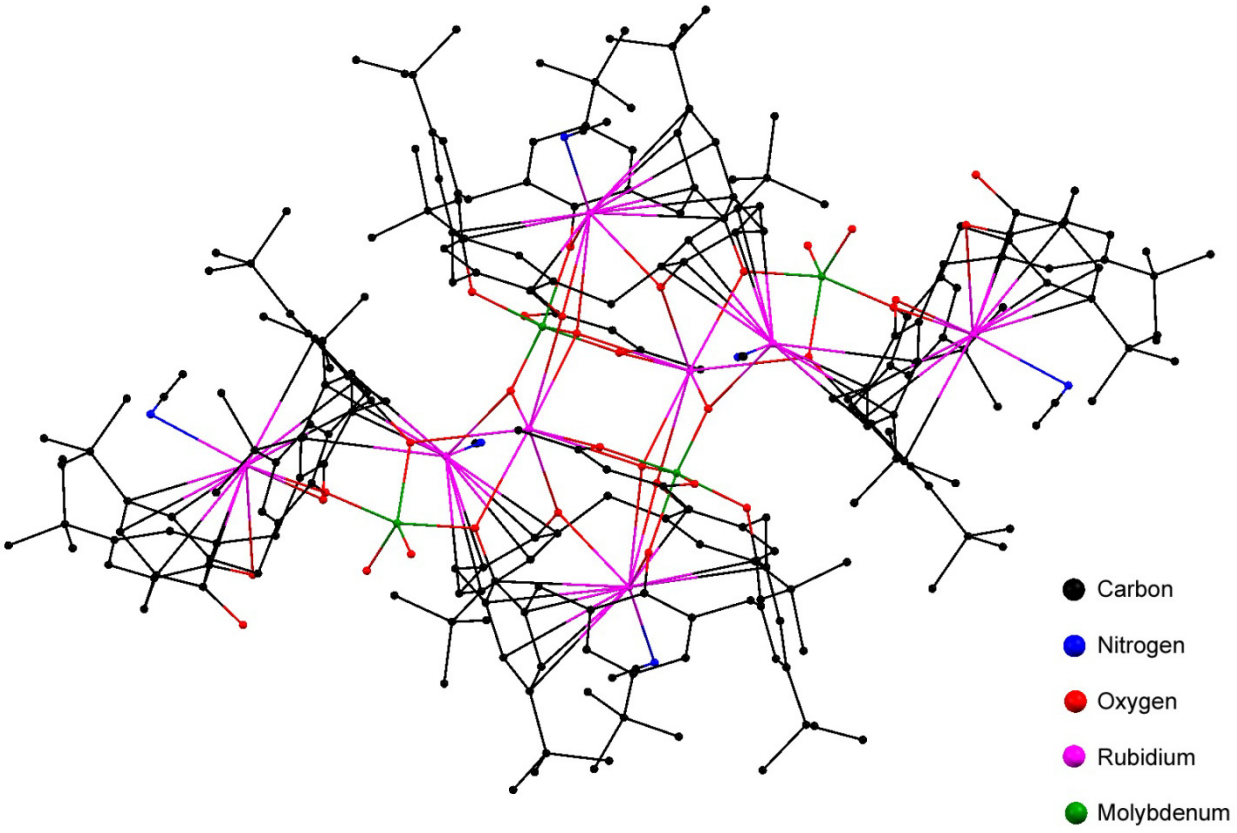

Figure 4.9 X-ray structure of the dimeric structure of **4.4a**. A ball and stick drawing is used for clarity. Non-coordinating acetonitrile molecules and hydrogen atoms have been omitted for clarity.

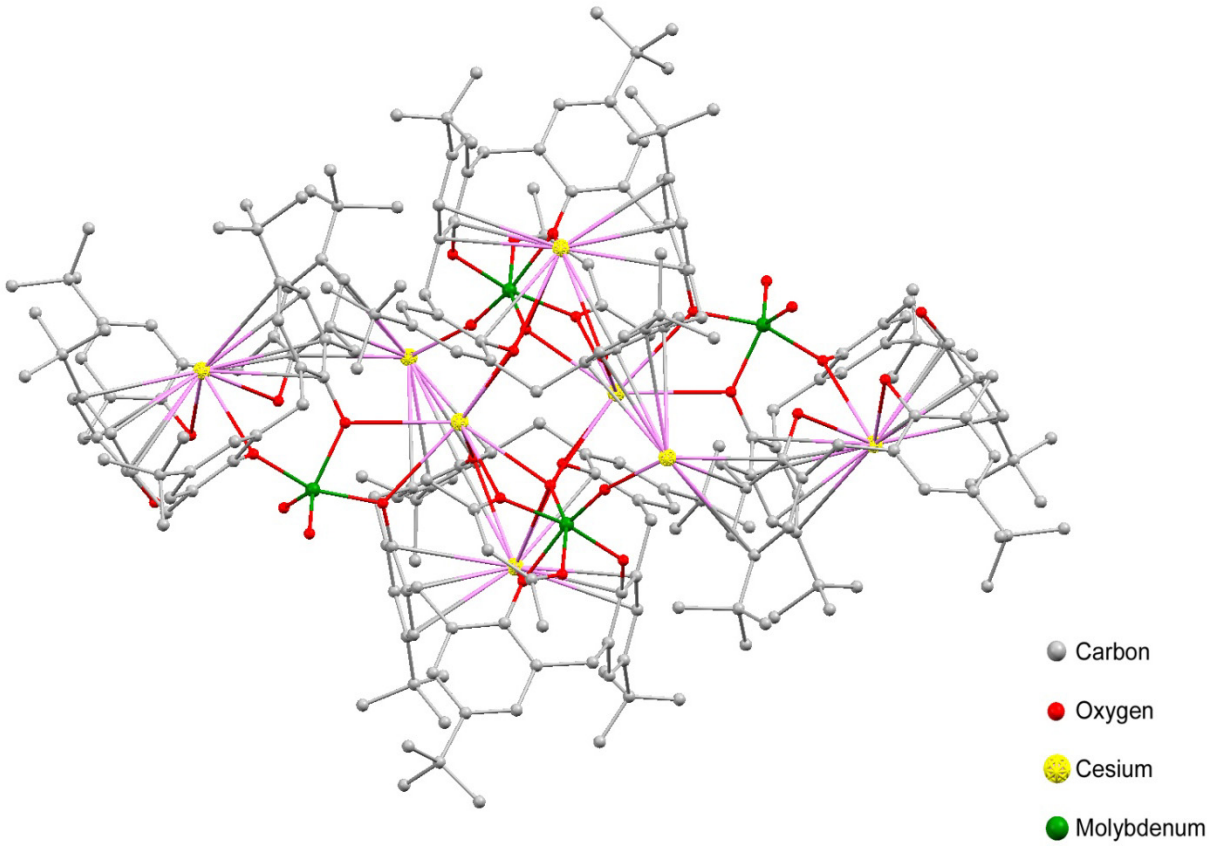

Figure 4.10 X-ray structure of the dimeric structure of **4.4b** displaying the atom connectivity. Ball and stick drawing is used for clarity. Hydrogen atoms have been omitted for clarity.

Complex **4.4a** contains two molybdenum atoms with two different geometries (Figure 4.11). Mo(1) is penta-coordinated and displays a distorted trigonal bipyramidal geometry with axial O(8,4) (O-Ar), and equatorial O(6,7) (Mo=O) and O(3) (O-Ar) atoms. The apical angle is O(4)-Mo(1)-O(8) = 161.57(2)^{o}, and the equatorial angles are O(3)-Mo(1)-O(6) = 122.91(15)^{o}, O(3)-Mo(1)-O(7) = 127.80(16)^{o}, and O(6)-Mo(1)-O(7) = 109.25(19)^{o}. The remaining angles range from 79.30(12) - 97.28(14)^{o}, two of these angles being below the ideal value of 90°. The distance *d*(Mo(1)-O) range from 1.686(3) – 2.014(3) Å with the shortest distance for the Mo=O bond.

Few crystal structures displaying five-coordinate geometry around molybdenum have been reported;[176-181] most exhibit trigonal bipyramidal geometry, though one example of square pyramidal[182] geometry has been reported.

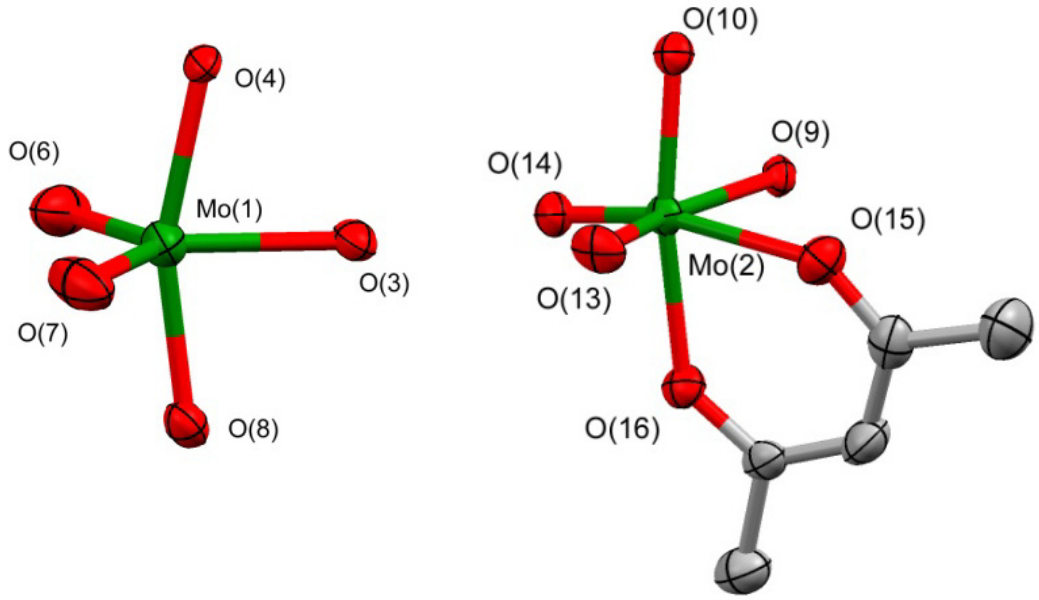

Figure 4.11 ORTEP drawing of the partial X-ray structure of compound **4.4a** showing the geometries around Mo(1) and Mo(2) centers.

Mo(2) is hexa-coordinated and can be described as distorted octahedral geometry, with the oxo ligands *cis* to each other. The apical angle defined as O(10)-Mo(2)-O(16) = 170.39(12)^{o} is close to the ideal value of 180°. The equatorial angles range from 80.50(12) – 102.62(15)^{o}. The distance *d*(Mo(2)-O) = 1.704(3) – 2.174(3) Å with the shortest distance for the Mo=O bond.

Table 4.3 Selected bond lengths (Å) and angles (º) of complex [**4.4a**]$_2$·8CH_3CN

Mo=O		Mo=O		Rb(1)-O_{Cx5}	2.846(3)-3.214(3)
Mo(1)-O(6)	1.686(3)	Mo(2)-O(13)	1.716(3)	Rb(1)-C_{Cx5}	3.247(4)-3.451(4)
Mo(1)-O(7)	1.693(3)	Mo(2)-O(14)	1.704(3)	Rb(1)-N(1)	3.016(6)
				Rb(2)-O_{Cx5}	2.916(3)-3.033(3)
		Mo-O_{acac}		Rb(2)-O(14)$_{M=O}$	3.064(3)
-	-	Mo(2)-O(15)	2.174(3)	Rb(2)-C_{Cx5}	3.292(4)-3.447(4)
-	-	Mo(2)-O(16)	2.101(3)	Rb(2)-N(2)	2.940(6)
				Rb(3)-O_{Cx5}	3.020(3)-3.074(3)
Mo-O_{Cx5}		Mo-O_{Cx5}		Rb(3)-O_{acac}	3.298(3)
Mo(1)-O(3)	2.014(3)	Mo(2)-O(9)	2.023(3)	Rb(3)-O(14,14a)$_{M=O}$	2.853(3)-3.340(3)
Mo(1)-O(4)	1.971(3)	Mo(2)-O(10)	1.951(3)	Rb(4)-O(13)$_{M=O}$	2.798(3)
Mo(1)-O(8)	1.997(3)			Rb(4)-C_{Cx5}	3.233(5)-3.473(5)
O(6)-Mo(1)-O(7)		109.25(19)		O(14)-Mo(2)-O(13)	102.62(15)
O(6)-Mo(1)-O(4)		94.93(15)		O(14)-Mo(2)-O(10)#1	101.36(14)
O(7)-Mo(1)-O(4)		91.93(15)		O(13)-Mo(2)-O(10)#1	91.91(14)
O(6)-Mo(1)-O(8)		97.28(14)		O(14)-Mo(2)-O(9)#1	92.22(13)
O(7)-Mo(1)-O(8)		97.00(14)		O(13)-Mo(2)-O(9)#1	165.16(14)
O(4)-Mo(1)-O(8)		161.57(12)		O(10)#1-Mo(2)-O(9)#1	85.42(12)
O(6)-Mo(1)-O(3)		122.91(15)		O(14)-Mo(2)-O(16)	84.39(13)
O(7)-Mo(1)-O(3)		127.80(16)		O(13)-Mo(2)-O(16)	94.36(14)
O(4)-Mo(1)-O(3)		82.48(12)		O(10)#1-Mo(2)-O(16)	170.39(12)
O(8)-Mo(1)-O(3)		79.30(12)		O(9)#1-Mo(2)-O(16)	86.67(12)
				O(14)-Mo(2)-O(15)	162.51(14)
				O(13)-Mo(2)-O(15)	85.13(14)
				O(10)#1-Mo(2)-O(15)	93.94(13)
				O(9)#1-Mo(2)-O(15)	80.50(12)
				O(16)-Mo(2)-O(15)	79.36(12)

Figure 4.12 illustrates the coordination environment around the rubidium atoms. One of the rubidium atoms in compound **4.4a** is localized in the calix[5]arene cavity. Rb(1) is coordinated to three oxygen atoms from the calix[5]arene ligand, to a nitrogen atom from a solvent molecule and to the arene rings through inner π-cation interactions (η^3-ring C and η^6-ring

E). Rb(2) is also coordinated to three oxygen atoms and a solvent molecule, with additional π-cation interactions (η^6-ring F, η^2-ring H and η^1-ring J). Rb(3) is found on the lower rim, sandwiched by the two calix[5]arene ligands and coordinated by eight oxygen atoms from the calix[5]arene ligand, acac and the Mo=O moiety. The remaining Rb(4) atom is *exo*, displaying two η^6-ring A,J π-cation interactions with a distance $d_{B,J\text{-}Rb(4)}$ (centroid B,J – Rb(4)) = 3.142 and 3.007 Å comparable to that observed in $d_{E\text{-}Rb(1)}$ (centroid E – Rb(1)) = 3.067 Å and $d_{E\text{-}Rb(2)}$ (centroid F – Rb(2)) = 3.108 Å (Table 4.4).

The calix[5]arene rings in compound **4.4a** and **4.4b** adopt a pinched cone conformation due to the inner π-cation interactions.

Table 4.4 Selected *d*(centroid-Rb(1)), *d*(centroid-Rb(2)) and *d*(centroid-centroid) distances (Å), centroid-O-Rb(1), centroid-O-Rb(2), centroid-Rb(2)-centroid and centroid-C(11/99)-centroid angles (º) in compound **4.4a**.

centroid A-Rb(1)	4.579	centroid A-O(1)-Rb(1)	99.61
centroid B-Rb(1)	4.711	centroid B-O(2)-Rb(1)	112.73
centroid C-Rb(1)	3.322	centroid C-O(3)-Rb(1)	54.84
centroid D-Rb(1)	4.786	centroid D-O(4)-Rb(1)	117.62
centroid E-Rb(1)	3.067	centroid E-O(5)-Rb(1)	52.12
centroid E-centroid C	6.017	centroid A-C(11)- centroid B	117.77
centroid B-Rb(4)	3.142		
		centroid B-Rb(4)- centroid J	125.20
centroid F-Rb(2)	3.108		
centroid G-Rb(2)	4.858	centroid F-O(8)-Rb(2)	47.75
centroid H-Rb(2)	3.554	centroid G-O(9)-Rb(2)	117.81
centroid I-Rb(2)	4.369	centroid H-O(10)-Rb(2)	61.84
centroid J-Rb(2)	4.788	centroid I-O(11)-Rb(2)	97.93
centroid F-centroid H	6.144	centroid J-O(12)-Rb(2)	97.93
centroid J-Rb(4)	3.007	centroid J-C(99)- centroid I	122.23

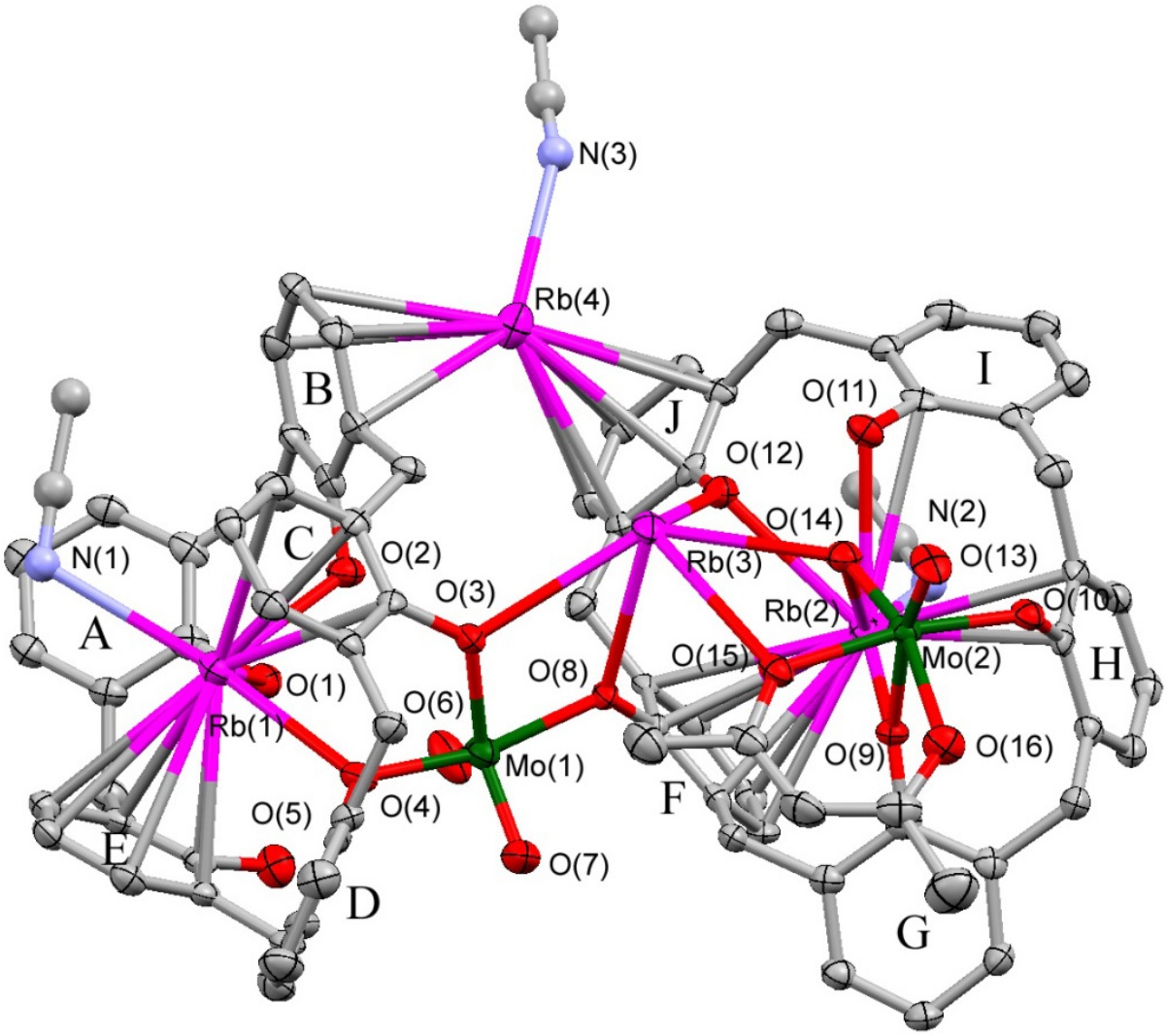

Figure 4.12 X-ray structure of the asymmetric unit of **4.4a**. The ball and stick and ORTEP drawing styles (50% probability ellipsoids) are used for clarity. Non-coordinating acetonitrile molecules, *tert*-butyl groups and hydrogen atoms have been omitted for clarity.

Attempts to increase the yield of compounds **4.4a** and **4.4b** were unsuccessful. The irreproducibility of our initial approach led us to seek better conditions for the isolation of **4.4a** or **4.4b**.

We envisioned that pure $Cs_2 \cdot$**^{t}BuC5(H)$_3$** salt might react with $MoO_2(acac)_2$ in a 1:1.5 ratio in anhydrous THF to give us the desired $(MoO_2)^{2+}$-calix[5]arene complex (Equation 4.6).

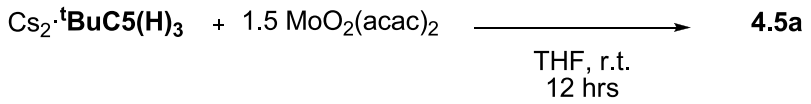

(4.6)

After workup a yellow solid was obtained, and its ^{1}H NMR spectrum is shown in Figure 4.13.

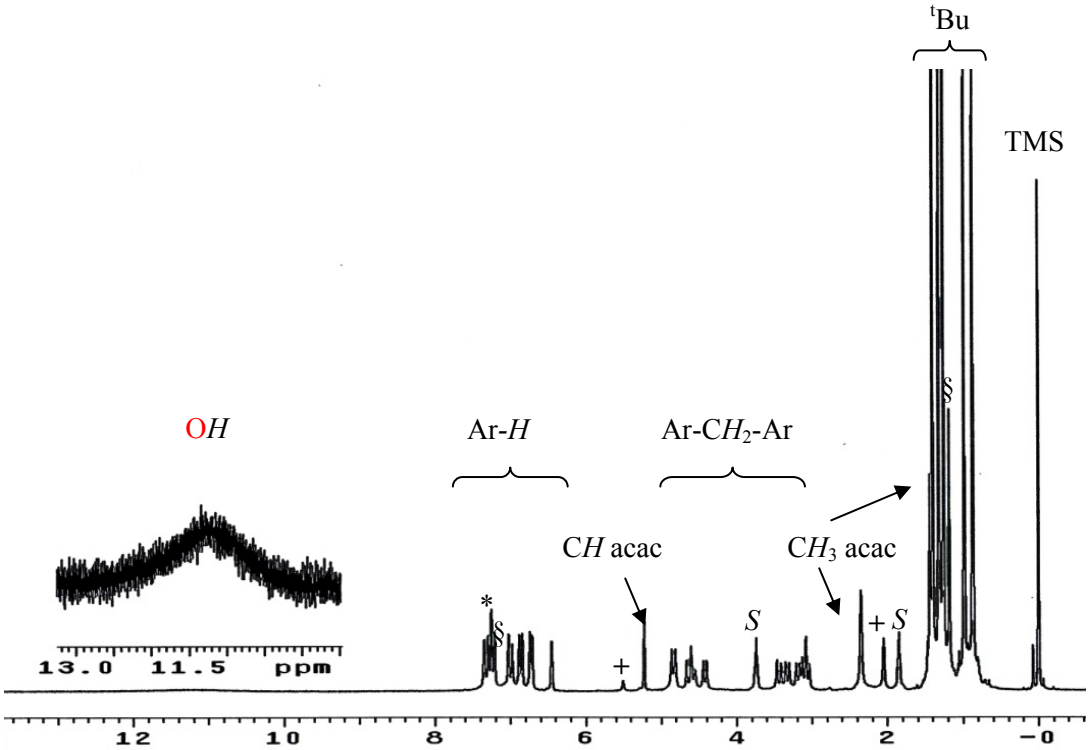

Figure 4.13 ^{1}H NMR spectrum of compound **4.5a** in *$CDCl_3$. § = $Cs_2 \cdot$**^{t}BuC5(H)$_3$**, + = Hacac, S = THF.

The ^{1}H NMR spectrum of sample **4.5a** showed a single compound with some impurities. The most difficult impurity to remove is the $Cs_2 \cdot$**^{t}BuC5(H)$_3$**, which has similar solubility to that of compound **4.5a** in common organic solvents. Attempts to purify the compound by crystallization resulted in the decomposition of **4.5a** to either parent calix[5]arene or $Cs_2 \cdot$**^{t}BuC5(H)$_3$**.

In order to find the best reaction conditions for the isolation of compound **4.5a**, we investigated the reaction in different molar ratios and solvents. We determined that the optimal conditions are $CHCl_3$ as reaction solvent and a 1:1.5 molar ratio ($Cs_2 \cdot$**^{t}BuC5(H)$_3$**:$MoO_2(acac)_2$).

The same procedure used for the synthesis of **4.5a** was used to isolate compounds **4.5b** and **4.5c** from the corresponding rubidium and potassium salts (Equation 4.7).

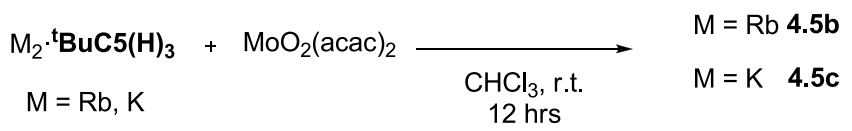

(4.7)

Compounds **4.5a-c** have limited solubility in pentane or hexane so they were purified by precipitation. Adding pentane or hexane to the crude product, and allowing the mixture to stand for one day at -34 ^{o}C, allowed **^{t}BuC5(H)$_5$** to be separated from the reaction mixture. Compounds **4.5a-c** generally decompose in solution in common organic solvents, resulting in the formation of $M_2 \cdot$**^{t}BuC5(H)$_3$** (M = K, Rb, Cs) and acetylacetone (Hacac). Long exposure to atmospheric moisture causes hydrolysis with liberation of Hacac.

The identity of complex **4.5a** (Figure 4.14) is suggested based on ^{1}H and ^{13}C NMR and IR spectroscopies, EDX (Electron Dispersion X-ray diffraction), elemental analysis and

confirmed by single crystal X-ray diffraction (Section 4.4). While the formulation for compounds **4.5b** and **4.5c** is still under current research.

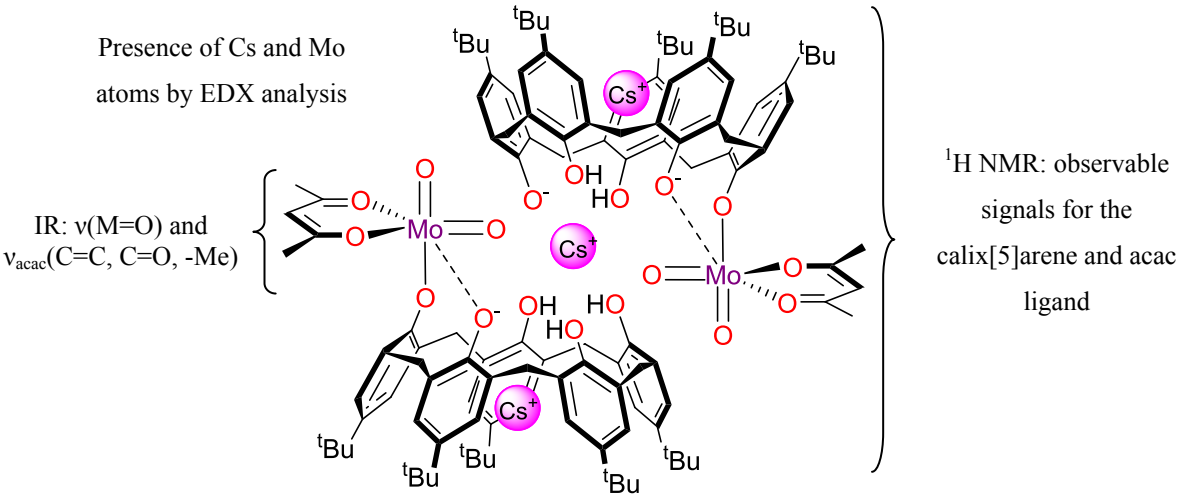

Cs[MoO_2(acac){Cs·**^{t}BuC5(H)$_{2.5}$**}]$_2$ **4.5a**

Figure 4.14 Molecular structure of compound **4.5a**.

4.2.3.1 ^{1}H NMR and infrared spectroscopies and EDX analysis

The ^{1}H NMR spectrum of complex **4.5a** (Figure 4.15) shows a broad signal at 10.71 ppm assigned to the OH groups, ten signals for the aromatic resonances (7.35 – 6.45 ppm), nine doublets for the methylene area (4.83 – 3.07 ppm, one pair overlapped), and finally five resonances for the *tert*-butyl area. This ^{1}H NMR pattern observed in compound **4.5a** is consistent with C_1 symmetry.[30]

The acac ligand displays a set of three sharp singlets, one at 5.25 ppm that is attributed to the C*H* group resonance. This value is consistent with the value of 4.93 ppm observed by Raston et al., in the compound [{MeOH·K·**^{t}BuC5(H)**}-μ-O-[Ti(acac)]$_2$ {THF·K·**^{t}BuC5(H)$_3$**}].[81] In the

aliphatic area at 2.37 and 1.44 ppm the resonances from two distinct $–CH_3$ groups were assigned to the acac ligand.

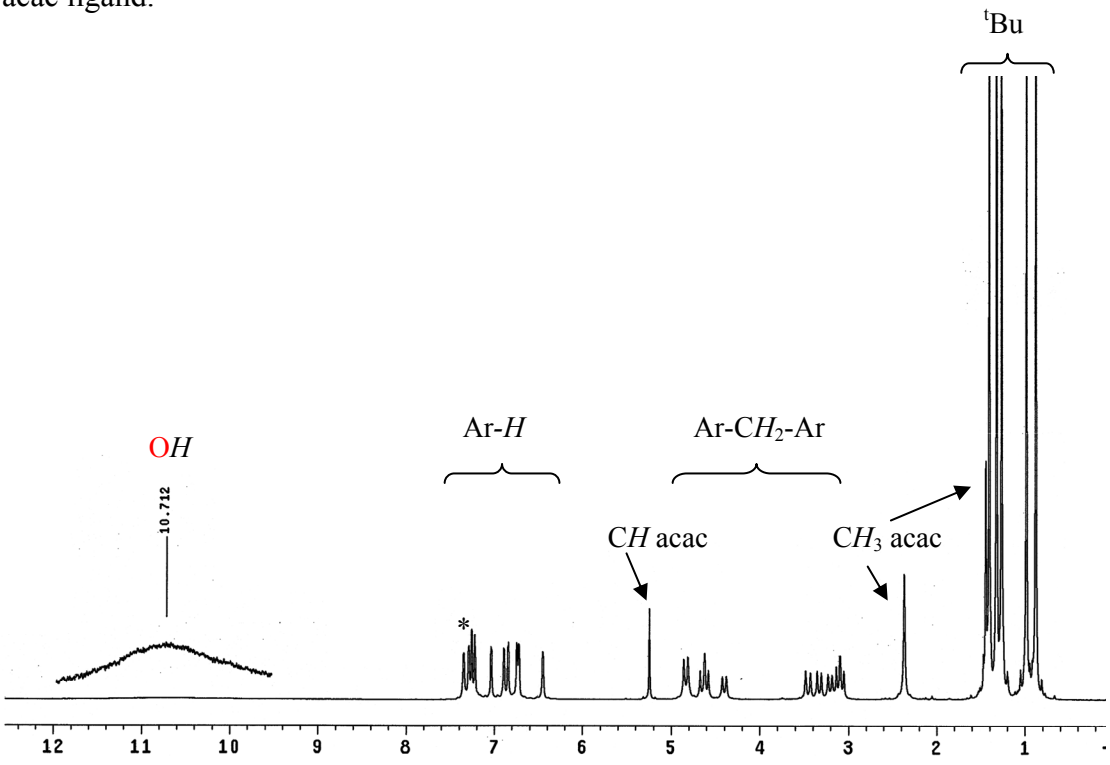

Figure 4.15 ^{1}H NMR spectrum of pure compound **4.5a** in *$CDCl_3$.

The ^{1}H NMR spectrum of complex **4.5b** (Figure 4.16) shows a similar pattern to that described for compound **4.5a**, with two notable differences. First, the OH resonances in compound **4.5b** appear as two singlets, at 8.85 and 7.48 ppm. Second, in compound **4.5b** there are also two different signals for two different coordinating acac ligands. The structure of complex **4.5b** could be similar to that of compound **4.5a**, but with an extra coordinated acac ligand.

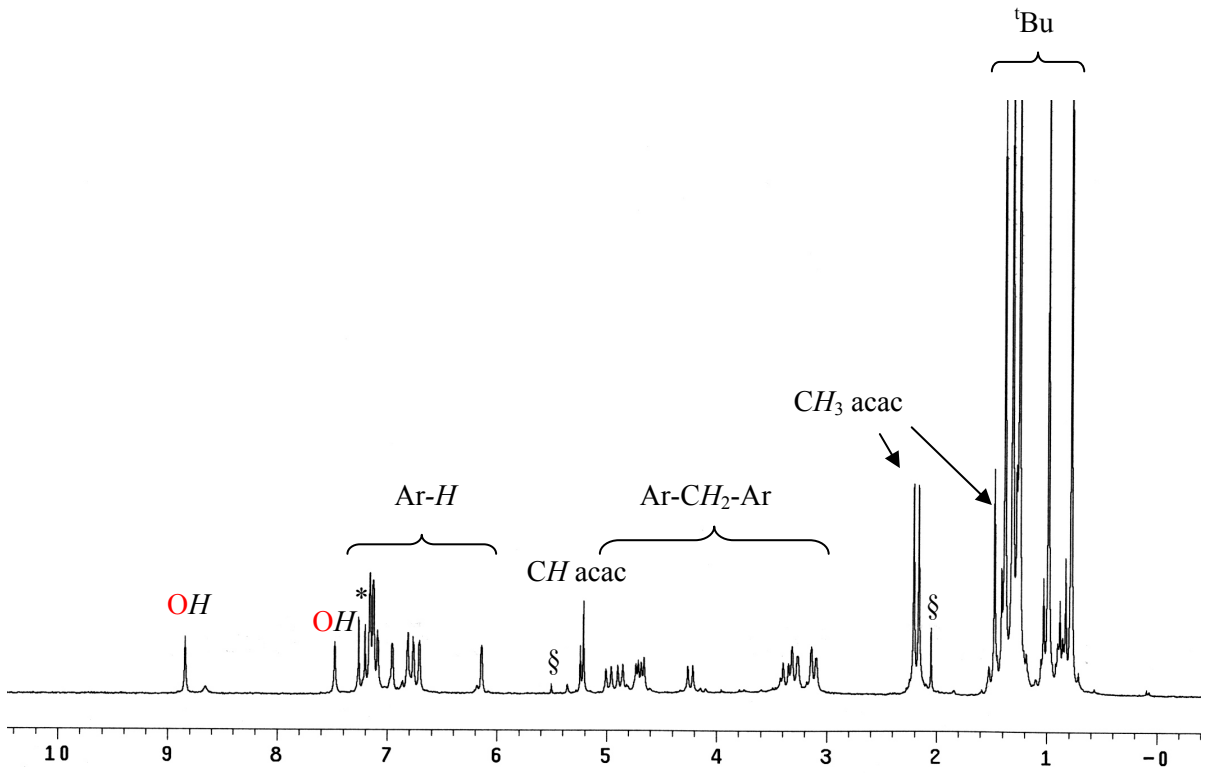

Figure 4.16 ^{1}H NMR spectrum of compound **4.5b** in *$CDCl_3$. § Hacac.

The ^{1}H NMR spectrum of compound **4.5c** is shown in Figure 4.17. This spectrum is more complicated than the previous ones, showing two non-equivalent calix[5]arene rings in the molecule, resulting in a C_1 symmetry. Eighteen signals out of expected twenty (some are overlapped) are found in the aromatic area (7.53 – 6.03 ppm), twenty different doublets are found in the methylene area (5.19 – 2.88 ppm), ten *tert*-butyl resonances (1.38 – 0.77 ppm) are found, and finally four resonances for four distinct OH groups appear at 10.81, 9.97, 8.60 and 4.70 ppm. The upfield signal for the OH group (4.70 ppm) has a similar chemical shift to that observed in dimeric phosphorus-bridged calix[5]arene compound (4.75 ppm) $\{$**^{t}BuC5(H)$_2$(P)**$\}_2$[138] but it is even more upfield than the value found for compound **3.2** (5.75 ppm).

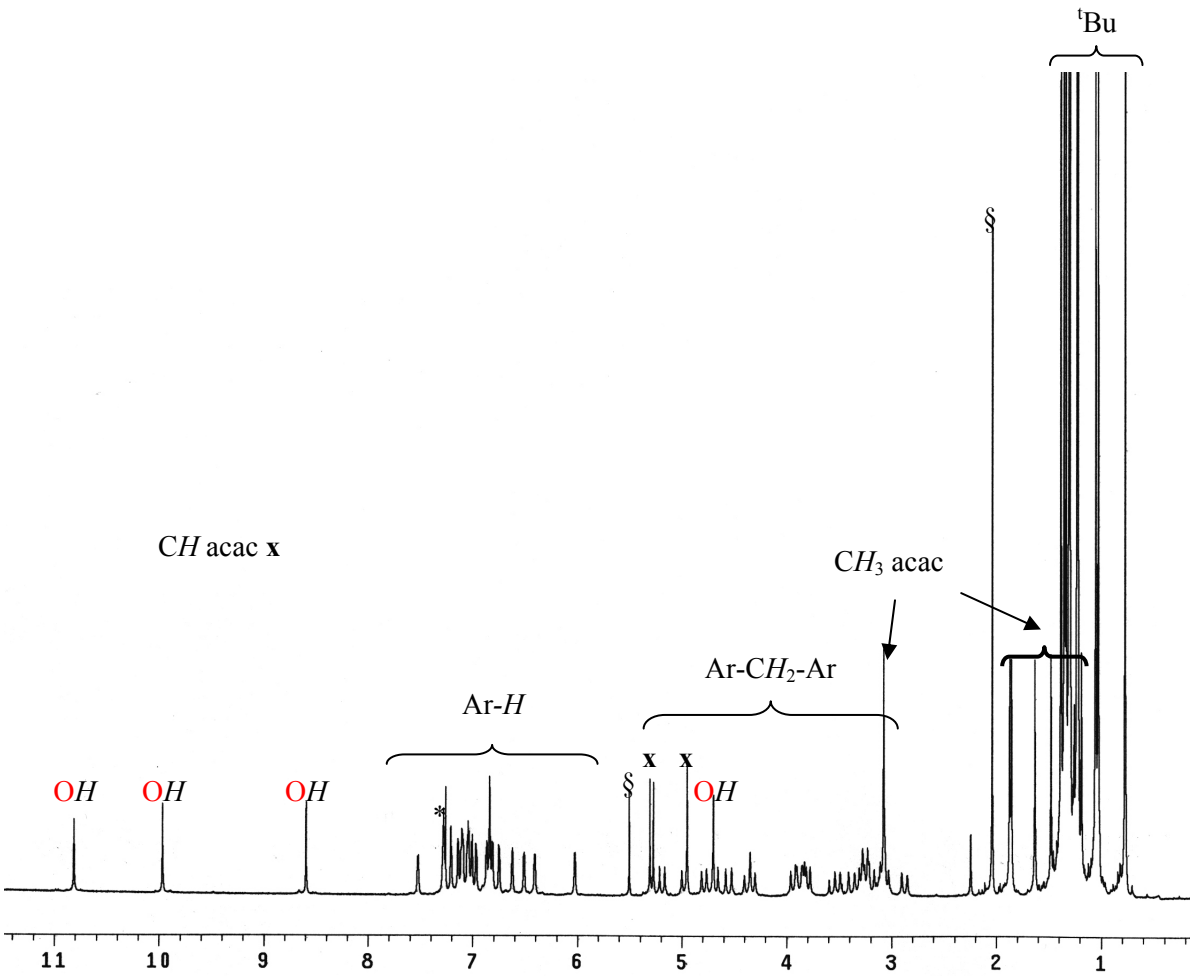

Figure 4.17 ^{1}H NMR spectrum of compound **4.5c** in *$CDCl_3$. § Hacac.

The differences between found in compound **4.5c** compared to compounds **4.5a** and **4.5b** might be caused by the π-cation interactions with the alkali metal. These π-cation interactions could be stronger with the K atom, making the framework of the calix[5]arene more rigid. Alternatively, the difference could be caused by the presence of an extra $MoO_2(acac)^+$ moiety disrupting the symmetry of the complex.

Indeed, three acac ligands and one free Hacac were observed in the spectrum of compound **4.5c**, while just two acac ligands were found in **4.5a**. The additional acac ligand

suggests the presence of an extra $MoO_2(acac)^+$ moiety in compound **4.5c**. Elemental analysis is also consistent with the presence of three $MoO_2(acac)^+$ moieties, two $K_2 \cdot$**^{t}BuC5(H)$_2$** and one molecule of Hacac. Currently, the connectivity and molecular structure of compound **4.5c** is under investigation. Table 4.5 gives a summary of the ^{1}H NMR data for complexes **4.5a** – **4.5c**.

Table 4.5 ^{1}H NMR chemical shifts (ppm) of compounds **4.5a** to **4.5c** in $CDCl_3$.

Compound	O*H*	Ar-*H*	Ar-C*H*$_2$-Ar	acac (C*H*)	acac C*H*$_3$	^{t}Bu (ratio)
4.5a	10.71	7.35-6.45 (10 signals)	4.83-3.07 (9 doublets)	(5.25)	2.37; 1.44	1.40-0.87 (1:1:1:1:1)
4.5b	8.85 7.48	7.16-6.14 (8 signals)	4.98-3.11 (10 doublets)	(5.24, 5.21)	2.21; 2.16; 2.05; 1.47	1.38-0.78 (1:1:1:1:1)
4.5c	10.81 9.97 8.60 4.70	7.53-6.03 (18 signals)	5.19-2.88 (20 doublets)	(5.30, 5.27, 4.95)	3.08; 1.87; 1.85; 1.63; 1.48; 1.19	1.38-0.77 (1:1:1:1:1:1:1:1:1:1)

Additional characterization of complexes **4.4a-b** was performed by EDX and IR spectroscopy. For example, the EDX experiment on compound **4.5a** showed that the sample contains both Mo and Cs atoms. The EDX result in compounds **4.5b** and **4.5c** was consistent with the proposed formulation i.e., Mo and Rb were contained in compound **4.4b** and Mo and K were contained compound **4.4c**.

In the infrared spectrum, two very strong ν(M=O) bands can be observed at 917, 879 cm^{-1} (**4.5a**), 914, 883 cm^{-1} (**4.5b**), and 914, 886 cm^{-1} (**4.5c**), characteristic of the symmetric and asymmetric stretching vibrations of the *cis*-$(MoO_2)^{2+}$ fragment.[171,183] The values found in

compounds **4.5a-c** are higher than those reported in *cis*-MoO_2^{2+}-containing calixarene literature (*sym* 904-877 and a*sym* 879-831 cm^{-1})[110] as well as those of noncalixarene Mo dioxo aryloxide $MoO_2(O\text{-}2,6\text{-}t\text{-}Bu_2C_6H_3)_2 \cdot HO\text{-}2,6\text{-}t\text{-}Bu_2C_6H_3$ (898, 884 cm^{-1})[184] but lower than the Mo dioxo alkoxides (947-945, 927-881 cm^{-1})[183] (Table 4.6).

Table 4.6 Principal Infrared frequencies (cm^{-1}) of compounds **4.1**, **4.2**, **4.3** and **4.5a-c** in KBr pellets.

Compound	ν(O-*H)*	ν(C=O); ν(C=C)	ν(C-O)	ν(-CH_3)*	ν(Mo=O)
MoO_2Cl_2	-	-	-	-	915, 864
$MoO_2(bipy)Cl_2$[171]	-	-	-	-	930, 908
$MoO_2(OR)_2$[183]	-	-	-	-	947-945, 927-881
$MoO_2(OPh_2)_2$[183]	-	-	1264	-	962, 875
$MoO_2(OPh_2)_2(py)_2$[183]	-	-	1249	-	932, 904
$MoO_2(OAr)_2$[184]	-	-	1264	-	898, 884
MoO_2-calix[4]arene[110]	-	-	1283-1262		904-877, 879-831
$MoO_2(acac)_2$	-	1591, 1510	1265	1362	935, 906
4.1	3433, 3296	-	1293	-	918, 885
4.2	3402, 3296	-	1295	-	907, 886
4.3	3433, 3307		1293	-	914, 883
4.5a	3411, 3263	1602, 1523	1296	1363	917, 879
4.5b	3413, 3294	1596, 1527	1295	1362	914, 883
4.5c	3475	1596, 1528	1294	1364	914, 886

*Characteristic -CH_3 of methyl ketone.[185] R = -Me, -Et, -^{n}Pr.[183] Ar = O-2,6-^{t}$Bu_2C_6H_3$.[184]

*4.2.3.2 Crystal and molecular structure of complex [**4.5a**]$_2$·2C$_5$H$_8$O$_2$*

The crystal structure of [**4.5a**]$_2$·2C$_5$H$_8$O$_2$ is shown in Figure 4.18, and selected bond distances and angles are listed in Table 4.7 and Table 4.8. Suitable crystals of compound **4.5a** were obtained by a slow evaporation of a concentrated pentane solution with some drops of THF at -34 ^{o}C.

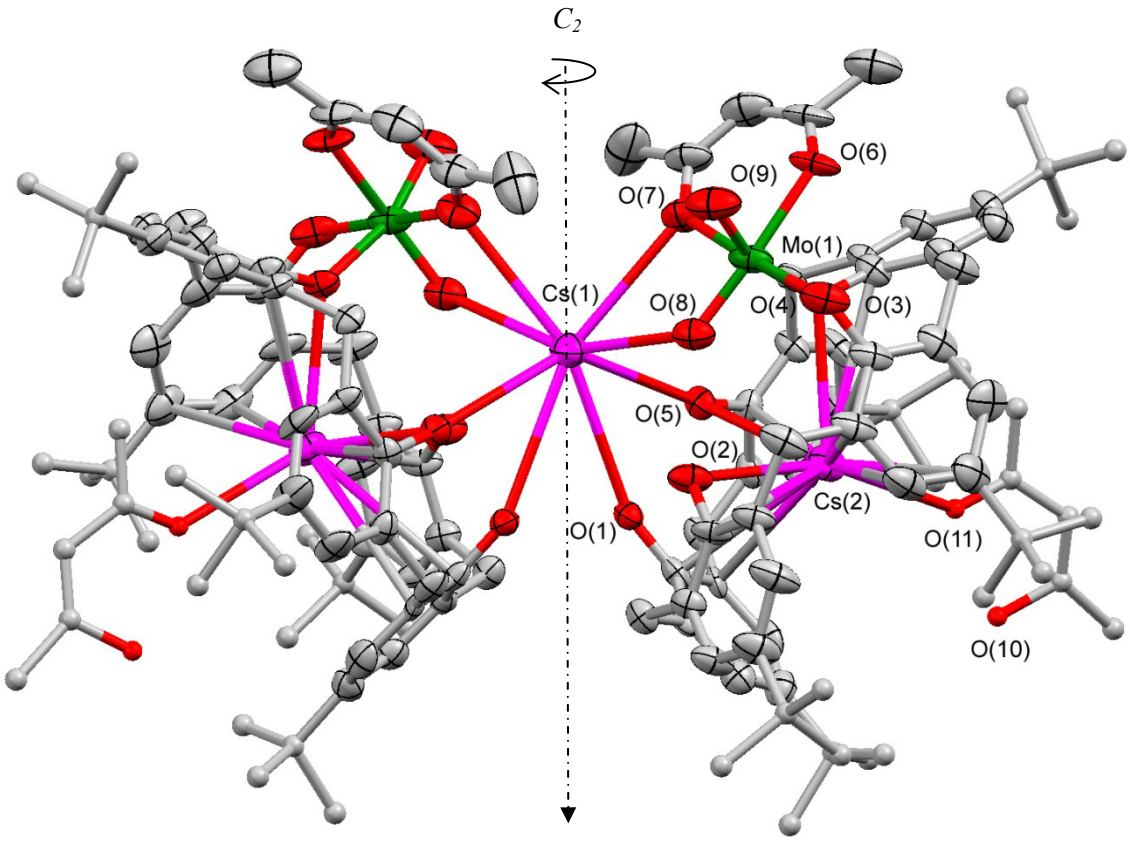

Figure 4.18 X-ray structure of [**4.5a**]$_2$·2C$_5$H$_8$O$_2$. ORTEP drawing (50% probability ellipsoids) and ball and stick drawing styles are used for clarity. Hydrogen atoms have been omitted for clarity.

Table 4.7 Selected bond lengths (Å) and angles (º) of complex [**4.5a**]$_2$·2$C_5H_8O_2$.

MoO_2(acac)			
Mo=O		Mo(1)#1-Cs(1)-Mo(1)	122.41(3)
Mo(1)-O(8)	1.717(15)	O(9)-Mo(1)-O(8)	104.9(2)
Mo(1)-O(9)	1.711(15)	O(9)-Mo(1)-O(3)	93.6(2)
		O(8)-Mo(1)-O(3)	99.0(2)
Mo-O_{acac}		O(9)-Mo(1)-O(4)	161.9(2)
Mo(1)-O(6)	2.157(5)	O(8)-Mo(1)-O(4)	93.13(19)
Mo(1)-O(7)	2.126(5)	O(3)-Mo(1)-O(4)	85.44(18)
		O(9)-Mo(1)-O(7)	93.3(2)
Mo-O_{Cx5}		O(8)-Mo(1)-O(7)	85.3(2)
Mo(1)-O(3)	1.950(5)	O(3)-Mo(1)-O(7)	170.75(19)
Mo(1)-O(4)	2.076(4)	O(4)-Mo(1)-O(7)	86.13(17)
		O(9)-Mo(1)-O(6)	84.9(2)
Cs(1)-O_{Cx5}	3.343(4) - 3.135(4)	O(8)-Mo(1)-O(6)	163.00(19)
Cs(1)-O(7)$_{acac}$	3.257(5)	O(3)-Mo(1)-O(6)	94.1(2)
Cs(1)-O(8)$_{Mo=O}$	3.033(5)	O(4)-Mo(1)-O(6)	77.12(18)
Cs(2)-O(11)$_{acac}$	3.199(13)	O(7)-Mo(1)-O(6)	80.3(2)
Cs(2)-O_{Cx5}	3.052(4) - 3.156(5)		
Cs(2)-C	3.416(6) – 3.868(6)		

Table 4.8 Selected *d*(centroid-Cs(2)), *d*(centroid E-centroid C) distances (Å) and centroid-O-Cs(2), centroid A-C(44)-centroid B angles (º) in compound [**4.5a**]$_2$·2$C_5H_8O_2$.

centroid A-Cs(2)	4.176	centroid A-O(4)-Cs(2)	104.35
centroid B-Cs(2)	3.730	centroid B-O(5)-Cs(2)	89.47
centroid C-Cs(2)	4.627	centroid C-O(1)-Cs(2)	66.01
centroid D-Cs(2)	3.351	centroid D-O(2)-Cs(2)	102.67
centroid E-Cs(2)	4.563	centroid E-O(3)-Cs(2)	49.62
centroid E-centroid C	6.582	centroid A-C(44)- centroid B	114.85

Compound [**4.5a**]$_2$·2$C_5H_8O_2$ is, to the best of our knowledge, the first fully characterized dioxomolydenum(VI)-containing calix[5]arene complex. The crystal structure contains two calix[5]arene ligands, three cesium and two molybdenum atoms, and additionally two molecules of Hacac. Cs(2) and Cs(2a) are each located in a calix[5]arene cavity. Each Cs(2, 2a) atom is coordinated to three calix[5]arene oxygen atoms (d(Cs(2)-O_{Cx5}) = 3.052(4) – 3.156(5) Å, d(Cs(2)-O(11)$_{Hacac}$ = 3.199(13) Å), and displays π-cation interactions with the five arene rings (η^2-ring A, η^1-ring B, η^4-ring C, η^1-ring D and η^1-ring E, d(Cs(2)-C_{Cx5}) = 3.416(6) – 3.868(6) Å). A C_2 axis passes through the Cs(1) atom (Figure 4.18). The Cs(1) atom is shared between the lower rims of both calix[5]arene ligands. Cs(1) atom is coordinated to a total of eight oxygen atoms, four coming from the calix[5]arene rings (2 each) and the rest from the MoO_2(acac) moiety (from the Mo=O and the acac ligand).

The apical angle defined by O(3)-Mo(1)-O(7) = 170.75(19)^o is similar to that found in the hexacoordinate Mo(2) in compound **4.4a** (O(10)-Mo(2)-O(16) = 170.39(12)^o) (Figure 4.19a). The equatorial angles in compound **4.5a** range from 77.12(18) – 104.9(2)^o, similar to those found in compound **4.4a** (80.50(12) – 102.62(15)^o). The d(Mo(1)-O) distances range from 1.711(15) – 2.157(5), with the short distance for the Mo=O bond. These distances are comparable to those reported in MoO_2-calixarene literature (d(M=O) = 1.694(3), 1.690(3) Å, d(Mo-O) = 1.916(3)-2.559(3) Å[165] and d(M=O) = 1.718(3), 1.735(3) Å, d(Mo-O) = 1.936(9)-2.1068(2) Å[110]). The distances observed for the Cs(1)-O bonds range from 3.033(5) – 3.343(4) Å, the shortest being O(8).

The calix[5]arene ligands in compound **4.5a** display a pinched cone conformation, previously observed in compound **4.4a** (Figure 4.19b). Finally, two molecules of Hacac are coordinated to the Cs(2) atom.

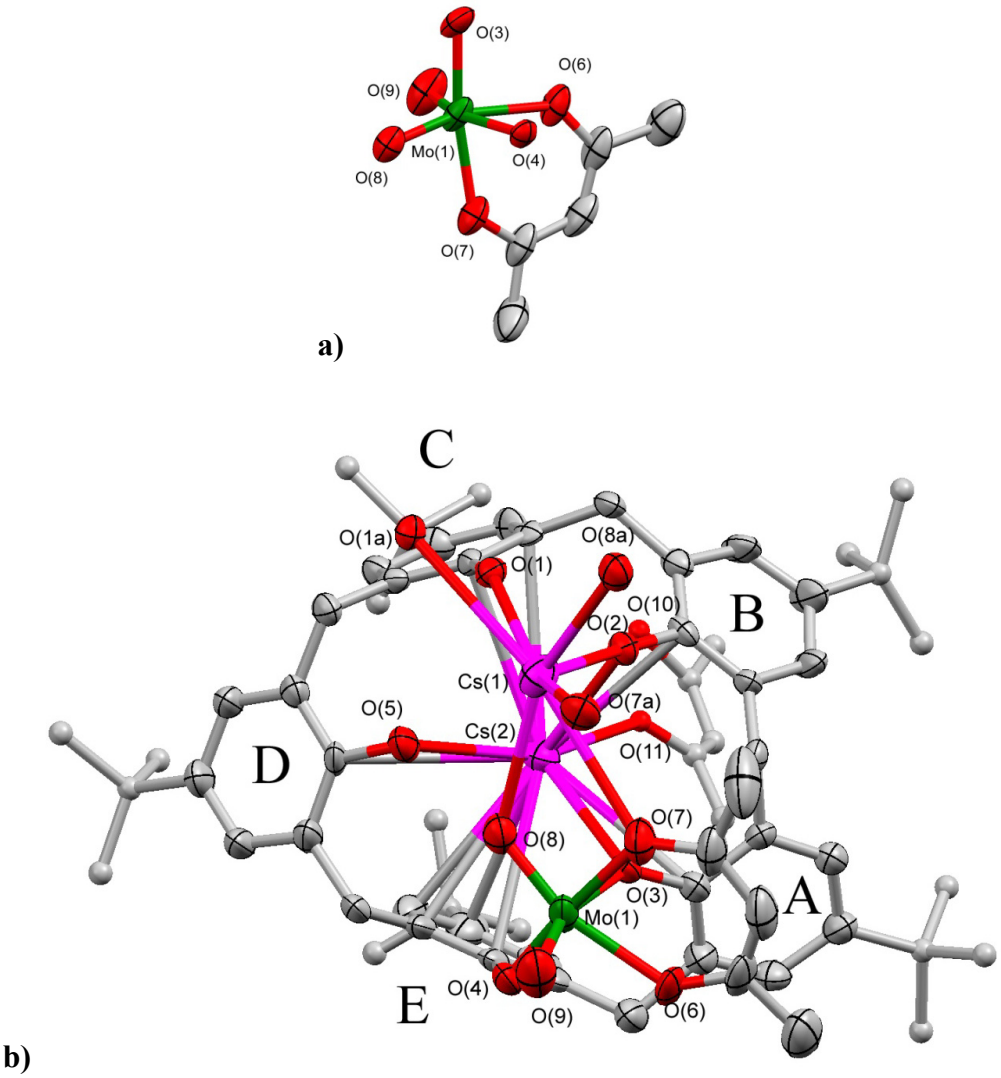

Figure 4.19 X-ray structure of the a) geometry around Mo(1) and of the b) top view of compound [**4.5a**]$_2$·2$C_5H_8O_2$. ORTEP drawing (50% probability ellipsoids) and ball and stick drawing styles are used for clarity. Half of the molecule and hydrogen atoms have been omitted for clarity.

4.3 Experimental Section

4.3.1 General Information

Unless otherwise noted, all manipulations were carried out in a dry nitrogen filled glove box. $M_2 \cdot$**^{t}BuC5(H)$_3$** (M = Na, K, Rb, Cs)[113] and dioxobis(2,4-pentanedionato)molybdenum(VI), ($MoO_2(acac)_2$),[186] were prepared by literature procedures. $M_2 \cdot$**^{t}BuC5(H)$_3$** (M = Rb, Cs) was left in the oven for 24 hrs before use (110 ^oC). MoO_2Cl_2 and 2,2'-bipyridine (bipy) were purchased from Aldrich and used without further purification. The melting points of all compounds were taken in capillary tubes on a Mel-Temp apparatus (Laboratory Devices, Cambridge, MA). A temperature proceeded by a ">" sign indicates that the compound starts to decompose. ^1H NMR and ^{13}C NMR spectra were recorded on a Varian XL-300 spectrometer at 300 and 75 MHz, respectively. Deuterated chloroform ($CDCl_3$) was dried over CaH_2 and was referenced to 7.26 ppm in ^1H NMR and 77.2 ppm in ^{13}C NMR. Microanalyses were performed by Atlantic Microlab, Inc, Norcross, GA. FTIR spectra were obtained as potassium bromide pellets in the range 400-4000 cm^{-1} with an Infinity Gold^{TM} FTIR spectrometer. UV/vis spectra were obtained on an Agilent 8453 spectrophotometer. All solvents were anhydrous and were stored over 4 Å molecular sieves for at least one day before use.

4.3.2 Synthesis of complexes

MoO_2Cl_2(bipy): A greenish blue solution of MoO_2Cl_2 (0.321 g, 1.61 mmol) in acetonitrile (3.0 mL) was added to a colorless solution of bipy (0.254 g, 1.63 mmol) in acetonitrile (5.0 mL). During addition the solution gradually turned to a white suspension. The reaction mixture was stirred at room temperature for 12 hrs. The resulting white suspension was filtered using a medium pore size frit. The white solid was washed with an additional ~15.0 mL

of anhydrous acetonitrile. The white solid was vacuum dried and identified as MoO_2Cl_2(bipy) (0.496 g, 1.40 mmol, 87% yield). Identification of the compound was performed by comparison of its IR vibration modes to those reported in the literature.[187] FTIR (KBr, cm^{-1}): 3435m (OH, from water), 3114w, 3084w, 3060w, 3037w, 1600s, 1573w, 1496s, 1475s, 1443s, 1318s, 1244w, 1226w, 1174w, 1155m, 1102w, 1074w, 1063w, 1028m, 936s (Mo=O), 905s (Mo=O), 776s, 734m, 654w, 636w, 421w. No further characterization was performed.

[MoO_2{^{t}**BuC5(H)$_3$**}] **4.1**: To a vigorously stirring solution of 0.133 g (0.150 mmol) of K_2·^{t}**BuC5(H)$_3$** in 2 mL of CH_3CN was added dropwise a light blue solution of 0.0308 g (0.155 mmol) MoO_2Cl_2 dissolved in 2 mL of CH_3CN. The addition took ~1 min, during which time the colorless solution turned into a red-brown suspension. The reaction mixture was stirred for 12 hrs at room temperature. The reaction mixture was then centrifuged for 25 min and the supernatant (light brown solution) discarded, while the black-blue solid was recovered and dried under vacuum. The dark blue solid was stirred with 10 mL of anhydrous hexane for 10 min and then filtered through ~1.0 g of Celite on a frit. The blue solution was recovered and the solvent removed by vacuum, to obtain 0.0981 g of a dark blue solid. Compound **4.1** can also be prepared with the sodium, rubidium and cesium dianionic salts: 0.0916 g (Na_2·^{t}**BuC5(H)$_3$**: 0.129 g, 0.151 mmol; MoO_2Cl_2: 0.0301 g, 0.151 mmol), 0.0858 g (Rb_2·^{t}**BuC5(H)$_3$**: 0.148 g, 0.151 mmol; MoO_2Cl_2: 0.0305 g, 0.153 mmol) and 0.0819 g (Cs_2·^{t}**BuC5(H)$_3$**: 0.162 g, 0.151 mmol; MoO_2Cl_2: 0.0303 g, 0.152 mmol). Mp: > 210 ^oC. ^1H NMR in $CDCl_3$ δ (ppm): 9.03 (s, 1H, OH), 8.66 (s, 2.5H, OH, Cx5), 8.27 (s, 2H, OH), 7.24 (d, 2H, *J* = 2.5 Hz, Ar-*H*), 7.21 (s, 7H, Ar-*H*, Cx5), 7.19 (d, 2H, *J* = 2.5 Hz, Ar-*H*), 7.16 (d, 2H, *J* = 2.2 Hz, Ar-*H*), 7.05 (d, 2H, *J* = 2.5 Hz, Ar-*H*), 4.87 (d, 2H, *J* = 14.0 Hz, Ar-CH_2-Ar), 4.81 (d, 1H, *J* = 14.3 Hz, Ar-CH_2-Ar), 4.48 (d,

2H, J = 13.8 Hz, Ar-CH_2-Ar), 3.76 (br, 5H, Ar-CH_2-Ar, Cx5), 3.51(d, 2H, J = 13.8 Hz, Ar-CH_2-Ar), 3.47 (d, 1H, J = 14.3 Hz, Ar-CH_2-Ar), 3.29 (d, 2H, J = 14.3 Hz, Ar-CH_2-Ar), 1.26 (s, 9H, ^{t}Bu), 1.25 (s, 22.5H, ^{t}Bu), 1.24 (s, 18H, ^{t}Bu), 1.22 (s, 18H, ^{t}Bu). The remaining ~38H observed in the aliphatic area accounts for 2.7 C_6H_{14} solvent molecules δ (ppm) = 1.28, 0.86. $^{13}C\{^1H\}$ NMR in $CDCl_3$ δ (ppm): 162.7, 158.7, 148.5, 148.2, 147.8, 147.1, 144.2, 143.4, 143.3, 132.5, 129.0, 127.4, 126.9, 126.4, 126.2, 126.1, 125.8, 125.7, 125.5, 124.9 (aromatic carbons), 35.3, 34.5 ($C(CH_3)_3$), 34.1 (Ar-CH$_2$-Ar), 32.2 ($C(CH_3)_3$), 31.7, 31.6 (C(CH$_3$)$_3$), 29.6, 29.1 (Ar-CH$_2$-Ar). FTIR (KBr, cm^{-1}): 3433s (OH), 3296s (OH), 3050m, 3028w, 2961s, 2907s, 2870s, 1600m, 1515w, 1505m, 1484s, 1461s, 1393m, 1364s, 1293s, 1244s, 1202s, 1122s, 1027w, 961m, 941m, 918m (Mo=O), 885m (Mo=O), 873s, 843m, 817m, 790s, 766w, 755w, 729w. UV/vis ($CHCl_3$) $\lambda_{max/nm}$: 241, 279, 286, 314, 356. At this point no % yield or ε values can be obtained because the pure compound cannot be isolated.

[MoO_2(bipy){K·^{t}**BuC5(H)$_2$**}] **4.2**: To a white suspension of MoO_2Cl_2(bipy) (0.0543 g, 0.153 mmol) in acetonitrile (3.0 mL) was added a suspension of K_2·^{t}**BuC5(H)$_2$** (0.134 g, 0.151 mmol) in acetonitrile (5.0 mL). Additional acetonitrile was used (~2.0 mL) in order to completely transfer the potassium salt. The reaction mixture gradually changed color during addition from a white suspension to yellow suspension and finally to an orange suspension. The reaction mixture was stirred for 12 hrs. A light brown suspension was obtained and was left to settle for 1 hr. The mixture was carefully decanted and the supernatant was discarded. Approximately 5 mL of acetonitrile was added and stirred for an additional 10 min. The solid was separated by centrifugation, and then washed with ~ 4.0 mL pentane. The light brown solid product recovered weighed 0.0886 g and was labeled as **4.2**. Mp: >208 ^oC. ^1H NMR ($CDCl_3$) δ

(ppm): 9.50 (s, 1H,* bipy), 8.93 (br, 1H, O*H*), 8.66 (s, §, OH, Cx5), 8.04 (d, 1H,* 7.4 Hz, bipy), 7.95 (br, 1H, O*H*), 7.90 (s, 1H, Ar-*H*), 7.89 (s, 1H, Ar-*H*), 7.55 (dd, 1H,* *J* = 4.4, 4.7 Hz, bipy), 7.30 (br, 1H,* bipy), 7.21 (s, §, Ar-CH_2-Ar, Cx5), 7.12 (d, 1H, *J* = 2.5 Hz, Ar-*H*), 7.07 (d, 1H, *J* = 2.5 Hz, Ar-*H*), 6.96 (d, 1H, *J* = 2.2 Hz, Ar-*H*), 6.80 (d, 1H, *J* = 2.2 Hz, Ar-*H*), 6.78 (d, 1H, *J* = 1.9 Hz, Ar-*H*), 6.73 (s, 2H, Ar-*H*), 6.67 (s, 1H, Ar-*H*), 4.61 (br, 1H, Ar-CH_2-Ar), 4.47 (d, 1H, *J* = 16.0 Hz, Ar-CH_2-Ar), 4.09 (d, 1H, *J* = 13.8 Hz, Ar-CH_2-Ar), 3.97 (d, 1H, *J* = 13.8 Hz, Ar-CH_2-Ar), 3.67 (br, 1H, Ar-CH_2-Ar), 3.64 (d, 1H, *J* = 16.8 Hz, Ar-CH_2-Ar), 3.43 (d, 1H, *J* = 13.8 Hz, Ar-CH_2-Ar), 3.12 (d, 1H, *J* = 14.0 Hz, Ar-CH_2-Ar), 2.77 (d, 1H, *J* = 13.8 Hz, Ar-CH_2-Ar), 2.02 (d, 1H, *J* = 14.6 Hz, Ar-CH_2-Ar), 1.99 (s, 2H,* CH_3CN), 1.32 (s, 9H, ^{t}Bu), 1.25 (s, §, ^{t}Bu, Cx5), 1.21 (s, 9H, ^{t}Bu), 1.16 (s, 9H, ^{t}Bu), 1.09 (s, 9H, ^{t}Bu), 0.93 (s, 10H,* ^{t}Bu). § = no integral was recorded. *The integral values reported for the compound are not consistent with the values required. This disagreement in values could be due to overlapping with solvent or impurities. No $^{13}C\{^1H\}$ NMR was obtained due to sample precipitation during the collection time. FTIR (KBr, cm^{-1}): 3402s (OH), 3296s (OH), 3084w, 3051w, 2960s, 2905s, 2869s, 1602m, 1505w, 1494m, 1484s, 1459s, 1445s, 1425w, 1393w, 1363m, 1313m, 1295m, 1262m, 1241m, 1207s, 1160w, 1118w, 1107w, 1064w, 1045w, 1028w, 995w, 907s (M=O), 886s (M=O), 876s, 843w, 834w, 819w, 792s, 765w, 733w. UV/vis ($CHCl_3$) $\lambda_{max/nm}$: 242, 285, 280, 312. At this point no % yield or ε values can be obtained because the compound cannot be isolated pure. No additional characterization was performed. [MoO_2(bipy){M·^{t}**BuC5(H)$_2$**}] (M = Na **(4.2a)**, Rb **(4.2b)**, Cs **(4.2c)**) can be prepared with the sodium, rubidium and cesium dianionic salts, respectively: 0.0288 g (Na_2·^{t}**BuC5(H)$_3$**: 0.0440 g, 0.0514 mmol; MoO_2Cl_2(bipy): 0.0197 g, 0.0555 mmol), 0.0233 g (Rb_2·^{t}**BuC5(H)$_3$**: 0.0491 g, 0.0501 mmol; MoO_2Cl_2(bipy): 0.0181 g, 0.0510 mmol) and 0.0259 g (Cs_2·^{t}**BuC5(H)$_3$**: 0.0547 g, 0.0509 mmol; MoO_2Cl_2(bipy): 0.0187 g, 0.0527 mmol).

The ^{1}H NMR spectra of compounds **4.2a-c** have been omitted due to their similarity to that described for compound **4.2**.

[MoO_2{K·^{t}**BuC5(H)$_2$**}] **4.3**: To a suspension of K_2·^{t}**BuC5(H)$_2$** (0.133 g, 0.150 mmol) in 7.0 mL of hexanes, 0.0586 g (0.165 mmol) of MoO_2Cl_2(bipy) was added with vigorous stirring. At this point no reaction was observed and the reaction mixture remained a suspension. Addition of 2.0 mL of acetonitrile produced (in about 5 minutes of stirring) a color change in the reaction mixture from a white suspension to a yellow suspension. The yellow suspension was stirred for 12 hrs. At the end of the reaction time two phases were obtained. The hexane phase (top one) produced an orange-red solution, containing parent ^{t}**BuC5(H)$_5$** and free bipy ligand with traces of **4.3**. The hexane phase was carefully decanted and discarded. The dark brown bottom phase (acetonitrile) contained a yellow solid at the bottom. The yellow solid was separated by centrifugation and washed with cold hexanes (3 x 2.0 mL), then vacuum dried. The amount of product recovered was 0.0533 g and identified as **4.3**. At this point no % yield can be obtained because the compound cannot be isolated pure. Mp: > 320 ^{o}C. ^{1}H NMR ($CDCl_3$) δ (ppm): 10.41 (s, 1H,* O*H*), 8.67 (s, 5H,* O*H*, Cx5), 8.14 (s, 1H,* O*H*), 7.25 (d, 1H,* *J* = 2.2 Hz, Ar-*H*), 7.23 (d, 1H,* *J* = 3.0 Hz, Ar-*H*), 7.22 (s, 10H,* Ar-*H*, Cx5), 7.07 (d, 1H,* *J* = 2.2 Hz, Ar-*H*), 7.04 (d, 1H,* *J* = 1.9 Hz, Ar-*H*), 6.89 (d, 1H,* *J* = 2.2 Hz, Ar-*H*), 6.80 (d, 1H,* *J* = 2.5 Hz, Ar-*H*), 6.66 (d, 1H,* *J* = 2.2 Hz, Ar-*H*), 6.56 (d, 1H,* *J* = 2.5 Hz, Ar-*H*), 6.38 (d, 1H,* *J* = 2.2 Hz, Ar-*H*), 6.04 (d, 1H,* *J* = 1.9 Hz, Ar-*H*), 4.96 (d, 1H,* *J* = 14.3 Hz, Ar-CH_2-Ar), 4.88 (d, 1H,* *J* = 15.4 Hz, Ar-CH_2-Ar), 4.69 (d, 1H,* *J* = 14.6 Hz, Ar-CH_2-Ar), 4.39 (d, 1H,* *J* = 14.0 Hz, Ar-CH_2-Ar), 4.20-3.20 (br, 10H,* Hz, Ar-CH_2-Ar, Cx5), 3.99 (d, 1H,* *J* = 15.4 Hz, Ar-CH_2-Ar), 3.82 (d, 1H,* *J* = 14.6 Hz, Ar-CH_2-Ar), 3.45 (d, 2H,* *J* = 14.6 Hz, Ar-CH_2-Ar), 3.42 (d, 1H,* *J* = 14.9

Hz, Ar-CH_2-Ar), 2.28 (d, 1H,* J = 14.9 Hz, Ar-CH_2-Ar), 1.85 (s, CH_3CN, residual solvent), 1.33 (s, 9H,* ^{t}Bu), 1.29 (s, 9H,* ^{t}Bu), 1.26 (s, 45H,* ^{t}Bu, Cx5), 1.16 (s, 9H,* ^{t}Bu), 0.99 (s, 9H,* ^{t}Bu), 0.77 (s, 9H,* ^{t}Bu). *The integral values were not recorded and are fixed to the expected values based on the proposed molecular formula. FTIR (KBr, cm^{-1}): 3433s (OH), 3307s (OH), 3051m, 3028w, 2966s, 2904s, 2869s, 1606m, 1487s, 1462s, 1393m, 1362s, 1293s, 1246s, 1203s, 1124m, 914s (Mo=O), 883s (Mo=O), 833m, 789m, 762w, 689w, 638w, 571w, 546w. No additional characterization was performed.

4.4a, **4.4b**: To a solid mixture of 0.0100 g (0.123 mmol) of **^{t}BuC5(H)$_5$**, 0.0569 g (0.246 mmol) of Rb_2CO_3 and 0.0462 g (0.142 mmol) of $MoO_2(acac)_2$ in a 20 mL pressure tube was added 10 mL of anhydrous acetonitrile, resulting in a light yellow suspension. The pressure tube was placed in an isotemp oil bath at 85 ^oC. After 30 minutes of reaction a change in color was observed from the initial yellow suspension to a dark green suspension. After ~10 hrs of reaction time, the color of the reaction mixture was red-orange with a white precipitate at the bottom of the pressure tube. After 24 hrs of reaction time, tiny crystals were observed on the wall of the pressure tube. After 36 hrs, a good size X-ray quality crystal was observed. The reaction mixture was stopped at ~48 hrs and no more formation of crystals was observed. ~10 mg of red-orange crystals were obtained, and a suitable crystal was used for X-ray analysis. Insufficient product was obtained for further analysis. A similar procedure was followed for **4.4b**: (**^{t}BuC5(H)$_5$**, 0.0996 g (0.123 mmol); Cs_2CO_3: 0.0829 g (0.254 mmol); $MoO_2(acac)_2$: 0.0470 g (0.144 mmol)).

$Cs[MoO_2(acac)\{Cs\cdot$**^{t}BuC5(H)$_{1.5}$**$\}]_2$ **4.5a**: To a colorless solution of 0.108 g (0.100 mmol) of $Cs_2\cdot$**^{t}BuC5(H)$_3$** in 5 mL of $CHCl_3$ was added dropwise a light green solution of 0.0519 g (0.159 mmol) $MoO_2(acac)_2$ dissolved in 3 mL of $CHCl_3$, with vigorous stirring. The addition

took ~1 min, during which time the colorless solution turned orange. The reaction mixture was stirred for 12 hrs at room temperature. The crude product was centrifuged for 25 min. The solid was discarded, while the supernatant (orange solution) was dried under vacuum. Anhydrous hexanes (~4.0 mL) were added to the red-orange solid and the resulting solution was kept in the freezer at -34 ^{o}C. Yellow crystalline solid was observed after 6 h. Centrifugation of the mixture, further washing with 2 x 3.0 mL portions of cold hexanes, and drying under vacuum yielded Cs[MoO_2(acac){Cs·^{t}**BuC5(H)$_{2.5}$**}]$_2$ **4.5a** as an off-yellow solid (0.0752 g, 0.0304 mmol, 30% yield). Mp: >275 ^{o}C. ^{1}H NMR ($CDCl_3$) δ (ppm): 10.71 (br, 2H, OH), 7.35 (d, 1H, *J* = 1.9 Hz, Ar-*H*), 7.29 (d, 1H, *J* = 2.2 Hz, Ar-*H*), 7.26 (d, 1H, *J* = 1.9 Hz, Ar-*H*), 7.22 (d, 1H, *J* = 2.5 Hz, Ar-*H*), 7.04 (d, 1H, *J* = 2.2 Hz, Ar-*H*), 6.89 (d, 1H, *J* = 2.2 Hz, Ar-*H*), 6.85 (d, 1H, *J* = 2.7 Hz, Ar-*H*), 6.74 (d, 1H, *J* = 2.5 Hz, Ar-*H*), 6.72 (d, 1H, *J* = 2.2 Hz, Ar-*H*), 6.45 (s, 1H, Ar-*H*), 5.25 (s, 1H, C*H* acac), 4.83 (d, 2H, *J* = 13.7 Hz, Ar-CH_2-Ar), 4.65 (d, 1H, *J* = 15.9 Hz, Ar-CH_2-Ar), 4.60 (d, 1H, *J* = 12.1 Hz, Ar-CH_2-Ar), 4.40 (d, 1H, *J* = 13.5 Hz, Ar-CH_2-Ar), 3.45 (d, 1H, *J* = 16.5 Hz, Ar-CH_2-Ar), 3.33 (d, 1H, *J* = 14.3 Hz, Ar-CH_2-Ar), 3.21 (d, 1H, *J* = 13.5 Hz, Ar-CH_2-Ar), 3.11 (d, 1H, *J* = 13.7 Hz, Ar-CH_2-Ar), 3.07 (d, 1H, *J* = 13.2 Hz, Ar-CH_2-Ar), 2.37 (s, 3H, CH_3 acac), 1.44 (s, 3H, CH_3 acac), 1.40 (s, 9H, ^{t}Bu), 1.32 (s, 9H, ^{t}Bu), 1.26 (s, 9H, ^{t}Bu), 0.98 (s, 9H, ^{t}Bu), 0.87 (s, 9H, ^{t}Bu). ^{13}C{^{1}H} NMR ($CDCl_3$) δ (ppm): 192.3, 186.7 (*C*=O, acac), 160.7, 156.2, 149.0, 148.5, 143.1, 142.8, 141.3, 133.0, 132.4, 131.7, 131.3, 131.0, 128.8, 128.3, 128.2, 127.6, 126.6, 126.3, 126.1, 125.6, 125.2, 124.4 (aromatic carbons), 102.1 (*C*H, acac), 36.3 (*C*(CH_3)$_3$), 34.3, 34.2, 34.1 (Ar-*C*H_2-Ar), 34.0, 33.9 (*C*(CH_3)$_3$), 31.99, 31.96, 31.8, 31.75 (C(*C*H_3)$_3$), 30.0, 28.2, 28.0 (Ar-*C*H_2-Ar), 27.0, 26.5 (*C*H_3, acac). FTIR (KBr, cm^{-1}): 3411m (OH), 3263m (OH), 3047w, 2959s, 2908s, 2868s, 1602s (C=O_{acac}), 1561w, 1523s (C=C_{acac}), 1481s, 1467s, 1460s, 1391m, 1363s (CH_3 acac), 1296s, 1277m, 1244w, 1206s, 1125m, 1026m,

917s (Mo=O), 879s (Mo=O), 832m, 820w, 766m, 799m, 670w, 602w, 552w, 416w. UV/vis (C_6H_6) $\lambda_{max/nm}$ (ε/dm^3 mol^{-1} cm^{-1}): 281 (6.06 x 10^4), 337 (1.42 x 10^3). Anal. Calcd for $C_{120}H_{149}Cs_3Mo_2O_{18}$: C 58.35, H 6.08. Found: C 58.23, H 5.98.

A similar procedure was followed for the rubidium and potassium salts to make **4.5b** and **4.5c**.

[MoO_2(acac){Rb_2·^{t}**BuC5(H)$_2$**}] **4.5b**: (Rb_2·^{t}**BuC5(H)$_3$**: 0.0988 g, 0.101 mmol; $MoO_2(acac)_2$: 0.0545 g, 0.167 mmol). Compound **4.5b** was obtained as a yellow solid (0.0438 g). Mp: >255 ^{o}C. ^{1}H NMR ($CDCl_3$) δ (ppm): 8.85 (s, 1H, O*H*), 7.48 (s, 1H, O*H*), 7.16 (s, 2H, Ar-*H*), 7.13 (d, 2H, *J* = 2.5 Hz, Ar-*H*), 7.09 (d, 1H, *J* = 2.5 Hz, Ar-*H*), 6.96 (d, 1H, *J* = 2.5 Hz, Ar-*H*), 6.82 (d, 1H, *J* = 2.5 Hz, Ar-*H*), 6.76 (d, 1H, *J* = 2.5 Hz, Ar-*H*), 6.71 (d, 1H, *J* = 2.8 Hz, Ar-*H*), 6.14 (d, 1H, *J* = 2.2 Hz, Ar-*H*), 5.01 (s, 0.2H*, C*H*, Hacac), 5.24 (s, 1H, C*H*, acac), 5.21 (s, 1H, C*H* acac), 4.98 (d, 1H, *J* = 14.3 Hz, Ar-CH_2-Ar), 4.87 (d, 1H, *J* = 14.0 Hz, Ar-CH_2-Ar), 4.71 (d, 1H, *J* = 14.3 Hz, Ar-CH_2-Ar), 4.68 (d, 1H, *J* = 15.7 Hz, Ar-CH_2-Ar), 4.23 (d, 1H, *J* = 13.5 Hz, Ar-CH_2-Ar), 3.37 (d, 1H, *J* = 15.1 Hz, Ar-CH_2-Ar), 3.29 (d, 1H, *J* = 14.0 Hz, Ar-CH_2-Ar), 3.29 (d, 1H, *J* = 17.1 Hz, Ar-CH_2-Ar), 3.12 (d, 1H, *J* = 13.5 Hz, Ar-CH_2-Ar), 3.11 (d, 1H, *J* = 14.3 Hz, Ar-CH_2-Ar), 2.21 (s, 3H, CH_3 acac), 2.16 (s, 3H, CH_3 acac), 2.05 (s, 1H,* CH_3, Hacac), 1.47 (s, 3H, CH_3 acac), 1.38 (s, 9H, ^{t}Bu), 1.31 (s, 11H,* CH_3 acac overlapped with ^{t}Bu), 1.25 (s, 9H, ^{t}Bu), 0.99 (s, 9H, ^{t}Bu), 0.78 (s, 9H, ^{t}Bu). *The integral values reported for the compound are not consistent with the values required. This disagreement in values could be due to overlapping with solvent or impurities. ^{13}C{^{1}H} NMR ($CDCl_3$) δ (ppm): 192.6 (*C*=O, acac), 191.2 (*C*=O, Hacac), 187.1 (*C*=O, acac), 159.7, 158.1, 156.8, 156.6, 148.9, 148.5, 148.0, 147.7, 144.2, 143.7, 143.3, 143.2, 143.0, 141.1, 132.8, 132.7, 132.3, 131.8, 131.6, 130.8, 130.5, 129.6,

129.4, 128.6, 128.3, 128.1, 127.62, 127.56, 126.4, 126.0, 125.8, 125.7, 125.6, 125.2, 124.7, 124.4, 123.6 (aromatic carbons), 105.2, 102.3 (*C*H, acac), 100.6 (*C*H, Hacac), 36.2 ($C(CH_3)_3$), 34.3, 34.13, 34.08, 33.9 (Ar-CH_2-Ar), 33.5 ($C(CH_3)_3$), 32.0, 31.91, 31.87, 31.69, 31.66, 31.6 ($C(CH_3)_3$), 31.0, 30.4, 30.2 (Ar-CH_2-Ar), 27.52, 27.49, 26.4, 25.0 (CH_3, Hacac), 22.8, 14.3 (CH_3, acac). FTIR (KBr, cm^{-1}): 3413m (OH), 3294m (OH), 3045w, 3028w, 2963s, 2905s, 2867s, 1701w, 1638w, 1596s ($C{=}O_{acac}$), 1538m, 1527s ($C{=}C_{acac}$), 1519m, 1513w, 1509w, 1494w, 1484s, 1393m, 1362s (CH_3 acac), 1295s, 1245m, 1207s, 1126m, 1027m, 914s (Mo=O), 883s (Mo=O), 834m, 819w, 769w, 673w, 552w. At this point no % yield or ε values can be obtained because the compound cannot be isolated pure. No additional characterization was performed.

$MoO_2(acac)[MoO_2(acac)\{K_2\cdot$**^{t}BuC5(H)$_2$**$\}]_2\cdot$Hacac **4.5c**: ($K_2\cdot$**^{t}BuC5(H)$_3$**: 0.133 g, 0.150 mmol; $MoO_2(acac)_2$: 0.0729 g, 0.223 mmol). Compound **4.5c** was obtained as a yellow solid (0.0550 g). Mp: >230 ^oC. ^1H NMR ($CDCl_3$) δ (ppm): 10.81 (s, 1H, O*H*), 9.97 (s, 1H, O*H*), 8.60 (s, 1H, O*H*), 7.53 (d, 1H, *J* = 2.2 Hz, Ar-*H*), 7.28 (d, 2H, *J* = 2.5 Hz, Ar-*H*), 7.21 (d, 1H, *J* = 1.9 Hz, Ar-*H*), 7.14 (d, 1H, *J* = 2.5 Hz, Ar-*H*), 7.11 (d, 1H, *J* = 2.8 Hz, Ar-*H*), 7.10 (d, 1H, *J* = 3.6 Hz, Ar-*H*), 7.05 (d, 1H, *J* = 3.0 Hz, Ar-*H*), 7.04 (d, 1H, *J* = 2.8 Hz, Ar-*H*), 7.01 (d, 1H, *J* = 1.9 Hz, Ar-*H*), 6.97 (d, 1H, *J* = 2.5 Hz, Ar-*H*), 6.87 (d, 1H, *J* = 2.2 Hz, Ar-*H*), 6.84 (s, 2H, Ar-*H*), 6.81 (d, 1H, *J* = 2.5 Hz, Ar-*H*), 6.75 (d, 1H, *J* = 2.2 Hz, Ar-*H*), 6.62 (d, 1H, *J* = 2.2 Hz, Ar-*H*), 6.51 (s, 1H, Ar-*H*), 6.41 (d, 1H, *J* = 2.2 Hz, Ar-*H*), 6.03 (d, 1H, *J* = 2.2 Hz, Ar-*H*), 5.50 (s, 1H, C*H,* Hacac), 5.30 (s, 1H, C*H*, acac), 5.27 (s, 1H, C*H*, acac), 5.19 (d, 1H, *J* = 14.6 Hz, Ar-CH_2-Ar), 4.98 (d, 1H, *J* = 15.4 Hz, Ar-CH_2-Ar), 4.95 (s, 1H, C*H*, acac), 4.79 (d, 1H, *J* = 14.3 Hz, Ar-CH_2-Ar), 4.70 (s, 1H, O*H*), 4.68 (d, 1H, *J* = 13.2 Hz, Ar-CH_2-Ar), 4.55 (d, 1H, *J* = 16.8 Hz, Ar-CH_2-Ar), 4.38 (d, 1H, *J* = 15.7 Hz, Ar-CH_2-Ar), 4.32 (d, 1H, *J* = 14.6 Hz, Ar-CH_2-Ar), 3.94 (d,

1H, J = 13.2 Hz, Ar-CH_2-Ar), 3.88 (d, 1H, J = 16.2 Hz, Ar-CH_2-Ar), 3.84 (d, 1H, J = 13.0 Hz, Ar-CH_2-Ar), 3.80 (d, 1H, J = 16.0 Hz, Ar-CH_2-Ar), 3.57 (d, 1H, J = 16.5 Hz, Ar-CH_2-Ar), 3.52 (d, 1H, J = 14.9 Hz, Ar-CH_2-Ar), 3.38 (d, 1H, J = 16.8 Hz, Ar-CH_2-Ar), 3.28 (d, 1H, J = 14.9 Hz, Ar-CH_2-Ar), 3.25 (d, 1H, J = 14.6 Hz, Ar-CH_2-Ar), 3.19 (d, 1H, J = 15.4 Hz, Ar-CH_2-Ar), 3.09 (d, 1H, J = 9.4 Hz, Ar-CH_2-Ar), 3.08 (s, 3H, CH_3, acac), 3.05 (d, 1H, J = 14.6 Hz, Ar-CH_2-Ar), 2.88 (d, 1H, J = 16.2 Hz, Ar-CH_2-Ar), 2.04 (s, 5H,* CH_3, Hacac), 1.87 (s, 3H, CH_3, acac), 1.85 (s, 3H, CH_3, acac), 1.63 (s, 3H, CH_3, acac), 1.48 (s, 3H, CH_3, acac), 1.38 (s, 9H, ^{t}Bu), 1.35 (s, 9H, ^{t}Bu), 1.34 (s, 9H, ^{t}Bu), 1.31 (s, 9H, ^{t}Bu), 1.30 (s, 9H, ^{t}Bu), 1.23 (s, 9H, ^{t}Bu), 1.22 (s, 9H, ^{t}Bu), 1.19 (s, 3H, CH_3, acac), 1.06 (s, 9H, ^{t}Bu), 1.03 (s, 9H, ^{t}Bu), 0.77 (s, 9H, ^{t}Bu). *The integral values reported for the compound are not consistent with the values required. This disagreement in values could be due to overlapping with solvent or impurities. ^{13}C{^{1}H} NMR ($CDCl_3$) δ (ppm): 194.5, 193.2, 191.6 (C=O, acac), 191.4 (C=O, Hacac), 188.4, 188.3 (C=O, acac), 186.2, 160.6, 160.5, 159.1, 158.8, 157.0, 154.8, 150.7, 150.4, 149.2, 148.5, 147.7, 144.8, 144.1, 144.0, 143.5, 143.1, 142.6, 142.2, 141.7, 141.6, 141.1, 133.2, 132.5, 131.9, 130.9, 130.7, 130.6, 130.4, 130.3, 130.2, 129.6, 129.5, 129.2, 129.1, 129.0, 128.7, 128.6, 128.5, 128.2, 127.4, 127.2, 126.8, 126.4, 126.1, 125.8, 125.6, 125.4, 124.8, 124.6, 124.4, 124.3, 123.7, 122.9, 122.4 (aromatic carbons), 105.4, 103.1, 101.1 (CH, acac), 100.6 (CH, Hacac), 38.1, 36.3, 35.4, 34.7 (C(CH_3)$_3$), 34.4, 34.3, 34.24, 34.19, 34.1, 34.04, 33.99 (Ar-CH$_2$-Ar), 33.7, 33.5 (C(CH_3)$_3$), 32.1, 32.0, 31.8, 31.73, 31.69, 31.6 (C(CH$_3$)$_3$), 30.3, 30.1 (Ar-CH$_2$-Ar), 27.9, 26.8, 26.6, 26.5, 26.1, 26.0 (CH$_3$, acac), 25.0 (CH$_3$, Hacac). FTIR (KBr, cm^{-1}): 3475m (OH), 3049w, 2960s, 2905s, 2869s, 1701w, 1686w, 1596s (C=O$_{acac}$), 1572w, 1561w, 1550w, 1528s (C=C$_{acac}$), 1514m, 1480s, 1460s, 1364s (CH_3 acac), 1294s, 1245m, 1204s, 1124m, 1027m, 914s (Mo=O), 886s (Mo=O), 834s, 797m, 767s, 674w, 551m, 425w. UV/vis ($CHCl_3$) $\lambda_{max/nm}$: 242, 277, 326. Anal. Calcd for

$C_{128}H_{159}K_4Mo_3O_{24}$: C 60.87, H 6.34. Found: C 61.02, H 6.49. At this point no % yield or ε values can be obtained because the compound cannot be isolated pure. No additional characterization was performed.

4.4 General X-ray crystal structure information

The crystallographic data and some details of the data collection and refinement of complexes [**4.4a**]$_2$·8CH_3CN and **4.5a**·2$C_5H_8O_2$·C_5H_{12} are given in Table 4.9. Absorption corrections were applied by SADABS.[155] All X-ray structures were solved by direct methods and subsequent difference Fourier syntheses and refined by full matrix least-squares methods against F^2 (SHELX 97).[121] Disorder for some *tert*-butyl groups was due to a two-fold axis, and was modeled using partial occupancies (PART instruction) and isotropic displacement parameters.[121] The H atoms in structures were taken in calculated positions. The programs Mercury[157] and POVRay[158] were used to generate the X-ray structural diagrams pictured in this Chapter.

Table 4.9 Crystallographic data for complexes [**4.4a**]$_2$·8CH_3CN and **4.5a**·2$C_5H_8O_2$·C_5H_{12}.

	[**4.4a**]$_2$·8CH_3CN	**4.5a**·2$C_5H_8O_2$·C_5H_{12}
Formula	$C_{246}H_{294}Mo_4N_8O_{32}Rb_8$	$C_{135}H_{170}Cs_3Mo_2O_{22}$
FW	4952.49	2753.32
cryst syst	Triclinic	Monoclinic
space group	P -1	C 2/c
T, K	213(2)	223.(2)
a, Å	19.344(2)	21.619(4)
b, Å	20.316(3)	23.820(4)
c, Å	21.147(3)	29.027(5)
α, deg	66.486(2)	90
β, deg	66.327(2)	97.282(5)
γ, deg	67.918(2)	90
V, A^3	6745.1(14)	14827(5)
Z	1	4
d_{calcd}, g·cm^{-3}	1.217	1.193
μ, mm^{-1}	1.675	0.951
refl collected	47747	34702
T_{min} / T_{max}	0.889	0.931
N_{measd}	19351	10643
[R_{int}]	[0.0708]	[0.0927]
R [I>2sigma(I)]	0.0422	0.0595
R (all data)	0.0697	0.0940
R_w [I>2sigma(I)]	0.1027	0.1446
R_w (all data)	0.1088	0.1594
GOF	0.911	1.043

4.5 Conclusions

Eight dioxomolybdenum(VI) complexes were synthesized by reacting MoO_2Cl_2, MoO_2Cl_2(bipy), or $MoO_2(acac)_2$ with $M_2 \cdot$ **^{t}BuC5(H)$_3$** (M = Na, K, Rb, Cs). Formation of new compounds was established by IR, EDX, elemental analysis and ^{1}H and ^{13}C NMR experiments. We reported the synthesis of the first dioxomolydenum-calix[5]arene complex (**4.5a**) and its full characterization. A key factor of these reactions is how to favor product formation; selection of solvents with suitable polarity can help to precipitate out the products or drive the reaction to completion.

CHAPTER 5

CALIXARENE PALLADIUM(II) COMPLEXES

5.1 Introduction

While the coordination of transition metal ions to the oxygen atoms of the calixarene lower rim has been extensively studied during the last two decades, almost all of these studies involved highly oxophilic early transition metals.[11,16,29] The chemistry of late transition metal (Ru, Os, Rh, Ir, Pd, Pt) derivatives of calixarenes has primarily been studied with calixarenes that are chemically modified with soft donor ligands, like phosphine derivatives.[22,136,188-190]

Early studies performed by Atwood et al.[191-194] on the reactivity of the parent calix[4,5]arene (with no pendant binding sites) toward Ru, Rh, and Ir, showed a competition between η^6 coordination to the aromatic rings of the calixarene, and direct interaction with the phenoxide oxygen atoms of the lower rim. These two modes of coordination were confirmed by X-ray studies (Figure 5.1a).[194] Such competition was demonstrated experimentally by Ishii et al.,[151] who proved that it is possible to coordinate the Rh center to the lower rim only after one of the metal ions is attached to the phenoxide aromatic ring (Figure 5.1b).[151]

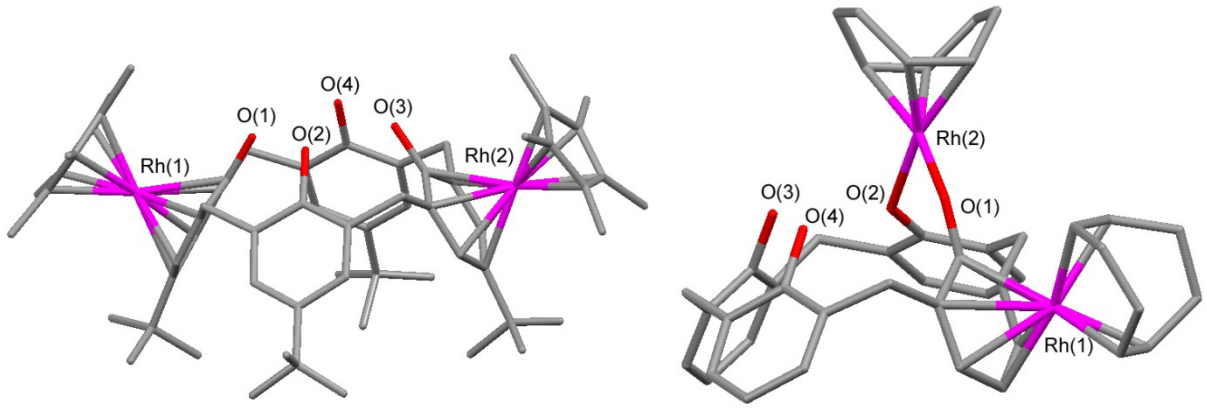

a) **b)**

Figure 5.1 Structural drawing of Rh(II) calix[4]arene complexes.[151,194]

After those experiments, two different approaches have been used to obtain late transition M-O (calixarene) bonds (M = Pd or Pt).[51,152] Ishii described the stepwise construction of a bimetallic Re-Pd calix[4]arene complex. The Ishii approach was based on the initial insertion of the Re ion onto the phenoxide oxygen surface, and then the introduction of the Pd moiety (Scheme 1.4).[51]

The second approach described in literature was the use of silyl-protected calixarene[74] by Vigalok et al.[152] The silyl-protected calixarene was allowed to react with a highly active P_2PtF_2 complex (P_2 = either 1,3-diphenylphosphinopropane or 2 Ph_3P) resulting in the displacement of the silyl protective groups (Scheme 5.1), leaving the Pt ion on the lower rim.[152] The authors reported that when they started with a 1,3-substituted silylcalixarene the product obtained was the 1,2-substituted metallocalixarene. They claimed the observed effect was not caused by steric factors but instead was due to the square planar geometry adopted by the metal center.[152]

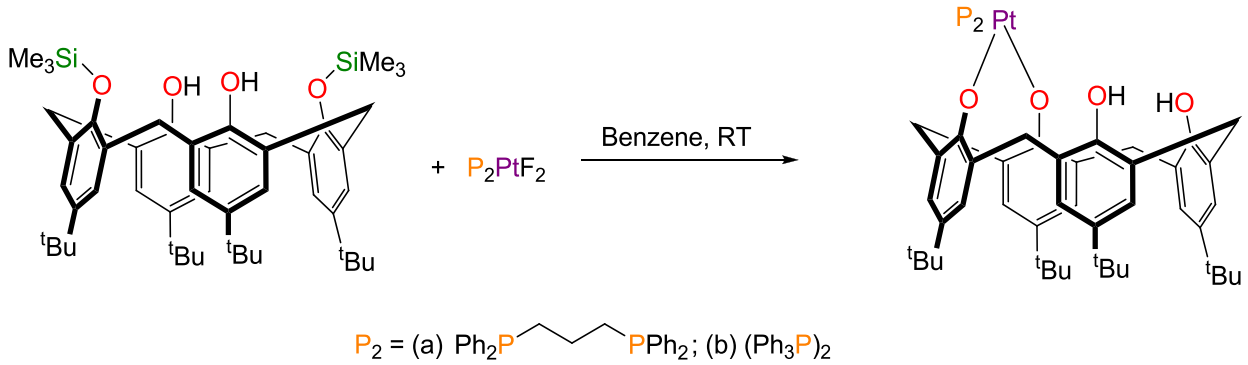

Scheme 5.1 Synthesis of a monometallic late transition metal calixarene complex with a metal-O coordination mode.[152]

There are several disadvantages with the Ishii and Vigalok syntheses: i) the time-consuming procedure and the anhydrous reaction conditions that were carried out to place both metals, Re- and Pd, on the lower rim, ii) the cumbersome initial silylcalixarene synthesis, and iii) the need to use a fluorinated transition metal derivative, which immediately reduces the synthesis to only a few transition metals. To avoid these problems, we decide to use simple metathesis reactions to place late transition metals onto the lower rim.

Calixanions[107-108,113] appear to be a suitable precursors because alkali metals M^+ (M = Li, Na, K, Rb or Cs) can generally be removed by the reaction with chloride ion.[58,85,110]

In this chapter, we describe the synthesis and characterization of heterobimetallic palladium(II)–M(I) (M = Na, K, Rb, Cs) calix[5]arene complexes and monometallic palladium(II) calix[4]arene complexes, achieved by using calixanions. This is the first part of two investigations involving Pd complexation to calix[4,5]arenes. The second part will be presented in Chapter 6 where the reactivity of the Pd calix[5]arene complexes will be discussed.

In this chapter, we will discuss both the synthetic approaches used and the structural trends encountered upon changing the nature of the calixarene ring.

5.2 Results and discussion

In Chapter 2 we described the interesting features found in the calix[5]arene mono- and dianions containing Rb or Cs ions. The reactivity of those calix[5]arene dianions was tested using titanium derivatives Cp_2TiCl_2 and $CpTiCl_3$ (Chapter 3) and molybdenum derivatives (MoO_2Cl_2, MoO_2Cl_2(bipy), $MoO_2(acac)_2$) (Chapter 4). The use of chlorotitanium derivatives or the chloromolybdenum derivative (MoO_2Cl_2) resulted in the loss of alkali ions (Na^+, K^+, Rb^+ or Cs^+) from the calix[5]arene ligand. We therefore hypothesize that the use of chloropalladium derivatives will allow us to prepare a mono-palladium calix[5]arene complex.

5.2.1 Synthesis of ***^{t}BuC5(H)$_5$*** *palladium complexes*

5.2.1.1 First approach using [Pd(CH$_3$CN)$_2$Cl$_2$]

Our initial reaction explored the reactivity of $Cs_2\cdot$**^{t}BuC5(H)$_3$** with a well known palladium complex, [Pd(CH_3CN)$_2$Cl$_2$]. The synthesis of [Pd(CH_3CN)$_2$Cl$_2$] is performed *in situ* when solid $PdCl_2$ is dissolved in hot acetonitrile.[195] Once the palladium chloride was dissolved, a suspension of $Cs_2\cdot$**^{t}BuC5(H)$_3$** in acetonitrile was added, with a 1:1.5 $Cs_2\cdot$**^{t}BuC5(H)$_3$**:$PdCl_2$ ratio. The ^{1}H NMR spectrum showed a mixture of parent **^{t}BuC5(H)$_5$** and only traces of an unknown compound **1**. In order to obtain a better yield of the unknown compound **1**, we increased the ratio to 1:5 $Cs_2\cdot$**^{t}BuC5(H)$_3$**: $PdCl_2$. We observed an increase in the amount of the unknown compound **1**, but it was still mixed with the parent calix[5]arene.

Contrary to expectations, ^{1}H NMR analysis showed that our unknown compound **1** was in fact the known monospirodienone[196] **1** (Equation 5.1). Monospirodienone **1** has been reported by Biali et al.,[196] prepared in 63% yield using phenyltrimethylammonium tribromide as an oxidizing agent.

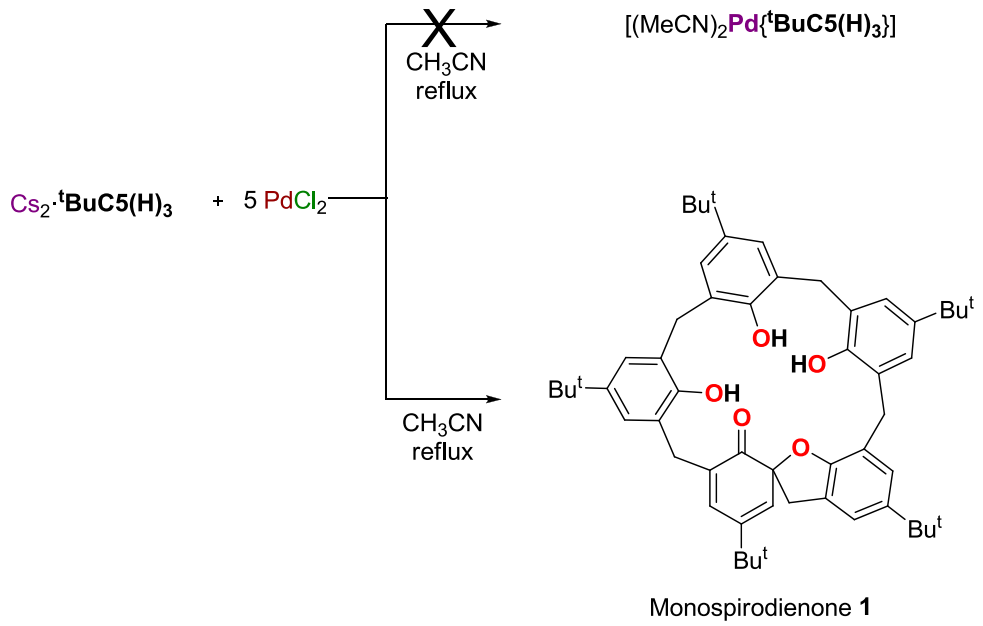

(5.1)

5.2.1.2 Second approach using [Pd(bipy)Cl$_2$] generated in situ

Not to be discouraged by this initial result we decided to use another synthetic route van Koten et al.[197-198] described a reaction using sodium phenoxide and palladium(II) acetate (Pd(OAc)$_2$) in the presence of a bidentate N-donor ligand such as 2,2'-bipyridine (bipy), in a 2:1:1 ratio to afford N-ligated bis(aryloxo)palladium(II) complexes (Scheme 5.2).[198]

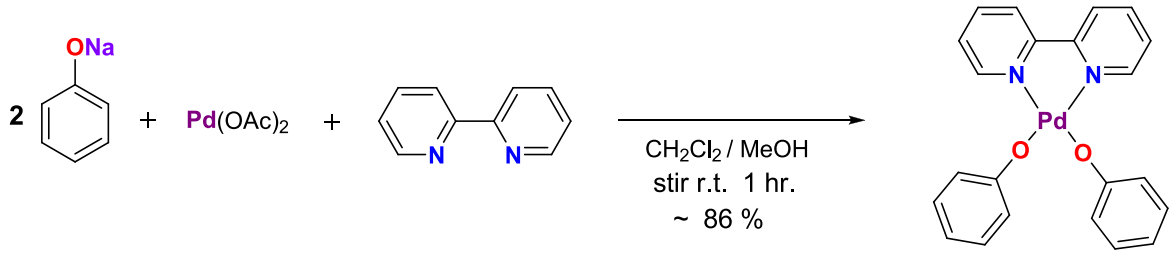

Scheme 5.2 Synthesis of N-ligated bis(aryloxo)palladium(II) complex.[198]

The procedure described by Koten seemed to be a practical approach for our purpose. We decided to generate the complex [Pd(bipy)Cl_2][195] *in situ* in acetonitrile and allow it to react with the dianionic calix[5]arene salt.

The reaction of two equivalents of the dianionic calix[5]arene salts $M_2 \cdot$**^{t}BuC5(H)$_3$** (M = Na, K, Rb, Cs)[113] with one equivalent of [Pd(bipy)Cl_2][195] in acetonitrile for 30 minutes at 90 ^{o}C, produced complexes [Pd(bipy){M·**^{t}BuC5(H)$_2$**}] (M = Na (**5.1a**), K (**5.1b**), Rb (**5.1c**) and Cs (**5.1d**)) (Scheme 5.3). The reaction generally produced a suspension within 5 min of the addition of the corresponding calixarene salt. Purification of the products from the reaction mixture by filtration, successive water washing cycles (to remove the MCl side product (M = Na, K, Rb, Cs)), and finally rinsing with acetonitrile, produced complexes **5.1a-d** in yields of 69 –74%.

Evidence for the alkali metal (Na, K, Rb, Cs) contained in the products was based on elemental analysis and further corroborated by X-ray studies.

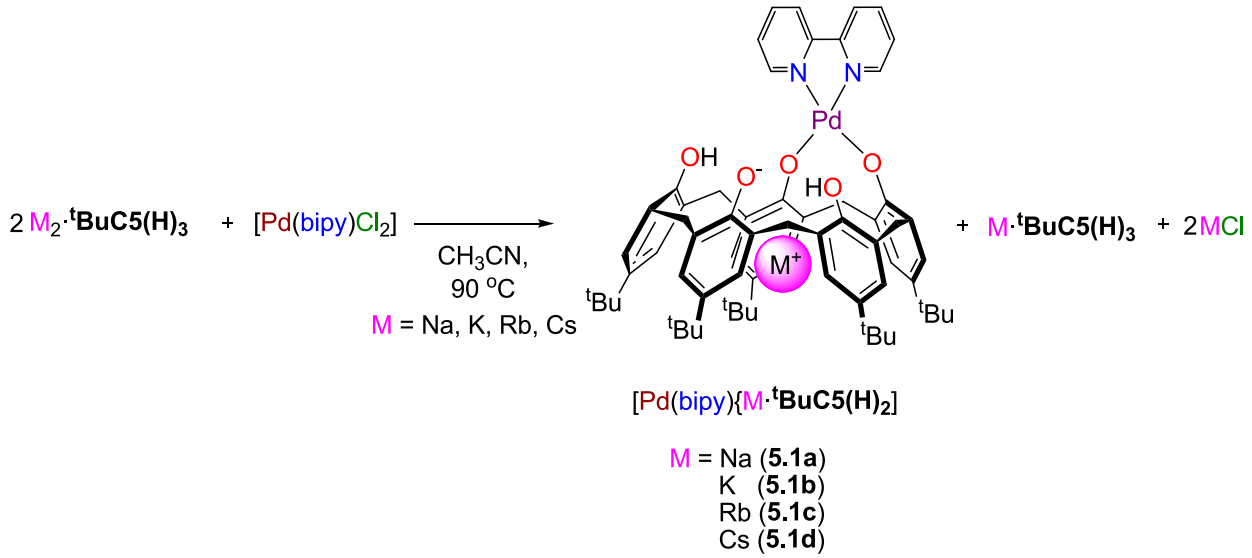

Scheme 5.3 Preparation of heterobimetallic palladium(II)-M(I) (M = Na, K, Rb, Cs) calix[5]arene complexes **5.1a-d**.

Complexes **5.1a-d** are soluble in chloroform, toluene and benzene at room temperature, but they are completely insoluble in any saturated hydrocarbon solvent or acetonitrile. Complexes **5.1a-d** are air and water stable but they decompose to the parent calixarene when they are exposed to an acidic solution.

X-ray quality crystals of complex **5.1d** were obtained from a concentrated benzene solution containing a few drops of DMSO. The X-ray structure of compound **5.1d** revealed the presence of the cesium ion inside the cavity of the calix[5]arene, coordinated by π–arene interactions. Analogous alkali metal-calixarene interactions have been observed before.[52-53,64,81,110]

When ligands (4-Me)$_2$bipy (2,2'-4,4'-dimethylbipyridine), phen (1,10-phenanthroline), dpa (2,2'-dipyridylamine) or the bidentate ligand tmeda (*N*,*N*,*N*',*N*'-tetramethylethylenediamine)

were used, no palladium-containing calix[5]arene complex was produced. In the case of (4-Me)$_2$bipy, phen or dpa, it was necessary first to isolate the corresponding [Pd(L)Cl$_2$] (L = (4-Me)$_2$bipy, phen, dpa) complex, then prepare the Pd-calix[5]arenes **5.2a-d**, **5.3a-d**, and **5.4-d**. In the case of [Pd(tmeda)Cl$_2$] no product could be isolated.

5.2.1.2.1 Synthesis of palladium precursors [Pd(L)Cl$_2$]

The general method first described by Wimmer and co-workers[195] for the synthesis and isolation of [Pd(bipy)Cl$_2$] can be applied for the synthesis of [Pd(L)Cl$_2$] (L = (4-Me)$_2$bipy, phen, dpa, tmeda) complexes (Equation 5.2). This synthesis is based on the initial formation of the [Pd(CH$_3$CN)$_2$Cl$_2$], which is generated *in situ* when solid PdCl$_2$ is added to boiling acetonitrile resulting in a red-brown solution.[195] Slow addition of the coordinating ligand produces the desired palladium complex as a microcrystalline solid. The microcrystalline solid is removed from the reaction mixture by filtration and then is vacuum dried.

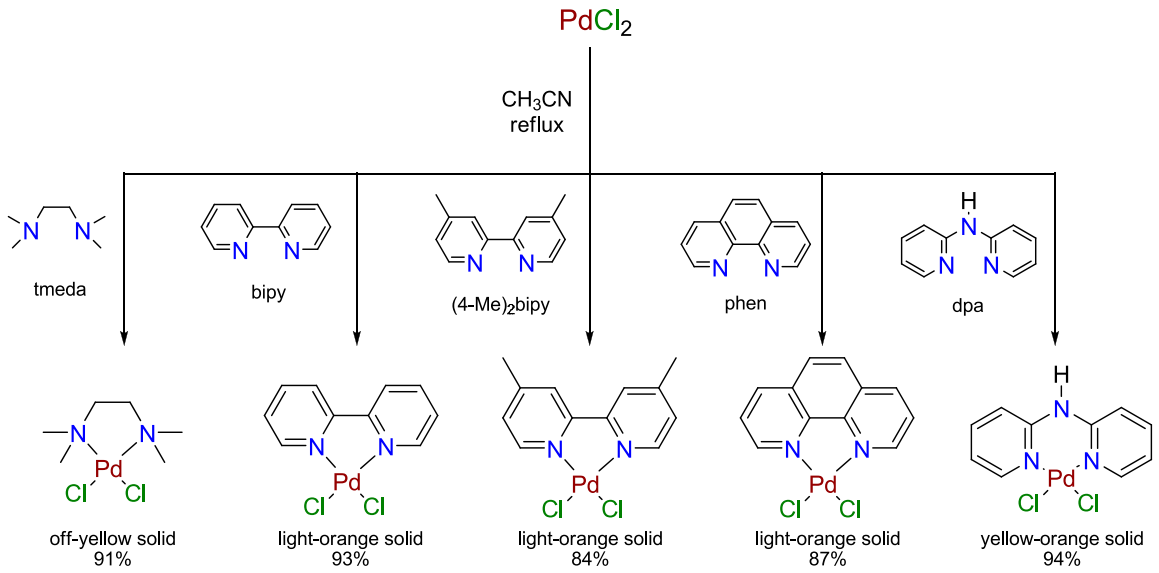

(5.2)

All the palladium complexes $[Pd(L)Cl_2]$ (L = bipy, $(4\text{-Me})_2$bipy, phen, dpa, tmeda) were obtained in good yields ranging from 84-94%. They are insoluble in all common solvents except DMSO. The palladium complexes are also partially soluble in hot acetonitrile (25 mg in 15.0 mL, at 90 ^{o}C).

When the $[Pd(L)Cl_2]$ (L = bipy, $(4\text{-Me})_2$bipy, phen, dpa, tmeda) complexes are initially isolated and then reacted with the corresponding calix[5]arene salt then it is possible to synthesize and isolate the corresponding palladium-containing calix[5]arene complexes. Table 5.1 presents a summary of yields for complexes containing the coordinating N-heterocyclic ligands bipy, $(4\text{-Me})_2$bipy, phen and dpa.

Table 5.1 Yields for complexes containing coordinating N-heterocyclic ligands.

Compound / L =	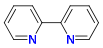	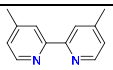	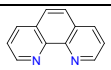	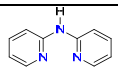
	bipy	$(4\text{-Me})_2$bipy	phen	dpa
$[Pd(L)\{Na\cdot^{t}\mathbf{BuC5(H)_2}\}]$	74%, **5.1a**	69%, **5.2a**	69%, **5.3a**	65%, **5.4a**
$[Pd(L)\{K\cdot^{t}\mathbf{BuC5(H)_2}\}]$	83%, **5.1b**	60%, **5.2b**	61%, **5.3b**	83%, **5.4b**
$[Pd(L)\{Rb\cdot^{t}\mathbf{BuC5(H)_2}\}]$	95%, **5.1c**	93%, **5.2c**	89%, **5.3c**	77%, **5.4c**
$[Pd(L)\{Cs\cdot^{t}\mathbf{BuC5(H)_2}\}]$	83%, **5.1d**	92%, **5.2d**	90%, **5.3d**	82%, **5.4d**

5.2.1.3 Proposed mechanism for the formation of palladium calix[5]arene complexes

In the formation of the palladium-containing calix[5]arene complex, we did not expect the alkali metal to be inside the cavity of the calix[5]arene, but in retrospect it can be rationalized on the basis of literature precedent[110] and experimental data. Scheme 5.4 shows the proposed mechanism for the formation of the [Pd(bipy){Cs·^{t}**BuC5(H)$_2$**}] complex, taking into account that the calixarene is in a cone conformation and the other alkali metal is localized inside the cavity. Two equivalents of the calix[5]arene dianion are necessary per one equivalent of the [Pd(L)Cl$_2$] complex in order to produce the desired product (see Scheme 5.3).

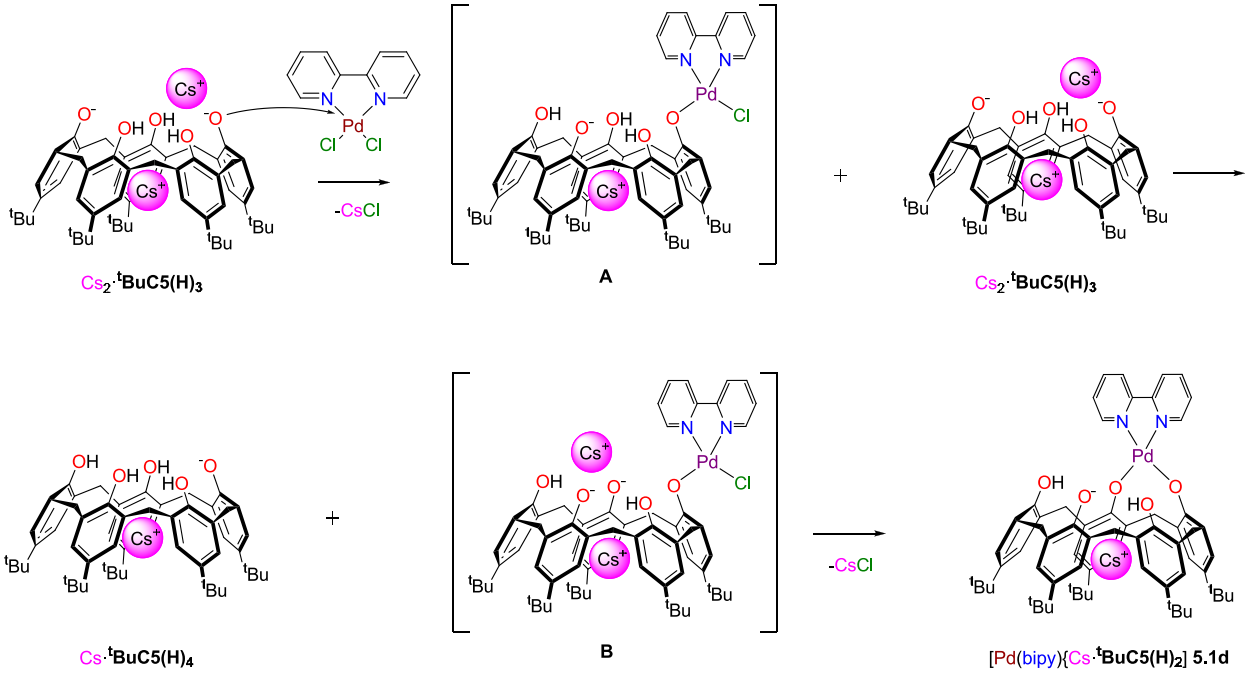

Scheme 5.4 Proposed mechanism for the formation of [Pd(bipy){Cs·^{t}**BuC5(H)$_2$**}] **5.1d**.

Initially one equivalent of the calix[5]arene dianion $Cs_2 \cdot$**^{t}BuC5(H)$_3$** reacts with one of the chlorides of the [Pd(bipy)Cl_2] complex to form intermediate **A**. Introduction of the (bipy)PdCl moiety makes the remaining calix-OH groups more acidic, so **A** can further react with the extra equivalent of $Cs_2 \cdot$**^{t}BuC5(H)$_3$** to give intermediate **B** and Cs·**^{t}BuC5(H)$_4$**.[113] The formation of Cs·**^{t}BuC5(H)$_4$** was verified by ^{1}H NMR. We suggest that deprotonation in the 2 position occurs to form **B** based on the X-ray structure of [Pt(dppp){**^{t}BuC4(H)$_2$**}][152] and the resulting X-ray structure of compound **5.1d**. The structure of **B** as depicted also allows for maximum H-bonding stabilization of the anionic oxygen. Intramolecular elimination of CsCl and simultaneous Pd-O bond formation leads to the formation of the compound **5.1d**.

Although this is formally a transmetallation, i.e., replacement of the alkali metal cation with the palladium moiety, we do not see significant differences in the reaction based on the identity of the alkali metal.

5.2.2 Synthesis of ***^{t}BuC4(H)$_4$, HC4(H)$_4$*** *and* ***^{t}BuC6(H)$_6$*** *palladium complexes*

Encouraged by our results, we decided to apply our synthetic approach in order to get analogous palladium complexes with *tert*-butylcalix[4]arene, **^{t}BuC4(H)$_4$** or *p*-H-calix[4]arene **HC4(H)$_4$**. In an optimized procedure the reaction between **RC4(H)$_4$** (R= ^{t}Bu, H) and potassium carbonate (K_2CO_3) in a 1:4 molar ratio in anhydrous acetonitrile at 90° C for 24 hrs, followed by addition of 1 equivalent of [Pd(L)Cl_2] complex (L = bipy, (4-Me)$_2$bipy, phen, dpa, tmeda), yielded compounds **5.5a** to **5.5e** and **5.6a** to **5.6c,** as depicted in Scheme 5.5. The palladium-containing calix[4]arene complexes were obtained in good yields (55-80%) after washing with water and acetonitrile.

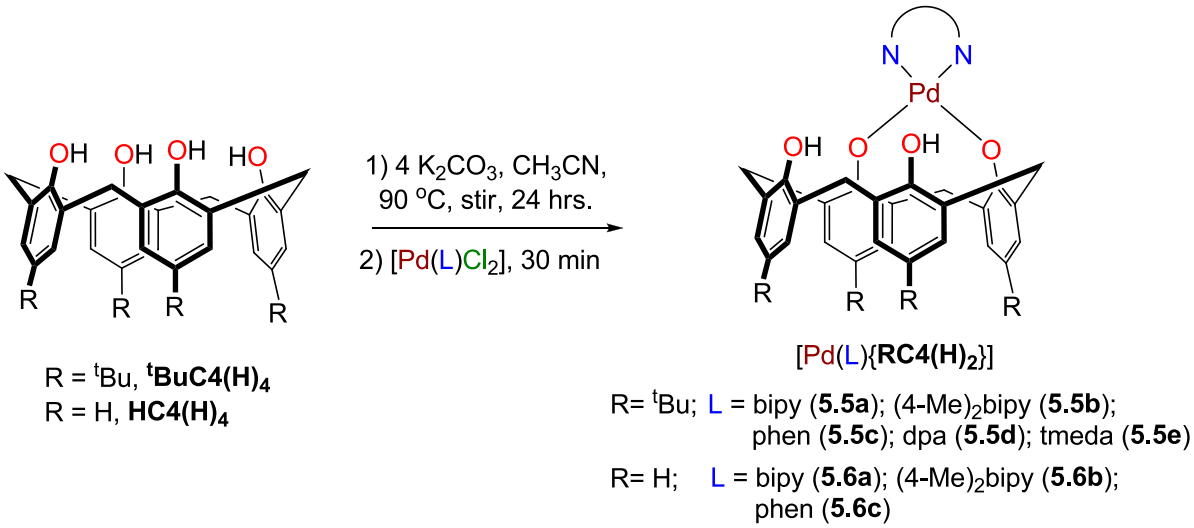

Scheme 5.5 Preparation of complexes **5.5a** to **5.5e** and **5.6a** to **5.6c**.

Complexes **5.5a** to **5.5e** and **5.6a** to **5.6c** are air and water stable and were isolated as orange to red solids. Complexes **5.5a** to **5.5e** are soluble in chloroform and benzene. Complexes **5.6a** and **5.5c** are soluble only in DMSO. Complex **5.6b** is soluble in DMSO and is slightly soluble in hot CH_3CN. In the case of **HC4(H)$_4$** with [Pd(dpa)Cl_2] or [Pd(tmeda)Cl_2] we were unable to separate a mixture of calixanion and the palladium complex. All palladium-calix[4]arene complexes were characterized by ^{1}H and ^{13}C NMR, FTIR, and elemental analysis.

X-ray analysis of single crystals of complexes **5.5a**, **5.5b**, **5.5e** and **5.6b** confirmed the structures assigned by spectroscopy. Crystals of complexes **5.5a** and **5.5b** were obtained after slow evaporation of a concentrated solution of benzene while crystals of **5.5e** and **5.6b** were obtained from slow evaporation of an acetonitrile solution.

In a similar manner to that described for the palladium calix[n]arene (n = 4 or 5) complexes we were able to isolate the palladium-containing calix[6]arene complex. Reaction of

^{t}BuC6(H)$_6$ with cesium carbonate (Cs_2CO_3) in a 1:2 ratio in dry acetonitrile for 24 hrs, followed by addition of 1 equivalent of [Pd((4-Me)$_2$bipy)Cl$_2$], afforded the [Pd((4-Me)$_2$bipy){Cs·**^{t}BuC6(H)$_3$**}] complex **5.7**, in 91% yield (Equation 5.3). To the best of our knowledge, complex **5.7** is the first example of a d^8 transition metal coordinated to the calix[6]arene lower rim. X-ray quality crystals of **5.7** were obtained after slow evaporation of a concentrated solution of benzene. The crystal structure of complex **5.7** shows a Cs^+ ion in the cavity, similar to the one observed in complex **5.1d**. The calix[6]arene ligand in compound **5.7** adopts a double cone conformation, similar to that described in [CpTi{**^{t}BuC6(H)$_3$**}] and [(CpTi)$_2${**^{t}BuC6**}], mono and bimetallic titanium(IV) calix[6]arene compounds, respectively.[90] The yields of [Pd(L){**RC4(H)$_4$**}] (R = ^{t}Bu, H) **5.5a-e** and [Pd((4-Me)$_2$bipy){Cs·**^{t}BuC6(H)$_6$**}] **5.7** are presented in Table 5.2.

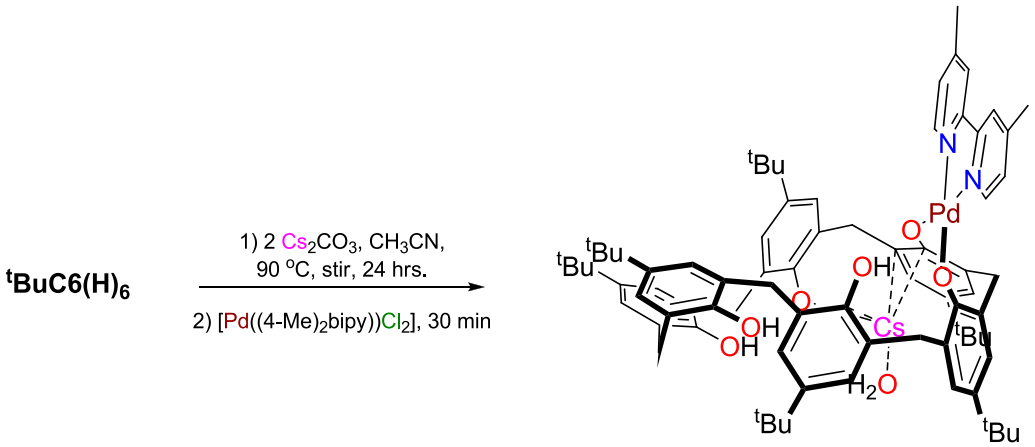

(5.3)

[Pd((4-Me)$_2$bipy){Cs·**^{t}BuC6(H)$_3$**}]·H$_2$O

5.7

Table 5.2 Summary of yields of **RC4(H)$_4$** (R = ^{t}Bu, H) and **^{t}BuC6(H)$_6$** palladium complexes.

Compound / L =	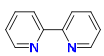	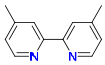	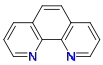		
	bipy	(4-Me)$_2$bipy	phen	dpa	tmeda
[Pd(L){**^{t}BuC4(H)$_2$**}]	66%, **5.5a**	63%, **5.5b**	66%, **5.5c**	66%, **5.5d**	80%, **5.5e**
[Pd(L){**HC4(H)$_2$**}]	66%, **5.6a**	55%, **5.6b**	68%, **5.6c**	mixture	mixture
[Pd(L){Cs·**^{t}BuC6(H)$_3$**}]	[a]	91%, **5.7**	[a]	[a]	[a]

[a] Not determined.

5.3 Spectral data

5.3.1 Spectral data for palladium calix[5]arene complexes

The ^{1}H NMR of spectra of complexes **5.1a-d**, **5.2a-d**, **5.3a-d** and **5.4a-d** have several similar aspects (Figures 5.2 to 5.5). First of all, the overall C_s symmetry of the calix[5]arene ligand[30] is retained in all of the complexes: three resonances are observed for the *tert*-butyl groups (integrating in a 2:2:1 ratio). Six doublets (due to $^2J_{HH}$ geminal coupling) are found for the methylene bridging groups (integrating in a 2:2:2:2:1:1 ratio). Finally, four, three, four, and four resonances for the bipy, (4-Me)$_2$bipy, phen, and dpa protons respectively, are observed in the aromatic region.

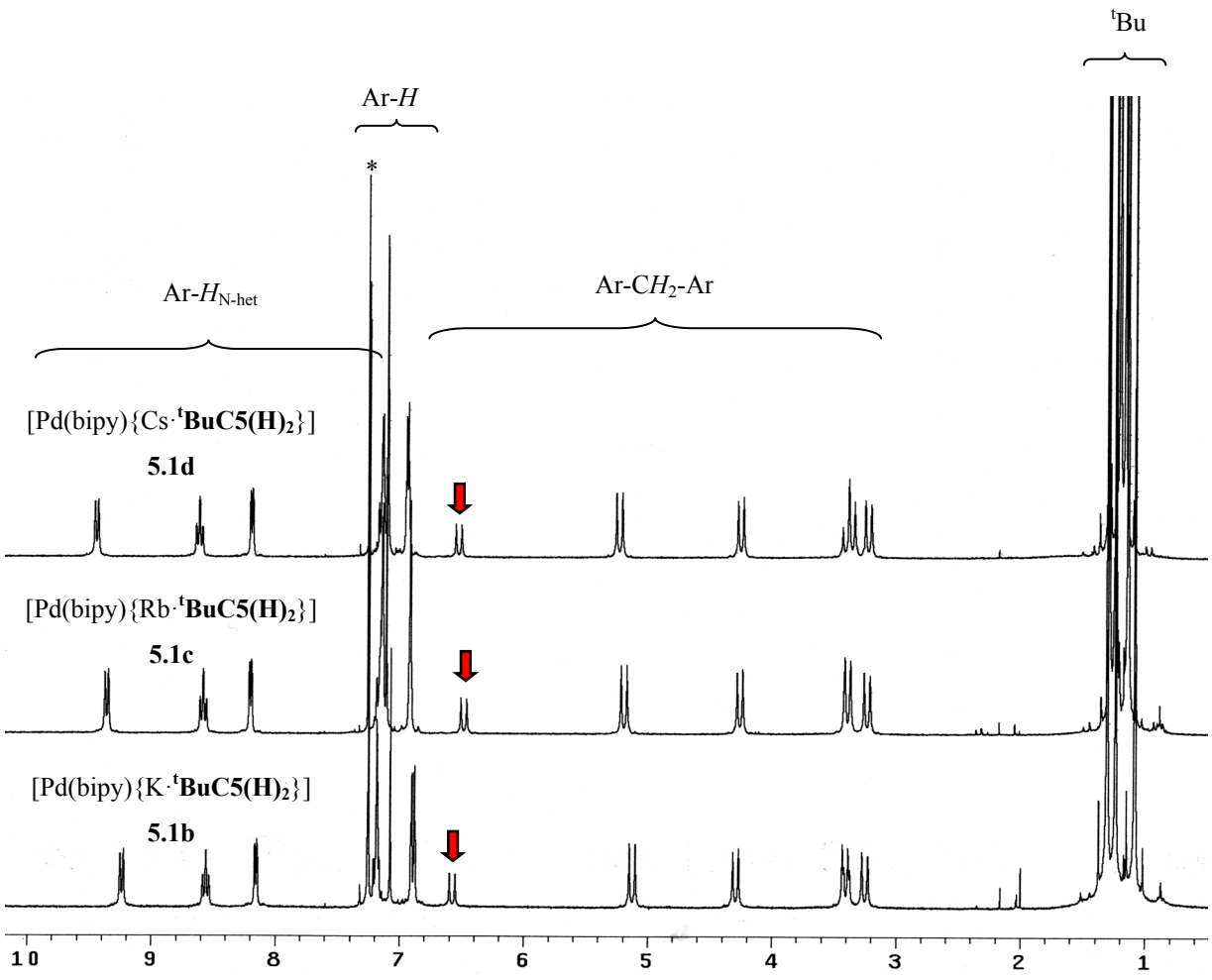

Figure 5.2 ^{1}H NMR spectra of [Pd(bipy){K·^{t}**BuC5(H)$_2$**}] **5.1b**, [Pd(bipy){Rb·^{t}**BuC5(H)$_2$**}] **5.1c**, and [Pd(bipy){Cs·^{t}**BuC5(H)$_2$**}] **5.1d** in *$CDCl_3$. The arrow highlights the methylene Pd···H interaction.

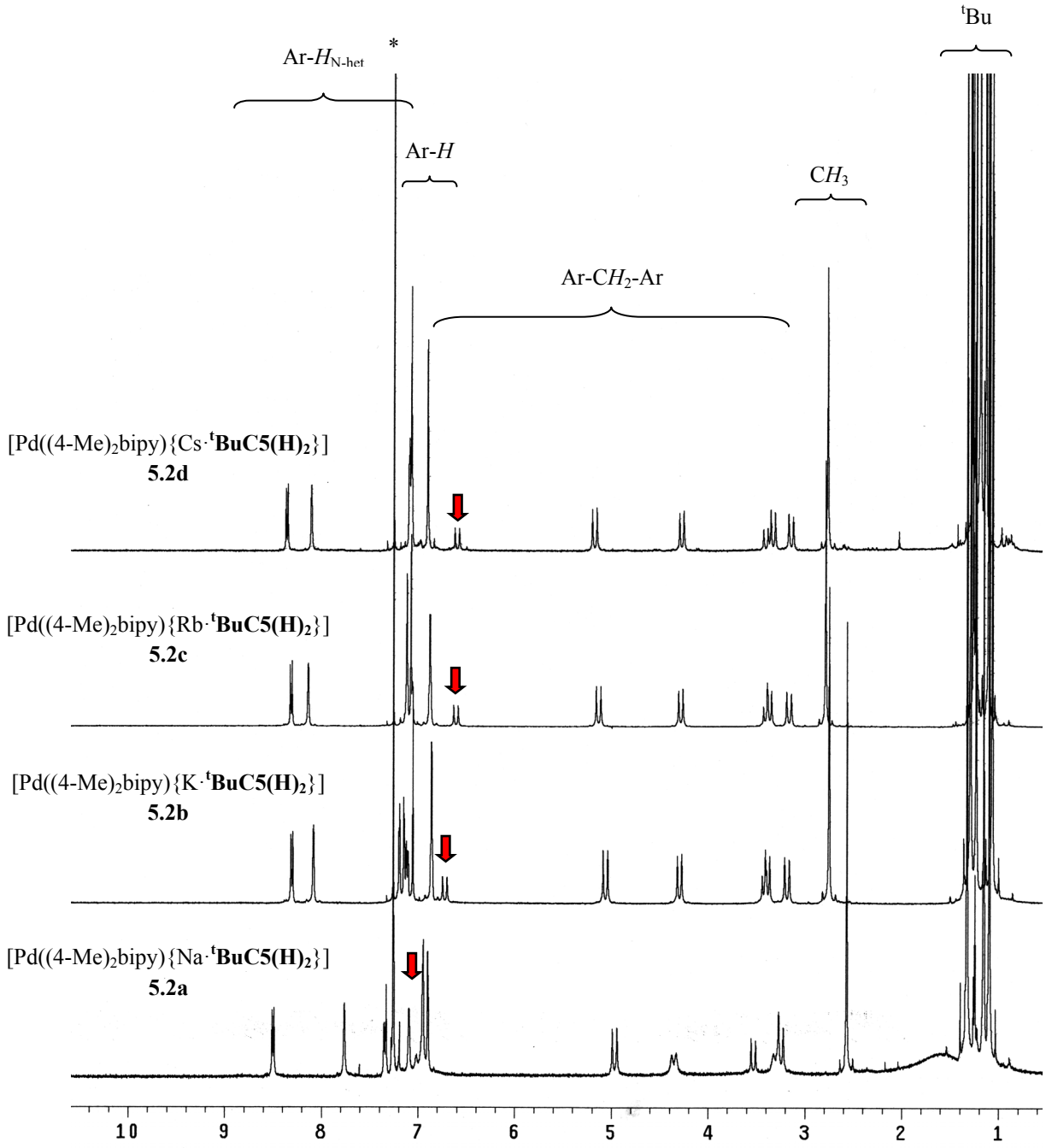

Figure 5.3 ^{1}H NMR spectra of [Pd((4-Me$_2$)bipy){Na·^{t}**BuC5(H)$_2$**}] **5.2a**, [Pd((4-Me$_2$)bipy){K·^{t}**BuC5(H)$_2$**}] **5.2b**, [Pd((4-Me$_2$)bipy){Rb·^{t}**BuC5(H)$_2$**}] **5.2c**, and [Pd((4-Me$_2$)bipy){Cs·^{t}**BuC5(H)$_2$**}] **5.2d** in *CDCl$_3$. The arrow highlights the methylene Pd···H interaction.

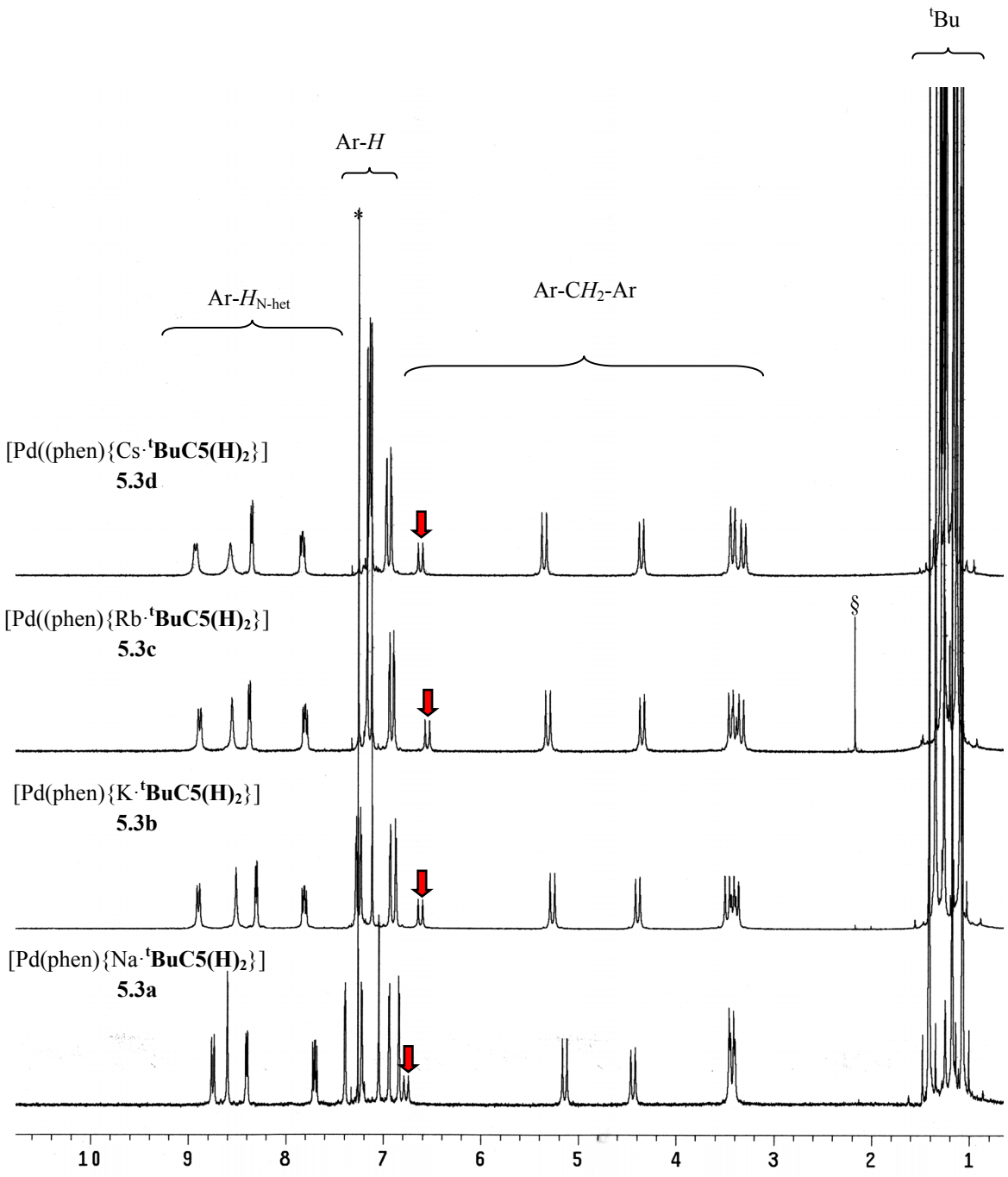

Figure 5.4 ^{1}H NMR spectra of [Pd(phen){Na·^{t}**BuC5(H)$_2$**}] **5.3a**, [Pd(phen){K·^{t}**BuC5(H)$_2$**}] **5.3b**, [Pd(phen){Rb·^{t}**BuC5(H)$_2$**}] **5.3c**, and [Pd(phen){Cs·^{t}**BuC5(H)$_2$**}] **5.3d** in *$CDCl_3$. §Residual solvent impurity (acetone). The arrow highlights the methylene Pd···H interaction.

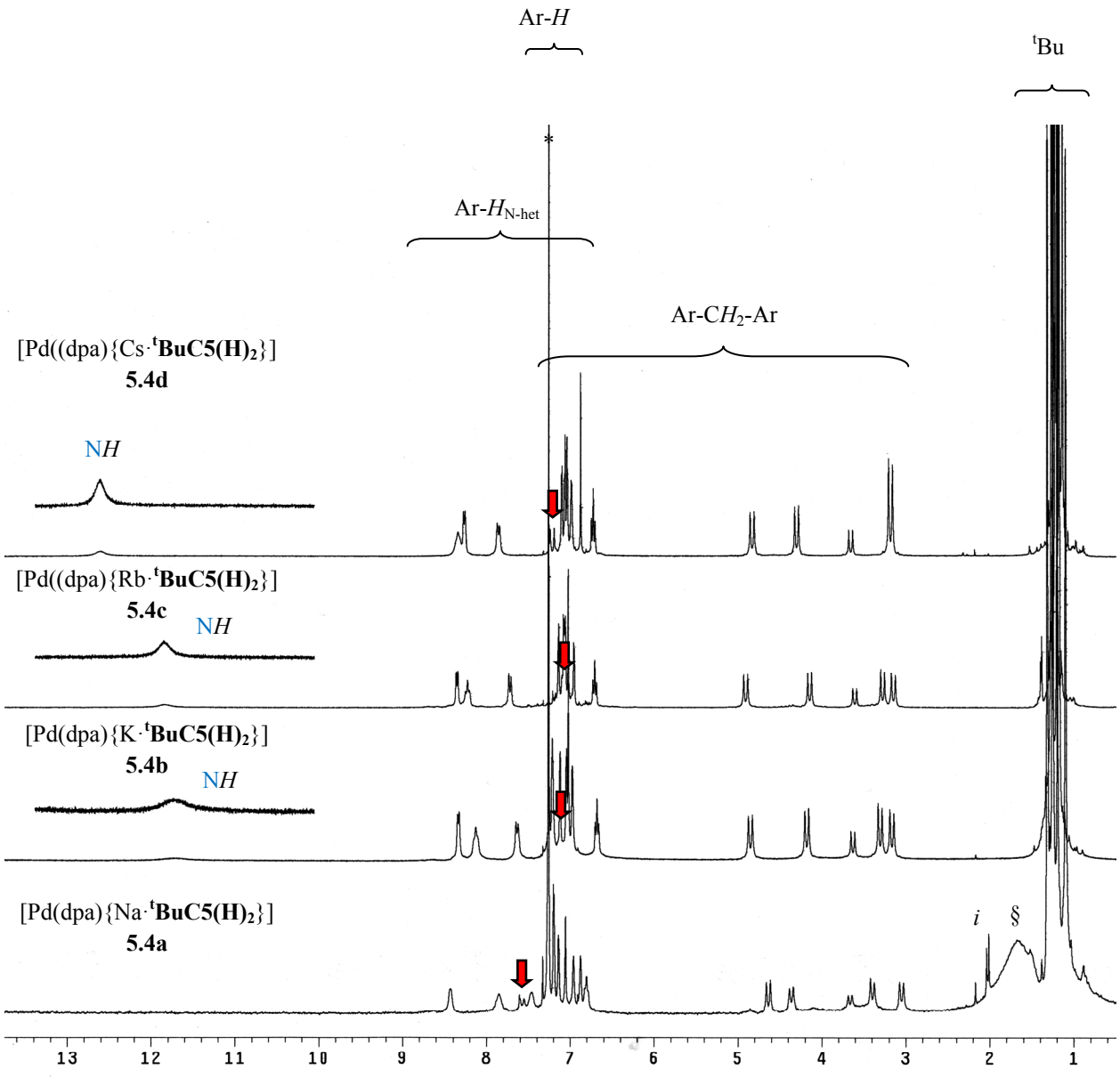

Figure 5.5 ^{1}H NMR spectra of [Pd(dpa){Na·^{t}**BuC5(H)$_2$**}] **5.4a**, [Pd(dpa){K·^{t}**BuC5(H)$_2$**}] **5.4b**, [Pd(dpa){Rb·^{t}**BuC5(H)$_2$**}] **5.4c**, and [Pd(dpa) {Cs·^{t}**BuC5(H)$_2$**}] **5.4d** in *$CDCl_3$. *i* = Impurities. $^{\S}H_2O$. The arrow highlights the methylene Pd···H interaction.

An interesting resonance from one of the protons on a methylene bridge in complexes **5.1a-d**, **5.2a-d**, **5.3a-d** and **5.4a-d** is observed very far downfield. A downfield methylene group was also observed in compound **3.1** and described in Chapter 3. In compound **3.1** a boat-chair conformation was observed and the M···H interaction was not responsible for the downfield shift. (Figure 5.6).

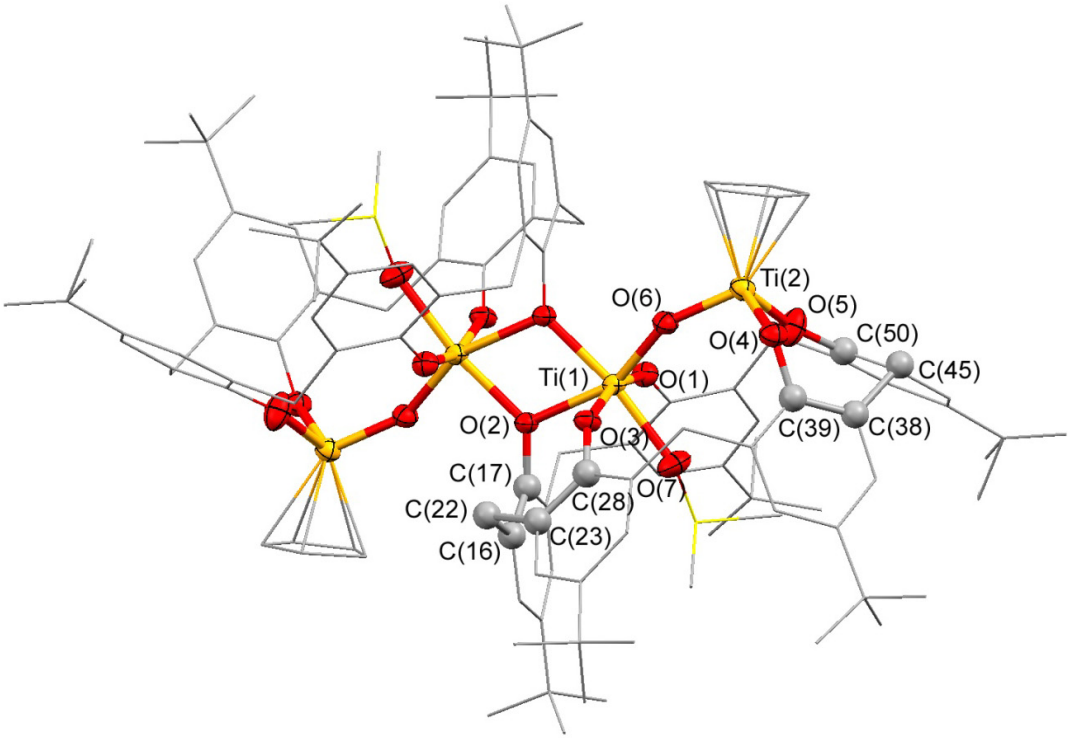

Figure 5.6 X-ray structure of compound **3.1** showing the boat-chair conformation. Thermal ellipsoids are shown at 50% probability. Molecules of crystallization and hydrogen atoms are omitted for clarity. Part of the molecule is drawn in wireframe style for clarity.

Table 5.3 summarizes the chemical shifts found in complexes **5.1a-d**, **5.2a-d**, **5.3a-d** and **5.4a-d**.

Table 5.3 ^{1}H NMR chemical shifts in ppm for complexes **5.1a-d**, **5.2a-d**, **5.3a-d** and **5.4a-d** in $CDCl_3$.

Compound	OH	L	Ar-H	Pd···H	Ar-CH_2-Ar	^{t}Bu
[Pd(bipy){Na·^{t}**BuC5(H)$_2$**}] **5.1a**	-	-	-	-	-	-
[Pd(bipy){K·^{t}**BuC5(H)$_2$**}] **5.1b**	14.48	9.25-7.19	7.26-6.89	6.59	6.59-3.26	1.32-1.09
[Pd(bipy){Rb·^{t}**BuC5(H)$_2$**}] **5.1c**	14.24	9.37-7.16	7.15-6.92	6.49	6.49-3.24	1.29-1.14
[Pd(bipy){Cs·^{t}**BuC5(H)$_2$**}] **5.1d**	13.95	9.45-7.15	7.15-6.95	6.54	6.54-3.23	1.30-1.17
[Pd((4-Me)$_2$bipy)){Na·^{t}**BuC5(H)$_2$**}] **5.2a**	*	8.50-7.34 2.57 (CH_3)	7.26-6.90	6.99	6.99-3.25	1.33-1.10
[Pd((4-Me)$_2$bipy)){K·^{t}**BuC5(H)$_2$**}] **5.2b**	14.03	8.31-7.12 2.76 (CH_3)	7.20-6.86	6.73	6.73-3.18	1.30-1.07
[Pd((4-Me)$_2$bipy)){Rb·^{t}**BuC5(H)$_2$**}] **5.2c**	13.58	8.32-7.08 2.79 (CH_3)	7.12-6.89	6.62	6.62-3.17	1.27-1.11
[Pd((4-Me)$_2$bipy)){Cs·^{t}**BuC5(H)$_2$**}] **5.2d**	*	8.37-7.09 2.77 (CH_3)	7.10-6.91	6.61	6.61-3.16	1.28-1.14
[Pd(phen){Na·^{t}**BuC5(H)$_2$**}] **5.3a**	*	8.75-7.70	7.39-6.84	6.76	6.76-3.42	1.41-1.07
[Pd(phen){K·^{t}**BuC5(H)$_2$**}] **5.3b**	14.44	8.90-7.81	7.28-6.88	6.62	6.62-3.39	1.35-1.10
[Pd(phen){Rb·^{t}**BuC5(H)$_2$**}] **5.3c**	14.25	8.89-7.81	7.17-6.90	6.55	6.55-3.34	1.29-1.14
[Pd(phen){Cs·^{t}**BuC5(H)$_2$**}] **5.3d**	13.82	8.94-7.84	7.15-6.93	6.63	6.63-3.32	1.30-1.17
[Pd(dpa){Na·^{t}**BuC5(H)$_2$**}] **5.4a**	*	8.43-6.81	7.20-6.88	7.56	7.56-3.05	1.31-1.19
[Pd(dpa){K·^{t}**BuC5(H)$_2$**}] **5.4b**	14.04	11.73 (NH) 8.33-6.69	7.21-6.97	7.23	7.23-3.17	1.26-1.17
[Pd(dpa){Rb·^{t}**BuC5(H)$_2$**}] **5.4c**	*	11.85 (NH) 8.35-6.71	7.14-6.96	7.12	7.12-3.15	1.22-1.20
[Pd(dpa){Cs·^{t}**BuC5(H)$_2$**}] **5.4d**	*	12.61 (NH) 8.35-6.73	7.10-6.88	7.22	7.22-3.18	1.23-1.14

*Not observed at room temperature.

An unusual chemical shift displacement for a doublet in a methylene proton was observed in complexes **5.1a-d**, **5.2a-d**, **5.3a-d** and **5.4a-d** downfield methylene (range 7.56-6.49 ppm). Similar chemical shifts were observed previously in metallocalixarene compounds reported by Ishii[151] (7.10 ppm), Vigalok[152] (6.50 ppm), and Matt[150] (7.34 ppm). Authors described that this downfield chemical shift was produced by an interaction between the transition metal and the methylene proton (M···H).[150-152] While regular agostic interactions normally cause an upfield shift of the hydrogen resonance[199] (see for example the methylene proton in $[Mo(PMe_3)_3(H)_2\{^t\mathbf{BuC4(H)_2}\}]$ complex, at -4.58 ppm in C_6D_6, Figure 5.7),[200] the opposite effect has been observed in d^8 square planar complexes and called anagostic interactions.[201] In these cases, the large downfield shift was proposed to be a result of the metal orbital anisotropy effect directed toward an axial or pseudoaxial H atom.[202]

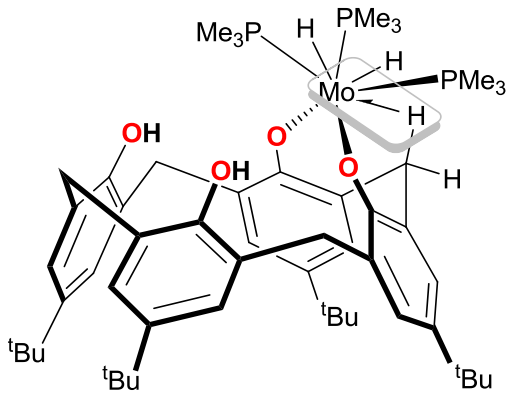

Figure 5.7 Line drawing of $[Mo(PMe_3)_3(H)_2\{^t\mathbf{BuC4(H)_2}\}]$ complex. Agostic interaction is highlighted.[200]

The chemical shifts observed in complexes **5.1a-d**, **5.2a-d**, **5.3a-d** and **5.4a-d** suggest that an interaction between the Pd and a methylene H atom might be responsible for the downfield

chemical shift of the methylene proton. This interaction between Pd and H was corroborated by X-ray diffraction studies performed on compound **5.1d**. The structure revealed a boat-boat conformation in the eight membered heterometallocycle (see Section 5.4).

The ^{13}C NMR spectra of all palladium-calix[5]arene complexes show a pattern consistent with C_s symmetry. Therefore, in the aromatic area are observed 17-21 resonance signals in the range 159.5 – 115.5 ppm (some of them overlapping) in agreement with the expected twenty-one resonance signals. In the aliphatic area (36.8 – 29.1 ppm) a total of 8 – 9 signals are observed (one of them overlapping). There are nine signals corresponding to Ar-CH$_2$-Ar, C(CH$_3$)$_3$, and C(CH$_3$)$_3$ groups, three signals for each group.

5.3.2 Spectral data for palladium calix[4,6]arene complexes

The ^{1}H NMR spectra of the compounds **5.5a** to **5.5e** display a similar symmetric pattern consistent with the expected 1,2-coordination mode. The *tert*-butyl groups appear as two sharp singlets in a 1:1 ratio. The NMR pattern shows six sets of doublets for the Ar-CH_2-Ar groups (2:2:1:1:1:1 ratio). One of these signals appears at 8.42 – 7.93 ppm, a very low field resonance for this proton, but it is similar to methylene resonances found in complexes **5.1a-d**, **5.2a-d**, **5.3a-d** and **5.4a-d**. From the X-ray structure of some of these compounds and literature precedent[150-152] we suggest that the Pd···H interaction is responsible for this downfield shift.

The resonance for the OH group is a sharp singlet at 11.79 – 10.25 ppm, downfield from the OH singlet for the parent **^{t}BuC4(H)$_4$** (10.39 ppm). Similar downfield shifts of the OH group and the axial hydrogen atom, accompanied by the short metal-H distance, have previously been observed for late transition metal calixarene systems.[150-152]

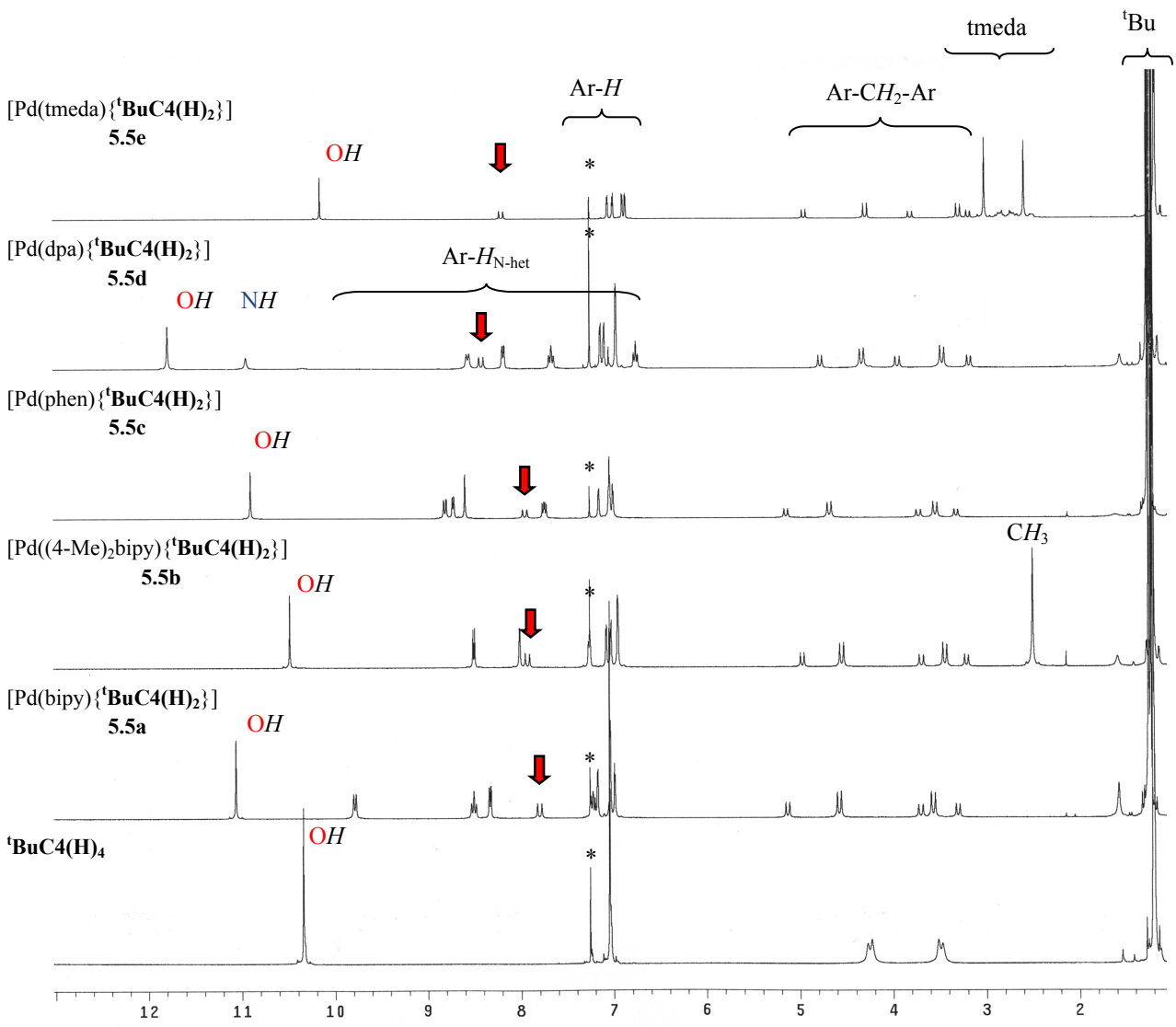

Figure 5.8 ^{1}H NMR spectra of complexes **5.5a-5.5e** and **^{t}BuC4(H)$_4$** in *$CDCl_3$. The arrow highlights the methylene Pd···H interaction.

The ^{1}H NMR spectra of compounds **5.6a** to **5.6c** display a symmetric pattern similar to that of the spectra of compounds **5.5a** to **5.5c**, consistent with the expected 1,2-coordination (Figure 5.9). A singlet for the resonance of the OH group is localized around 10.34 – 10.28 ppm. The downfield shift of the methylene proton was also observed (7.99-7.96 ppm). The

replacement of the ^{t}Bu by H in the *para* position makes the ^{1}H NMR pattern quite different in the aromatic area. The coupling of the *para* H results in two different sets of triplets. The aromatic N-heterocyclic and the remaining methylene protons fall in the expected range.

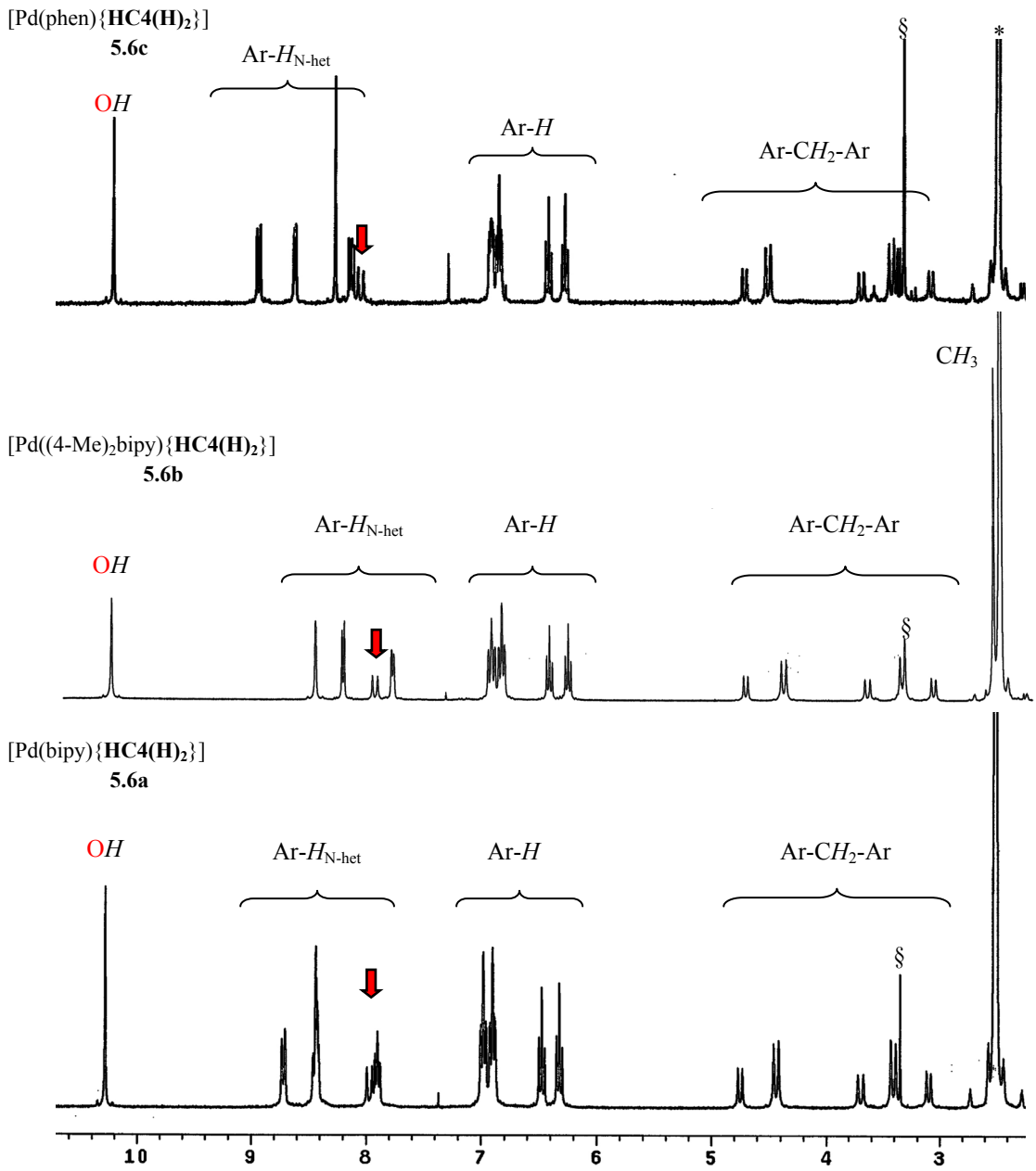

Figure 5.9 ^{1}H NMR spectra of complexes **5.6a-5.6c** and **^{t}BuC4(H)$_4$** in *DMSO-d$_6$. §H$_2$O. The arrow highlights the methylene Pd···H interactions.

The ^{1}H NMR spectrum of [Pd((4-Me)$_2$bipy))\{Cs·^{t}**BuC6(H)$_3$**\}] (**5.7**) displays a highly unsymmetrical NMR pattern due to the partial metallation (Figure 5.10). Complex **5.7** produced twelve methylene doublets (integrating to 1 hydrogen each, with some overlapped), six resonances for the ^{t}Bu groups (two overlapped), and two broad peaks at 14.13 and 10.66 ppm (in a 1:2 ratio) for the unreacted OH groups. As expected, the methylene proton that interacts with the metal (Pd···H) is observed in the downfield region, at 7.58 ppm.

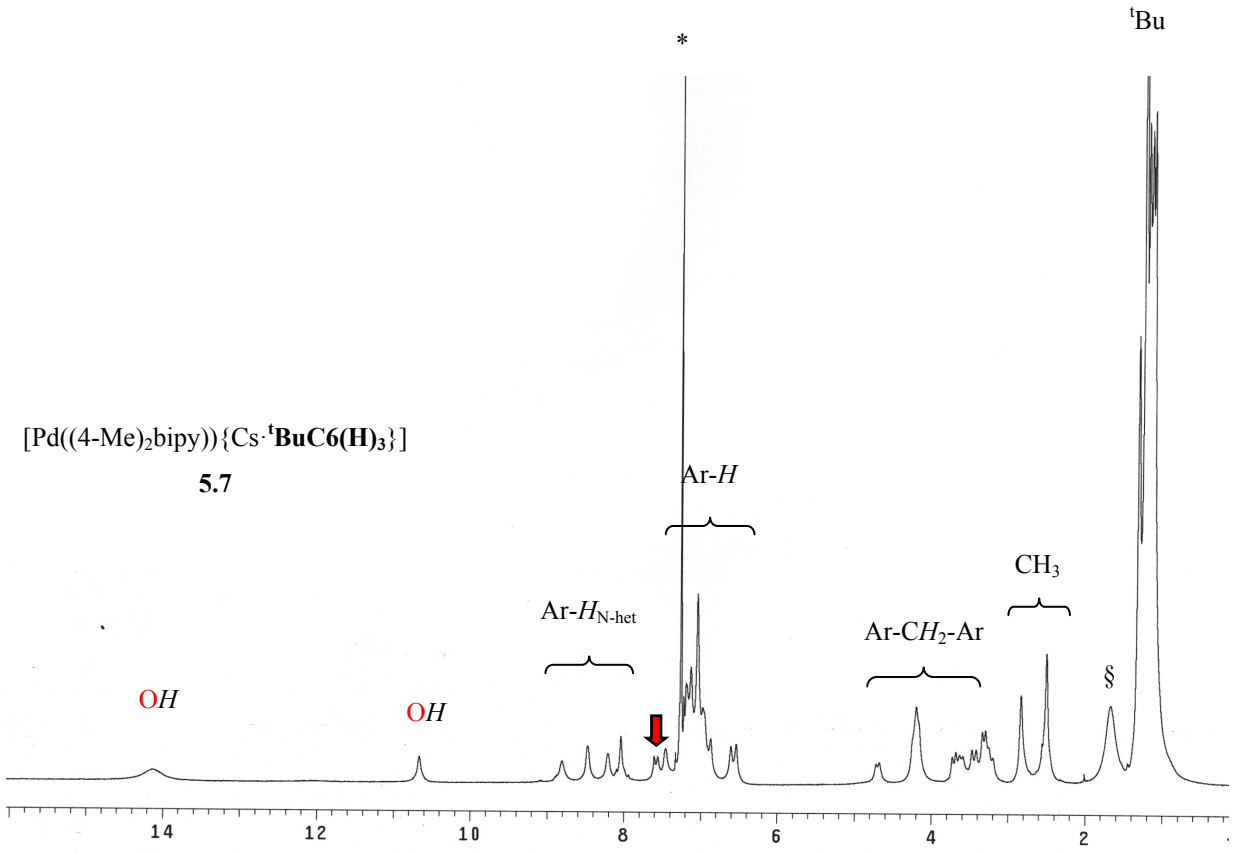

Figure 5.10 ^{1}H NMR spectrum of [Pd((4-Me)$_2$bipy))\{Cs·^{t}**BuC6(H)$_3$**\}] **5.7** complex in *CDCl$_3$. §H$_2$O. The arrow highlights the methylene Pd···H interactions.

Table 5.4 shows the chemical shifts found in palladium calix[4,6]arene complexes.

Table 5.4 ^{1}H NMR chemical shifts in ppm for palladium calix[4,6]arene complexes **5.5a-5.5e** and **5.7**.

Compound	OH	L	Ar-H	Pd···H	Ar-CH_2-Ar	^{t}Bu
[Pd(bipy){^{t}**BuC4(H)$_2$**}]^{a} **5.5a**	11.07	9.79-7.23	7.18-6.99	7.80	7.80-3.30	1.26; 1.23
[Pd((4-Me)$_2$bipy)){^{t}**BuC4(H)$_2$**}]^{a} **5.5b**	10.49	8.51-7.27 2.50 (CH_3)	7.08-6.96	7.93	7.93-3.21	1.21; 1.20
[Pd(phen){^{t}**BuC4(H)$_2$**}]^{a} **5.5c**	10.90	8.81-7.75	7.16-7.01	7.96	7.96-3.32	1.27; 1.24
[Pd(dpa){^{t}**BuC4(H)$_2$**}]^{a} **5.5d**	11.80	10.96 (NH) 8.57-6.76	7.14-6.98	8.43	8.43-3.18	1.27; 1.22
[Pd(tmeda){^{t}**BuC4(H)$_2$**]^{a} **5.5e**	10.16	3.02-2.59	7.07-6.87	8.21	8.21-3.19	1.19; 1.18
[Pd(bipy){**HC4(H)$_2$**}]^{b} **5.6a**	10.28	8.72-7.90	6.98-6.32	7.97	7.97-3.10	-
[Pd((4-Me)$_2$bipy)){**HC4(H)$_2$**}]^{b} **5.6b**	10.28	8.51-7.83 2.56 (CH_3)	6.97-6.30	7.99	7.99-3.09	-
[Pd(phen){**HC4(H)$_2$**}]^{b} **5.6c**	10.34	9.05-8.23	6.99-6.34	8.15	8.15-3.10	-
[Pd((4-Me)$_2$bipy)){Cs·^{t}**BuC6(H)$_3$**}]^{a} **5.7**	14.13 10.66	8.80-7.46 2.83 (CH_3) 2.50 (CH_3)	7.22-6.54	7.58	7.58-3.22	1.32-1.12

^{a} $CDCl_3$, ^{b} DMSO-d_6

5.4 Crystal structures

Crystal structures of **5.1d**·2DMSO, **5.5a**·5C_6H_6, **5.5b**·5.5C_6H_6, **5.5e**·3CH_3CN, **5.6b**·2CH_3CN and **5.7**·7.5C_6H_6·H_2O are shown in Figures 5.11-5.13, respectively, and selected bond distances and angles are listed in Table 5.5.

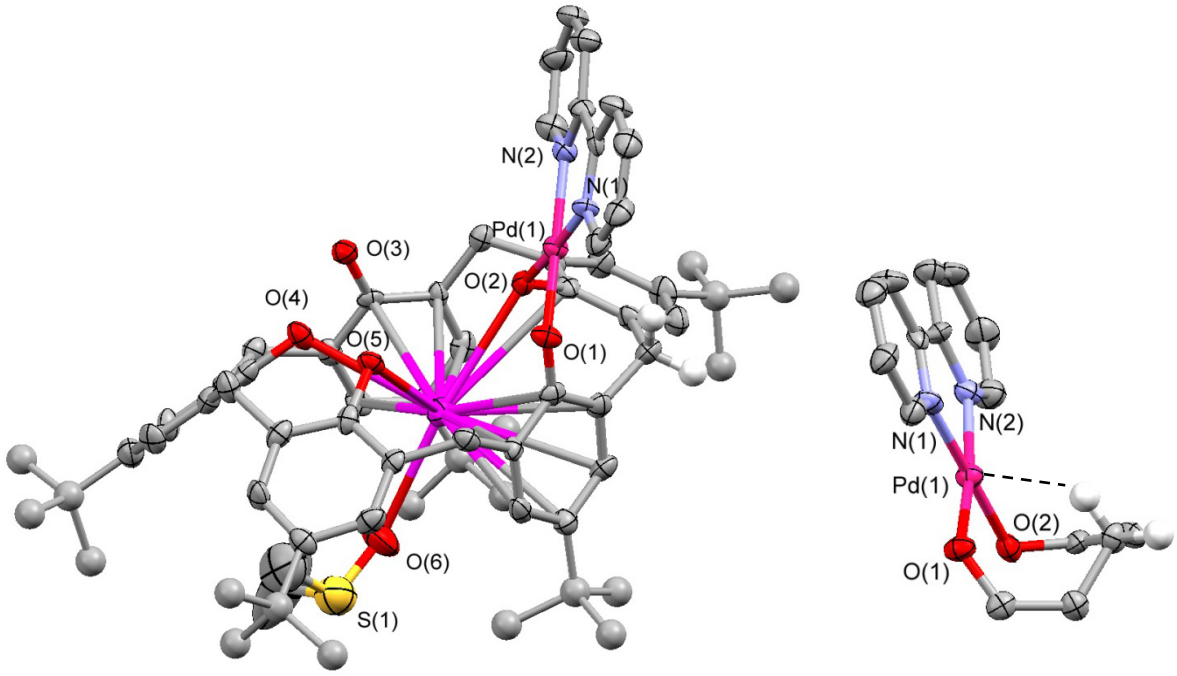

a) **b)**

Figure 5.11 ORTEP diagram of compound a) **5.1d**·2DMSO and b) eight-membered cycle. Thermal ellipsoids at the 50% probability level. H atoms and non-coordinating solvent are omitted for clarity.

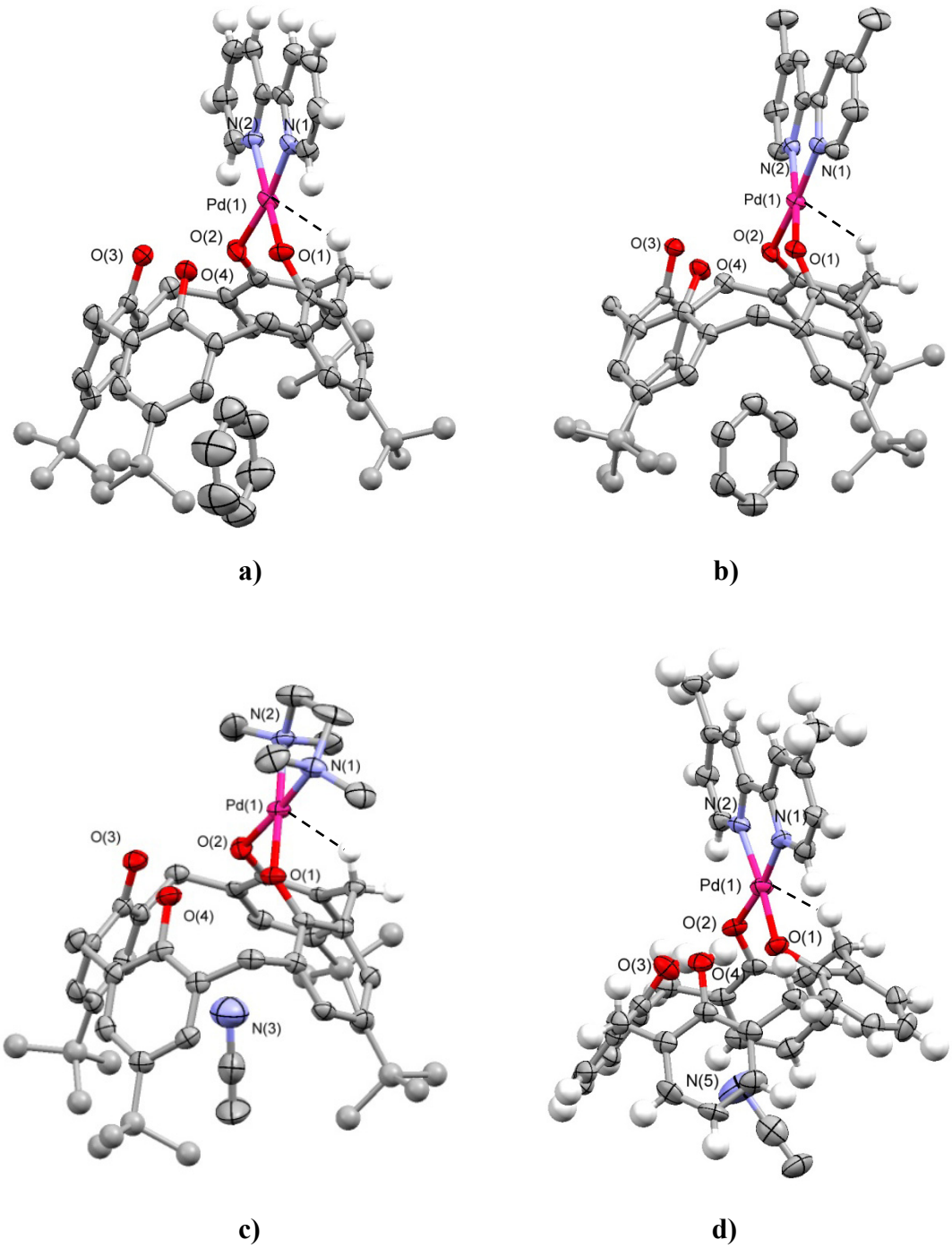

Figure 5.12 ORTEP diagrams of compounds a) **5.5a**·$5C_6H_6$, b) **5.5b**·$5.5C_6H_6$, c) **5.5e**·$3CH_3CN$ and d) **5.6b**·$2CH_3CN$ with thermal ellipsoids at the 50% probability level. H atoms and non-coordinating solvent are omitted for clarity.

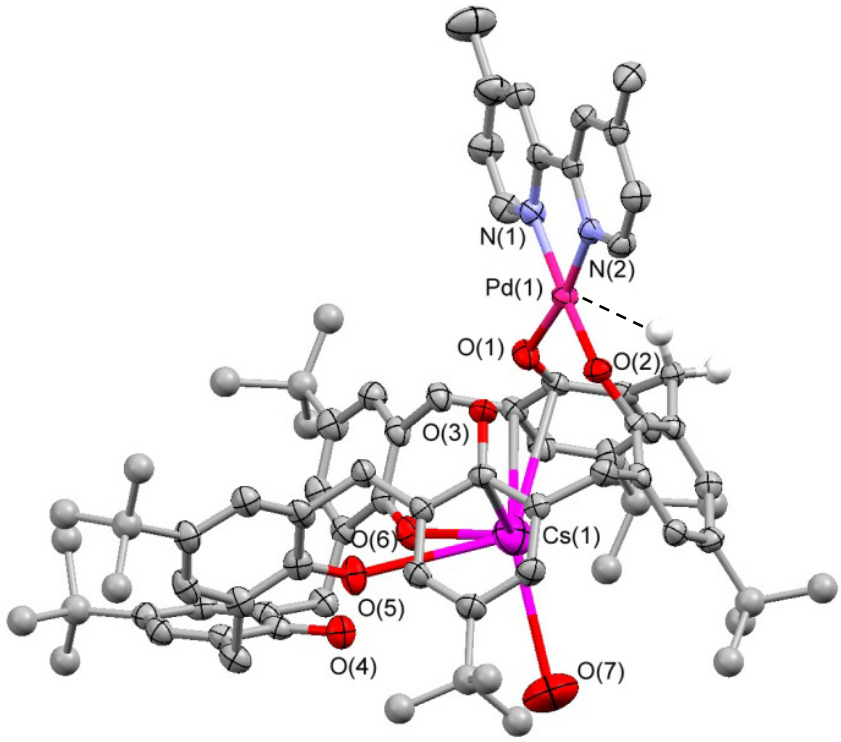

Figure 5.13 ORTEP diagram of compound **5.7**·7.5C_6H_6·H_2O with thermal ellipsoids at the 50% probability level. Some H atoms and non-coordinating solvent are omitted for clarity.

Table 5.5 Selected bond lengths (Å) and angles (º) of complexes **5.1d**·2DMSO, **5.5a**·5C_6H_6, **5.5b**·5.5C_6H_6, **5.5e**·3CH_3CN, **5.6**·2CH_3CN and **5.7**·7.5C_6H_6·H_2O.

	5.1d·2DMSO	**5.5a**·5C_6H_6	**5.5b**·5.5C_6H_6	**5.5e**·3CH_3CN	**5.6b**·2CH_3CN	**5.7**·7.5C_6H_6·H_2O
Pd(1)-O(1)	1.997(4)	1.990(4)	1.997(3)	2.007(3)	1.979(5)	1.999(4)
Pd(1)-O(2)	1.999(5)	1.997(4)	1.988(3)	2.004(3)	1.983(5)	1.994(4)
Pd(1)-N(1)	1.989(6)	1.996(4)	1.999(3)	2.044(4)	2.004(6)	2.004(5)
Pd(1)-N(2)	2.027(6)	2.004(4)	2.001(3)	2.048(4)	1.992(6)	1.997(5)
Cs(1)-O(2)	3.127(5)	-	-	-	-	-
Cs(1)-O(4)	3.248(5)	-	-	-	-	3.388(4)
Cs(1)-O(5)	3.182(5)	-	-	-	-	-
Cs(1)-O(6)	3.007(6)	-	-	-	-	3.152(4)
Cs(1)-O(7)	-	-	-	-	-	3.278(7)
N(1)-Pd(1)-O(1)	90.3(2)	91.24(16)	93.28(11)	90.82(15)	94.6(2)	93.64(19)
N(1)-Pd(1)-O(2)	177.3(2)	171.90(17)	174.49(11)	176.60(16)	171.9(2)	170.41(18)
O(1)-Pd(1)-O(2)	91.86(18)	92.41(16)	91.68(11)	90.31(14)	91.8(2)	95.25(17)
N(1)-Pd(1)-N(2)	80.4(2)	81.05(17)	80.58(12)	86.32(17)	80.8(2)	80.61(19)
O(1)-Pd(1)-N(2)	170.3(2)	171.58(16)	171.46(11)	176.51(15)	171.4(2)	171.14(18)
O(2)-Pd(1)-N(2)	97.4(2)	94.82(17)	94.24(12)	92.43(16)	92.2(2)	90.13(18)

All five complexes possess an approximate square planar coordination geometry around the metal with adjacent, interligand angles around the palladium center falling in the range 80.4(2)-97.4(2)°. Complexes **5.1d**·2DMSO, **5.5a**·5C_6H_6, **5.5b**·5.5C_6H_6, **5.5e**·3CH_3CN, **5.6**·2CH_3CN and **5.7**·7.5C_6H_6·H_2O possess eight-membered heterometallocycles formed by Pd(1)-O(1)-C(1)-C(2)-C(11)-C(12)-C(17)-O(2), with an approximate boat-boat conformation. Similar heterometallocycle conformations are observed in [Rh(cod){^{t}**BuC4(H)$_2$**·η^6-Rh(cod)}][151] (cod = 1,5-cyclooctadiene) and [Pt(dppp){^{t}**BuC4(H)$_2$**}][152] (dppp = diphenylphosphinopropane) complexes. In all complexes this conformation results in a short distance between the axial H atom of the methylene bridging C(11)H_2 group, and the Pd center, *d*(Pd···H) 2.170 – 2.443 Å

(dashed line in Figures 5.12-5.17). This short interaction is responsible for the downfield chemical shift of the methylene proton (Table 5.6).

Table 5.6 Pd···H interactions (Å) of complexes **5.1d**·2DMSO, **5.5a**·5C_6H_6, **5.5b**·5.5C_6H_6, **5.5e**·3CH_3CN, **5.6**·2CH_3CN and **5.7**·7.5C_6H_6·H_2O.

	5.1d·2DMSO	**5.5a**·5C_6H_6	**5.5b**·5.5C_6H_6	**5.5e**·3CH_3CN	**5.6b**·2CH_3CN	**5.7**·7.5C_6H_6·H_2O
Pd···H	2.443	2.273	2.254	2.170	2.290	2.303

Complexes **5.5a**·5C_6H_6, **5.5b**·5.5C_6H_6, **5.5e**·3CH_3CN and **5.6**·2CH_3CN crystallize with a solvent molecule (C_6H_6 or CH_3CN) entrapped inside the calixarene cavity. In the case of compound **5.1d**·2DMSO one molecule of DMSO is coordinated to the Cs ion.

The Pd-O distances fall within the range of Pd-O distances found in related palladium alkoxide and aryloxide complexes (Table 5.7).

Table 5.7 Overview of characteristic bond distances for palladium alkoxide and aryloxide compounds.

Compound	*d*(Pd–O) (Å)	Ref
[Pd(Me)(CH(CF_3)$_2$)(tmeda)]	2.020(2)	[203]
[Pd(Me)(OC_6H_5)(tmeda)]	2.024(3)	[203]
[Pd(Me)(OC_6H_4-NO_2)(tmeda)]	2.029(4)	[203]
[Pd(OPh)$_2$(bipy)]	1.983(6) – 1.996(7)	[198]
[Pd(OC_6F_5)$_2$(bipy)]	2.013(3) – 2.013(4)	[198]
[Pd(OPh)(OCH(CF_3)$_2$)(bipy)]·HOPh	1.984(6) – 1.997(5)	[204]
5.1d·2DMSO	1.997(4) –1.999(5)	This work
5.5a·5C_6H_6	1.990(4) – 1.997(4)	This work
5.5b·5.5C_6H_6	1.988(3) – 1.997(3)	This work
5.5e·3CH_3CN	2.004(3) – 2.007(3)	This work
5.6b·2CH_3CN	1.979(5) – 1.983(5)	This work
5.7·7.5C_6H_6·H_2O	1.994(4) –1.999(4)	This work

For the calix[5]arene and calix[6]arene palladium derivatives an alkali ion is incorporated in the structure, but not in the calix[4]arene derivatives.

*5.4.1 Crystal structures of by-products [Pd(bipy){^{t}**BuC5(H)$_3$**}]·4CH$_3$CN (**5.1**·4CH$_3$CN) and [Pd((4-Me)$_2$bipy){^{t}**BuC5(H)$_3$**}]·4CH$_3$CN (**5.2**·4CH$_3$CN)*

X-ray structures of byproducts **5.1**·4CH$_3$CN and **5.2**·4CH$_3$CN were obtained from the mother liquor from the first part of the purification procedure (hot filtration). A small amount of crystals (<10 mg) of **5.1**·4CH$_3$CN was obtained from the slow evaporation of the filtrate (acetonitrile solution) from the reaction between Na$_2$·^{t}**BuC5(H)$_3$** and [Pd(bipy)Cl$_2$], and crystals of **5.2**·4CH$_3$CN from the reaction between Rb$_2$·^{t}**BuC5(H)$_3$** and [Pd((4-Me)$_2$bipy)Cl$_2$]. Attempts to reproduce those compounds for additional characterization were unsuccessful. Figure 5.14 illustrates a line drawing of compounds Pd(bipy){^{t}**BuC5(H)$_3$**}] **5.1** and [Pd((4-Me)$_2$bipy){^{t}**BuC5(H)$_3$**}] **5.2**.

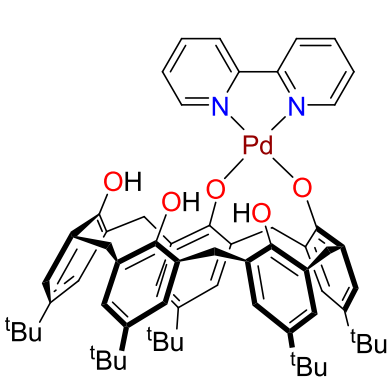

[Pd(bipy){^{t}**BuC5(H)$_3$**}] **5.1**

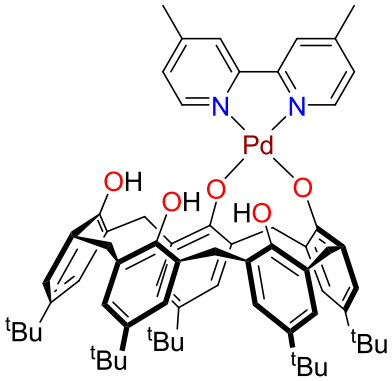

[Pd((4-Me)$_2$bipy){^{t}**BuC5(H)$_3$**}] **5.2**

Figure 5.14 Line drawings of compounds **5.1** and **5.2**.

Several interesting features were found in the solid state structures of complexes **5.1**·4CH_3CN and **5.2**·4CH_3CN. First, neither of them contains the alkali metal inside the calix[5]arene cavity. Instead of the alkali metal a solvent molecule was found for **5.1**·4CH_3CN and two molecules in **5.2**·4CH_3CN (Figure 5.15).

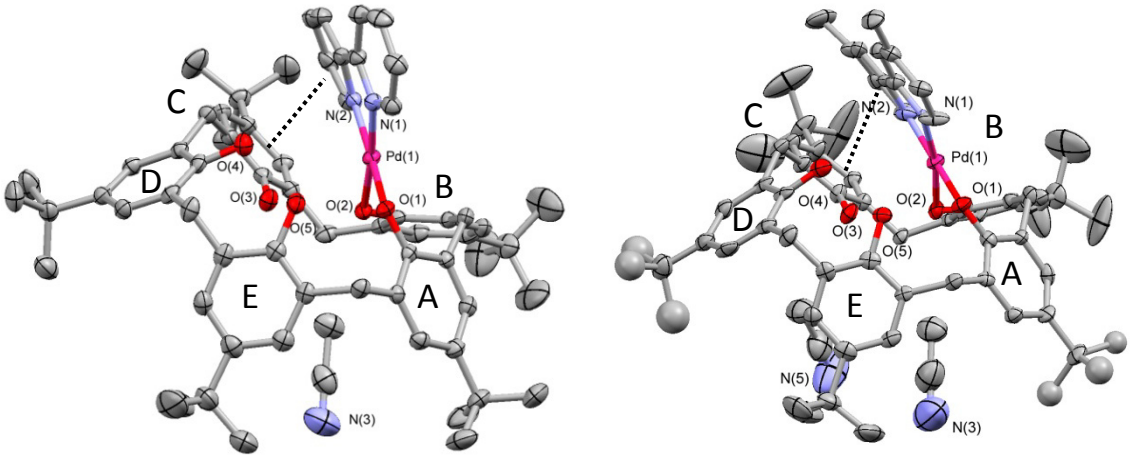

a) **b)**

Figure 5.15 ORTEP diagram of compound a) **5.1**·4CH_3CN and b) **5.2**·4CH_3CN with thermal ellipsoids at the 50% probability level. Some H atoms and non-coordinating solvent are omitted for clarity.

Second, π-π stacking interactions were observed between the calix[5]arene ring labeled C (Figure 5.14) and one of the pyridyl rings. The distances are $d_{\pi\text{-}\pi}$(ring C – bipy ring) = 3.987 Å in **5.1**·4CH_3CN and $d_{\pi\text{-}\pi}$(ring C – (4-Me)$_2$bipy ring) = 3.893 Å, both slightly higher than the maximum value reported for the ring centroid-centroid distance $d_{c\text{-}c}$ = 3.8 Å in aromatic π-stacking.[205]

The d(Pd···H) = 2.367 and 2.427 Å distances for **5.1**·4CH_3CN and **5.2**·4CH_3CN, respectively, are in the typical range reported in this chapter. Selected bond distances and angles are tabulated in Table 5.8.

Finally the calix[5]arene rings in complexes **5.1**·4CH_3CN and **5.2**·4CH_3CN are much more distorted than in complex **5.1d**·2DMSO.

Table 5.8 Selected bond lengths (Å) and angles (º) of complexes **5.1**·4CH_3CN and **5.2**·4CH_3CN.

	5.1·4CH_3CN	**5.2**·4CH_3CN	Ranges from Table 5.5
Pd(1)-O(1)	2.0024(19)	2.006(6)	1.979(5) – 2.007(3)
Pd(1)-O(2)	2.0195(19)	2.007(7)	1.983(5) – 2.004(3)
Pd(1)-N(1)	2.008(2)	2.005(8)	1.989(6) – 2.044(4)
Pd(1)-N(2)	2.002(2)	1.985(8)	1.992(6) – 2.048(4)
Pd···H	2.367	2.427	2.170 – 2.443
$d_{c\text{-}c}$(arene-pyridyl)	3.987	3.893	-
N(1)-Pd(1)-O(1)	91.62(9)	90.9(3)	90.3(2) – 94.6(2)
N(1)-Pd(1)-O(2)	174.59(8)	169.8(2)	170.41(18) – 177.3(2)
O(1)-Pd(1)-O(2)	91.61(8)	90.5(3)	90.31(14) – 95.25(17)
N(1)-Pd(1)-N(2)	80.81(10)	80.9(3)	80.4(2)- 86.32(17)
O(1)-Pd(1)-N(2)	171.61(9)	171.8(3)	170.3(2) – 176.51(15)
O(2)-Pd(1)-N(2)	95.67(9)	97.2(3)	90.13(18) – 97.4(2)

5.5 Experimental Section

5.5.1 General information

Unless otherwise noted, all manipulations were carried out in air. $M_2 \cdot$**^{t}BuC5(H)$_3$** (M = Na, K, Rb, Cs) were prepared as previously described.[113] Potassium carbonate (K_2CO_3), N,N,N',N'-tetramethylenediamine (tmeda), 2,2'-bipyridyl (bipy), 4,4'dimethyl-2,2'-dipyridyl ((4-Me)$_2$bipy), 1,10-phenanthroline (phen), 2,2'-dipyridylamine (dpa), and $PdCl_2$ were obtained from Aldrich and were used without further purification. *p*-H-calix[4]arene (**HC4(H)$_4$**),[206] *p-tert*-butylcalix[4]arene (**^{t}BuC4(H)$_4$**),[6] *p-tert*-butylcalix[5]arene (**^{t}BuC5(H)$_5$**),[120] *p-tert*-butylcalix[6]arene (**^{t}BuC6(H)$_6$**),[7] (2,2'-dipyridine)dichloropalladium(II) [Pd(bipy)Cl_2], (4,4'dimethyl-2,2'-dipyridine)dichloropalladium(II) [Pd((4-Me)$_2$bipy)Cl_2], (1,10-phenanthroline)dichloropalladium(II) [Pd(phen)Cl_2], (N,N,N',N'-tetramethylenediamine)dichloropalladium(II) [Pd(tmeda)Cl_2], and (2,2'-dipyridylamine)dichloropalladium(II) [Pd(dpa)Cl_2] were all prepared by literature procedures.[195] The melting points of all compounds were taken in capillary tubes on a Mel-Temp apparatus (Laboratory Devices, Cambridge, MA). A temperature preceded by a ">" sign indicates that the compound starts to decompose at that temperature but appears to actually melt at some higher temperature. ^{1}H NMR and ^{13}C NMR spectra were recorded on a Varian XL-300 spectrometer at 300 and 75 MHz, respectively. Microanalyses were performed by Atlantic Microlab, Inc, Norcross, GA. IR and UV/Vis spectra were obtained with an Infinity Gold^{TM} FTIR spectrometer and Agilent 8453 spectrophotometer, respectively. Filtrations used a medium sintered glass filter. All solvents were anhydrous and were stored over 4Å molecular sieves prior to use.

5.5.1.1 Preparation of compounds

5.5.1.1.1 General procedure for the synthesis of [Pd(L)Cl_2] (L = bipy, tmeda, (4-Me)$_2$bipy, 1,10-phen, dpa)[195]

A representative synthesis of complex [Pd(bipy)Cl_2] is given. Ligand bipy (0.192 g, 1.23 mmol) in acetonitrile (10.0 mL) was added by syringe to a refluxing deep red solution of $PdCl_2$ (0.212 g, 1.19 mmol) in acetonitrile (55 mL). The resulting yellow solution was stirred vigorously for 30 minutes and microcrystals of [Pd(bipy)Cl_2] gradually separated out from the reaction mixture while stirring. The crystalline solid was filtered, washed with acetonitrile (15 mL), and dried under vacuum to obtain a light orange solid (0.370 g, 1.11 mmol, 93% yield). Mp: 376 - 378 ^{o}C. ^{1}H NMR (DMSO-d_6) δ (ppm): 9.12 (dd, 2H, *J* = 5.8, 1.4 Hz), 8.59 (dd, 2H, *J* = 7.6, 0.8 Hz), 8.36 (ddd, 2H, *J* = 7.9, 8.0, 1.6 Hz), 7.81 (ddd, 2H, *J* = 5.9, 7.6, 1.4 Hz). FTIR (KBr, cm^{-1}): 3109m, 3084m, 3074m, 3049m, 1603s, 1564w, 1498w, 1468s, 1448s, 1313w, 1165m, 1111w, 1038w, 1024w, 762s, 719m.

[Pd(tmeda)Cl_2]: (tmeda 0.308 g, 2.65 mmol and $PdCl_2$ 0.465 g, 2.62 mmol). Off-yellow solid (0.702 g, 2.39 mmol, 91% yield). Mp: 248-250 ^{o}C. ^{1}H NMR (DMSO-d_6) δ (ppm): 2.72 (s, 4H, CH_2), 2.64 (s, 12H, CH_3). FTIR (KBr, cm^{-1}): 3022m, 2988m, 2913m, 2843w, 1468s, 1437m, 1402m, 1281m, 1200w, 1125m, 1105w, 1064w, 1046s, 1009s, 955m, 808s, 772m, 507w.

[Pd((4-Me)$_2$bipy)Cl_2]: ((4-Me)$_2$bipy 0.252 g, 1.37 mmol and $PdCl_2$ 0.242 g, 1.37 mmol). Light orange solid (0.414 g, 1.14 mmol, 84% yield). Mp: 382 – 384 ^{o}C. ^{1}H NMR (DMSO-d_6) δ (ppm): 8.85 (d, 2H, *J* = 5.8 Hz), 8.42 (s, 2H), 7.60 (d, 2H, *J* = 5.2 Hz), 2.52 (s, 6H, CH_3). FTIR (KBr, cm^{-1}): 3113m, 3060m, 3032m, 2966w, 2920w, 1616s, 1556w, 1481m, 1448m, 1419m, 1381w, 1221m, 1032m, 926w, 833m, 567w, 517m.

[Pd(phen)Cl_2]: (phen 0.474 g, 2.63 mmol and $PdCl_2$ 0.465 g, 2.62 mmol). Light orange solid (0.812 g, 2.27 mmol, 87% yield). Mp: 438 - 440 ^oC. ^1H NMR (DMSO-d_6) δ (ppm): 9.35 (dd, 2H, *J* = 5.4, 1.1 Hz), 8.99 (dd, 2H, *J* = 8.2, 1.1 Hz), 8.29 (s, 2H), 8.14 (dd, 2H, *J* = 8.0, 5.4 Hz). FTIR (KBr, cm^{-1}): 3078m, 3058m, 1631w, 1603w, 1581w, 1515m, 1425s, 1409w, 1153w, 842s, 710m.

[Pd(dpa)Cl_2]: (dpa 0.284 g, 1.66 mmol and $PdCl_2$ 0.296 g, 1.67 mmol). Yellow-orange solid (0.545 g, 1.56 mmol, 94% yield). Mp: 364 – 366 ^oC. ^1H NMR (DMSO-d_6) δ (ppm): 11.13 (s, 1H, NH), 8.59 (d, 2H, *J* = 6.0 Hz), 7.97 (dd, 2H, *J* = 8.0, 7.7 Hz), 7.28 (d, 2H, *J* = 8.5 Hz), 7.16 (dd, 2H, *J* = 7.1, 6.3 Hz). FTIR (KBr, cm^{-1}): 3280m, 3233m, 3198m, 3137m, 3036w, 1631s, 1584s, 1523m, 1472s, 1435m, 1361w, 1235m, 1159m, 1030w, 904w, 766s, 533w.

*5.5.1.1.2 Synthesis of [Pd(L){M·^{t}**BuC5(H)$_2$**}] (L = bipy, (4-Me)$_2$bipy, 1,10-phen, dpa) complexes*

All palladium-containing calix[5]arene complexes were prepared following a similar procedure. A solution or suspension of M_2·^{t}**BuC5(H)$_3$** (M = Na, K, Rb, Cs) in anhydrous acetonitrile (10 mL) was added to a hot solution (90 ^oC, oil bath) of anhydrous acetonitrile (25 mL) of the corresponding [Pd(L)Cl_2] (L = bipy, (4-Me)$_2$bipy, 1,10-phen, dpa) in a 2:1 mol ratio. A change in color was observed from light yellow to orange with formation of a precipitate. The reaction mixture was stirred for additional 30 min. At the end of this time the heat was removed and the solution was vacuum filtered while hot using a medium pore size frit. An orange solid was recovered. The orange solid was washed with DI water (10 mL) twice and with acetonitrile (10 mL) twice affording complexes **5.1a-d**, **5.2a-d**, **5.3a-d**, and **5.4a-d**.[207]

[Pd(bipy){Na·^{t}**BuC5(H)$_2$**}] **(5.1a)**: (^{t}**BuC5(H)$_5$**: 0.101 g, 0.124 mmol; NaO^{t}Bu: 0.0243 g, 0.253 mmol, [Pd(bipy)Cl_2]: 0.0213 g, 0.0639 mmol). **5.1a** was obtained as an orange solid (0.0520 g, 0.0475 mmol, 74% yield). Mp: >318 ^{o}C. No ^{1}H or ^{13}C{^{1}H} NMR were performed due to its poor solubility. FTIR (KBr, cm^{-1}): 3422m (OH), 3074w, 3047m, 2959s, 2903s, 2866s, 1605m, 1566w, 1480s, 1469s, 1452s, 1391m, 1361m, 1296s, 1261m, 1252m, 1206s, 1174m, 1161m, 1127m, 1058w, 1043w, 1026w, 945w, 917w, 878m, 821m, 801m, 768m, 725m, 671w, 602w, 568w, 550w, 527w, 495w. UV/vis λ_{max}/nm (C_6H_6) (ε/dm^3 mol^{-1} cm^{-1}): 280 (2.64 x 10^4), 491 (3.86 x 10^3), 461 (3.85 x 10^3). By slow evaporation of the filtrate solution, red block crystals of (>10 mg) compound **5.1** were obtained, however the yield was quite low, so no further characterization was performed.

[Pd(bipy){K·^{t}**BuC5(H)$_2$**}] **(5.1b)**: (^{t}**BuC5(H)$_5$**: 0.0530 g, 0.0653 mmol; KO^{t}Bu: 0.0148 g, 0.132 mmol, [Pd(bipy)Cl_2]: 0.0114 g, 0.0342 mmol). **5.1b** was obtained as an orange-red solid (0.0315 g, 0.0284 mmol, 83% yield). Mp: >340 ^{o}C. ^{1}H NMR ($CDCl_3$) δ (ppm): 14.48 (br, 2H, OH), 9.25 (d, 2H, *J* = 8.0 Hz, bipy), 8.57 (dd, 2H, J = 7.4 Hz, 6.6 Hz, bipy), 8.17 (d, 2H, *J* = 4.4 Hz, bipy), 7.26 (d, 2H, *J* = 2.2 Hz, Ar-*H*), 7.19 (dd, 2H, *J* = 6.6, 5.8 Hz, bipy), 7.18 (d, 2H, *J* = 2.5 Hz, Ar-*H*), 7.09 (s, 2H, Ar-*H*), 6.92 (d, 2H, *J* = 2.5 Hz, Ar-*H*), 6.89 (d, 2H, *J* = 2.5 Hz, Ar-*H*), 6.59 (d, 1H, *J* = 13.7 Hz, Ar-C*H*$_2$-Ar), 5.13 (d, 2H, *J* = 14.3 Hz, Ar-C*H*$_2$-Ar), 4.30 (d, 2H, *J* = 13.7 Hz, Ar-C*H*$_2$-Ar), 3.42 (d, 2H, *J* = 13.5 Hz, Ar-C*H*$_2$-Ar), 3.40 (d, 1H, *J* = 14.0 Hz, Ar-C*H*$_2$-Ar), 3.26 (d, 2H, 14.3 Hz, Ar-C*H*$_2$-Ar), 1.32 (s, 18H, ^{t}Bu), 1.25 (s, 9H, ^{t}Bu), 1.09 (s, 18H, ^{t}Bu). ^{13}C{^{1}H} NMR ($CDCl_3$) δ (ppm): 157.8, 157.7, 155.5, 151.1, 148.3, 141.7, 141.6, 139.7, 137.6, 131.6, 130.9, 129.4, 128.1, 127.1, 126.9, 126.1, 125.8, 125.4, 125.3, 124.9, 124.4 (aromatic carbons), 36.1, 35.9 (*C*(CH$_3$)$_3$), 34.1 (Ar-*C*H$_2$-Ar), 33.8 (*C*(CH$_3$)$_3$), 32.0, 31.9, 31.5 (C(*C*H$_3$)$_3$),

29.3 (Ar-*C*H_2-Ar). IR (KBr, cm^{-1}): 3429m (OH), 3112w, 3080w, 3044m, 2958s, 2904s, 2867m, 1607m, 1494w, 1479s, 1453s, 1392m, 1362s, 1295s, 1260m, 1249m, 1208s, 1160w, 1125w, 1057w, 1040w, 1026w, 970w, 946w, 915w, 881m, 820w, 797w, 768m, 726w, 671w. UV/vis λ_{max}/nm (C_6H_6) (ε/dm^3 mol^{-1} cm^{-1}): 291 (1.29 x 10^4), 437 (1.53 x 10^3), 461 (1.49 x 10^3). E. A. for $C_{65}H_{75}KN_2O_5Pd{\cdot}CH_3CN{\cdot}H_2O$ calc(found): C: 68.84 (68.81); H: 6.90 (6.88).

[Pd(bipy){Rb·^{t}**BuC5(H)$_2$**}] **(5.1c)**: (**^{t}BuC5(H)$_5$**: 0.104 g, 0.128 mmol; Rb_2CO_3: 0.0305 g, 0.132 mmol, [Pd(bipy)Cl_2]: 0.0234 g, 0.0702 mmol). **5.1c** was obtained as an orange solid (0.0774 g, 0.0669 mmol, 95% yield.). Mp: >285 ^oC. ^1H NMR ($CDCl_3$) δ (ppm): 14.24 (br, 2H, OH), 9.37 (d, 2H, *J* = 8.0 Hz, bipy), 8.59 (dd, 2H, *J* = 7.7, 6.9 Hz, bipy), 8.21 (d, 2H, *J* = 4.7 Hz, bipy), 7.16 (dd, 2H, *J* = 8.5, 7.7 Hz, bipy), 7.15 (d, 2H, *J* = 2.5 Hz, Ar-*H*), 7.14 (d, 2H, *J* = 2.5 Hz, Ar-*H*), 7.11 (s, 2H, Ar-*H*), 6.92 (s, 4H, Ar-*H*), 6.49 (d, 1H, *J* = 13.7 Hz, Ar-C*H*$_2$-Ar), 5.20 (d, 2H, *J* = 14.3 Hz, Ar-C*H*$_2$-Ar), 4.26 (d, 2H, *J* = 13.5 Hz, Ar-C*H*$_2$-Ar), 3.39 (d, 3H, *J* = 13.7 Hz, Ar-C*H*$_2$-Ar), 3.24 (d, 2H, *J* = 14.3 Hz, Ar-C*H*$_2$-Ar), 1.29 (s, 9H, ^{t}Bu), 1.24 (s, 18H, ^{t}Bu), 1.14 (s, 18H, ^{t}Bu). $^{13}C\{^1H\}$ NMR ($CDCl_3$) δ (ppm): 158.4, 158.2, 155.5, 151.3, 148.2, 141.7, 141.5, 139.5, 137.2, 132.2, 131.4, 129.5, 128.7, 127.9, 126.6, 126.0, 125.9, 125.7, 125.4, 125.1,124.8 (aromatic carbons), 36.1 (*C*$(CH_3)_3$), 34.1 (Ar-*C*H_2-Ar), 34.0 (*C*$(CH_3)_3$), 33.9 (*C*$(CH_3)_3$), 32.0, 31.8, 31.6 (C(*C*$H_3)_3$), 29.4 (Ar-*C*H_2-Ar). IR (KBr, cm^{-1}): 3434m (OH), 3116w, 3086w, 3044m, 2957s, 2904s, 2867s, 1607m, 1479s, 1459s, 1392m, 1362s, 1295s, 1261s, 1208s, 1161m, 1125m, 1057w, 1041w, 1026w, 972w, 945w, 915w, 881m, 820m, 797w, 767m, 726m, 669m, 562w. UV/vis λ_{max}/nm (C_6H_6) (ε/dm^3 mol^{-1} cm^{-1}): 286 (3.56 x 10^4), 419 (5.05 x 10^3), 425 (5.03 x 10^3).

[Pd(bipy){Cs·^{t}**BuC5(H)$_2$**}] **(5.1d)**: (**^{t}BuC5(H)$_5$**: 0.104 g, 0.128 mmol; Cs_2CO_3: 0.0460 g, 0.141 mmol, [Pd(bipy)Cl_2]: 0.0231 g, 0.0693 mmol). **5.1d** was obtained as an orange solid (0.0692 g, 0.0575 mmol, 83% yield). Mp: >295 ^{o}C. ^{1}H NMR ($CDCl_3$) δ (ppm): 13.95 (s, 2H, OH), 9.45 (d, 2H, *J* = 8.0 Hz, bipy), 8.62 (dd, 2H, *J* = 7.7, 8.0 Hz, bipy), 8.20 (d, 2H, *J* = 4.4 Hz, bipy), 7.15 (dd, 2H, *J* = 7.7, 8.0 Hz, bipy), 7.15 (d, 4H, *J* = 2.5 Hz, Ar-*H*), 7.11 (s, 2H, Ar-*H*), 6.95 (m, 4H, Ar-*H*), 6.54 (d, 1H, *J* = 13.7 Hz, Ar-CH_2-Ar), 5.24 (d, 2H, *J* = 14.0 Hz, Ar-CH_2-Ar), 4.26 (d, 2H, *J* = 13.5 Hz, Ar-CH_2-Ar), 3.41 (d, 1H, *J* = 15.1 Hz, Ar-CH_2-Ar), 3.36 (d, 2H, *J* = 13.7 Hz, Ar-CH_2-Ar), 3.23 (d, 2H, *J* = 14.3 Hz, Ar-CH_2-Ar), 1.30 (s, 9H, ^{t}Bu), 1.21 (s, 18H, ^{t}Bu), 1.17 (s, 18H, ^{t}Bu). ^{13}C{^{1}H} NMR ($CDCl_3$) δ (ppm): 159.0, 158.4, 155.5, 151.7, 148.2, 141.7, 141.6, 139.3, 136.9, 132.1, 131.7, 129.9, 128.9, 128.7, 126.7, 126.0, 125.9, 125.7, 125.5, 125.2 (aromatic carbons), 36.4, 36.2 (*C*(CH_3)$_3$), 34.1, 34.0 (Ar-*C*H_2-Ar), 33.8 (*C*(CH_3)$_3$), 32.1, 31.8, 31.7 (C(*C*H_3)$_3$), 29.2 (Ar-*C*H_2-Ar). IR (KBr, cm^{-1}): 3435m (OH), 3111w, 3087w, 3044w, 2957s, 2903s, 2866s, 1605m, 1479s, 1468s, 1458s, 1392w, 1362m, 1295s, 1261s, 1208s, 1160w, 1127w, 1039w, 915w, 881m, 820m, 799m, 767m, 726m, 670w, 561w. UV/vis λ_{max}/nm (C_6H_6) (ε/dm^3 mol^{-1} cm^{-1}): 292 (4.00 x 10^4), 432 (5.92 x 10^3), 426 (5.88 x 10^3). E. A. for $C_{65}H_{75}CsN_2O_5Pd{\cdot}CH_3CN$ calc(found): C: 64.65 (64.21); H: 6.32 (6.35).

[Pd((4-Me)$_2$bipy){Na·^{t}**BuC5(H)$_2$**}] **(5.2a)**: (**^{t}BuC5(H)$_5$**: 0.102 g, 0.126 mmol; NaO^{t}Bu: 0.0244 g, 0.254 mmol, [Pd((4-Me)$_2$bipy)Cl_2]: 0.0239 g, 0.0661 mmol). **5.2a** was obtained as a red solid (0.0510 g, 0.455 mmol, 69% yield). Mp: >270 ^{o}C. ^{1}H NMR ($CDCl_3$) δ (ppm): 8.50 (d, 2H, *J* = 5.5 Hz, (4-Me)$_2$bipy), 7.76 (s, 2H, (4-Me)$_2$bipy), 7.34 (d, 2H, *J* = 6.3 Hz, (4-Me)$_2$bipy), 7.26 (d, 2H, *J* = 2.5 Hz, Ar-*H*), 7.10 (s, 2H, Ar-*H*), 6.99 (d, 1H, *J* = 15.1 Hz, Ar-CH_2-Ar), 6.95 (d, 4H, 2.5 Hz, Ar-*H*), 6.90 (d, 2H, 2.7 Hz, Ar-*H*), 4.97 (d, 2H, *J* = 14.0 Hz, Ar-CH_2-Ar), 4.35

(d, 2H, J = 13.2 Hz, Ar-CH_2-Ar), 3.53 (d, 1H, J = 14.0 Hz, Ar-CH_2-Ar), 3.30 (d, 2H, J = 15.1 Hz, Ar-CH_2-Ar), 3.25 (d, 2H, J = 14.0 Hz, Ar-CH_2-Ar), 2.57 (s, 6H, CH_3, (4-Me)$_2$bipy), ~1.70 (H_2O), 1.33 (s, 18H, ^{t}Bu), 1.25 (s, impurity), 1.16 (s, 9H, ^{t}Bu), 1.10 (s, 18H, ^{t}Bu). No $^{13}C\{^1H\}$ NMR was obtained due to sample precipitation during the collection time. IR (KBr, cm^{-1}): 3448m (OH), 3047w, 2955s, 2900m, 2866m, 1619m, 1560w, 1481s, 1459s, 1390w, 1361m, 1297m, 1263m, 1246w, 1208s, 1126w, 1036w, 918w, 876m, 827m, 796w, 750w, 727w, 600w, 578w, 518w. UV/vis λ_{max}/nm (C_6H_6) (ε/dm^3 mol^{-1} cm^{-1}): 289 (2.41 x 10^4), 312 (1.46 x 10^4), 449 (2.91 x 10^3).

[Pd((4-Me)$_2$bipy){K·**^{t}BuC5(H)$_2$**}] **(5.2b)**: (**^{t}BuC5(H)$_5$**: 0.0598 g, 0.0737 mmol; KO^{t}Bu: 0.0165 g, 0.147 mmol, [Pd((4-Me)$_2$bipy)Cl$_2$]: 0.0135 g, 0.0373 mmol). **5.2b** was obtained as an orange solid (0.0256 g, 0.0225 mmol, 60% yield). Mp: > 288 ^{o}C. ^{1}H NMR ($CDCl_3$) δ (ppm): 14.03 (s, 2H, OH); 8.31 (d, 2H, J = 5.5 Hz, (4-Me)$_2$bipy), 8.09 (s, 2H, (4-Me)$_2$bipy), 7.20 (d, 2H, J = 2.5 Hz, Ar-H), 7.15 (d, 2H, J = 2.5 Hz, Ar-H), 7.12 (d, 2H, J = 5.2 Hz, (4-Me)$_2$bipy), 7.06 (s, 2H, Ar-H), 6.87 (s, 2H, Ar-H), 6.86 (s, 2H, Ar-H), 6.73 (d, 1H, J = 14.0 Hz, Ar-CH_2-Ar), 5.07 (d, 2H, J = 14.3 Hz, Ar-CH_2-Ar), 4.30 (d, 2H, J = 13.5 Hz, Ar-CH_2-Ar), 3.42 (d, 1H, J = 13.7 Hz, Ar-CH_2-Ar), 3.39 (d, 2H, J = 13.5 Hz, Ar-CH_2-Ar), 3.18 (d, 2H, J = 14.6 Hz, Ar-CH_2-Ar), 2.76 (s, 6H, CH_3, (4-Me)$_2$bipy), 1.30 (s, 18H, ^{t}Bu), 1.24 (s, 9H, ^{t}Bu), 1.07 (s, 18H, ^{t}Bu). $^{13}C\{^1H\}$ NMR ($CDCl_3$) δ (ppm):158.4, 158.1, 154.8, 153.4, 151.1, 148.4, 141.2, 139.4, 137.0, 131.5, 131.0, 129.2, 128.0, 127.1, 126.8, 125.6, 125.4, 125.2, 124.5, 123.5 (aromatic carbons), 36.2, 35.9 (C(CH_3)$_3$), 34.1 (Ar-CH$_2$-Ar), 33.8 (C(CH_3)$_3$), 32.0, 31.9, 31.5 (C(CH$_3$)$_3$), 29.2 (Ar-CH$_2$-Ar), 22.7 (CH$_3$). IR (KBr, cm^{-1}): 3427m (OH), 3047w, 2656s, 2904m, 2866m, 1619m, 1480s, 1459s, 1392w, 1361m, 1296s, 1261m, 1246m, 1208s, 1126w, 1035w, 922w, 880m,

826m, 797m, 767w, 729w. UV/Vis λ_{max}/nm (C_6H_6) (ε/dm^3 mol^{-1} cm^{-1}): 290 (3.07 x 10^4), 433 (3.24 x 10^3). E. A. for $C_{67}H_{79}KN_2O_5Pd{\cdot}CH_3CN{\cdot}H_2O$ calc(found): C: 69.24 (69.37); H: 7.07 (6.91).

[Pd((4-Me)$_2$bipy){Rb·**^{t}BuC5(H)$_2$**}] **(5.2c)**: (**^{t}BuC5(H)$_5$**: 0.101 g, 0.125 mmol; Rb_2CO_3: 0.0295 g, 0.128 mmol, [Pd((4-Me)$_2$bipy)Cl_2]: 0.0242 g, 0.0669 mmol). **5.2c** was obtained as an orange solid (0.0736 g, 0.0621 mmol, 93% yield). Mp: 303-305 ^{o}C. ^{1}H NMR ($CDCl_3$) δ (ppm): 13.58 (s, 2H, OH), 8.32 (d, 2H, *J* = 5.8 Hz, (4-Me)$_2$bipy), 8.14 (s, 2H, (4-Me)$_2$bipy), 7.12 (s, 4H, Ar-*H*), 7.08 (s, 2H, Ar-*H*), 7.08 (d, 2H, *J* = 4.4 Hz, (4-Me)$_2$bipy), 6.89 (m, 4H, Ar-*H*), 6.62 (d, 1H, *J* = 13.7 Hz, Ar-C*H*$_2$-Ar), 5.14 (d, 2H, *J* = 14.0 Hz, Ar-C*H*$_2$-Ar), 4.29 (d, 2H, *J* = 13.5 Hz, Ar-C*H*$_2$-Ar), 3.41 (d, 1H, *J* = 13.7 Hz, Ar-C*H*$_2$-Ar), 3.38 (d, 2H, *J* = 13.7 Hz, Ar-C*H*$_2$-Ar), 3.17 (d, 2H, *J* = 14.6 Hz, Ar-C*H*$_2$-Ar), 2.79 (s, 6H, CH_3, (4-Me)$_2$bipy), 1.27 (s, 9H, ^{t}Bu), 1.24 (s, 18H, ^{t}Bu), 1.11 (s, 18H, ^{t}Bu). ^{13}C{^{1}H} NMR ($CDCl_3$) δ (ppm): 158.9, 158.8, 154.7, 153.4, 151.3, 148.3, 141.3, 139.3, 136.5, 132.0, 131.6, 129.4, 128.5, 127.8, 127.0, 126.5, 125.7, 125.5, 125.2, 124.8, 123.6 (aromatic carbons), 36.1 (*C*(CH_3)$_3$), 34.1, 34.0 (Ar-*C*H$_2$-Ar), 33.8 (*C*(CH_3)$_3$), 32.0, 31.8, 31.6 (C(*C*H$_3$)$_3$), 29.2 (Ar-*C*H$_2$-Ar), 22.8 (*C*H$_3$). IR (KBr, cm^{-1}): 3436m (OH), 3045w, 2957s, 2904m, 2867m, 1619s, 1480s, 1459s, 1392m, 1362s, 1297s, 1263s, 1208s, 1126w, 1035w, 968w, 945w, 916w, 881m, 826m, 798m, 768w, 746w, 728w, 669w, 576w, 520m. UV/vis λ_{max}/nm (C_6H_6) (ε/dm^3 mol^{-1} cm^{-1}): 290 (2.93 x 10^4), 432 (4.40 x 10^3), 436 (4.36 x 10^3). By slow evaporation of the filtrate solution, red block crystals (>10 mg) of compound **5.2** were obtained, however the yield was quite low, so no further characterization was performed.

[Pd((4-Me)$_2$bipy){Cs·**^{t}BuC5(H)$_2$**}] **(5.2d)**: (**^{t}BuC5(H)$_5$**: 0.104 g, 0.128 mmol; Cs_2CO_3: 0.0467 g, 0.143 mmol, [Pd((4-Me)$_2$bipy)Cl_2]: 0.0243 g, 0.0672 mmol). **5.2d** was obtained as an

orange solid (0.0763 g, 0.0619 mmol, 92% yield). Mp: 308 – 310 ^{o}C. ^{1}H NMR ($CDCl_3$) δ (ppm): 8.37 (d, 2H, *J* = 5.8 Hz, (4-Me)$_2$bipy), 8.12 (s, 2H, (4-Me)$_2$bipy), 7.10 (d, 2H, *J* = 2.2 Hz, Ar-*H*), 7.09 (d, 2H, *J* = 5.8 Hz, (4-Me)$_2$bipy), 7.08 (s, 4H, Ar-*H*), 6.91 (s, 4H, Ar-*H*), 6.61 (d, 1H, *J* = 13.7 Hz, Ar-C*H*$_2$-Ar), 5.19 (d, 2H, *J* = 14.3 Hz, Ar-C*H*$_2$-Ar), 4.29 (d, 2H, *J* = 13.7 Hz, Ar-C*H*$_2$-Ar), 3.42 (d, 1H, *J* = 14.0 Hz, Ar-C*H*$_2$-Ar), 3.34 (d, 2H, *J* = 13.5 Hz, Ar-C*H*$_2$-Ar), 3.16 (d, 2H, *J* = 14.6 Hz, Ar-C*H*$_2$-Ar), 2.77 (s, 6H, CH_3, (4-Me)$_2$bipy), 1.28 (s, 9H, ^{t}Bu), 1.20 (s, 18H, ^{t}Bu), 1.14 (s, 18H, ^{t}Bu). ^{13}C{^{1}H} NMR ($CDCl_3$) δ (ppm):159.5, 159.2, 154.8, 153.3, 151.8, 148.5, 141.3, 139.0, 136.3, 132.0, 129.9, 128.9, 128.8, 127.0, 126.6, 125.9, 125.6, 125.4, 123.5 (aromatic carbons), 36.4, 36.1 (*C*(CH$_3$)$_3$), 34.2, 34.1 (Ar-*C*H$_2$-Ar), 33.9 (*C*(CH$_3$)$_3$), 32.1, 31.9, 31.7 (C(*C*H$_3$)$_3$), 29.9, 29.1 (Ar-*C*H$_2$-Ar), 22.8 (*C*H$_3$). IR (KBr, cm^{-1}): 3436m (OH), 3043w, 2957s, 2904m, 2866m, 1619m, 1558w, 1480s, 1459s, 1392w, 1361m, 1297s, 1263m, 1208s, 1127w, 1035w, 916w, 881m, 826m, 798w, 767w, 746w, 727w, 669w, 598w, 575w, 520w. UV/vis λ_{max}/nm (C_6H_6) (ε/dm^3 mol^{-1} cm^{-1}): 292 (4.12 x 10^4), 425 (5.53 x 10^3), 419 (5.51 x 10^3).

[Pd(phen){Na·^{t}**BuC5(H)$_2$**}] **(5.3a)**: (**^{t}BuC5(H)$_5$**: 0.101 g, 0.124 mmol; NaO^{t}Bu: 0.0225 g, 0.234 mmol, [Pd(phen)Cl$_2$]: 0.0226 g, 0.0632 mmol). **5.3a** was obtained as a red-orange solid (0.0485 g, 0.0434 mmol, 69% yield). Mp: >323 ^{o}C. ^{1}H NMR ($CDCl_3$) δ (ppm): 8.75 (d, 2H, *J* = 8.0 Hz, phen), 8.60 (s, 2H, phen), 8.40 (d, 2H, *J* = 4.1 Hz, phen), 7.70 (dd, 2H, *J* = 5.2, 8.2 Hz, phen), 7.39 (d, 2H, *J* = 2.2 Hz, Ar-*H*), 7.22 (d, 2H, *J* = 2.2 Hz, Ar-*H*), 7.05 (s, 2H, Ar-*H*), 6.94 (d, 2H, *J* = 2.5 Hz, Ar-*H*), 6.84 (d, 2H, *J* = 2.5 Hz, Ar-*H*), 6.76 (d, 1H, *J* = 13.5 Hz, Ar-C*H*$_2$-Ar), 5.14 (d, 2H, *J* = 14.0 Hz, Ar-C*H*$_2$-Ar), 4.44 (d, 2H, *J* = 14.0 Hz, Ar-C*H*$_2$-Ar), 3.43 (d, 3H, *J* = 14.0 Hz, Ar-C*H*$_2$-Ar), 3.42 (d, 2H, *J* = 14.0 Hz, Ar-C*H*$_2$-Ar), 1.41 (s, 18H, ^{t}Bu), 1.18 (s, 9H, ^{t}Bu), 1.07 (s, 18H, ^{t}Bu). ^{13}C{^{1}H} NMR ($CDCl_3$) δ (ppm): 157.9, 157.0, 151.6, 148.7, 145.8,

141.3, 140.1, 139.0, 137.8, 130.3, 128.9, 128.6, 127.3, 127.2, 125.9, 125.5, 125.2, 124.9, 124.5 (aromatic carbons), 37.4, 35.7 ($C(CH_3)_3$), 34.1 (Ar-CH_2-Ar), 33.8 ($C(CH_3)_3$), 32.0, 31.9, 31.5 ($C(CH_3)_3$), 29.7 (Ar-CH_2-Ar). IR (KBr, cm^{-1}): 3435m (OH), 3086w, 3051w, 2958s, 2903m, 2867m, 1605m, 1516w, 1481s, 1459s, 1427s, 1392m, 1362m, 1293s, 1261s, 1246m, 1205s, 1147w, 1126w, 1109w, 879m, 844m, 822m, 797m, 766w, 746w, 717m, 590w, 561w, 439w. UV/vis λ_{max}/nm (C_6H_6) (ε/dm^3 mol^{-1} cm^{-1}): 279 (3.11 x 10^4), 439 (2.34 x 10^3).

[Pd(phen){K·**^{t}BuC5(H)$_2$**}] **(5.3b)**: (**^{t}BuC5(H)$_5$**: 0.0588 g, 0.0725 mmol; KO^{t}Bu: 0.0163 g, 0.145 mmol, [Pd(phen)Cl_2]: 0.0134 g, 0.0375 mmol). **5.3b** was obtained as a yellow-orange solid (0.0261 g, 0.0230 mmol, 61% yield). Mp: > 306 ^oC. ^1H NMR ($CDCl_3$) δ (ppm): 14.44 (br, 2H, OH), 8.90 (d, 2H, *J* = 8.2 Hz, phen), 8.51 (s, 2H, phen), 8.31 (d, 2H, *J* = 4.4 Hz, phen), 7.81 (dd, 2H, *J* = 5.2, 8.2 Hz, phen), 7.28 (d, 2H, *J* = 2.2 Hz, Ar-*H*), 7.23 (d, 2H, *J* = 2.5 Hz, Ar-*H*), 7.12 (s, 2H, Ar-*H*), 6.93 (d, 2H, *J* = 2.5 Hz, Ar-*H*), 6.88 (d, 2H, *J* = 2.5 Hz, Ar-*H*), 6.62 (d, 1H, *J* = 13.7 Hz, Ar-CH_2-Ar), 5.27 (d, 2H, *J* = 14.3 Hz, Ar-CH_2-Ar), 4.39 (d, 2H, *J* = 13.5 Hz, Ar-CH_2-Ar), 3.48 (d, 2H, *J* = 13.7 Hz, Ar-CH_2-Ar), 3.41 (d, 1H, *J* = 14.0 Hz, Ar-CH_2-Ar), 3.39 (d, 2H, *J* = 14.6 Hz, Ar-CH_2-Ar), 1.35 (s, 18H, ^{t}Bu), 1.26 (s, 9H, ^{t}Bu), 1.10 (s, 18H, ^{t}Bu). $^{13}C\{^1H\}$ NMR ($CDCl_3$) δ (ppm): 158.3, 158.2, 151.2, 148.4, 144.7, 141.6, 139.8, 139.5, 137.4, 131.5, 131.4, 129.9, 129.3, 128.6, 128.1, 127.5, 127.0, 125.7, 125.4, 125.2, 124.6 (aromatic carbons), 36.4, 36.0 ($C(CH_3)_3$), 34.1 (Ar-CH_2-Ar), 33.9 ($C(CH_3)_3$), 32.0, 31.9, 31.5 ($C(CH_3)_3$), 29.4 (Ar-CH_2-Ar). IR (KBr, cm^{-1}): 3436m (OH), 3049w, 2957s, 2904m, 2867m, 1606m, 1516w, 1480s, 1459s, 1430m, 1412w, 1392m, 1362s, 1294s, 1263m, 1248m, 1206s, 1151w, 1126m, 916w, 881m, 844m, 820m, 797w, 768w, 748w, 726w, 716m. UV/vis λ_{max}/nm (C_6H_6) (ε/dm^3 mol^{-1} cm^{-}

^{1}): 279 (2.64 x 10^4), 449 (1.51 x 10^3), 439 (1.51 x 10^3). E. A. for $C_{67}H_{75}KN_2O_5Pd{\cdot}CH_3CN{\cdot}H_2O$ calc(found): C: 69.47 (69.42); H: 6.76 (6.71).

[Pd(phen){Rb·^{t}**BuC5(H)$_2$**}] **(5.3c)**: (^{t}**BuC5(H)$_5$**: 0.101 g, 0.124 mmol; Rb_2CO_3: 0.0307 g, 0.133 mmol, [Pd(phen)Cl_2]: 0.0232 g, 0.0649 mmol). **5.3c** was obtained as an orange color solid (0.0685 g, 0.0580 mmol, 89% yield). Mp: > 300 ^{o}C. ^{1}H NMR ($CDCl_3$) δ (ppm): 14.25 (br, 2H, OH), 8.89 (d, 2H, *J* = 8.0 Hz, phen), 8.56 (s, 2H, phen), 8.38 (d, 2H, *J* = 4.9 Hz, phen), 7.81 (dd, 2H, *J* =5.2, 8.0 Hz, phen), 7.17 (s, 4H, Ar-*H*), 7.12 (s, 2H, Ar-*H*), 6.94 (s, 2H, Ar-*H*), 6.90 (d, 2H, *J* = 2.2 Hz, Ar-*H*), 6.55 (d, 1H, *J* = 13.7 Hz, Ar-CH_2-Ar), 5.32 (d, 2H, *J* = 14.3 Hz, Ar-CH_2-Ar), 4.35 (d, 2H, *J* = 13.7 Hz, Ar-CH_2-Ar), 3.44 (d, 2H, *J* = 13.5 Hz, Ar-CH_2-Ar), 3.41 (d, 1H, *J* = 13.7 Hz, Ar-CH_2-Ar), 3.34 (d, 2H, *J* = 14.6 Hz, Ar-CH_2-Ar), 1.29 (s, 9H, ^{t}Bu), 1.27 (s, 18H, ^{t}Bu), 1.14 (s, 18H, ^{t}Bu). ^{13}C{^{1}H} NMR ($CDCl_3$) δ (ppm): 158.9, 158.6, 151.4, 148.4, 144.7, 141.6, 139.6, 139.4, 136.9, 132.0, 131.9, 129.9, 129.5, 128.6, 128.2, 126.7, 125.8, 125.6, 125.3, 125.0 (aromatic protons), 36.4, 36.2 (*C*(CH_3)$_3$), 34.2, 34.1 (Ar-*C*H_2-Ar), 33.9 (*C*(CH_3)$_3$), 32.0, 31.9, 31.6 (C(*C*H_3)$_3$), 29.4 (Ar-*C*H_2-Ar). IR (KBr, cm^{-1}): 3435m (OH), 3047w, 2958s, 2904m, 2866m, 1608m, 1480s, 1459s, 1430m, 1412w, 1392m, 1362m, 1294s, 1263m, 1207s, 1124m, 1111m, 916w, 881m, 843m, 820m, 797m, 767w, 748w, 727w, 716m, 669w, 577w, 523w. UV/vis λ_{max}/nm (C_6H_6) (ε/dm^3 mol^{-1} cm^{-1}): 280 (5.72 x 10^4), 432 (6.68 x 10^3), 426 (6.66 x 10^3).

[Pd(phen){Cs·^{t}**BuC5(H)$_2$**}] **(5.3d)**: (^{t}**BuC5(H)$_5$**: 0.0996 g, 0.123 mmol; Cs_2CO_3: 0.0455 g, 0.140 mmol, [Pd(phen)Cl_2]: 0.0221 g, 0.0618 mmol). **5.3d** was obtained as an orange solid (0.0683 g, 0.0556 mmol, 90% yield). Mp: > 320 ^{o}C. ^{1}H NMR ($CDCl_3$) δ (ppm): 13.82 (br, 2H, OH), 8.94 (d, 2H, *J* = 7.4 Hz, phen), 8.58 (s, 2H, phen), 8.36 (d, 2H, *J* = 4.9 Hz, phen), 7.84 (dd, 2H, *J* = 5.2, 8.0 Hz, phen), 7.15 (s, 3H, Ar-*H*), 7.13 (s, 3H, Ar-*H*), 6.98 (d, 2H, *J* = 2.5 Hz, Ar-

H), 6.93 (d, 2H, *J* = 2.5 Hz, Ar-*H*), 6.63 (d, 1H, *J* = 14.0 Hz, Ar-CH_2-Ar), 5.36 (d, 2H, *J* = 14.3 Hz, Ar-CH_2-Ar), 4.36 (d, 2H, *J* = 13.7 Hz, Ar-CH_2-Ar), 3.43 (d, 3H, *J* = 13.5 Hz, Ar-CH_2-Ar), 3.32 (d, 2H, *J* = 14.6 Hz, Ar-CH_2-Ar), 1.30 (s, 9H, ^{t}Bu), 1.24 (s, 18H, ^{t}Bu), 1.17 (s, 18H, ^{t}Bu). $^{13}C\{^1H\}$ NMR ($CDCl_3$) δ (ppm): 159.5, 158.8, 151.7, 148.4, 144.6, 141.5, 139.6, 139.3, 136.7, 132.2, 131.8, 129.9, 128.9, 128.6, 126.9, 125.9, 125.4, 125.3 (aromatic carbons), 36.8, 36.1 ($C(CH_3)_3$), 34.2, 34.1 (Ar-CH_2-Ar), 33.9 ($C(CH_3)_3$), 32.1, 31.9, 31.7 ($C(CH_3)_3$), 29.2 (Ar-CH_2-Ar). FTIR (KBr, cm^{-1}): 3447m (OH), 3045w, 2959s, 2906m, 2868m, 1604m, 1560w, 1480s, 1459s, 1392w, 1362m, 1295s, 1265m, 1208s, 1126m, 916m, 881m, 843m, 820m, 798m, 767w, 746w, 716m, 669w, 592w, 577w, 561w. UV/vis λ_{max}/nm (C_6H_6) (ε/dm^3 mol^{-1} cm^{-1}): 278 (6.03 x 10^4), 432 (6.90 x 10^3), 426 (6.88 x 10^3). E. A. for $C_{67}H_{75}CsN_2O_5Pd{\cdot}CH_3CN$ calc(found): C: 65.32 (64.99); H: 6.20 (6.15).

[Pd(dpa){Na·**^{t}BuC5(H)$_2$**}] **(5.4a)**: (**^{t}BuC5(H)$_5$**: 0.102 g, 0.126 mmol; NaO^{t}Bu: 0.0243 g, 0.253 mmol, [Pd(dpa)Cl_2]: 0.0238 g, 0.0683 mmol). **5.4a** was obtained as a red-orange solid (0.0495 g, 0.0446 mmol, 65% yield). Mp: >290 ^{o}C. ^{1}H NMR ($CDCl_3$) δ (ppm): 8.43 (br, 2H, dpa), 7.86 (br, 2H, dpa), 7.56 (d, 1H, *J* = 12.9 Hz, Ar-CH_2-Ar), 7.45 (br, 2H, dpa), 7.28 (s, §, impurity), 7.20 (s, 2H, Ar-*H*), 7.14 (s, 2H, Ar-*H*), 7.06 (s, 2H, Ar-*H*), 6.96 (s, 2H, Ar-*H*), 6.88 (s, 2H, Ar-*H*), 6.81 (dd, 2H, *J* = 6.3, 7.1 Hz, dpa), 4.64 (d, 2H, *J* = 14.3 Hz, Ar-CH_2-Ar), 4.36 (d, 2H, *J* = 12.9 Hz, Ar-CH_2-Ar), 3.66 (d, 2H,* *J* = 12.6 Hz, Ar-CH_2-Ar), 3.40 (d, 3H,* *J* = 12.9 Hz, Ar-CH_2-Ar), 3.05 (d, 2H, *J* = 14.6 Hz, Ar-CH_2-Ar), 1.31 (s, 19H,* ^{t}Bu), 1.25 (s, 18H, ^{t}Bu), 1.19 (s, 9H, ^{t}Bu), 1.10 (s, 14H, impurity). § = integral not available. *The integral value reported for the compound is not consistent with the value required. This disagreement in the value could be due to overlapping with solvent or impurities. No $^{13}C\{^1H\}$ NMR was not performed due to its

poor solubility. FTIR (KBr, cm^{-1}): 3424m (OH), 3253w, 3205w, 3138w, 3087w, 3043w, 2959s, 2904m, 2867m, 1627m, 1589m, 1535w, 1478s, 1460s, 1437s, 1392m, 1361m, 1295m, 1245m, 1207s, 1160m, 1127w, 1023w, 913w, 876m, 821m, 796m, 766m, 669w, 528w, 454w. UV/vis λ_{max}/nm (C_6H_6) (ε/dm^3 mol^{-1} cm^{-1}): 288 (2.08 x 10^4).

[Pd(dpa){K·**^{t}BuC5(H)$_2$**}] **(5.4b)**: (**^{t}BuC5(H)$_5$**: 0.0502 g, 0.0619 mmol; KO^{t}Bu: 0.0141 g, 0.126 mmol, [Pd(dpa)Cl_2]: 0.0105 g, 0.0301 mmol). **5.4b** was obtained as an orange solid (0.0281 g, 0.0250 mmol, 83% yield). Mp: > 280 ^oC. ^1H NMR ($CDCl_3$) δ (ppm): 14.04 (br, 2H, OH), 11.73 (br, 1H, NH), 8.33 (d, 2H, *J* = 5.5 Hz, dpa), 8.13 (dd, 2H, *J* = 6.9, 7.4 Hz, dpa), 7.67 (d, 2H, *J* = 8.2 Hz, dpa), 7.23 (d, 1H, *J* = 13.5 Hz, Ar-C*H*$_2$-Ar), 7.21 (d, 2H, *J* = 2.5 Hz, Ar-*H*), 7.12 (d, 2H, *J* = 2.5 Hz, Ar-*H*), 7.05 (d, 2H, *J* = 2.5 Hz, Ar-*H*), 7.02 (s, 2H, Ar-*H*), 6.97 (d, 2H, *J* = 2.2 Hz, Ar-*H*), 6.69 (dd, 2H, *J* = 6.6, 6.6 Hz, dpa), 4.86 (d, 2H, *J* = 14.3 Hz, Ar-C*H*$_2$-Ar), 4.19 (d, 2H, *J* = 13.5 Hz, Ar-C*H*$_2$-Ar), 3.63 (d, 1H, *J* = 13.5 Hz, Ar-C*H*$_2$-Ar), 3.29 (d, 2H, *J* = 13.7 Hz, Ar-C*H*$_2$-Ar), 3.17 (d, 2H, *J* = 14.3 Hz, Ar-C*H*$_2$-Ar), 1.26 (s, 18H, ^{t}Bu), 1.19 (s, 9H, ^{t}Bu), 1.17 (s, 18H, ^{t}Bu). $^{13}C\{^1H\}$ NMR ($CDCl_3$) δ (ppm): 156.7, 153.7, 152.0, 149.0, 147.7, 141.0, 140.7, 139.9, 139.5, 132.1, 131.7, 129.0, 128.2, 127.5, 126.5, 125.8, 125.6, 125.1, 124.7, 117.1, 115.5 (aromatic carbons), 36.8, 34.5 (*C*(CH_3)$_3$), 34.1, 34.0 (Ar-*C*H$_2$-Ar), 33.9 (*C*(CH_3)$_3$), 31.8, 31.8, 31.6 (C(*C*H$_3$)$_3$), 29.9 (Ar-*C*H$_2$-Ar). FTIR (KBr, cm^{-1}): 3407m (OH), 3247w, 3205w, 3138w, 3080w, 3041m, 2958s, 2904m, 2867m, 1642m, 1628m, 1589m, 1536w, 1477s, 1437s, 1392m, 1362s, 1295s, 1279s, 1244s, 1207s, 1160m, 1127m, 1023w, 913w, 880m, 819m, 795m, 767m, 727w, 677w, 534w. UV/vis λ_{max}/nm (C_6H_6) (ε/dm^3 mol^{-1} cm^{-1}): 292 (3.59 x 10^4).

[Pd(dpa){Rb·**^{t}BuC5(H)$_2$**}] **(5.4c)**: (**^{t}BuC5(H)$_5$**: 0.102 g, 0.125 mmol; Rb_2CO_3: 0.0283 g, 0.122 mmol, [Pd(dpa)Cl_2]: 0.0209 g, 0.0600 mmol). **5.4c** was obtained as an orange color solid

(0.0542 g, 0.0463 mmol, 77% yield). Mp: >290 ^{o}C. ^{1}H NMR ($CDCl_3$) δ (ppm): 11.85 (br, 1H, NH), 8.35 (d, 2H, *J* = 5.5 Hz, dpa), 8.23 (dd, 2H, *J* = 7.1, 7.7 Hz, dpa), 7.72 (d, 2H, *J* = 8.5 Hz, dpa), 7.14 (d, 2H, *J* = 2.2 Hz, Ar-*H*), 7.12 (d, 1H, *J* = 13.7 Hz, Ar-CH_2-Ar), 7.08 (d, 2H, *J* = 2.5 Hz, Ar-*H*), 7.06 (d, 2H, *J* = 2.7 Hz, Ar-*H*), 7.03 (s, 2H, Ar-*H*), 6.96 (d, 2H, *J* = 2.2 Hz, Ar-*H*), 6.71 (dd, 2H, *J* = 6.3, 6.3 Hz, dpa), 4.91 (d, 2H, *J* = 14.3 Hz, Ar-CH_2-Ar), 4.14 (d, 2H, *J* = 13.7 Hz, Ar-CH_2-Ar), 3.61 (d, 1H, *J* = 13.7 Hz, Ar-CH_2-Ar), 3.28 (d, 2H, *J* = 13.7 Hz, Ar-CH_2-Ar), 3.15 (d, 2H, *J* = 14.3 Hz, Ar-CH_2-Ar), 1.22 (s, 9H, ^{t}Bu), 1.21 (s, 18H, ^{t}Bu), 1.20 (s, 18H, ^{t}Bu). ^{13}C{^{1}H} NMR ($CDCl_3$) δ (ppm): 157.4, 154.1, 152.3, 149.2, 147.7, 140.9, 140.7, 139.5, 139.3, 132.7, 132.2, 128.6, 128.5, 128.2, 126.4, 125.6, 124.9, 117.0, 115.6 (aromatic carbons), 36.6, 34.9 (*C*(CH_3)$_3$), 34.1, 34.0 (Ar-*C*H_2-Ar), 33.9 (*C*(CH_3)$_3$), 31.9, 31.8, 31.7 (C(*C*H_3)$_3$), 30.0 (Ar-*C*H_2-Ar). FTIR (KBr, cm^{-1}): 3433m (OH), 3043w, 2958s, 2902m, 2867m, 1655m, 1601m, 1588m, 1535w, 1479s, 1437s, 1392w, 1362m, 1295m, 1247m, 1209m, 1162w, 1126w, 1023w, 914w, 880m, 821m, 800w, 765m, 656w, 536w. UV/Vis λ_{max}/nm (C_6H_6), (ε/dm^3 mol^{-1} cm^{-1}): 289 (5.30 x 10^4), 425 (3.93 x 10^3), 488 (2.22 x 10^3).

[Pd(dpa){Cs·**^{t}BuC5(H)$_2$**}] **(5.4d)**: (**^{t}BuC5(H)$_5$**: 0.103 g, 0.127 mmol; Cs_2CO_3: 0.0461 g, 0.141 mmol, [Pd(dpa)Cl_2]: 0.0228 g, 0.0654 mmol). **5.4d** was obtained as an orange solid (0.0652 g, 0.0535 mmol, 82% yield). Mp: 280 - 281 ^{o}C. ^{1}H NMR ($CDCl_3$) δ (ppm): 12.61 (br, 1H, NH), 8.35 (br, 2H, dpa), 8.27 (d, 2H, *J* = 5.8 Hz, dpa), 7.86 (d, 2H, *J* = 7.7 Hz, dpa), 7.22 (d, 1H, *J* = 14.3 Hz, Ar-CH_2-Ar), 7.10 (d, 2H, *J* = 2.2 Hz, Ar-*H*), 7.07 (d, 2H, *J* = 2.2 Hz, Ar-*H*), 7.04 (d, 2H, *J* = 2.2 Hz, Ar-*H*), 6.99 (s, 2H, Ar-*H*), 6.88 (s, 2H, Ar-*H*), 6.73 (dd, 2H, *J* = 6.3, 6.9 Hz, dpa), 4.83 (d, 2H, *J* = 14.0 Hz, Ar-CH_2-Ar), 4.30 (d, 2H, *J* = 13.5 Hz, Ar-CH_2-Ar), 3.66 (d, 1H, *J* = 14.0 Hz, Ar-CH_2-Ar), 3.18 (d, 4H, *J* = 14.0 Hz, Ar-CH_2-Ar), 1.23 (s, 18H, ^{t}Bu), 1.18 (s,

18H, ^{t}Bu), 1.14 (s, 9H, ^{t}Bu). $^{13}C\{^{1}H\}$ NMR ($CDCl_3$) δ (ppm): 157.2, 153.3, 149.3, 147.5, 140.6, 140.1, 139.9, 139.1, 132.4, 129.3, 128.9, 126.0, 125.8, 125.5, 125.0, 116.9, 116.2 (aromatic carbons), 36.7 ($C(CH_3)_3$), 34.1, 34.0 (Ar-CH_2-Ar), 33.9 ($C(CH_3)_3$), 33.7, 31.8, 31.8 ($C(CH_3)_3$), 30.7 (Ar-CH_2-Ar). FTIR (KBr, cm^{-1}): 3436m (OH), 3041w, 2958s, 2904m, 2866m, 1637m, 1600m, 1587m, 1541w, 1478s, 1436s, 1392m, 1362m, 1321m, 1296s, 1247m, 1209s, 1161w, 1127w, 1022w, 913w, 881m, 821m, 798w, 766w, 737w, 669w, 656w, 563w, 537w. UV/vis λ_{max}/nm (C_6H_6) (ε/dm^3 mol^{-1} cm^{-1}): 288 (4.49 x 10^4), 307 (4.45 x 10^4), 432 (4.33 x 10^4).

*5.5.1.1.3 General synthesis of [Pd(L){^{t}**BuC4(H)$_2$**}] (L = bipy, (4-Me)$_2$bipy, 1,10-phen, dpa, tmeda) complexes*

All palladium-containing calix[4]arene complexes were prepared as follows: To a suspension of **RC4(H)$_4$** (R = ^{t}Bu, H) in anhydrous acetonitrile (20 mL) was added K_2CO_3 in a 1:4 ratio. The reaction mixture was stirred at acetonitrile reflux temperature under a nitrogen gas flow. After one day of reflux, [Pd(bipy)Cl_2] was added to the resulting light yellow solution, in a 1:1 ratio with respect to the calix[4]arene. A change in color was observed from light yellow solution to orange or red with formation of a precipitate. The resulting mixture was left to stir for 30 minutes more. The resulting red or orange suspension was hot filtered using a medium pore frit. The red or orange solid was washed with DI water (10 mL) twice, then with acetonitrile (5 mL) twice, affording complexes **5.5a-e** and **5.6a-c**.[207]

[Pd(bipy){^{t}**BuC4(H)$_2$**}] (**5.5a**): (^{t}**BuC4(H)$_4$**: 0.0519 g, 0.0800 mmol; K_2CO_3: 0.0465 g, 0.336 mmol; [Pd(bipy)Cl_2]: 0.0269 g, 0.0807 mmol). **5.5a** was obtained as a red solid (0.0479 g, 0.0527 mmol, 66% yield). Mp: 270 - 272 ^{o}C. ^{1}H NMR ($CDCl_3$) δ (ppm): 11.07 (s, 2H, OH), 9.79 (d, 2H, *J* = 8.0 Hz, bipy), 8.51 (dd, 2H, *J* = 7.7, 7.4 Hz, bipy), 8.34 (d, 2H, *J* = 4.9 Hz, bipy),

7.80 (d, 1H, J = 14.0 Hz, Ar-CH_2-Ar), 7.23 (dd, 2H, J = 6.6, 6.6 Hz, bipy), 7.18 (d, 2H, J = 2.2 Hz, Ar-H), 7.04 (d, 4H, J = 1.9 Hz, Ar-H), 6.99 (d, 2H, J = 2.5 Hz, Ar-H), 5.13 (d, 1H, J = 11.8 Hz, Ar-CH_2-Ar), 4.58 (d, 2H, J = 12.6 Hz, Ar-CH_2-Ar), 3.70 (d, 1H, J = 13.7 Hz, Ar-CH_2-Ar), 3.57 (d, 2H, J = 12.9 Hz, Ar-CH_2-Ar), 3.30 (d, 1H, J = 12.1 Hz, Ar-CH_2-Ar), 1.58 (s, 3H, possibly H_2O), 1.26 (s, 18H, ^{t}Bu), 1.23 (s, 18H, ^{t}Bu), 0.73 (s, 2H, possibly CH_3CN). $^{13}C\{^1H\}$ NMR ($CDCl_3$) δ (ppm): 155.9, 155.5, 150.5, 148.6, 142.6, 142.1, 139.4, 131.5, 130.5, 130.3, 126.7, 126.3, 126.1, 126.0, 125.4, 125.1, 124.5 (aromatic carbons), 38.0, 35.3 ($C(CH_3)_3$), 34.1, 33.8 (Ar-CH$_2$-Ar), 31.8 (C(CH$_3$)$_3$). FTIR (KBr, cm^{-1}): 3448m (OH), 3109w, 3086w, 3046w, 2959s, 2905s, 2866m, 1605m, 1560w, 1481s, 1467s, 1460s, 1452s, 1391w, 1361m, 1305s, 1259s, 1207s, 1159w, 1128w, 1056w, 1043w, 912w, 871m, 827w, 765m, 725w, 670w, 580w. UV/vis (C_6H_6) λ_{max}/nm (ε/dm^3 mol^{-1} cm^{-1}): 292 (2.95 x 10^4), 461 (2.41 x 10^3), 469 (2.40 x 10^3). E. A. for $C_{54}H_{62}N_2O_4Pd{\cdot}CH_3CN$ calc(found): C: 70.76 (70.57); H: 6.89 (6.83).

[Pd((4-Me)$_2$bipy){**^{t}BuC4(H)$_2$**}] (**5.5b**): (**^{t}BuC4(H)$_4$**: 0.0523 g, 0.0806 mmol; K_2CO_3: 0.0440 g, 0.318 mmol; [Pd((4-Me)$_2$bipy)Cl$_2$]: 0.0301 g, 0.0832 mmol). **5.5b** was obtained as an orange solid (0.0479 g, 0.0511 mmol, 63% yield). Mp: 298 - 300 ^{o}C. ^{1}H NMR ($CDCl_3$) δ (ppm): 10.49 (s, 2H, OH), 8.51 (d, 2H, J = 5.8 Hz, (4-Me)$_2$bipy), 8.01 (s, 2H, (4-Me)$_2$bipy), 7.93 (d, 1H, J = 13.7 Hz, Ar-CH_2-Ar), 7.27 (d, 2H, J = 3.6 Hz, (4-Me)$_2$bipy), 7.08 (d, 2H, J = 2.2 Hz, Ar-H), 7.03 (d, 2H, J = 2.5 Hz, Ar-H), 6.96 (s, 4H, Ar-H), 4.97 (d, 1H, J = 12.1 Hz, Ar-CH_2-Ar), 4.55 (d, 2H, J = 12.9 Hz, Ar-CH_2-Ar), 3.69 (d, 1H, J = 13.7 Hz, Ar-CH_2-Ar), 3.44 (d, 2H, J = 12.9 Hz, Ar-CH_2-Ar), 3.21 (d, 1H, J = 12.1 Hz, Ar-CH_2-Ar), 2.50 (s, 6H, CH_3, (4-Me)$_2$bipy), 1.58 (s, 1H, possibly H_2O), 1.21 (s, 18H, ^{t}Bu), 1.20 (s, 18H, ^{t}Bu), 0.73 (s, 3H, possibly CH_3CN). $^{13}C\{^1H\}$ NMR ($CDCl_3$) δ (ppm): 156.0, 155.2, 153.2, 150.6, 149.0, 141.9, 138.9, 131.2, 130.9, 130.0,

127.6, 126.8, 126.0, 125.2, 124.9, 124.3, 123.1 (aromatic carbons), 37.9, 34.9 ($C(CH_3)_3$), 34.0, 33.8 (Ar-CH_2-Ar), 31.8, 31.7 ($C(CH_3)_3$), 21.9 (CH_3 of $(4\text{-Me})_2$bipy)). FTIR (KBr, cm^{-1}): 3436s (OH), 3045w, 2959s, 2904m, 2866m, 1618m, 1482s, 1468s, 1459m, 1452m, 1439m, 1391w, 1361m, 1303m, 1275m, 1258m, 1207s, 1159w, 1131w, 1048w, 1037w, 922w, 912w, 870w, 829m, 786w, 758w, 722w, 579w. UV/vis (C_6H_6) λ_{max}/nm (ε/dm^3 mol^{-1} cm^{-1}): 296 (1.10 x 10^4), 463 (7.31 x 10^2). E. A. for $C_{56}H_{66}N_2O_4Pd{\cdot}CH_3CN$ calc(found): C: 71.18 (71.13); H: 7.11 (7.05).

[Pd(phen){**^{t}BuC4(H)$_2$**}] (**5.5c**): (**^{t}BuC4(H)$_4$**: 0.0513 g, 0.0791 mmol; K_2CO_3: 0.0441 g, 0.319 mmol; [Pd(phen)Cl_2]: 0.0282 g, 0.0789 mmol). **5.5c** was obtained as a red solid (0.0488 g, 0.0523 mmol, 66% yield). Mp: 310 - 312 ^oC. ^1H NMR ($CDCl_3$) δ (ppm): 10.90 (s, 2H, OH), 8.81 (d, 2H, *J* = 8.2 Hz, phen), 8.73 (d, 2H, *J* = 4.1 Hz, phen), 8.60 (s, 2H, phen), 7.96 (d, 1H, *J* = 13.7 Hz, Ar-CH_2-Ar), 7.75 (dd, 2H, *J* = 5.2, 8.2 Hz, phen), 7.16 (d, 2H, *J* = 2.2 Ar-*H*), 7.05 (d, 2H, *J* = 2.5 Hz, Ar-*H*), 7.04 (d, 2H, *J* = 2.5 Hz, Ar-*H*), 7.01 (d, 2H, *J* = 2.5 Hz, Ar-*H*), 5.15 (d, 1H, *J* = 11.8 Hz, Ar-CH_2-Ar), 4.68 (d, 2H, *J* = 12.6 Hz, Ar-CH_2-Ar), 3.72 (d, 1H, *J* = 13.7 Hz, Ar-CH_2-Ar), 3.54 (d, 2H, *J* = 12.9 Hz, Ar-CH_2-Ar), 3.32 (d, 1H, *J* = 11.8 Hz, Ar-CH_2-Ar), 1.58 (s, 1H, possibly H_2O), 1.27 (s, 18H, ^{t}Bu), 1.24 (s, 18H, ^{t}Bu), 0.73 (s, 1H, possibly CH_3CN). $^{13}C\{^1H\}$ NMR ($CDCl_3$) δ (ppm): 156.0, 150.8, 149.2, 145.6, 142.1, 139.4, 139.1, 131.1, 130.8, 130.1, 130.0, 128.6, 126.6, 126.2, 125.5, 125.2, 124.6 (aromatic carbons), 38.0, 35.2 ($C(CH_3)_3$), 34.1, 33.9 (Ar-CH_2-Ar), 31.8 ($C(CH_3)_3$). FTIR (KBr, cm^{-1}): 3435m (OH), 3050m, 2957s, 2904m, 2865m, 1604w, 1516w, 1481s, 1466s, 1460s, 1428m, 1412w, 1391w, 1361m, 1342w, 1301s, 1275m, 1260m, 1205s, 1148w, 1128w, 1110w, 912w, 881w, 870m, 843m, 828w, 786w, 757w, 717m, 675w, 619w, 579w. UV/vis (C_6H_6) λ_{max}/nm (ε/dm^3 mol^{-1} cm^{-1}): 278 (2.96 x 10^4), 470 (2.38 x 10^3), 461 (2.36 x 10^3).

[Pd(dpa){^{t}**BuC4(H)$_2$**}] (**5.5d**): (^{t}**BuC4(H)$_4$**: 0.0751 g, 0.116 mmol; K_2CO_3: 0.0633 g, 0.458 mmol; [Pd(dpa)Cl_2]: 0.0442 g, 0.127 mmol). **5.5d** was obtained as a red solid (0.0702 g, 0.0759 mmol, 66% yield). Mp: 260 - 261 ^oC. ^1H NMR ($CDCl_3$) δ (ppm): 11.80 (s, 2H, OH), 10.96 (s, 1H, NH, dpa), 8.57 (d, 2H, *J* = 8.2 Hz, dpa), 8.43 (d, 1H, *J* = 13.7 Hz, Ar-C*H*$_2$-Ar), 8.19 (d, 2H, *J* = 6.0 Hz, dpa), 7.67 (dd, 2H, *J* = 6.9, 7.4 Hz, dpa), 7.14 (d, 2H, *J* = 2.5 Hz, Ar-*H*), 7.10 (d, 2H, *J* = 2.2 Hz, Ar-*H*), 6.98 (d, 4H, *J* =1.9 Hz, Ar-*H*), 6.76 (dd, 2H, *J* = 6.6, 6.6 Hz, dpa), 4.78 (d, 1H, *J* = 11.8 Hz, Ar-C*H*$_2$-Ar), 4.33 (d, 2H, *J* = 12.9 Hz, Ar-C*H*$_2$-Ar), 3.95 (d, 1H, *J* = 14.0 Hz, Ar-C*H*$_2$-Ar), 3.47 (d, 2H, *J* = 12.9 Hz, Ar-C*H*$_2$-Ar), 3.18 (d, 1H, *J* = 12.1 Hz, Ar-C*H*$_2$-Ar), 1.58 (s, 1H, possibly H_2O), 1.27 (s, 18H, ^{t}Bu), 1.22 (s, 18H, ^{t}Bu), 0.80 (s, 1H, possibly CH_3CN). $^{13}C\{^1H\}$ NMR ($CDCl_3$) δ (ppm): 154.3, 150.0, 148.5, 147.8, 146.9, 144.5, 142.8, 140.5, 139.6, 131.6, 131.2, 129.9, 127.9, 126.6, 126.1, 125.5, 125.4, 124.6, 117.9, 116.1 (aromatic carbons), 38.5, 35.4 (*C*(CH_3)$_3$), 34.1, 33.9 (Ar-*C*H$_2$-Ar), 32.8, 32.5, 31.8, 31.7, 31.6 (C(*C*H$_3$)$_3$). *Extra peaks in ^{13}C NMR spectrum possibly due to sample decomposition during collection time. FTIR (KBr, cm^{-1}): 3424m (OH), 3313w, 3282w, 3202m, 3141m, 3088m, 3046m, 2959s, 2906s, 2866m, 1650m, 1631m, 1589m, 1538m, 1504w, 1479s, 1461m, 1434s, 1392w, 1361m, 1303s, 1270m, 1257w, 1240s, 1207s, 1163m, 1130w, 1065w, 1025w, 912w, 887w, 870w, 826w, 768s, 725w, 579w. UV/vis (C_6H_6) λ_{max}/nm (ε/dm^3 mol^{-1} cm^{-1}): 288 (1.47 x 10^4), 406 (8.65 x 10^2), 421 (7.87 x 10^2).

[Pd(tmeda){^{t}**BuC4(H)$_2$**}] (**5.5e**): (^{t}**BuC4(H)$_4$**: 0.0509 g, 0.0784 mmol; K_2CO_3: 0.0434 g, 0.314 mmol; [Pd(tmeda)Cl_2]: 0.0249 g, 0.0848 mmol). Unlike previous reactions no precipitate was formed. The resulting yellow solution was filtered on a bed of celite supported on a medium pore size frit. Yellow crystals were obtained after slow evaporation of the solvent. The crystals

lose solvent quickly to produce **5.5e** as an orange solid (0.0675 g, 0.0776 mmol, 99% yield). Mp: 80 ^{o}C loses solvent > 190 ^{o}C. ^{1}H NMR ($CDCl_3$) δ (ppm): 10.16 (s, 2H, OH), 8.21 (d, 1H, *J* = 13.5 Hz, Ar-C*H*$_2$-Ar), 7.07 (d, 2H, *J* = 2.5 Hz, Ar-*H*), 7.01 (d, 2H, *J* = 2.5 Hz, Ar-*H*), 6.91 (d, 2H, *J* = 2.2 Hz, Ar-*H*), 6.87 (d, 2H, *J* = 2.5 Hz, Ar-*H*), 4.95 (d, 1H, *J* = 11.8 Hz, Ar-C*H*$_2$-Ar), 4.29 (d, 2H, *J* = 12.4 Hz, Ar-C*H*$_2$-Ar), 3.81 (d, 1H, *J* = 13.5 Hz, Ar-C*H*$_2$-Ar), 3.30 (d, 2H, *J* = 12.6 Hz, Ar-C*H*$_2$-Ar), 3.19 (d, 1H, *J* = 11.8 Hz, Ar-C*H*$_2$-Ar), 3.02 (s, 6H, CH_3, tmeda), 2.83-2.74 (m, 4H, CH_2, tmeda), 2.59 (s, 6H, CH_3, tmeda), 1.19 (s, 18H, ^{t}Bu), 1.18 (s, 18H, ^{t}Bu), 0.84 (s, 8H, possible CH_3CN). $^{13}C\{^{1}H\}$ NMR ($CDCl_3$) δ (ppm): 155.3, 150.1, 142.5, 138.8, 131.5, 131.1, 130.5, 126.0, 125.9, 124.9, 124.6, 124.0 (aromatic carbons), 116.9 (CH_3CN), 62.1 (*C*H$_2$, tmeda), 51.4, 50.1 (*C*H$_3$, tmeda), 37.4, 34.5 (*C*(CH$_3$)$_3$), 34.0, 33.7 (Ar*C*H$_2$Ar), 31.7, 31.6 (C(*C*H$_3$)$_3$). FTIR (KBr, cm^{-1}): 3436m (OH), 3046m, 2958s, 2905s, 2867s, 1668m, 1606m, 1503w, 1481s, 1467s, 1408m, 1393m, 1361s, 1303s, 1273s, 1258s, 1206s, 1158w, 1131m, 1042w, 1010w, 959w, 911w, 870m, 826w, 809s, 788m, 766w, 720w, 579w, 518w. UV/vis (C_6H_6) λ_{max}/nm (ε/dm^3 mol^{-1} cm^{-1}): 289 (1.24 x 10^4), 451 (7.04 x 10^2), 488 (5.57 x 10^2). E. A. for $C_{50}H_{70}N_2O_4Pd{\cdot}4CH_3CN{\cdot}3H_2O$ calc(found): C: 64.04 (64.24); H: 8.15 (8.17).

*5.5.1.1.4 Synthesis of [Pd(L){**HC4(H)$_2$**}] (L = bipy, (4-Me)$_2$bipy, 1,10-phen) complexes*

[Pd(bipy){**HC4(H)$_2$**}] (**5.6a**): (**HC4(H)$_4$**: 0.0503 g, 0.119 mmol; K_2CO_3: 0.0773 g, 0.559 mmol; [Pd(bipy)Cl_2]: 0.0411 g, 0.123 mmol). **5.6a** was obtained as an orange solid (0.0535 g, 0.0781 mmol, 66% yield). Mp: >310 ^{o}C. ^{1}H NMR (DMSO-d$_6$) δ (ppm): 10.28 (s, 2H, OH), 8.72 (d, 2H, *J* = 8.0 Hz, bipy), 8.44 (dd, 2H, *J* = 6.3, 8.0 Hz, bipy), 8.43 (d, 2H, *J* = 5.2 Hz, bipy), 7.97 (d, 1H, *J* = 14.0 Hz, Ar-C*H*$_2$-Ar), 7.90 (dd, 2H, *J* = 6.3, 6.9 Hz, bipy), 6.98 (dd, 4H, *J* = 6.3, 7.4 Hz, Ar-*H*), 6.90 (dd, 4H, *J* = 6.3, 6.0 Hz, Ar-*H*), 6.47 (dd, 2H, *J* = 7.4, 7.4 Hz, Ar-*H*),

6.32 (dd, 2H, J = 7.4, 7.4 Hz, Ar-H), 4.75 (d, 1H, J = 11.5 Hz, Ar-CH_2-Ar), 4.44 (d, 2H, J = 12.6 Hz, Ar-CH_2-Ar), 3.69 (d, 1H, J = 14.0 Hz, Ar-CH_2-Ar), 3.41 (d, 2H, J = 12.9 Hz, Ar-CH_2-Ar), 3.10 (d, 1H, J = 11.5 Hz, Ar-CH_2-Ar). $^{13}C\{^1H\}$ NMR (DMSO-d_6) δ (ppm): 158.4, 156.0, 152.7, 148.0, 141.6, 131.1, 131.0, 130.5, 130.2, 130.0, 127.8, 127.5, 127.3, 124.1, 119.3, 116.2 (aromatic carbons), 36.4, 33.3 (ArCH$_2$Ar). FTIR (KBr, cm^{-1}): 3448m (OH), 3103m, 3080m, 3057m, 2924s, 2860m, 2835m, 2763m, 2713m, 2617m, 1601m, 1592m, 1560w, 1465s, 1450s, 1429s, 1308m, 1274s, 1252s, 1218m, 1172m, 1160m, 1092m, 1058w, 1043w, 912m, 857m, 762s, 753s, 722m, 670w, 656w, 626w, 570w. UV/vis λ_{max}/nm (DMSO) (ε/dm^3 mol^{-1} cm^{-1}): 291 (1.27 x 10^4), 374 (3.34 x 10^2). E. A. for $C_{38}H_{30}N_2O_4Pd{\cdot}CH_3CN$ calc(found): C: 66.16 (65.95); H: 4.58 (4.37).

[Pd((4-Me)$_2$bipy){**HC4(H)$_2$**}] (**5.6b**): (**HC4(H)$_4$**: 0.103 g, 0.243 mmol; K_2CO_3: 0.136 g, 0.984 mmol; [Pd((4-Me)$_2$bipy)Cl$_2$]: 0.0883 g, 0.244 mmol). **5.6b** was obtained as an orange solid (0.0953 g, 0.134 mmol, 55% yield). Mp: >300 ^oC decomposes. ^1H NMR (DMSO-d_6) δ (ppm): 10.28 (s, 2H, OH), 8.51 (s, 2H, (4-Me)$_2$bipy), 8.27 (d, 2H, J = 5.8 Hz, (4-Me)$_2$bipy), 7.99 (d, 1H, J = 14.0 Hz, Ar-CH_2-Ar), 7.83 (d, 2H, J = 5.8 Hz, (4-Me)$_2$bipy), 6.97 (dd, 4H, J = 8.0, 8.0 Hz, Ar-H), 6.88 (dd, 4H, J = 6.9, 7.4 Hz, Ar-H), 6.46 (dd, 2H, J = 7.4, 7.4 Hz, Ar-H), 6.30 (dd, 2H, J = 7.4, 7.5 Hz, Ar-H), 4.75 (d, 1H, J = 11.5 Hz, Ar-CH_2-Ar), 4.41 (d, 2H, J = 12.6 Hz, Ar-CH_2-Ar), 3.67 (d, 1H, J = 13.7 Hz, Ar-CH_2-Ar), 3.37 (d, 3H*, J = 12.6 Hz, Ar-CH_2-Ar), 3.09 (d, 1H, J = 11.8 Hz, Ar-CH_2-Ar), 2.56 (s, 6H, CH_3, (4-Me)$_2$bipy). * due to overlap with H_2O. $^{13}C\{^1H\}$ NMR (DMSO-d_6) δ (ppm): 159.2, 156.0, 154.4, 153.4, 147.9, 131.8, 131.6, 130.9, 129.9, 128.9, 128.4, 128.2, 127.9, 125.1, 120.0, 116.8 (aromatic carbons), 33.9 (ArCH$_2$Ar), 21.8 (CH$_3$ of (4-Me)$_2$bipy)). FTIR (KBr, cm^{-1}): 3435m (OH), 3055m, 2922m, 1619s, 1591m, 1465s, 1449s,

1427s, 1384m, 1262s, 1218m, 1090w, 911w, 834w, 752s, 701w, 517w. UV/vis λ_{max}/nm (DMSO) (ε/dm^3 mol^{-1} cm^{-1}): 295 (1.76 x 10^4).

[(Pd(phen){**HC4(H)$_2$**}] (**5.6c**): (**HC4(H)$_4$**: 0.0525 g, 0.124 mmol; K_2CO_3: 0.0783 g, 0.567 mmol; [Pd(phen)Cl_2]: 0.0444 g, 0.124 mmol). **5.6c** was obtained as an orange solid (0.0598 g, 0.0843 mmol, 68% yield). Mp: 320 - 322 ^{o}C. ^{1}H NMR (DMSO-d$_6$) δ (ppm): 10.34 (s, 2H, OH), 9.05 (d, 2H, *J* = 8.3 Hz, phen), 8.73 (d, 2H, *J* = 4.1 Hz, phen), 8.37 (s, 2H, phen), 8.23 (dd, 2H, *J* = 5.2, 8.2 Hz, phen), 8.15 (d, 1H, *J* = 13.4 Hz, Ar-C*H*$_2$-Ar), 6.99 (dd, 4H, *J* = 5.8, 5.8 Hz, Ar-*H*), 6.92 (dd, 4H, *J* = 5.8, 5.5 Hz, Ar-*H*), 6.48 (dd, 2H, *J* = 7.4, 7.4 Hz, Ar-*H*), 6.34 (dd, 2H, *J* = 7.4, 7.4 Hz, Ar-*H*), 4.75 (d, 1H, *J* = 11.8 Hz, Ar-C*H*$_2$-Ar), 4.54 (d, 2H, *J* = 12.6 Hz, Ar-C*H*$_2$-Ar), 3.71 (d, 1H, *J* = 13.7 Hz, Ar-C*H*$_2$-Ar), 3.45 (d, 2H, *J* = 12.9 Hz, Ar-C*H*$_2$-Ar), 3.10 (d, 2H,* *J* = 11.8 Hz, Ar-C*H*$_2$-Ar). *The integral value reported for the compound is not consistent with the value required. This disagreement in the value could be due to overlapping with solvent or impurities. No ^{13}C{^{1}H} data is available because of the poor solubility in DMSO. FTIR (KBr, cm^{-1}): 3438m (OH), 3067m, 2952w, 2924m, 2862w, 2833w, 1591m, 1561w, 1516w, 1465s, 1451s, 1427s, 1388m, 1343w, 1275s, 1259s, 1215w, 1146w, 1092w, 911w, 849m, 753s, 714m, 659w, 569w. UV/vis λ_{max}/nm (DMSO) (ε/dm^3 mol^{-1} cm^{-1}): 291 (3.34 x 10^4). E. A. for $C_{40}H_{30}N_2O_4Pd{\cdot}CH_3CN{\cdot}0.5H_2O$ calc(found): C: 66.45 (66.04); H: 4.51 (4.08).

*5.5.1.1.5 Synthesis of [Pd((4-Me)$_2$bipy){Cs·**^{t}BuC6(H)$_3$**}] complex **5.7***

[Pd((4-Me)$_2$bipy){Cs·**^{t}BuC6(H)$_3$**}] (**5.7**): To a suspension of **^{t}BuC6(H)$_6$** (0.0794 g, 0.0816 mmol) in anhydrous acetonitrile (20 mL) was added Cs_2CO_3 (0.0513 g, 0.157 mmol). The reaction mixture was stirred at acetonitrile reflux temperature under a nitrogen gas flow. After one day of reflux, solid [Pd((4-Me)$_2$bipy)Cl_2] (0.0276 g, 0.0763 mmol) was added to the

resulting white suspension. A change in color was observed from white suspension to orange with formation of a precipitate. The resulting mixture was left to stir for 30 minutes more. The resulting orange suspension was hot filtered using a medium pore size frit. The red or orange solid was washed with DI water (10 mL) twice, then with acetonitrile (10 mL) twice, affording complex **5.7**. (0.0970 g, 0.0696 mmol, 91% yield). Mp: > 333 ^{o}C. ^{1}H NMR ($CDCl_3$) δ (ppm): 14.13 (s, 2H, OH), 10.66 (s, 1H, OH), 8.80 (br, 1H, $(4\text{-Me})_2$bipy), 8.47 (br, 1H, $(4\text{-Me})_2$bipy), 8.21 (br, 1H, $(4\text{-Me})_2$bipy), 8.04 (br, 1H, $(4\text{-Me})_2$bipy), 7.58 (d, 1H, *J* = 14.3 Hz, Ar-CH_2-Ar), 7.46 (br, 1H, $(4\text{-Me})_2$bipy), 7.22 (s, 1H, Ar-*H*), 7.19 (s, 1H, Ar-*H*), 7.13 (s, 2H, Ar-*H*), 7.04 (s, 3H, Ar-*H*), 6.97 (s, 3H, Ar-*H*, $(4\text{-Me})_2$bipy), 6.87 (s, 1H, Ar-*H*), 6.60 (s, 1H, Ar-*H*), 6.54 (s, 1H, Ar-*H*), 4.70 (d, 1H, *J* = 13.7 Hz, Ar-CH_2-Ar), 4.20 (br, 4H, Ar-CH_2-Ar), 3.70 (d, 1H, *J* = 13.7 Hz, Ar-CH_2-Ar), 3.61 (d, 1H, *J* = 14.0 Hz, Ar-CH_2-Ar), 3.44 (d, 1H, *J* = 17.0 Hz, Ar-CH_2-Ar), 3.31 (d, 2H, *J* = 12.4 Hz, Ar-CH_2-Ar), 3.22 (d, 1H, *J* = 17.3 Hz, Ar-CH_2-Ar), 2.83 (s, 3H, $(4\text{-Me})_2$bipy), 2.50 (s, 3H, $(4\text{-Me})_2$bipy), 1.67 (b, H_2O), 1.32 (s, 9H, ^{t}Bu), 1.24 (s, 18H, ^{t}Bu), 1.20 (s, 9H, ^{t}Bu), 1.16 (s, 9H, ^{t}Bu), 1.12 (s, 9H, ^{t}Bu). No $^{13}C\{^{1}H\}$ NMR was obtained due to sample precipitation during the collection time. FTIR (KBr, cm^{-1}): 3436m (OH), 3041w, 2956s, 2906m, 2866m, 1618m, 1483s, 1458s, 1392w, 1361m, 1298s, 1282m, 1260s, 1207s, 1124m, 1049w, 1036w, 924w, 912w, 872m, 826m, 804w, 744w, 578w, 418w. UV/vis ($CHCl_3$) λ_{max}/nm (ε/dm^3 mol^{-1} cm^{-1}): 289 (1.43 x 10^4), 299 (1.35 x 10^4), 309 (1.19 x 10^4).

5.5.2 General X-ray crystal structure information

The crystallographic data and some details of the data collection and refinement of complexes **5.1d**·2DMSO, **5.5a**·$5C_6H_6$, **5.5b**·$6C_6H_6$, **5.5e**·$3CH_3CN$, **5.6**·$4CH_3CN$ and **5.7**·$8C_6H_6$·H_2O are given in Table 5.9, while in Table 5.10 the data for crystals **5.1**·$4CH_3CN$ and **5.2**·$4CH_3CN$ is shown. Absorption corrections were applied by SADABS.[155] All X-ray structures were solved by direct methods and subsequent difference Fourier syntheses and refined by full matrix least-squares methods against F^2 (SHELX 97).[121] Disorder for some *tert*-butyl groups was due to a two-fold axis, and was modeled using partial occupancies (PART instruction) and isotropic displacement parameters.[121] The H atoms in structures were taken in calculated positions. The programs Mercury[157] and POVRay[158] were used to generate the X-ray structural diagrams pictured in this chapter.

Table 5.9 Crystallographic data and summary of data collection and structure refinement of complexes **5.1d**·2DMSO, **5.5a**·5C_6H_6, **5.5b**·6C_6H_6, **5.5e**·3CH_3CN, **5.6**·4CH_3CN and **5.7**·8C_6H_6·H_2O

	5.1d·2DMSO	**5.5a**·5C_6H_6	**5.5b**·5.5C_6H_6
Formula	$C_{69}H_{87}CsN_2O_7PdS_2$	$C_{84}H_{92}CsN_2O_4Pd$	$C_{89}H_{99}CsN_2O_4Pd$
FW	1359.84	1300.00	1367.10
cryst syst	Monoclinic	Triclinic	Triclinic
space group	C 2/c	P -1	P -1
T, K	213(2)	223(2)	213(2)
a, Å	43.596(8)	12.8420(16)	15.413(4)
b, Å	16.583(3)	12.8541(16)	15.721(4)
c, Å	21.447(4)	23.050(3)	16.733(4)
α, deg	90	82.731(3)	71.785(4)
β, deg	91.897(4)	76.861(2)	82.626(4)
γ, deg	90	89.165(2)	80.006(4)
V, A^3	15496(5)	3675.1(8)	3781.0(16)
Z	8	2	2
d_{calcd}, $g\cdot cm^{-3}$	1.166	1.175	1.201
μ, mm^{-1}	0.801	0.302	0.297
refl collected	31358	26091	26562
T_{min} / T_{max}	0.946	0.968	0.972
N_{measd}	11175	12708	10855
[R_{int}]	0.0962	[0.1096]	[0.0552]
R [I>2sigma(I)]	0.0595	0.0712	0.0444
R (all data)	0.1037	0.1077	0.0532
R_w [I>2sigma(I)]	0.1413	0.1606	0.1201
R_w (all data)	0.1564	0.1900	0.1272
GOF	0.891	1.045	1.074
	5.5e·3CH_3CN	2[**5.6b**·2CH_3CN]	**5.7**·7.5C_6H_6·H_2O
Formula	$C_{56}H_{79}N_5O_4Pd$	$C_{88}H_{80}N_8O_8Pd$	$C_{123}H_{140}CsN_2O_7Pd$
FW	992.64	1590.4	1997.68
cryst syst	Monoclinic	Triclinic	Triclinic
space group	P 21/c	P-1	P-1
T, K	213(2)	218(2)	213(2)
a, Å	12.1693(15)	11.886(2)	16.970(3)
b, Å	19.380(2)	15.831(3)	17.483(4)
c, Å	25.985(3)	20.493(4)	22.660(5)
α, deg	90	86.233(4)	67.545(3)
β, deg	117.495(5)	73.193(4)	82.449(4)
γ, deg	90	88.305(4)	63.291(4)
V, A^3	5436.1(11)	3683.2(12)	5544(2)
Z	4	2	2
d_{calcd}, $g\cdot cm^{-3}$	1.205	1.426	1.196
μ, mm^{-1}	0.388	0.553	0.545
refl collected	23640	15015	30281
T_{min} / T_{max}	0.979	0.964	0.933
N_{measd}	7824	10456	15791
[R_{int}]	[0.0626]	[0.0576]	0.0677
R [I>2sigma(I)]	0.0503	0.0520	0.0734
R (all data)	0.0805	0.1169	0.0976
R_w [I>2sigma(I)]	0.1363	0.1050	0.1902
R_w (all data)	0.1493	0.1336	0.2123
GOF	0.964	0.865	1.009

Table 5.10 Crystallographic data and summary of data collection and structure refinement of complexes **5.1**·4CH_3CN and **5.2**·4CH_3CN

	5.1·4CH_3CN	**5.2**·4CH_3CN
Formula	$C_{73}H_{88}N_6O_5Pd$	$C_{75}H_{92}N_6O_5Pd$
FW	1235.90	1263.95
cryst syst	Triclinic	Triclinic
space group	P -1	P -1
T, K	213(2)	223(2)
a, Å	13.788(2)	13.763(3)
b, Å	14.793(2)	16.86(3)
c, Å	17.838(3)	18.31(3)
α, deg	99.764(3)	74.39(3)
β, deg	92.285(2)	69.15(3)
γ, deg	108.748(2)	67.17(3)
V, A^3	3378.0(9)	3608(12)
Z	2	2
d_{calcd}, $g \cdot cm^{-3}$	1.203	1.152
μ, mm^{-1}	0.327	0.308
refl collected	2207	18269
T_{min} / T_{max}	0.934	0.974
N_{measd}	9649	10284
[R_{int}]	[0.0412]	[0.1008]
R [I>2sigma(I)]	0.0362	0.0968
R (all data)	0.0467	0.1436
R_w [I>2sigma(I)]	0.1007	0.2424
R_w (all data)	0.1060	0.2878
GOF	1.040	1.022

5.6 Conclusions

The results presented in this chapter demonstrate that calixanions can be used as an efficient entrance point for the synthesis of O-bound palladium calix[4-6]arene complexes. The palladium complexes strongly favor the 1,2-binding mode. The resulting eight-membered heteropalladacycle forms a boat-boat conformation. This conformation favors a short Pd-H interaction that is observable as a downfield resonance in the ^{1}H NMR spectrum and demonstrated in the X-ray studies.

CHAPTER 6

HETEROBIMETALLIC PALLADIUM(II)/TITANIUM(IV) AND PALLADIUM(II)/MOLYBDENUM(VI) COMPLEXES

6.1 Introduction

Interest in bimetallic surface and catalytic reactions, for example the SOHIO catalytic process,[208] has led to extensive research in bimetallic model systems. Our interest in metal aryloxo complexes bearing molybdenum[181,184,209] or bismuth[210-211] atoms as catalyst models for the SOHIO process[208] has led us to investigate the properties of calixarenes as polyoxo supportive ligands.[58,93,109-110] In particular, calix[5]arene has proven to be excellent for the insertion of more than one heteroatom in the lower rim.[82-83,87,130,212] Recently our group described the synthesis and structural characterization of the first example of soluble M^{III}/Mo^{VI} (M = Bi, Sb) calixarene compounds utilizing the **^{t}BuC5(H)$_5$** ligand as an oxygen-rich platform, to mimic the catalytic active site of the SOHIO process. The synthesis was performed in a rational manner in which one Bi^{III} or Sb^{III} metal center was selectively placed on the lower rim of the calix[5]arene[85] followed by the addition of the Mo^{VI} reactant as a final step (Scheme 6.1).[213]

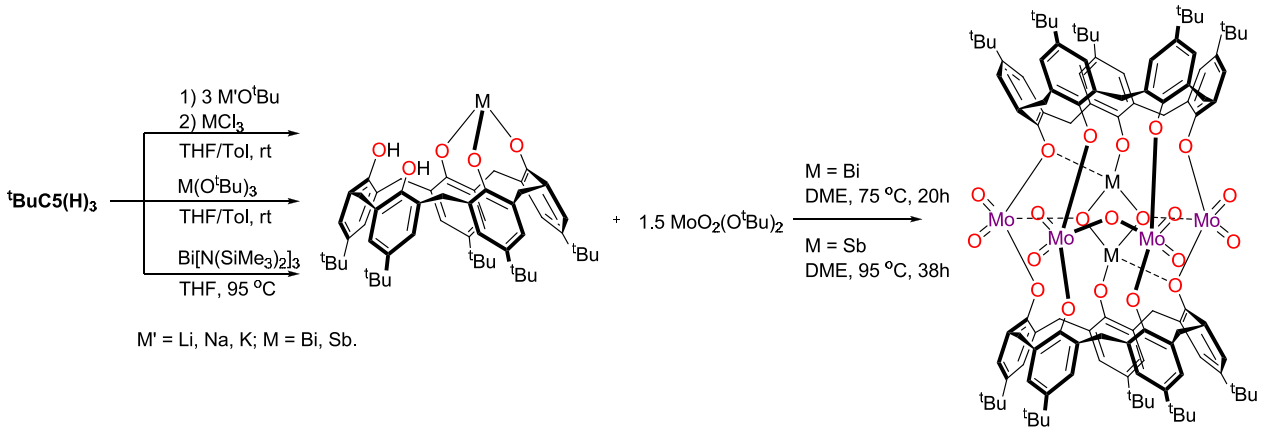

Scheme 6.1 Preparation of monometallic bismuth or antimony[85] and heterobimetallic Mo/M (M = Bi, Sb) calix[5]arene complexes.[213]

Motivated by the reactivity of the calix[5]arene, we decided to explore new systems containing two different transition metals in the lower rim. Following an approach similar to that used in the synthesis of the Mo^{VI}/Bi^{III} calix[5]arene complex, we selectively place one transition metal in the lower rim, while leaving some hydroxyl oxygens for further reactivity. In this fashion we may explore the reactivity of palladium-calix[5]arene complexes.

In Chapter 5 we observed that when our palladium-calix[5]arene complex, for example [Pd(bipy){Cs·**^{t}BuC5(H)$_2$**}] **5.1d**, was exposed to air or water, neither the alkali metal nor the palladium ions were lost. In contrast, the complex reacted quickly when aqueous HCl was added. Both metals were lost, to obtain parent **^{t}BuC5(H)$_5$**.

In this chapter we describe the synthesis and full characterization of the first examples of heterobimetallic Pd^{II}/Ti^{IV} and Pd^{II}/Mo^{VI} calix[5]arene complexes. This work provides further examples of rational synthesis of metallocalixarenes containing two different transition metals.

6.2 Results and discussion

6.2.1 Synthesis of palladium(II)/titanium(IV) complexes

In order to explore the reactivity of the alkali metal and the remaining two hydroxyl oxygens in palladium-calix[5]arene complexes [Pd(L){M·^{t}**BuC5(H)$_2$**} **5.1c-d**, **5.2c-d**, and **5.3c-d**, we screened several titanium precursors (e.g. $TiCl_4$·2THF, Cp_2TiCl_2, $CpTiCl_3$). We hypothesized that metal chlorides could react with the alkali metal to perform a salt elimination reaction resulting in the formation of the heterobimetallic complex. However, we were unable to isolate any compounds using chlorotitanium derivatives. We decided to use titanium-containing strong bases, for example $Ti(O^iPr)_4$ and $Ti(NEt_2)_4$. In the case of $Ti(O^iPr)_4$, we ended with a mixture of compounds that we were unable to separate.

The best results were obtained using the precursor $Ti(NEt_2)_4$, leading to the formation of dimeric titanium bridged complexes Ti[Pd(L){M·^{t}**BuC5**}]$_2$ (**6.1 - 6.6**) as depicted in equation 6.1.

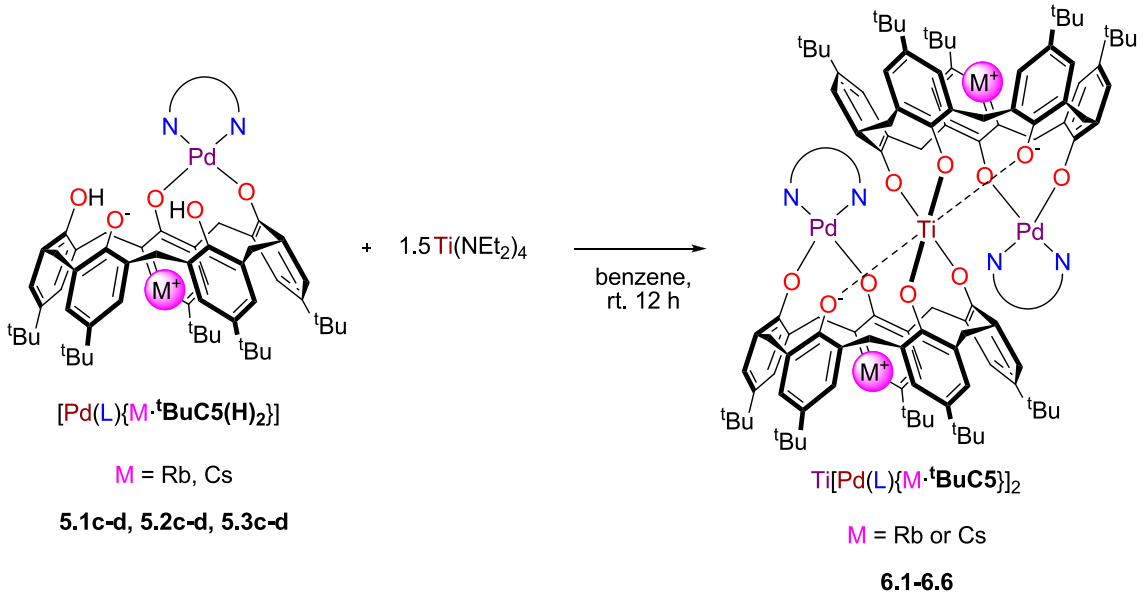

(6.1)

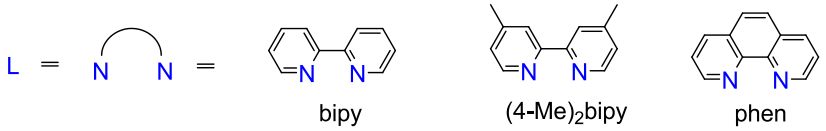

	bipy	(4-Me)$_2$bipy	phen
Ti[Pd(L){Rb·^{t}BuC5}]$_2$	**6.1**	**6.2**	**6.3**
Ti[Pd(L){Cs·^{t}BuC5}]$_2$	**6.4**	**6.5**	**6.6**

The reaction occurs when 1.5 equivalents of $Ti(NEt_2)_4$ react with one equivalent of [Pd(L){M·^{t}**BuC5(H)$_2$**}] (**5.1c-d**, **5.2c-d**, or **5.3c-d**) in anhydrous benzene at room temperature. The products **6.1 - 6.6** are not soluble in benzene, therefore purification is simple; the product precipitates from the reaction mixture. Successive washing with hexane or pentane helped to remove any remaining impurities. Using this methodology we were able to isolate the heterobimetallic complexes **6.1** – **6.6** in good yield (70-92%) after an easy purification.

The formation of the metallo-bridged complexes can be rationalized by the elimination of all four ligands from the titanium precursor by the remaining acidic protons of the compounds

5.1c-d, **5.2c-d**, and **5.3c-d**. Other examples where titanium serves as bridge between two calixarene ligands such as **^{t}BuC4(H)$_4$** or **^{t}BuC6(H)$_6$** have been described in the literature.[31,91]

6.2.1.1 NMR spectroscopy

The solubility of the heterobimetallic complexes **6.1** – **6.6** in chloroform allowed their solution analysis by ^{1}H NMR spectroscopy. Complexes **6.1** – **6.6** give very similar patterns (Figure 6.1). The overall C_s symmetry of the palladium-calix[5]arene ligand is retained in the compounds: three resonances are observed for the *tert*-butyl groups (in a 2:1:2 ratio) located between 1.23 and 0.76 ppm. In addition, six doublets due to $^2J_{HH}$ geminal coupling for non-equivalent methylene hydrogens[30] are observed for the methylene bridging groups (in a 2:1:2:2:1:2 ratio) ranging from 5.29 to 1.07 ppm. The aromatic proton resonances from the calix[5]arene are observed in the range of 6.70 to 5.43 ppm. Finally, the aromatic resonances assigned to the N-heterocyclic ligands (bipy, (4-Me)$_2$bipy and phen) attached to the palladium center are observed in the range 9.54 to 7.11 ppm. The overall similarity of the ^{1}H NMR spectra suggests that the calixarene ring in compounds **6.1-6.6** adopts a cone conformation in solution similar to that for compounds **5**.

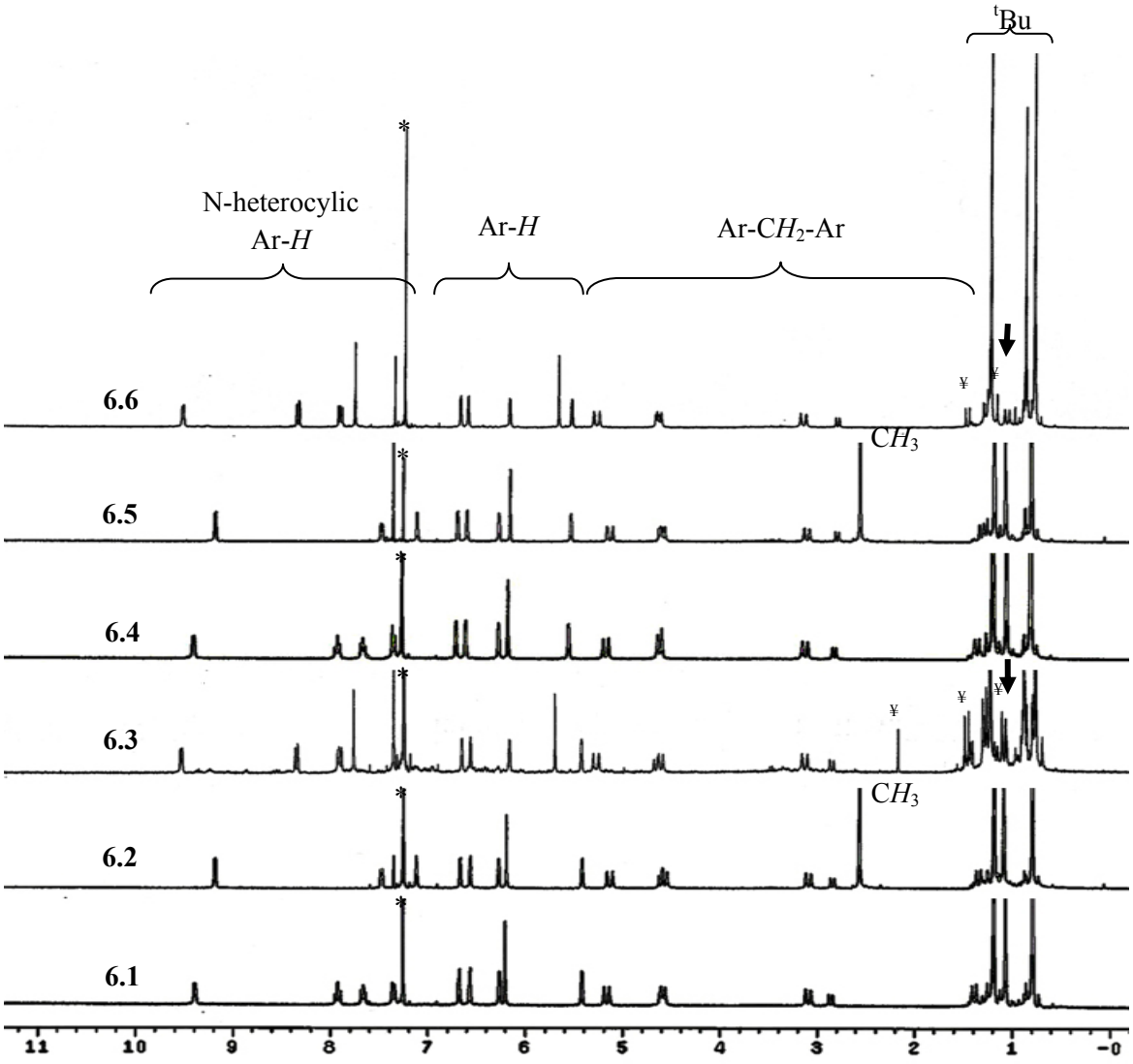

Figure 6.1 ^{1}H NMR spectra of complexes **6.1** to **6.6** in $CDCl_3$. *Residual solvent C_6H_6. ¥Impurities.

Clues to the differences between the products and the starting materials are found upon closer examination of the ^{1}H NMR spectra, especially the chemical shifts of the aromatic, methylene and *tert*-butyl protons from the calix[5]arene ligand. Figure 6.2 and Table 6.1 show comparative ^{1}H NMR spectra and data of complexes **5.1c** and **6.1** as an example. Compound **6.1** presents certain unusual chemical shifts in its ^{1}H NMR spectrum compared with those of compound **5.1c**.

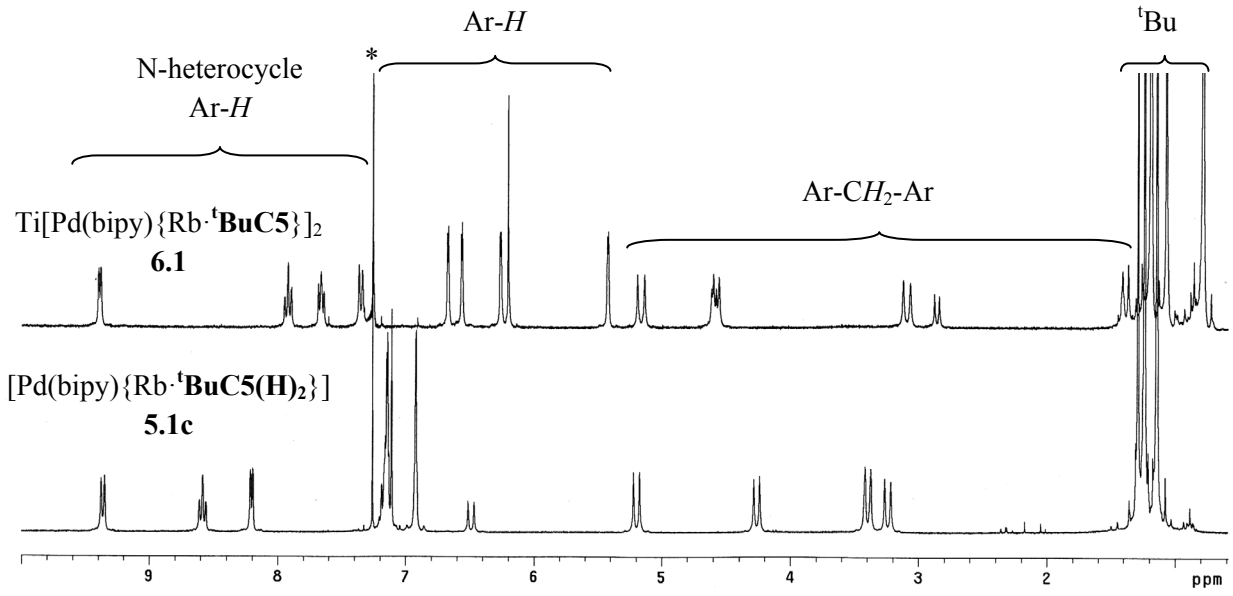

Figure 6.2 Comparison between ^{1}H NMR spectra of complexes **5.1c** and **6.1** in *$CDCl_3$.

Table 6.1 Comparative ^{1}H NMR data for compounds **5.1c** and **6.1** in $CDCl_3$. Highlighted values refer to the major changes found between compounds.

Protons	**5.1c**	**6.1**
-O*H*	14.24	-
N-heterocyclic Ar-*H*	**9.37 (d, 2H, 8.0 Hz)** 8.59 (dd, 2H, 7.7, 6.9 Hz) **8.21 (d, 2H, 4.7 Hz)** 7.16 (dd, 2H, 8.5, 7.7 Hz)	**9.39 (d, 4H, 4.7 Hz)** 7.92 (dd, 4H, 7.7, 6.3 Hz) 7.67 (dd, 4H, 5.8, 6.6 Hz) **7.35 (d, 4H, 7.7 Hz)**
Ar-*H*	7.15 (d, 2H, 2.5 Hz) 7.14 (d, 2H, 2.5 Hz) 7.11 (s, 2H) 6.92 (s, 4H)	6.67 (d, 4H. 2.8 Hz) 6.57 (d, 4H, 2.5 Hz) 6.27 (d, 4H, 2.5 Hz) 6.21 (s, 4H) 5.43 (d, 4H, 2.5 Hz)
Ar-C*H*$_2$-Ar	**6.49 (d, 1H, 13.7 Hz)** 5.20 (d, 2H,14.3 Hz) 4.26 (d, 2H, 13.5 Hz) **3.39 (d, 3H, 13.7 Hz)** 3.24 (d, 2H, 14.3 Hz)	5.17 (d, 4H, 16.5 Hz) **4.60 (d, 2H, 11.0 Hz)** 4.58 (d, 4H, 12.9 Hz) 3.09 (d, 4H, 16.2 Hz) 2.86 (d, 2H, 11.5 Hz) **1.39 (d, 4H, 13.5 Hz)**
^{t}Bu	1.29 (s, 9H) 1.24 (s, 18H) 1.14 (s, 18H)	1.19 (s, 36H) 1.07(s, 18H) 0.79 (s, 36H)

Two of the N-heterocyclic aromatic proton resonances in **6.1** show a notable chemical shift (Figure 6.3). The aromatic proton A at δ 7.35 (^3J = 7.7 Hz) has moved 2.02 ppm upfield relative to its position in compound **5.1c**. Proton C at δ 9.39 (^3J = 4.7 Hz) has moved 1.18 ppm downfield, suggesting that the aromatic proton A is shielded while the proton C is deshielded.

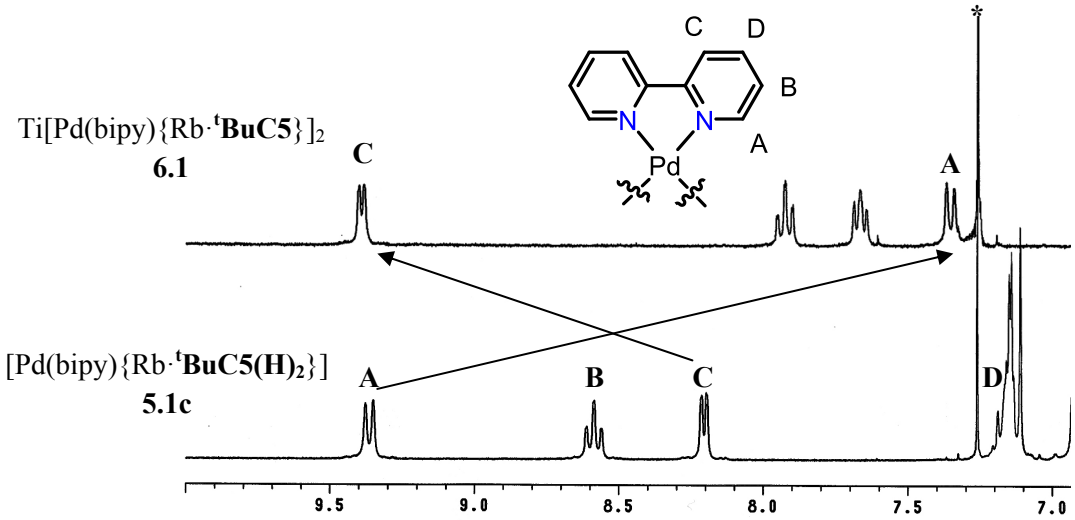

Figure 6.3 ^{1}H NMR spectra of expansions in the N-heterocyclic aromatic areas of complexes **5.1c** and **6.1** in *$CDCl_3$. The arrows depict the movement of the proton signals.

The aromatic proton Ar-*H* resonances in **6.1** at 6.67 – 5.43 ppm are significantly upfield compared with the values of **5.1c** (Ar-*H* from 7.15 – 6.92 ppm). This range is also about 0.95 (max) and 1.36 ppm (min) upfield of normal Ar-*H* positions in metallocalixarenes, compared for example to the compounds [W(N^{t}Bu)(NH^{t}Bu){^{t}**BuC5(PNMe$_2$)**}], [W(N^{t}Bu)(OTf){^{t}**BuC5(PNMe$_2$)**}], [(SiMe$_2$)$_2${^{t}**BuC5(H)**}], [(SiMePh)$_2${^{t}**BuC5(H)**}], [(SiMe$_2$){^{t}**BuC5(H)$_3$**}], [(SiMePh){^{t}**BuC5(H)$_3$**}], [Ti(NMe$_2$){^{t}**BuC5(PNMe$_2$)**}] and [Zr(NEt$_2$){^{t}**BuC5(PNMe$_2$)**}] (overall Ar-*H* range 7.62 – 6.79 ppm).[82-83,130] A compound containing two calix[5]arene moieties bridged by two titanium atoms [{MeOH·K·^{t}**BuC5(H)**}-μ-

O-[Ti(acac)]$_2${THF·K·^{t}**BuC5(H)$_3$**}], has a range for the Ar-*H* protons of 7.48 – 6.48 ppm[81] (see Table 6.2).

The methylene region also shows significant changes (Figure 6.4 **E** and **I** protons). First the doublet at δ 4.60 ppm labeled as **E**, which integrates to 1H (asymmetric molecule), is 1.89 ppm upfield of its position found in **5.1c** (6.49 ppm, 1H). This upfield shift is indicative of the rupture of the Pd-H interaction due to the change in the conformation of the metallocycle (ref. Chapter 5, Figure 5.11). Second, the doublet at δ 1.39 ppm labeled as **I**, which integrates to 1H (asymmetric molecule), is 2.00 ppm upfield of its position in compound **5.1c** (3.39 ppm, 1H). Upfield shifts in the aromatic and methylene area (Ar-*H*, Ar-C*H*$_2$-Ar) in compounds **6.1** to **6.6** are found because the protons are positioned above an aromatic ring. The increase of shielding for the aromatic rings is responsible for this chemical shift.[83]

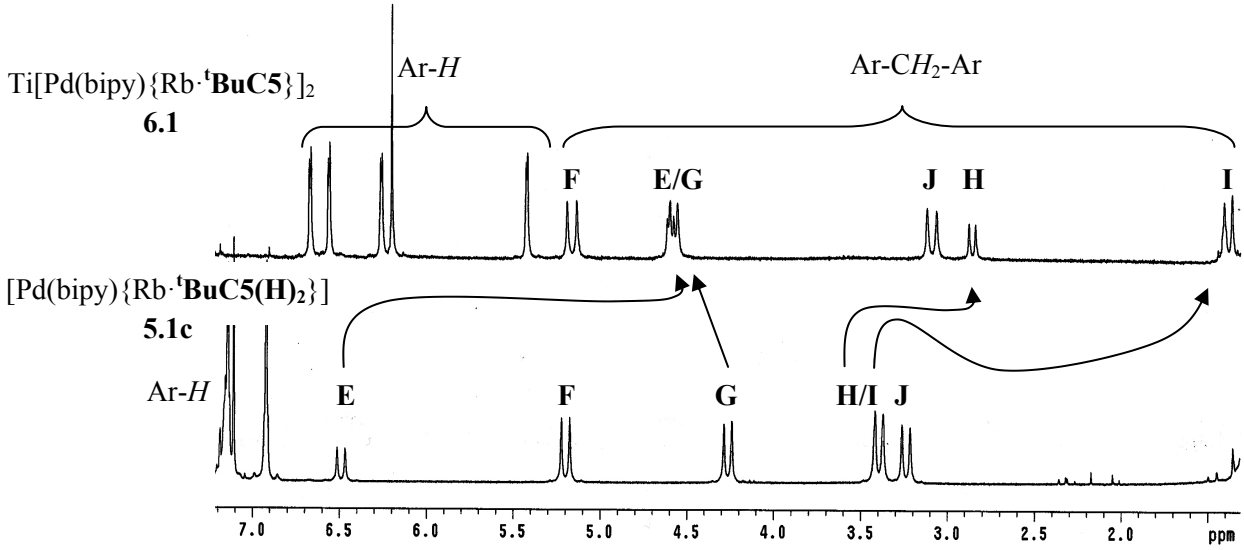

Figure 6.4 ^{1}H NMR spectra of expansions of the aromatic (Ar-H) and methylene (Ar-C*H*$_2$-Ar) areas of complexes **5.1c** and **6.1** in $CDCl_3$. The arrows depict the movement of the proton signals.

Table 6.2 Common ppm ranges found in literature for the Ar-*H*, Ar-CH_2-Ar and ^{t}Bu resonances in metallocalix[5]arenes in $CDCl_3$.

Compound	Ar-*H*	Ar-CH_2-Ar	^{t}Bu	conformation*	ref.
[W(N^{t}Bu)(NH^{t}Bu){^{t}**BuC5(PNMe$_2$)**}]	7.62-6.99	4.58-3.29	1.33-1.12	F-C	[82]
[W(N^{t}Bu)(OTf){^{t}**BuC5(PNMe$_2$)**}]	7.50-7.11	4.70-3.30	1.30-1.16	C	[82]
[(SiMe$_2$)$_2${^{t}**BuC5(H)**}]	7.15-6.92	4.16-3.39	1.28-1.14	1,2-A	[130]
[(SiMePh)$_2${^{t}**BuC5(H)**}]	7.25-6.79	4.88-3.23	1.37-1.08	C	[130]
[(SiMe$_2$){^{t}**BuC5(H)$_3$**}]	7.21-6.94	4.15-3.35	1.29-1.11	P-C	[130]
[(SiMePh){^{t}**BuC5(H)$_3$**}]	7.27-7.06	4.33-3.32	1.25-1.16	1,3-A	[130]
[Ti(NMe$_2$){^{t}**BuC5(PNMe$_2$)**}]	7.24-6.98	4.71-3.32	1.38-1.08	C	[83]
[Zr(NEt$_2$){^{t}**BuC5(PNMe$_2$)**}]	7.16-6.99	4.72-3.21	1.31-1.10	C	[83]
[{MeOH·K·^{t}**BuC5(H)**}-μ-O-[Ti(acac)]$_2${THF·K·^{t}**BuC5(H)$_3$**}]	7.48-6.48	5.54-2.96	1.33-0.78	C	[81]
[Pd(L){M·^{t}**BuC5(H)$_2$**} (**5.1c-d**, **5.2c-d**, and **5.3c-d**)	7.17-6.89	6.63-3.16	1.30-1.11	*p*-C	§
Ti[Pd(L){M·^{t}**BuC5**}]$_2$ (**6.1 – 6.6**)	6.70-5.43	5.29-1.07	1.23-0.76	F-C	§

*C = cone, F-C = flattened cone, P-C = partial cone, *p*-C = pinched cone 1,2-A = 1,2-alternate, 1,3-A =1,3-alternate. M = Rb, Cs. L = bipy, (4-Me)$_2$bipy, phen. §This work.

If moisture is introduced into an NMR tube containing compound **6.1,** it slowly decomposes to the starting material compound **5.1c**, as shown by ^{1}H NMR. The rate of the decomposition depends on the concentration of water; in the presence of trace water the product decomposes over a day but at high concentration (a drop) of water the decomposition is instantaneous. This result suggests that the Rb ion is still contained in compound **6.1**. A qualitative experiment using Energy Dispersive X-ray analysis (EDX) showed that M, Pd and Ti

(M = Rb or Cs) are present in compounds **6.1 - 6.6**. The EDX result was later confirmed by single crystal X-ray diffraction (Section 6.2.1.2).

6.2.1.2 Crystal and molecular structures

Single crystals of compound **6.1** were obtained by slow diffusion of a solution of $Ti(NEt_2)_4$ into a concentrated solution of [Pd(bipy){Rb·^{t}**BuC5(H)$_2$**] **5.1c** in benzene at room temperature. The crystal structure of complex **6.1** is displayed in Figure 6.5 and selected bond distances and angles are presented in Table 6.3. Complex **6.1** crystallizes in the P21/c space group and consists of a dimeric heterobimetallic Pd/Ti (ratio 2:1) unit with the calix[5]arene ligands adopting a flattened cone conformation. Complex **6.1** represents the first example of a metallocalix[5]arene containing both early and late transition metals on the lower rim.

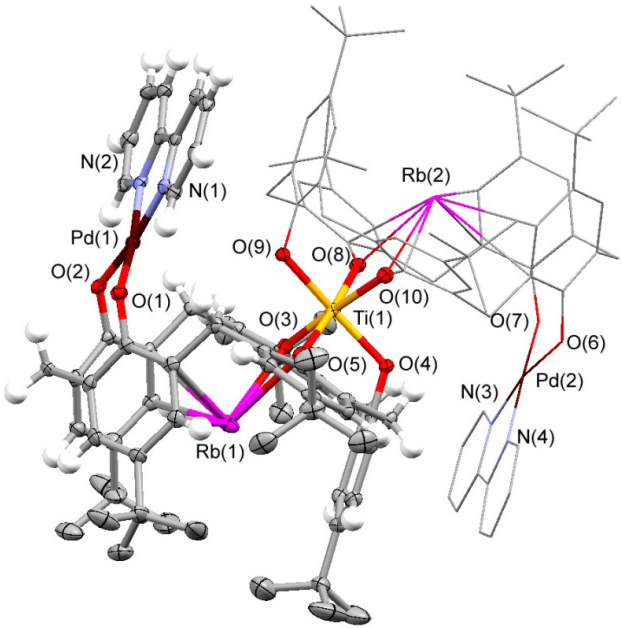

Figure 6.5 X-ray structure of complex **6.1**. Ellipsoids shown at 50% probability. The second part of the molecule is shown as wireframe model for clarity. Most H atoms and benzene crystallization molecules are not shown for clarity.

Table 6.3 Selected bond distances (Å) and angles (^{o}) for complex **6.1**.

Pd(1)-O(1)	1.975(3)	O(2)-Pd(1)-N(1)	169.97(12)	O(3)-Ti(1)-O(4)	87.90(11)
Pd(1)-O(2)	2.007(3)	O(1)-Pd(1)-N(2)	169.65(12)	O(10)-Ti(1)-O(4)	95.31(11)
Pd(1)-N(1)	2.019(3)	O(2)-Pd(1)-N(2)	92.68(12)	O(8)-Ti(1)-O(4)	86.62(11)
Pd(1)-N(2)	2.026(3)	N(1)-Pd(1)-N(2)	80.62(13)	O(5)-Ti(1)-O(4)	89.84(11)
Rb(1)-O(5)	2.723(3)	O(3)-Ti(1)-O(10)	173.68(12)	O(9)-Ti(1)-O(4)	170.63(11)
Rb(1)-O(3)	2.842(3)	O(3)-Ti(1)-O(8)	97.39(11)	O(3)-Ti(1)-Rb(1)	44.71(8)
Ti(1)-O(3)	1.937(3)	O(10)-Ti(1)-O(8)	88.24(11)	O(10)-Ti(1)-Rb(1)	129.94(8)
Ti(1)-O(4)	1.962(3)	O(3)-Ti(1)-O(5)	85.82(11)	O(8)-Ti(1)-Rb(1)	141.66(8)
Ti(1)-O(10)	1.945(3)	O(10)-Ti(1)-O(5)	88.75(11)	O(5)-Ti(1)-Rb(1)	41.19(8)
Ti(1)-O(8)	1.953(3)	O(8)-Ti(1)-O(5)	175.13(11)	O(9)-Ti(1)-Rb(1)	94.98(8)
Ti(1)-O(5)	1.957(3)	O(3)-Ti(1)-O(9)	86.60(11)	O(4)-Ti(1)-Rb(1)	86.40(8)
Ti(1)-O(9)	1.965(3)	O(10)-Ti(1)-O(9)	90.91(11)	Ti(1)-O(3)-Rb(1)	106.64(11)
O(1)-Pd(1)-O(2)	96.56(11)	O(8)-Ti(1)-O(9)	86.57(11)	Ti(1)-O(5)-Rb(1)	110.56(11)
O(1)-Pd(1)-N(1)	89.60(12)	O(5)-Ti(1)-O(9)	97.30(11)	Rb(2)-Ti(1)-Rb(1)	174.98(2)

Complex **6.1** crystallizes with six molecules of benzene, but none of the molecules are found inside the cavity due to the presence of the alkali ion and the *tert*-butyl groups that block the cavity (Figure 6.6).

The titanium center in complex **6.1** displays a coordination number of six and serves as a bridge between two palladium-calix[5]arene moieties (Figure 6.6). Each palladium-calix[5]arene unit provides three adjacent O atoms in order to complete the coordination sphere of titanium. All of the Ti-O bond distances and O-Ti-O angles fall in the normal ranges for hexacoordinated titanium(IV) calixarene complexes.[52-53,81,91-92] Complex **6.1** does not have remaining OH groups; each oxygen is associated with a palladium, titanium or rubidium center to balance the overall charge.

In compound **6.1**, the environments at the Pd(1) and Pd(2) centers are similar. Both metal centers possess an approximate square planar coordination geometry with adjacent interligand angles falling in the range 96.56(11)^{o} (O-Pd-O) to 80.18(14)^{o} (N-Pd-N). The Pd-O (1.975(3) to

2.007(3) Å) and Pd-N (2.013(3) to 2.026(3) Å) distances are consistent with those reported in the literature.[198,214]

The rubidium ions display π interactions with two of the calix[5]arene aromatic rings (A and B) in an η^2 fashion, and with the aromatic ring C in an η^1 fashion (Figure 6.6d).

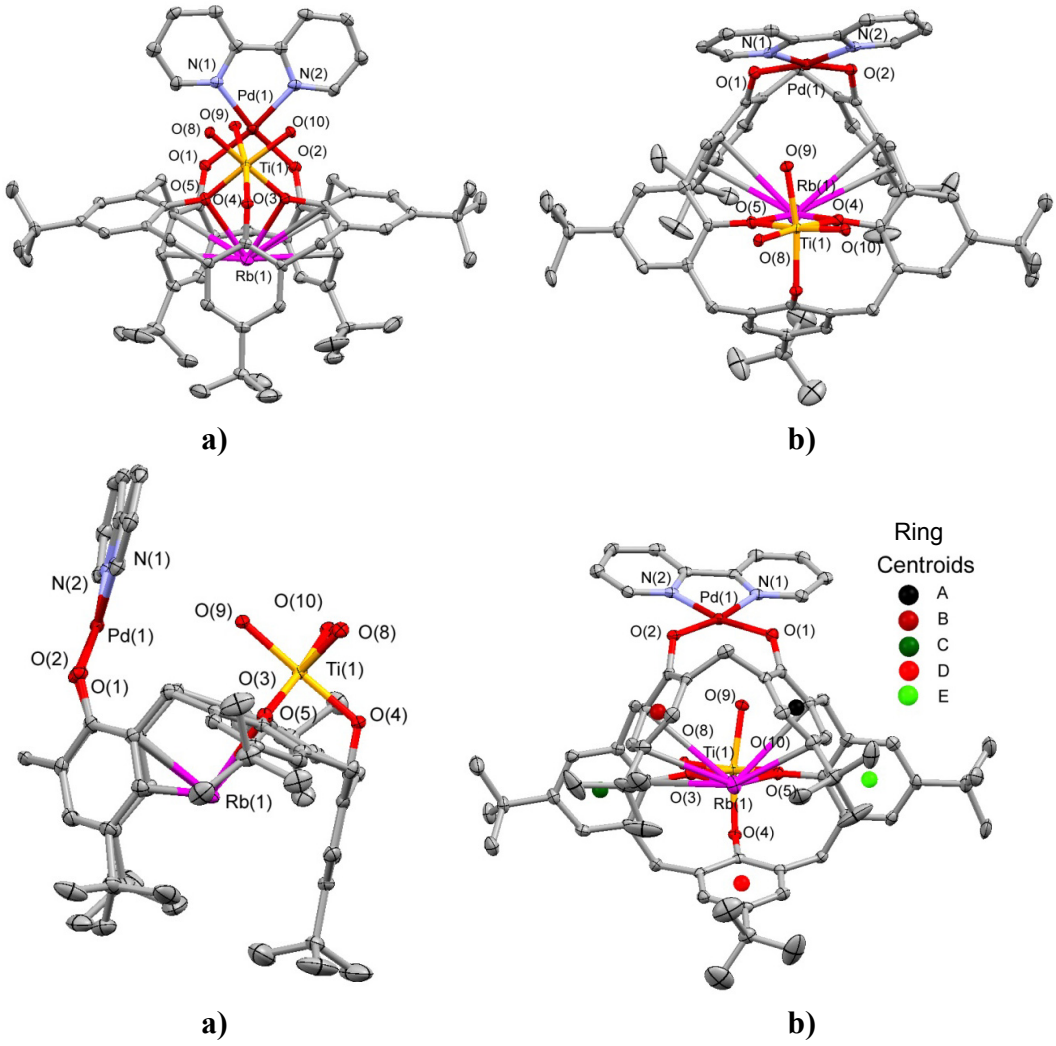

Figure 6.6 X-ray structure of complex **6.1**: a) front view, b) top view, c) side view and d) bottom view. Ellipsoids are shown at 50% probability. Crystallization molecules, H atoms and the second calix[5]arene ligand are not shown for clarity.

The main structural difference between compounds **5.1d** and **6.1** concerns the orientation of the Pd atom in the 8-membered metal-containing heterocycle (Figure 6.7). In compound **5.1d** the overall conformation of the metal-containing heterocycle could be described as a boat-boat (BB) conformation, while in compound **6.1** it is better described as a boat-chair (BC) conformation[1] (Figure 6.7). This change in conformation is consistent with the observation made in solution by ^{1}H NMR, in which the downfield methylene doublet returns to a normal position due to loss of the Pd···H interaction. The distances we observe for the Pd···H interaction in the CB conformation of **6.1** are 3.288 Å (Pd(1)) and 3.261 Å (Pd(2)); about ~0.8 Å greater than the Pd···H distances in **5.1d** (2.443 Å). Metal···H distance values for the BB conformation reported in the literature range from 2.254 to 2.550 Å.[151-152]

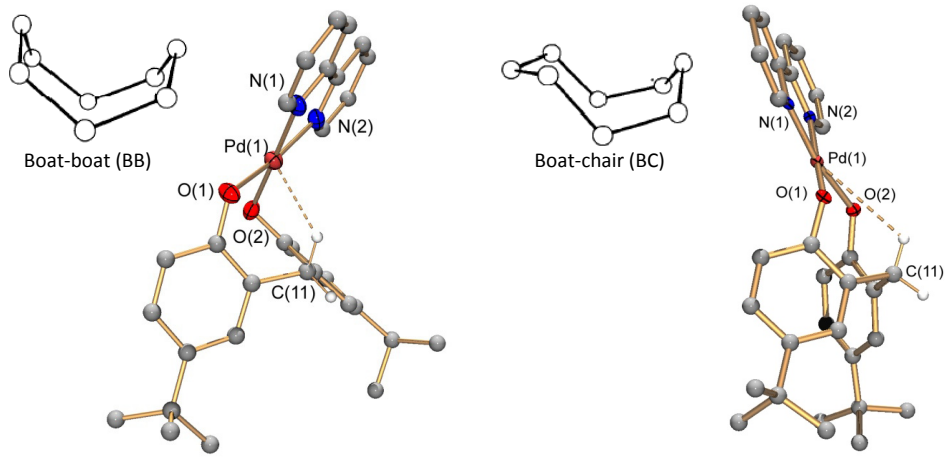

a) 5.1d **b) 6.1**

Figure 6.7 Approximate ideal conformations[1] observed in: a) **5.1d** boat-boat conformation and b) **6.1** boat-chair conformation. Only partial structures of compound **5.1d** and **6.1** are shown for clarity.

In order to determine what factors may affect the change in conformation in the metal-containing heterocyle we calculated the relative energy for the BB and BC conformations in collaboration with Dr. Benjamin Janesko. Calculations are based on density functional theory using the B3LYP exchange-correlation functional, the uncontracted LANL2DZ basis set and effective core potential on Pd, and the 6-31+G(d,p) basis set on other atoms.[215] Calculated geometries for the BB conformation and BC conformation with a model molecule are shown in Figure 6.8.

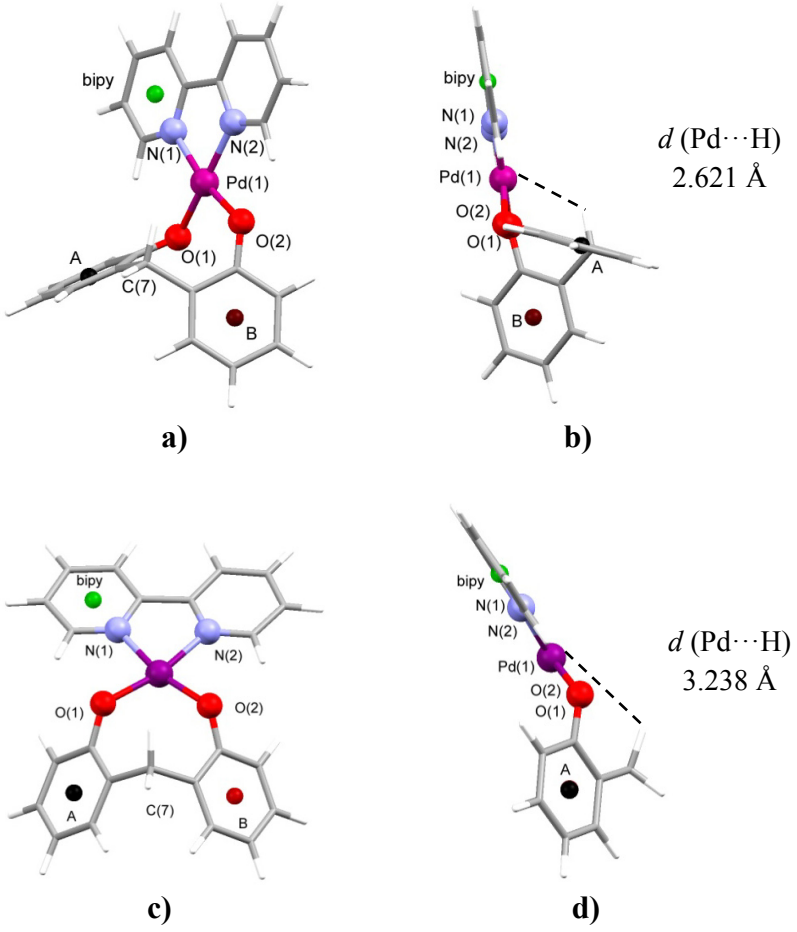

Figure 6.8 Calculated geometries for the model of an 8-membered palladium-containing heterocycle. a) BB conformation and b) side view of BB conformation, c) BC conformation and d) side view of BC conformation.

The BB geometry has a flattened aromatic ring (**A**) with a 2.621 Å Pd···H interaction (Figure 6.8a). The plane of the aromatic ring **A** is 105.89^{o} from the plane of the bipy ring (Figure 6.8b). In the case of the BC conformation the angle between the plane of the aromatic ring A and the plane of the bipy ring is 133.63^{o} (Figure 6.7d). As expected, the calculated distance for the Pd···H interaction in the BC conformation (3.238 Å) is larger than the Pd···H interaction in the BB conformation (2.621 Å).

The distances found in the calculated geometries for the Pd···H interaction are close to those found experimentally, but the angles show a significant deviation (see Table 6.4). Those deviations could be due to interactions not considered in the calculations, for example the interaction with the alkali metal.

Table 6.4 Selected bond distances and angles for calculated BB and BC conformations, and values found experimentally.

Conformer	source	A-O(1)-bipy (°)	B-O(2)-bipy (°)	Pd···H (Å)	A-C(7/11)-B (°)	*d* centroid A - B (Å)	*d* centroid A - bipy (Å)	*d* centroid A - bipy (Å)
Boat-boat BB	calc	105.89	171.31	2.621	114.14	4.930	5.616	6.743
	5.1d	94.27	156.63	2.443	115.77	4.941	5.212	6.600
difference		**11.62**	**14.68**	**0.178**	**1.63**	**0.011**	**0.404**	**0.143**
Boat-chair BC	calc	133.63	133.64	3.238	106.57	4.708	6.282	6.282
	6.1	145.48	143.06	3.288	91.91	4.169	6.553	6.379
difference		**11.85**	**9.42**	**0.050**	**14.66**	**0.539**	**0.271**	**0.097**

The boat-boat geometry was calculated to be 2.6 kcal/mol more stable than the boat-chair geometry. This value again suggests that there are other factors involved that promote the change in conformation.

A close look at the X-ray structure of **6.1** reveals two important intramolecular π interactions. First, the distances between the aromatic ring of the calix[5]arene and the pyridyl ring of the bipy ligands, D···bipyB' and D'···bipyB, average 3.633 Å (Figure 6.9a). Second, the aromatic rings C···C' and E···E' of the facing calix[5]arene ligands have centroid-centroid distances of 4.147 and 3.818 Å, respectively (Figure 6.9b).

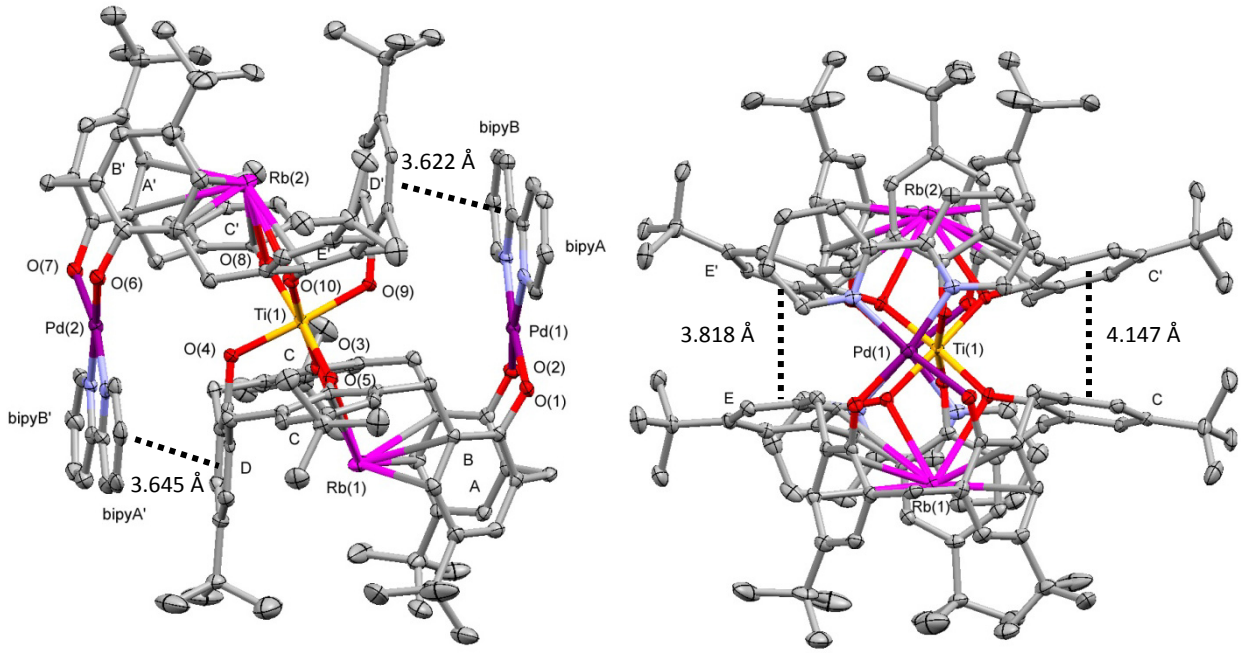

a) **b)**

Figure 6.9 X- ray structure of **6.1** showing the interactions **a)** between D···bipyB' and D'···bipyA and **b)** between the aromatic rings C···C' and E···E' of the calix[5]arene ligands.

These intramolecular interactions may promote the conformational change in the 8-membered heterocycle. If so, the π interactions between the aromatic rings must be stronger than the Pd···H interactions.

Another notable feature in the X-ray structure of **6.1** is the crystal packing. Interestingly, we observe layers of molecules of **6.1** (Figure 6.10). Intermolecular π-π stacking (denoted by a dotted line in Figure 6.10) produces polymeric chains, unlike the dimers observed for compound **5.1d**.

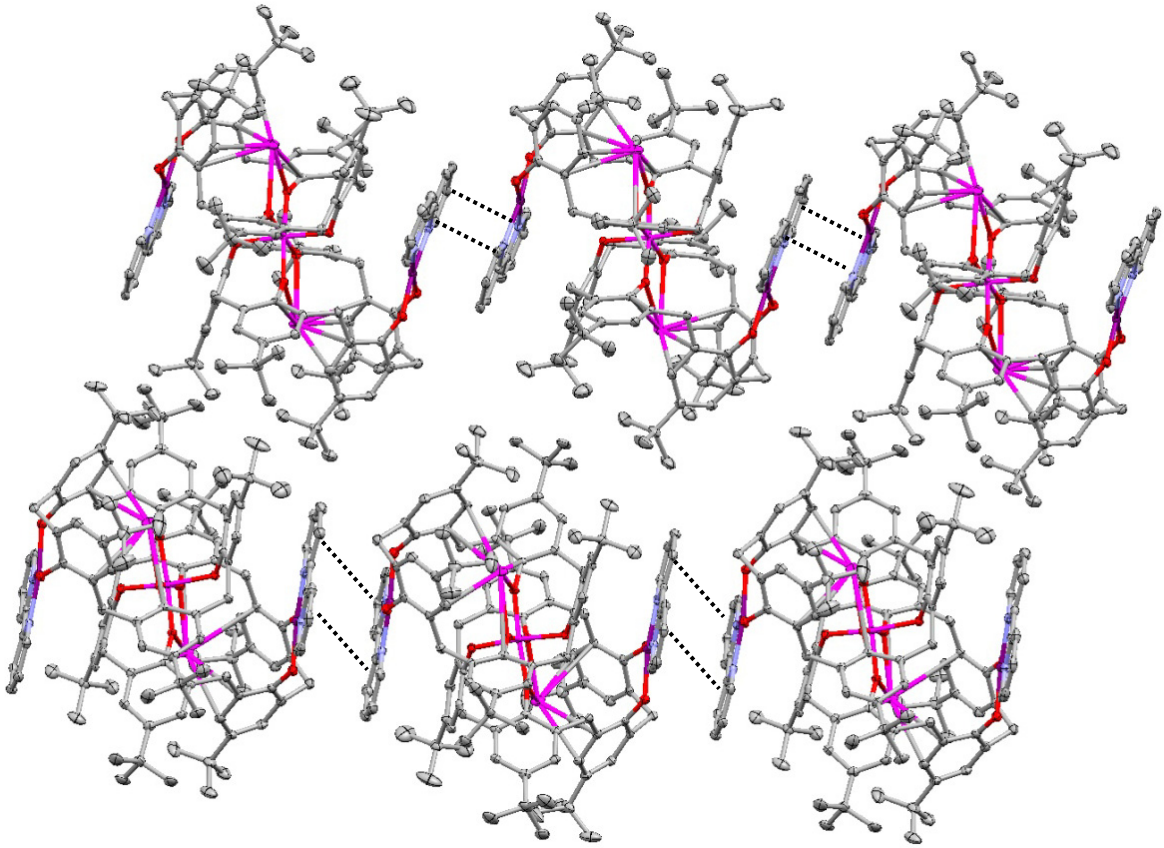

Figure 6.10 View of the crystal packing in complex **6.1**.

The planar Pd(1)bipy^{2+} and Pd(2)bipy^{2+} moieties in these chains are parallel but displaced with respect to one another (Figure 6.11). Both pyridyl rings of each bipy ligand are found to form an intermolecular π-π stack with a stacking distance of $d_{\pi\text{-}\pi}$(Pd(1)bipy^{2+}) = 3.199 Å and $d_{\pi\text{-}\pi}$(Pd(2)bipy^{2+}) = 3.259 Å, and a centroid-centroid pyridyl distance $d_{c\text{-}c}$(Pd(1)bipy^{2+}) = 3.773 Å and $d_{c\text{-}c}$(Pd(2)bipy^{2+}) = 3.781Å. Additional intramolecular interactions between one pyridyl ring (bipyB or bipyB') and the calix[5]arene aryl ring D' or D with a $d_{c\text{-}c}$(bipyB-D') = 3.622 Å and $d_{c\text{-}c}$(bipyB'-D) = 3.645 Å were observed.

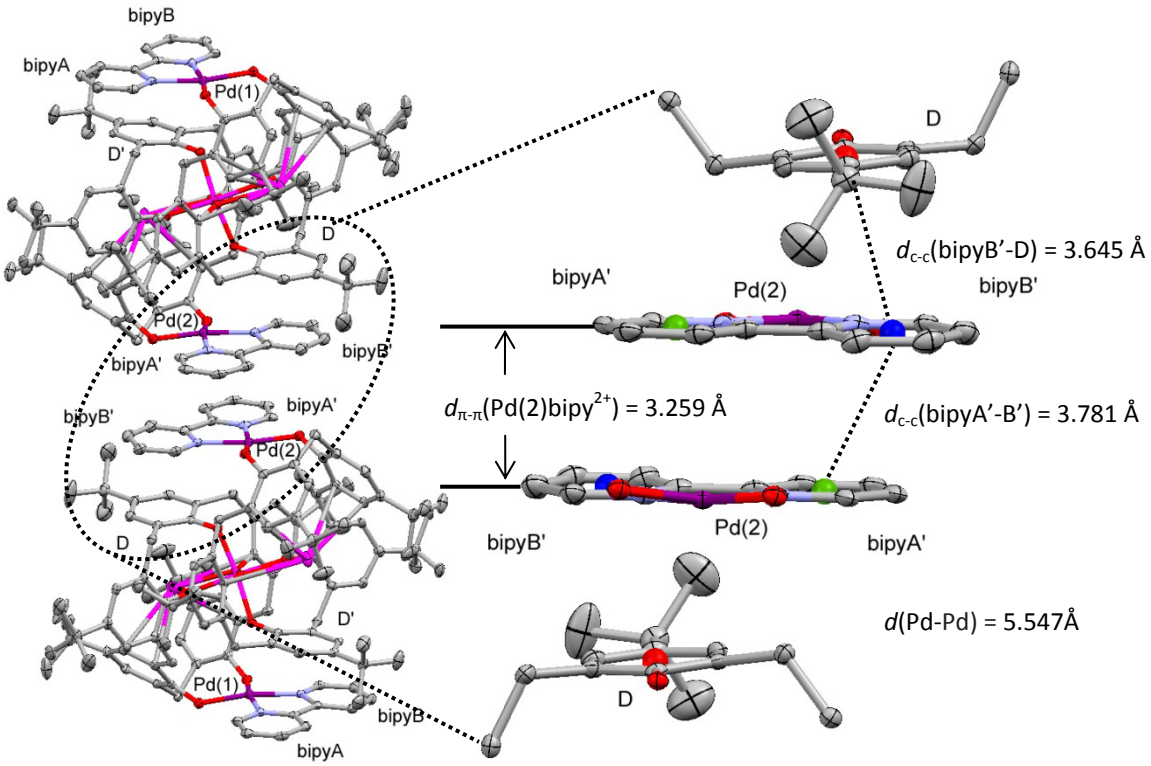

Figure 6.11 View of the crystal π-π stacking showing the parallel displacement and a close-up of the intermolecular π-π stacking with selected distances.

All the $d_{c\text{-}c}$ distances observed in compound **6.1** fall below the maximum value reported for the ring centroid-centroid distance $d_{c\text{-}c}$ = 3.8 Å[205] in aromatic π–stacking.

6.2.2 Synthesis of palladium(II)/molybdenum(IV) complexes

In a similar approach to that described in the synthesis of Pd/Ti heterobimetallic complexes, we initially reacted MoO_2Cl_2 with compounds **5.1c-d**, **5.2c-d**, and **5.3c-d** but no new product was observed by ^{1}H NMR. On the other hand, when we reacted one equivalent of compounds **5.1c-d**, **5.2c-d**, and **5.3c-d** with 1.2 equivalents of $MoO_2(acac)_2$ in benzene, we observed the formation of new products **6.7 - 6.12** as depicted by Equation 6.2. A precedent for the reactivity of $MoO_2(acac)_2$ with the dianions $M_2\cdot$**^{t}BuC5(H)$_3$** (M = K, Rb, Cs) was described in Chapter 4, in which the acac was able to deprotonate the calix[5]arene and produce the $MoO_2(acac)$-containing calix[5]arene compound.

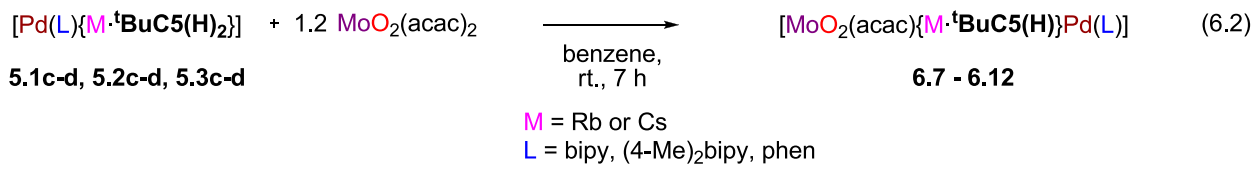

(6.2)

Compounds **6.7** – **6.12** can be isolated in 79 – 96% yield after workup. The compounds were characterized by ^{1}H NMR, ^{13}C NMR, IR, and UV-Vis spectroscopies and elemental analysis. Unfortunately no single crystals were obtained for X-ray studies. Nevertheless, a molecular structure can be proposed on the basis of the spectroscopic data (Figure 6.12).

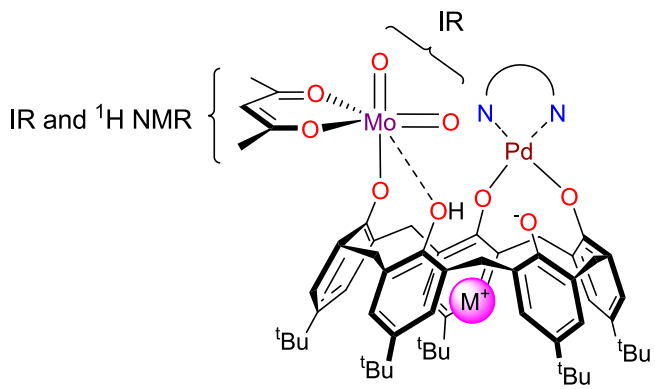

[MoO_2(acac){M·^{t}**BuC5(H)**}Pd(L)]

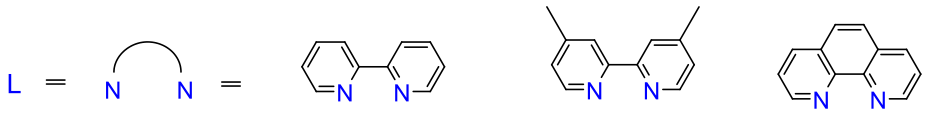

M = Rb or Cs

	bipy	(4-Me)$_2$bipy	phen
[MoO_2(acac){Rb·^{t}**BuC5(H)**}Pd(L)]	**6.7**	**6.8**	**6.9**
[MoO_2(acac){Cs·^{t}**BuC5(H)**}Pd(L)]	**6.10**	**6.11**	**6.12**

Figure 6.12 Proposed molecular structure for compounds **6.7 - 6.12**.

The combination of two spectroscopic techniques, IR and ^{1}H NMR, was used to propose the molecular structure of the products **6.7 – 6.12**. The structural prediction was validated with elemental analysis. In the IR spectrum five characteristic absorptions are observed for the MoO_2^{2+} and acetylacetonate anion (acac, ν(C=O), ν(C=C) and ν(-CH_3) of methyl ketone) moieties. The acac ligand was also observed by ^{1}H NMR where three new chemical shifts are observed. The final clue was elemental analysis which was consistent with the presence of Rb or Cs in the product.

6.2.2.1 Spectroscopy analysis

The solid state IR spectra (KBr pellets) of the [MoO_2(acac){M·^{t}**BuC5(H)**}Pd(L)] (**6.7 - 6.12**) complexes exhibit two strong bands in the ranges 915-917 and 886-891 cm^{-1}, corresponding to the stretching vibrations characteristic of the *cis*-MoO_2^{2+}arrangement.[171,183] The bands are shifted to longer wavelength compared to the vibrations of $MoO_2(acac)_2$ (935, 906 cm^{-1}). The ν(Mo=O) IR frequencies found for compounds **6.7** to **6.12** are higher than those reported in *cis*-MoO_2^{2+}-containing calixarene literature (*sym* 904-877 and a*sym* 879-831 cm^{-1})[110] as well as those of noncalixarene Mo dioxo aryloxide MoO_2(O-2,6-*t*-$Bu_2C_6H_3)_2$·HO-2,6-*t*-$Bu_2C_6H_3$ (898, 884 cm^{-1})[184] but lower than the Mo dioxo alkoxides (947-945, 927-881 cm^{-1}).[183] The observed values for complexes **6.7 – 6.12** are close to the values observed in compounds **4.1-3** (918-907, 886-883 cm^{-1}), **4.5a-c** (917-914, 886-879 cm^{-1}) and for bipy or phen-ligated organomolybdenum(VI) dioxo complexes[159] (934-892, 914-871 cm^{-1}) and MoO_2Cl_2 (915, 864 cm^{-1}) (Table 6.5). No significant changes were observed for the ν(C=O), ν(C=C) and ν(-CH_3) of methyl ketone from the acac ligand compared with those values in the starting $MoO_2(acac)_2$.

Table 6.5 Principal Infrared frequencies (cm^{-1}) of compounds **6.7** to **6.12** in KBr pellets, with comparative values from literature.

Compound	ν(O-*H)*	ν(C=O); ν(C=C)	ν(C-O)	ν(-CH_3)*	ν(Mo=O)
MoO_2Cl_2	-	-	-	-	915, 864
$MoO_2(L)Y_2$[159]	-	-	-	-	934-892, 914-871
$MoO_2(bipy)Cl_2$[171]	-	-	-	-	930, 908
$MoO_2(OR)_2$[183]	-	-	-	-	947-945, 927-881
$MoO_2(OPh_2)_2$[183]	-	-	1264	-	962, 875
$MoO_2(OPh_2)_2 \cdot Py_2$[183]	-	-	1249	-	932, 904
$MoO_2(OAr)_2$[184]	-	-	1264	-	898, 884
MoO_2-calix[4]arene[110]	-	-	1283-1262		904-877, 879-831
$MoO_2(acac)_2$	-	1591; 1510	1265	1362	935, 906
4.1	3433, 3296	-	1293	-	918, 885
4.2	3402, 3296	-	1295	-	907, 886
4.3	3433, 3307		1293	-	914, 883
4.5a	3411, 3263	1602, 1523	1296	1363	917, 879
4.5b	3413, 3294	1596, 1527	1295	1362	914, 883
4.5c	3475	1596, 1528	1294	1364	914, 886
6.7	3423	1604; 1523	1296; 1267	1362	915, 888
6.8	3421	1615; 1522	1299; 1266	1362	915, 886
6.9	3434	1604; 1522	1296; 1267	1362	916, 894
6.10	3435	1605; 1522	1297; 1264	1362	916, 887
6.11	3450	1615; 1522	1299; 1266	1362	916, 886
6.12	3444	1605; 1521	1297; 1264	1362	917, 891

*Characteristic -CH_3 of methyl ketone.[185] R = -Me, -Et, -^{n}Pr.[183] Ar = O-2,6-^{t}$Bu_2C_6H_3$.[184] L = N-heterocyclic ligand, Y = alkyl group, see reference.[159]

^{1}H NMR spectroscopy was the primary identification tool of the products **6.7** – **6.12**. ^{1}H NMR spectra can give information about the conformational behavior and symmetry adopted by the calix[5]arene framework in the product.[30]

In general the compounds **6.7** – **6.12** exhibit a ^{1}H NMR pattern characteristic of an asymmetric conformation[30] of the calix[5]arene framework. A summary of the proton chemical shifts of compounds **6.7** to **6.12** is presented in Table 6.6.

Table 6.6 Chemical shifts (ppm) of compounds **6.7** to **6.12** in $CDCl_3$.

Compound	O*H*	Ar-H_L	Ar-H_{cx}	$H^{\cdots}$Pd*	Ar-CH_2-Ar 10 doublets	acac$^-$ (C*H*); CH_3	^{t}Bu (1:1:1:1:1 ratio)
bipy							
6.7	9.63	9.38-7.13 (8 signals)	7.26-6.26 (8 signals)	6.64	6.64-3.11	(5.02); 1.46; 1.32	1.40-0.85
6.10	9.30	9.39-7.13 (8 signals)	7.31-6.43 (9 signals)	6.70	6.70-3.07	(5.00); 1.45; 1.31	1.41-0.89
(4-Me)2bipy							
6.8	9.84	9.60-6.61 -Me: 2.86, 2.58 (6 aromatic signals)	7.33-6.17 (9 signals)	7.23	7.23-3.02	(4.98); 1.63; 1.49	1.40-0.78
6.11	9.66	9.66-6.62 -Me: 2.86, 2.56 (6 aromatic signals)	7.28-6.35 (8 signals)	7.21	7.21-2.99	(4.96); 1.62; 1.47	1.41-0.84
phen							
6.9	9.84	8.92-7.98 (4 signals)	7.28-6.25 (~9 signals)	6.87	6.87-3.08	(4.94); 1.48; 1.04	1.37-0.85
6.12	9.56	8.93-7.98 (4 signals)	7.36-6.40 (~8 signals)	6.93	6.93-3.04	(4.90); 1.47; 1.02	1.38-0.88

* δ $H^{\cdots}$Pd in ppm in **5.1c** = 6.49; **5.1d** = 6.54; **5.2c** = 6.62; **5.2d** = 6.61; **5.3c** = 6.55; **5.3d** = 6.63.

Reaction between $MoO_2(acac)_2$ and complexes **5.1c-d**, **5.2c-d**, and **5.3c-d** affected the overall symmetry of the calix[5]arene ligand due to the attachment of the second transition metal. This change is reflected in the resonances of the Ar-*H*, Ar-CH_2-Ar and ^{t}Bu protons of the calix[5]arene ligand (Figure 6.13).

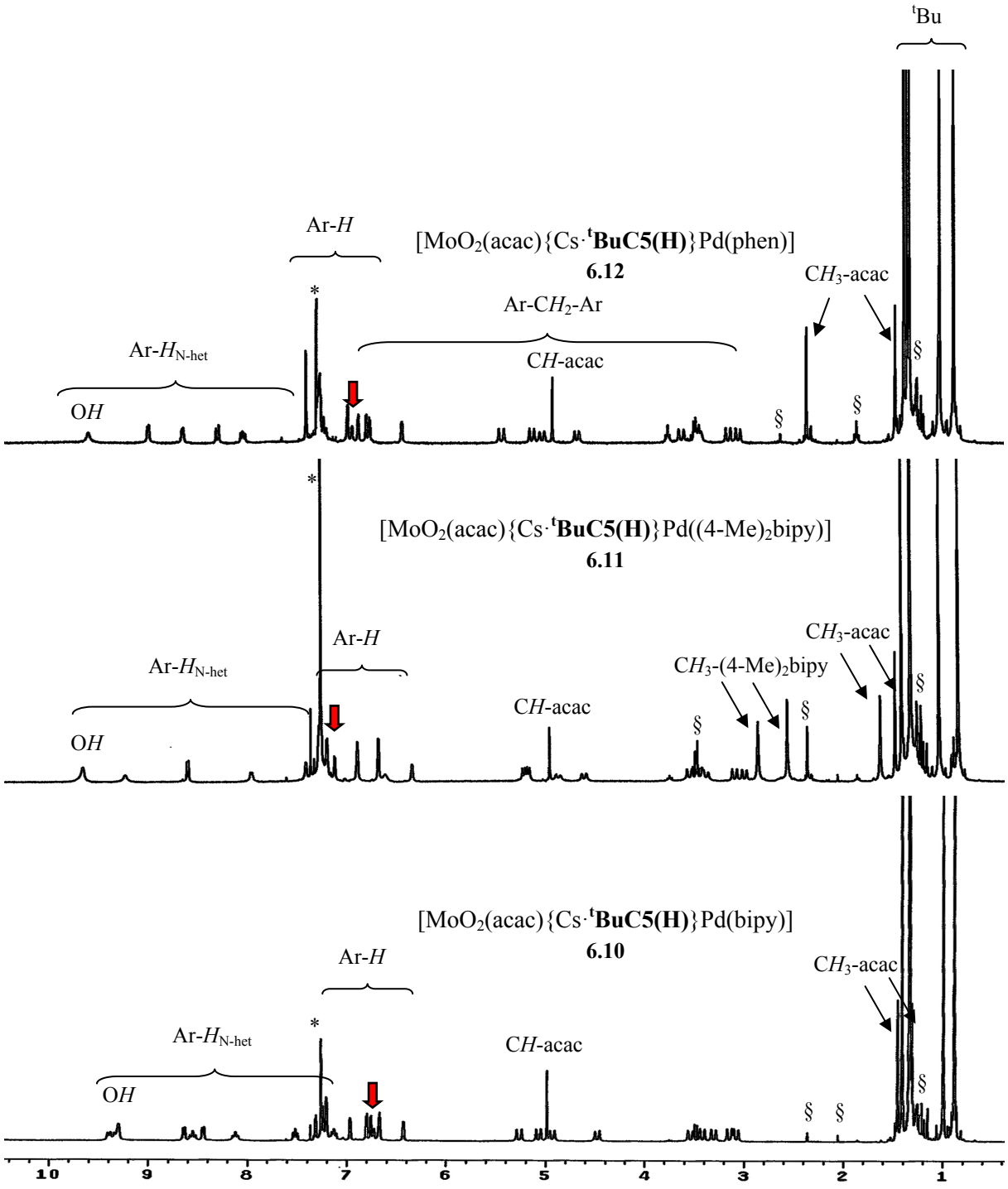

Figure 6.13 ^{1}H NMR spectra of complexes **6.10 – 6.12** in *$CDCl_3$. The arrow highlights the methylene Pd···H interaction proton. § = impurities or residual solvent.

The aromatic proton resonances (Ar-*H*) from the calix[5]arene in complexes **6.7** – **6.12** are found in the range of 7.36 to 6.17 ppm as a set of ten doublets (with some overlap) with a $^4J_{HH}$ = ~2.5 Hz.

Complexes **6.7** – **6.12** all exhibit five pairs of doublets for the methylene protons (1:1:1:1:1 ratio) resulting in 10 doublets; nine of the doublets can be observed in the range of 5.41 to 2.99 ppm. The remaining methylene resonances are found in the range of 7.23 to 6.64 ppm. These downfield methylene resonances display a variation in the chemical shift with respect to the starting complexes **5.1c-d, 5.2c-d, 5.3c-d** (see Table 6.7). This chemical shift variation suggests that the Pd···*H* interaction is stronger, resulting in a downfield movement. These NMR shifts also suggest that the boat-boat conformation is retained in the palladium-containing heterocycle (this Pd···*H* interaction was discussed in Chapter 5).

Table 6.7 Comparative chemical shifts (ppm) of the aromatic, methylene and *tert*-butyl area of compounds **6.7** to **6.12** with starting material and normal values found in literature.

Compound	Ar-H_{cx}	H···Pd*	Ar-CH_2-Ar	^{t}Bu
Literature value*	7.62-6.92	-	4.88-3.21	1.38-1.10
[{MeOH·K·**^{t}BuC5(H)**}-μ-O-[Ti(acac)]$_2${THF·K·**^{t}BuC5(H)$_3$**}]*	7.48-6.48	-	5.54-2.96	1.33-0.78
5.1c-d, 5.2c-d, 5.3c-d	7.17-6.89	6.63-6.49	6.63-3.16	1.30-1.11
6.1-6.6	6.70-5.43	-	5.29-1.07	1.23-0.76
6.7-6.12	7.36-6.17	7.23-6.64	7.23-2.99	1.41-0.78

* Data taken from metallocalix[5]arene compounds from Table 6.2

The resonances of the *tert*-butyl groups in complexes **6.7 - 6.12** are observed in the range of 1.41 to 0.78 ppm as a set of five singlets (1:1:1:1:1 ratio), and finally the O*H* group resonances are found in the range of 9.84 – 9.30 ppm.

The ^{1}H NMR spectra of the compounds **6.7** – **6.12** display three new signals corresponding to the acac ligand. The acac C*H* resonance (4.90 – 5.02 ppm) does not show a significant change between compounds **6.7** – **6.12**. Compounds **6.8** and **6.11** have the most downfield acac CH_3 resonances (~1.63 ppm, see Table 6.6), while compounds **6.9** and **6.12** have the most upfield ones (~1.03 ppm). It is not clear whether these differences are related to the electronic or steric properties of the (4-Me)$_2$bipy (**6.8**, **6.11**) and phenanthroline (**6.9**, **6.12**) ligands.

In the ^{1}H NMR spectra (see Figure 6.13), complexes **6.7, 6.8**, **6.10** and **6.11** indicate an asymmetric environment for the N-heterocyclic ligand due to the coordination of the molybdenum atom attached to the lower rim of the calix[5]arene ligand. The coordination of the molybdenum atom makes the pyridyl rings magnetically non-equivalent resulting in eight signals for eight different pyridyl protons in **6.7** and **6.10** (9.39 – 7.13 ppm) and six signals for the (4-Me)$_2$bipy aromatic protons in **6.8** and **6.11** (9.66 – 6.61 ppm). In the case of **6.9** and **6.12** complexes just four signals of the phen are observed in the 8.93 – 7.98 ppm range. We propose that this behavior is due to the restricted rotation of the pyridyl rings in the phen ligand compared to that in bipy and (4-Me)$_2$bipy (Figure 6.14). The bipy and (4-Me)$_2$bipy ligands can lose planarity upon Mo coordination resulting in a puckered 5-membered ring (asymmetric), but the phen ligand does not have that capability.

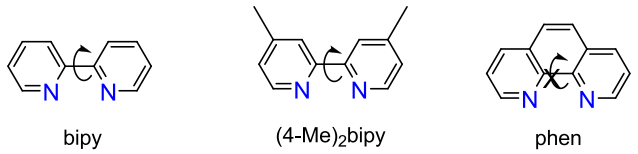

Figure 6.14 Proposed restricted rotation of the pyridyl rings in phen.

6.2.2.1.1. Conformational analysis and symmetry

Figures 6.15 and 6.16 show the changes that occur in the ^{1}H NMR spectra of **^{t}BuC5(H)$_5$**, Cs$_2$·**^{t}BuC5(H)$_2$**, [Pd(bipy){Cs·**^{t}BuC5(H)$_2$**}] **5.1d** and [MoO$_2$(acac){Cs·**^{t}BuC5(H)**}Pd(bipy)] **6.10**. Figures 6.15 and 6.16 illustrate how the symmetry around the calixarene framework (Ar-*H*, Ar-C*H*$_2$-Ar and ^{t}Bu groups) changes from the parent calix[5]arene through the formation of the trimetallic product.

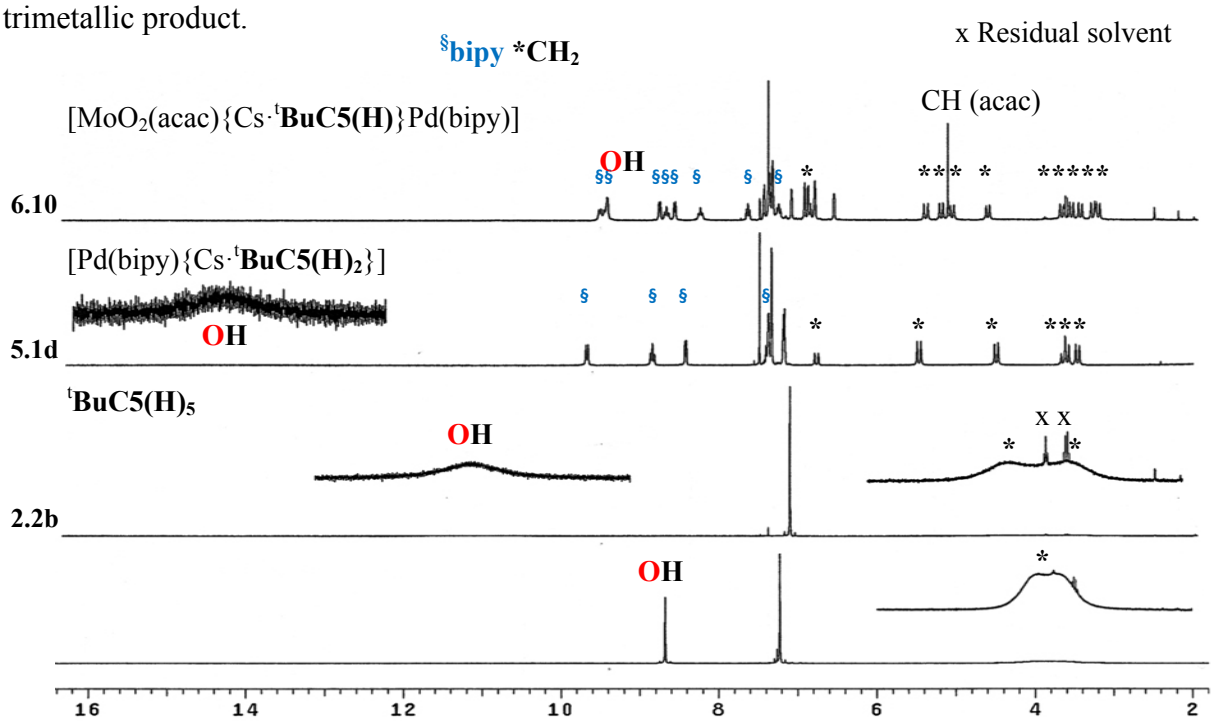

Figure 6.15 ^{1}H NMR spectra displaying the variation in the chemical shift behavior from **^{t}BuC5(H)$_5$** to [MoO$_2$(acac){**Cs·^{t}BuC5(H)**}Pd(bipy)] **6.10**, from the OH to the Ar-CH$_2$-Ar regions.

The ^{1}H NMR spectrum of the parent calix[5]arene gives a singlet for the O*H* group (8.66 ppm, 5H), a singlet for the Ar-*H* (7.21 ppm, 10H), a broad signal for the Ar-CH_2-Ar (3.80 ppm, 10H) and a singlet for the *tert*-butyl group (1.26 ppm, 45H). This ^{1}H NMR pattern is characteristic of a cone conformation with C_{5v} symmetry.

Only a small change is observed in the ^{1}H NMR spectrum when the parent calix[5]arene is converted to its dicesium salt. In compound Cs_2·**^{t}BuC5(H)$_2$** the calix[5]arene adopts a cone conformation with a C_{5v} symmetry in solution, on average. For both parent **^{t}BuC5(H)$_5$** and Cs_2·**^{t}BuC5(H)$_2$** the broadness of the methylene peaks indicates fluxional behavior.

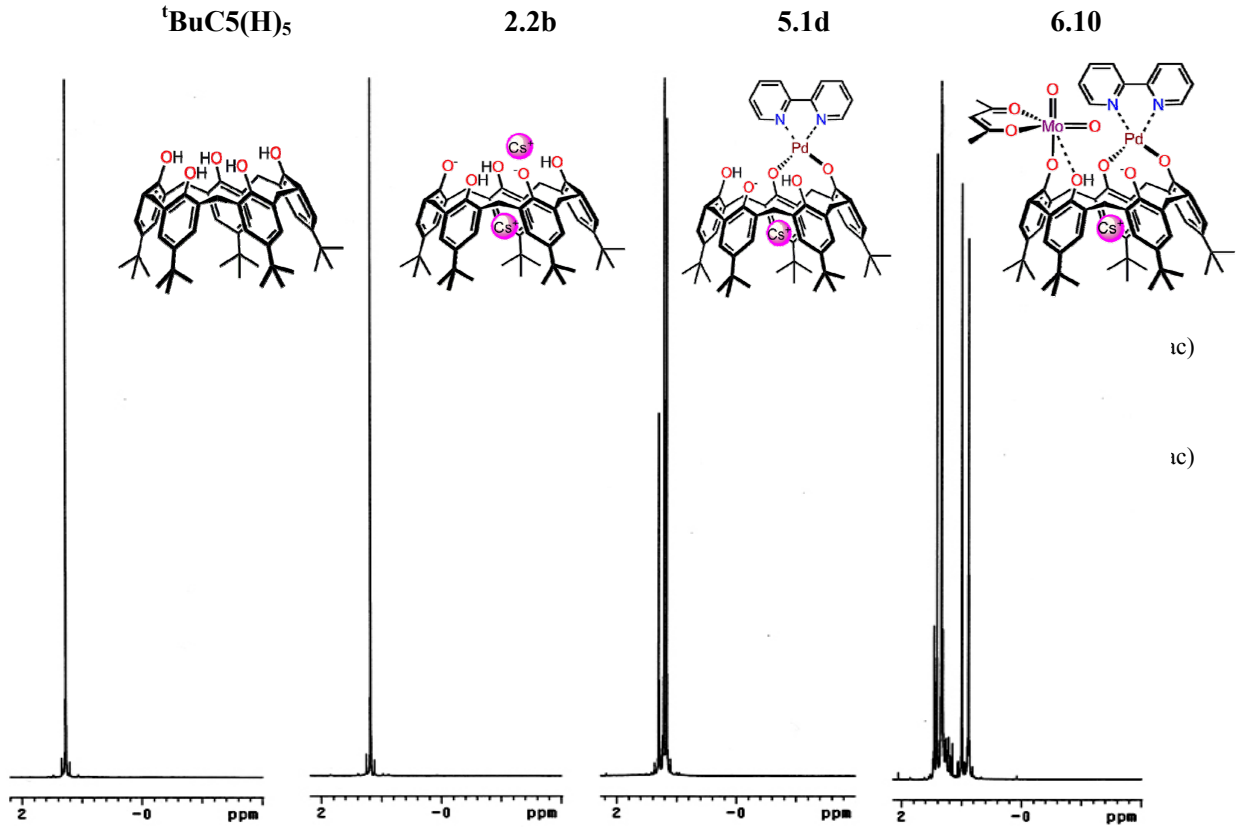

Figure 6.16 ^{1}H NMR spectra of the *tert*-butyl area displaying the variation in the chemical shift behavior from **^{t}BuC5(H)$_5$** to [MoO_2(acac){**Cs·^{t}BuC5(H)**}Pd(bipy)] **6.10**. *Impurity.

In contrast, in the [Pd(bipy){Cs·^{t}**BuC5(H)$_2$**}] (**5.1d**) ^{1}H NMR spectrum, four signals associated with the bipy aromatic protons (2:2:2:2 ratio), three singlets in the aromatic region (4:2:4 ratio), three pairs of methylene doublets (1:2:2 ratio), and three singlets for the ^{t}Bu groups (9:18:18 ratio) are observed. The overall ^{1}H NMR pattern suggests that a mirror plane crosses the molecule, consistent with a cone conformation with C_s symmetry adopted by the calix[5]arene ligand (Figure 6.17).[30] In compound [Pd(bipy){Cs·^{t}**BuC5(H)$_2$**}] **5.1d**, as well as the Mo/Pd one [MoO_2(acac){Cs·^{t}**BuC5(H)**}Pd(bipy)] **6.10**, all peaks are sharp, indicating no fluxional behavior.

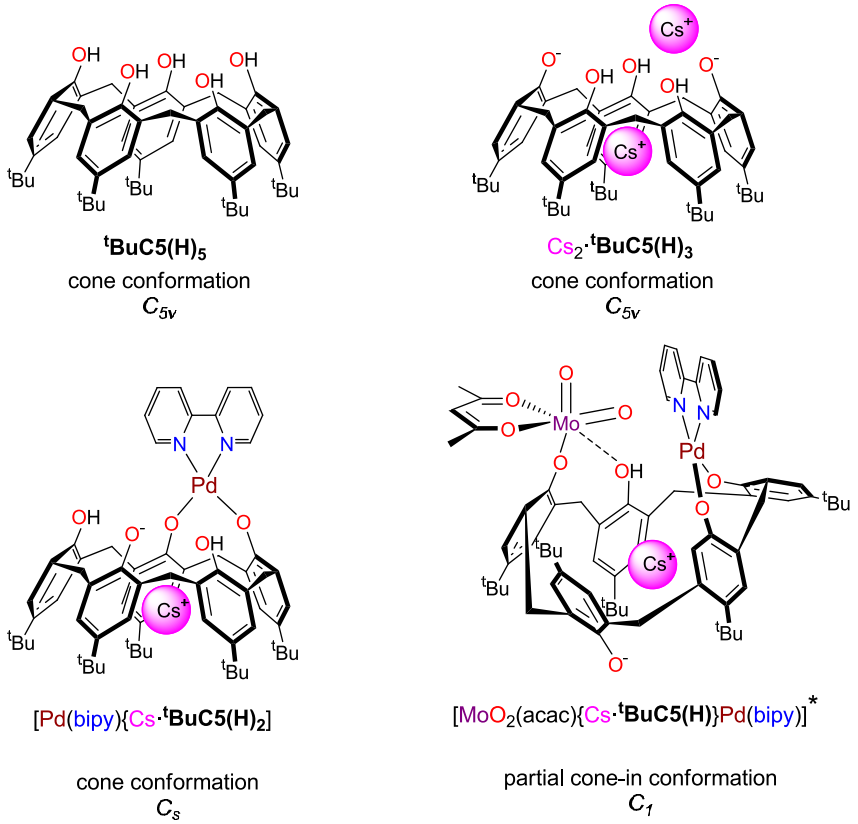

Figure 6.17 Conformation and symmetry adopted by the calix[5]arene ligand in ^{t}**BuC5(H)$_5$**, Cs$_2$·^{t}**BuC5(H)$_3$ 2.2b**, [Pd(bipy){Cs·^{t}**BuC5(H)$_2$**}] **5.1d** and [MoO_2(acac){Cs·^{t}**BuC5(H)**}Pd(bipy)] **6.10**. * Proposed structure.

Finally, the ^{1}H NMR spectrum of the product [MoO_2(acac){**Cs·^{t}BuC5(H)**}Pd(bipy)] **6.10** is consistent with C_1 symmetry corresponding to a partial cone-in conformer; an asymmetric conformation (Figure 6.17).[30] In this kind of symmetry the predicted ^{1}H NMR pattern shows five pairs of doublets (1:1:1:1:1 ratio) for the aromatic region (Ar-*H*), five pairs of doublets (1:1:1:1:1 ratio) in the methylene area (Ar-CH_2-Ar), and finally five singlets (1:1:1:1:1 ratio) in the *tert*-butyl area (see Figure 6.16).[30]

The conformation and symmetry adopted in solution for the calix[5]arene ligands in **^{t}BuC5(H)$_5$**, Cs_2·**^{t}BuC5(H)$_2$ 2.2b**, [Pd(bipy){Cs·**^{t}BuC5(H)$_2$**}] **5.1d** and [MoO_2(acac){Cs·**^{t}BuC5(H)**}Pd(bipy)] **6.10** are summarized and shown in Figure 6.17.

6.3 Experimental Section

6.3.1 General Information

Unless otherwise noted, all manipulations were carried out in a dry nitrogen filled glove box. [Pd(L){M·**^{t}BuC5(H)$_2$**}] (M = Rb, Cs; L = bipy **5.1c-d**, (4-Me)$_2$bipy **5.2c-d** and phen **5.3c-d**) were prepared from the procedure described in Chapter 5 and were left in the oven overnight before use (100 ^{o}C). Dioxobis(2,4-pentanedionato)molybdenum(VI), (MoO_2(acac)$_2$), was prepared using a literature procedure.[186] Tetrakis(diethylamino)titanium(IV) (Ti(NEt$_2$)$_4$) was purchased from Aldrich and was used as received. The melting points of all compounds were taken in capillary tubes on a Mel-Temp apparatus (Laboratory Devices, Cambridge, MA). A temperature proceeded by a “>” sign indicates that the compound starts to decompose at that temperature without melting. ^{1}H NMR and ^{13}C NMR spectra were recorded on a Varian XL-300 spectrometer at 300 and 75 MHz, respectively. Deuterated chloroform ($CDCl_3$) was dried over CaH_2 and was referenced to 7.26 ppm and 77.2 ppm for ^{1}H and ^{13}C NMR, respectively.

Microanalyses were performed by Atlantic Microlab, Inc, Norcross, GA. IR and UV/Vis spectra were obtained with an Infinity Gold™ FTIR spectrometer and Agilent 8453 spectrophotometer, respectively. All solvents were anhydrous and were stored over molecular sieves for one day before use.

6.3.2 Synthesis of complexes

*6.3.2.1 General procedure for the synthesis of Ti[(L)Pd{M·^{t}BuC5}]$_2$ (L = bipy, (4-Me)$_2$bipy, 1,10-phen, M = Rb, Cs) (**6.1-6.6**)*

All Ti/Pd calix[5]arene complexes were prepared following a similar procedure as follows:

Ti[Pd(bipy){Rb·**^{t}BuC5**}]$_2$ **(6.1)**: To a solution of [Pd(bipy){Rb·**^{t}BuC5(H)$_2$**}] **5.1c** (0.0580 g, 0.0501 mmol) in benzene (10.0 mL) was added a solution of Ti(NEt$_2$)$_4$ (0.0253 g, 0.0752 mmol) in benzene (3.0 mL). The reaction mixture was allowed to stir 12 hrs at room temperature. The resulting suspension was centrifuged for 20 min. The solid was recovered and was left to stir with 5.0 mL of benzene, then centrifuged one more time. The solid was recovered and vacuum dried affording **6.1** as an orange solid (0.0511 g, 0.0217 mmol, 87% yield). Mp: > 315 ^{o}C. ^{1}H NMR (CDCl$_3$) δ (ppm): 9.39 (d, 4H, *J* = 4.7 Hz, bipy), 7.92 (dd, 4H, *J* = 7.7, 6.3 Hz, bipy), 7.67 (dd, 4H, *J* = 5.8, 6.6 Hz, bipy), 7.35 (d, 4H, *J* = 7.7 Hz, bipy), 6.67 (d, 4H, *J* = 2.8 Hz, Ar-*H*), 6.57 (d, 4H, *J* = 2.5 Hz, Ar-*H*), 6.27 (d, 4H, *J* = 2.5 Hz, Ar-*H*), 6.21 (s, 4H, Ar-*H*), 5.43 (d, 4H, *J* = 2.5 Hz, Ar-*H*), 5.17 (d, 4H, *J* = 16.5 Hz, Ar-C*H*$_2$-Ar), 4.60 (d, 2H, *J* = 11.0 Hz, Ar-C*H*$_2$-Ar), 4.58 (d, 4H, *J* = 12.9 Hz, Ar-C*H*$_2$-Ar), 3.09 (d, 4H, *J* = 16.2 Hz, Ar-C*H*$_2$-Ar), 2.86 (d, 2H, *J* = 11.5 Hz, Ar-C*H*$_2$-Ar), 1.39 (d, 4H, *J* = 13.5 Hz, Ar-C*H*$_2$-Ar), 1.19 (s, 36H, ^{t}Bu), 1.07 (s, 18H, ^{t}Bu), 0.79 (s, 36H, ^{t}Bu). No ^{13}C{^{1}H} NMR was obtained due to sample precipitation

during the collection time. FTIR (KBr, cm^{-1}): 3437b (OH, from water), 3045w, 2953vs, 2903s, 2864s, 1621m, 1606m, 1478s, 1463vs, 1456vs, 1392w, 1361m, 1296s, 1260s, 1208s, 1123m, 880w, 827m, 757s, 535w. UV/vis $\lambda_{max/nm}$ ($CHCl_3$) ($\varepsilon/dm^3\ mol^{-1}\ cm^{-1}$): 255 (4.18 x 10^4), 249 (4.17 x 10^4), 261 (4.06 x 10^4), 312 (1.66 x 10^4), 401 (1.14 x 10^4). E. A. for $C_{130}H_{146}N_4O_{10}Pd_2Rb_2Ti{\cdot}C_6H_6$ calc(found): C: 67.10 (67.17); H: 6.29 (6.50).

Ti[Pd((4-Me)$_2$bipy){Rb·^{t}**BuC5**}]$_2$ **(6.2)**: ([Pd((4-Me)$_2$bipy){Rb·^{t}**BuC5(H)$_2$**}] **5.2c**: 0.0593 g, 0.0501 mmol; $Ti(NEt_2)_4$: 0.0256 g, 0.0761 mmol). **6.2** was obtained as a yellow-orange solid (0.0484 g, 0.0201 mmol, 80% yield). Mp: > 328 ^oC. ^1H NMR ($CDCl_3$) δ (ppm): 9.19 (d, 4H, *J* = 5.8 Hz, (4-Me)$_2$bipy), 7.49 (d, 4H, *J* = 6.1 Hz, (4-Me)$_2$bipy), 7.12 (s, 4H, (4-Me)$_2$bipy), 6.67 (d, 4H, *J* = 2.8 Hz, Ar-*H*), 6.57 (d, 4H, *J* = 2.5 Hz, Ar-*H*), 6.28 (d, 4H, *J* = 2.5 Hz, Ar-*H*), 6.20 (s, 4H, Ar-*H*), 5.43 (d, 4H, *J* = 2.5 Hz, Ar-*H*), 5.14 (d, 4H, *J* = 16.8 Hz, Ar-C*H*$_2$-Ar), 4.62 (d, 2H, *J* = 11.3 Hz, Ar-C*H*$_2$-Ar), 4.57 (d, 4H, *J* = 14.6 Hz, Ar-C*H*$_2$-Ar), 3.10 (d, 4H, *J* = 16.5 Hz, Ar-C*H*$_2$-Ar), 2.85 (d, 2H, *J* = 11.3 Hz, Ar-C*H*$_2$-Ar), 2.57 (s, 12H, (4-Me)$_2$bipy), 1.35 (d, 4H, *J* = 13.5 Hz, Ar-C*H*$_2$-Ar), 1.19 (s, 36H, ^{t}Bu), 1.09 (s, 18H, ^{t}Bu), 0.80 (s, 36H, ^{t}Bu). $^{13}C\{^1H\}$ NMR ($CDCl_3$) δ (ppm): 166.3, 159.3, 157.7, 155.1, 150.0, 146.9, 138.45, 138.38, 138.1, 136.4, 136.1, 133.5, 131.2, 128.5 (residual C_6H_6), 126.7, 126.5, 126.3, 123.9, 122.3, 121.7, 121.5, 120.8 (aromatic carbons), 36.1, 34.1 (*C*(CH_3)$_3$), 33.8, 33.5 (Ar-*C*H$_2$-Ar), 33.2 (*C*(CH_3)$_3$), 32.8, 32.1, 31.8 (C(*C*H$_3$)$_3$), 21.8 (*C*H$_3$, (4-Me)$_2$bipy). FTIR (KBr, cm^{-1}): 3438b,s (OH, from water), 3045w, 3016w, 2954vs, 2904s, 2866m, 1622s, 1479vs, 1456vs, 1392w, 1361m, 1296s, 1261s, 1207s, 1126m, 1034w, 920w, 879m, 827s, 800w, 758m, 569w, 538m. UV/vis $\lambda_{max/nm}$ ($CHCl_3$) ($\varepsilon/dm^3\ mol^{-1}\ cm^{-1}$): 247 (3.86 x 10^4), 252 (3.86 x 10^4), 257 (3.76 x 10^4), 310 (1.63 x 10^4), 400 (7.71 x 10^3).

Ti[Pd(phen){Rb·^{t}**BuC5**}]$_2$ **(6.3)**: ([Pd(phen){Rb·^{t}**BuC5(H)$_2$**}] **5.3c**: 0.0592 g, 0.0502 mmol; Ti(NEt$_2$)$_4$: 0.0253 g, 0.0752 mmol). **6.3** was obtained as a red solid (0.0446 g, 0.0185 mmol, 74% yield). Mp: > 300 ^{o}C. ^{1}H NMR (CDCl$_3$) δ (ppm): 9.54 (d, 4H, *J* = 3.9 Hz, phen), 8.35 (d, 4H, *J* = 7.2 Hz, phen), 7.92 (dd, 4H, *J* = 5.0, 8.0 Hz, phen), 7.77 (s, 4H, phen), 6.66 (d, 4H, *J* = 2.5 Hz, Ar-*H*), 6.57 (d, 4H, *J* = 2.8 Hz, Ar-*H*), 6.18 (d, 4H, *J* = 2.5 Hz, Ar-*H*), 5.71 (s, 4H, Ar-*H*), 5.44 (d, 4H, *J* = 2.2 Hz, Ar-*H*), 5.29 (d, 4H, *J* = 16.8 Hz, Ar-C*H*$_2$-Ar), 4.67 (d, 2H, *J* = 11.3 Hz, Ar-C*H*$_2$-Ar), 4.62 (d, 4H, *J* = 12.9 Hz, Ar-C*H*$_2$-Ar), 3.64 (d, 4H, *J* = 16.8 Hz, Ar-C*H*$_2$-Ar), 3.36 (d, 2H, *J* = 11.0 Hz, Ar-C*H*$_2$-Ar), 1.23 (s, 36H, ^{t}Bu), 1.09 (d, 4H, *J* = 12.4 Hz, Ar-C*H*$_2$-Ar), 0.88 (s, 18H, ^{t}Bu), 0.76 (s, 36H, ^{t}Bu). Unknown peaks at 1.49, 1.45, 1.31 and 1.29 ppm are probably impurities or residual solvent. No integration was performed in the ^{1}H NMR spectrum of **6.3**. However, the number of protons reported is based on compound **6.6** due to similarity. No ^{13}C{^{1}H} NMR was obtained due to sample precipitation during the collection time. FTIR (KBr, cm^{-1}): 3437b,s (OH, from water), 3080w, 3045w, 3016w, 2955vs, 2903s, 2866m, 1635m, 1479vs, 1459vs, 1430m, 1413w, 1392w, 1361m, 1296s, 1208s, 1127w, 916w, 880w, 841m, 827m, 800w, 760w, 716m, 675w, 539m. UV/vis $\lambda_{max/nm}$ (CHCl$_3$) (ε/dm^3 mol^{-1} cm^{-1}): 242 (6.52 x 10^4), 272 (5.97 x 10^4), 367 (1.06 x 10^4).

Ti[Pd(bipy){Cs·^{t}**BuC5**}]$_2$ **(6.4)**: ([Pd(bipy){Cs·^{t}**BuC5(H)$_2$**}] **5.1d**: 0.0604 g, 0.0501 mmol; Ti(NEt$_2$)$_4$: 0.0252 g, 0.0749 mmol). **6.4** was obtained as an orange solid (0.0543 g, 0.0221 mmol, 88% yield). Mp: > 323 ^{o}C. ^{1}H NMR (CDCl$_3$) δ (ppm): 9.39 (d, 4H, *J* = 4.4 Hz, bipy), 7.92 (ddd, 4H, *J* = 7.7, 8.0, 1.1 Hz, bipy), 7.66 (dd, 4H, *J* = 6.1, 6.3 Hz, bipy), 7.35 (d, 4H, *J* = 8.5 Hz, bipy), 6.70 (d, 4H, *J* = 2.5 Hz, Ar-*H*), 6.61 (d, 4H, *J* = 2.5 Hz, Ar-*H*), 6.27 (d, 4H, *J* = 2.5 Hz, Ar-*H*), 6.17 (s, 4H, Ar-*H*), 5.56 (d, 4H, *J* = 2.5 Hz, Ar-*H*), 5.17 (d, 4H, *J* = 16.5 Hz, Ar-

CH_2-Ar), 4.61 (d, 6H, J = 12.4 Hz, Ar-CH_2-Ar), 3.12 (d, 4H, J = 16.2 Hz, Ar-CH_2-Ar), 2.82 (d, 2H, J = 11.3 Hz, Ar-CH_2-Ar), 1.36 (d, 4H, J = 13.2 Hz, Ar-CH_2-Ar), 1.20 (s, 36H, ^{t}Bu), 1.06 (s, 18H, ^{t}Bu), 0.81 (s, 36H, ^{t}Bu). No $^{13}C\{^1H\}$ NMR was obtained due to sample precipitation during the collection time. FTIR (KBr, cm^{-1}): 3437b,s (OH, from water), 3044w, 3015w, 2955vs, 2904s, 2865m, 1607w, 1478s, 1465vs, 1459vs, 1393w, 1361m, 1297s, 1261m, 1208s, 1125w, 880w, 828w, 759m, 676w, 540w. UV/vis $\lambda_{max/nm}$ ($CHCl_3$) (ε/dm^3 mol^{-1} cm^{-1}): 260 (4.88 x 10^4), 311 (1.88 x 10^4), 388 (1.54 x 10^4).

Ti[Pd((4-Me)$_2$bipy){Cs·^{t}**BuC5**}]$_2$ **(6.5)**: ([Pd((4-Me)$_2$bipy){Cs·^{t}**BuC5(H)$_2$**}] **5.2d**: 0.0617 g, 0.0501 mmol; Ti(NEt$_2$)$_4$: 0.0252 g, 0.0749 mmol). **6.5** was obtained as a yellow solid (0.0577 g, 0.0230 mmol, 92% yield). Mp: > 335 ^{o}C. ^{1}H NMR ($CDCl_3$) δ (ppm): 9.19 (d, 4H, J = 5.8 Hz, (4-Me)$_2$bipy), 7.48 (d, 4H, J = 5.5 Hz, (4-Me)$_2$bipy), 7.11 (s, 4H, (4-Me)$_2$bipy), 6.70 (d, 4H, J = 2.5 Hz, Ar-H), 6.60 (d, 4H, J = 2.5 Hz, Ar-H), 6.28 (d, 4H, J = 2.8 Hz, Ar-H), 6.17 (s, 4H, Ar-H), 5.55 (d, 4H, J = 2.5 Hz, Ar-H), 5.14 (d, 4H, J = 16.5 Hz, Ar-CH_2-Ar), 4.62 (d, 2H, J = 11.0 Hz, Ar-CH_2-Ar), 4.59 (d, 4H, J = 12.9 Hz, Ar-CH_2-Ar), 3.12 (d, 4H, J = 16.5 Hz, Ar-CH_2-Ar), 2.81 (d, 2H, J = 11.3 Hz, Ar-CH_2-Ar), 2.57 (s, 12H, (4-Me)$_2$bipy), 1.33 (d, 4H, J = 13.8 Hz, Ar-CH_2-Ar), 1.20 (s, 36H, ^{t}Bu), 1.08 (s, 18H, ^{t}Bu), 0.82 (s, 36H, ^{t}Bu). $^{13}C\{^1H\}$ NMR ($CDCl_3$) δ (ppm): 166.6, 159.3, 158.5, 155.1, 150.0, 146.9, 139.4, 137.8, 133.8, 131.3, 126.8, 126.6, 126.3, 123.9, 122.3, 121.7, 121.3 (aromatic carbons), 36.1, 33.9 (C(CH$_3$)$_3$), 33.8 (Ar-CH$_2$-Ar), 33.5 (C(CH$_3$)$_3$), 32.8 (Ar-CH$_2$-Ar), 32.1(C(CH$_3$)$_3$), 32.0 (Ar-CH$_2$-Ar), 31.7 (C(CH$_3$)$_3$), 21.8 (CH$_3$, (4-Me)$_2$bipy). FTIR (KBr, cm^{-1}): 3438b,s (OH, from water), 3043w, 2956vs, 2903s, 2865m, 1621s, 1478vs, 1459vs, 1392m, 1361s, 1297s, 1262s, 1208s, 1126m, 1036w, 921w,

880m, 828s, 801w, 759m, 676w, 539m. UV/vis $\lambda_{max/nm}$ ($CHCl_3$) (ε/dm^3 mol^{-1} cm^{-1}): 259 (4.44 x 10^4), 345 (1.24 x 10^4), 392 (1.19 x 10^4), 489 (2.28 x 10^3).

Ti[Pd(phen){Cs·^{t}**BuC5**}]$_2$ **(6.6)**: ([Pd(phen){Cs·^{t}**BuC5(H)$_2$**}] **5.3d**: 0.0615 g, 0.0501 mmol; $Ti(NEt_2)_4$: 0.0253 g, 0.0752 mmol). **6.6** was obtained as a red solid (0.0438 g, 0.0175 mmol, 70% yield). Mp: > 349 ^oC. ^1H NMR ($CDCl_3$) δ (ppm): 9.54 (d, 4H, *J* = 4.9 Hz, phen), 8.35 (d, 4H, *J* = 8.0 Hz, phen), 7.92 (dd, 4H, *J* = 8.0, 5.2 Hz, phen), 7.77 (s, 4H, phen), 6.69 (d, 4H, *J* = 2.2 Hz, Ar-*H*), 6.61 (d, 4H, *J* = 2.5 Hz, Ar-*H*), 6.18 (d, 4H, *J* = 2.5 Hz, Ar-*H*), 5.68 (s, 4H, Ar-*H*), 5.55 (d, 4H, *J* = 2.5 Hz, Ar-*H*), 5.29 (d, 4H, *J* = 16.5 Hz, Ar-CH_2-Ar), 4.67 (d, 2H, *J* = 11.3 Hz, Ar-CH_2-Ar), 4.65 (d, 4H, *J* = 13.5 Hz, Ar-CH_2-Ar), 3.16 (d, 4H, *J* = 15.9 Hz, Ar-CH_2-Ar), 2.81 (d, 2H, *J* = 11.5 Hz, Ar-CH_2-Ar), 1.23 (s, 39H,* ^{t}Bu), 1.07 (d, 4H, *J* = 13.2 Hz, Ar-CH_2-Ar), 0.87 (s, 19H,* ^{t}Bu), 0.78 (s, 38H,* ^{t}Bu). *The integral value reported for the compound is not consistent with the value required. This disagreement in value could be due to overlapping with solvent or impurities. Unknown peaks at 1.49, 1.45, 1.31, 1.29, 1.27 ppm are probably impurities or residual solvent. No $^{13}C\{^1H\}$ NMR was performed due to sample precipitation during the collection time. FTIR (KBr, cm^{-1}): 3437b,s (OH, from water), 3080w, 3051w, 2954vs, 2903m, 2865m, 1630m, 1516w, 1479vs, 1459vs, 1426m, 1413w, 1392w, 1361m, 1297s, 1208s, 1127w, 916w, 881m, 841m, 828w, 759w, 716w, 539w. UV/vis $\lambda_{max/nm}$ ($CHCl_3$) (ε/dm^3 mol^{-1} cm^{-1}): 257 (5.38 x 10^4), 269 (5.35 x 10^4), 344 (1.45 x 10^4), 405 (1.25 x 10^4).

*6.3.2.2 General procedure for the synthesis of [MoO_2(acac){M·**^{t}BuC5(H)**}Pd(L)] (L = bipy, (4-Me)$_2$bipy, 1,10-phen, M = Rb, Cs) (**6.7-6.12**)*

All Mo/Pd calix[5]arene complexes were prepared following a similar procedure as follows:

[MoO_2(acac){Rb·**^{t}BuC5(H)**}Pd(bipy)] **(6.7)**: To a solution of [Pd(bipy){Rb·**^{t}BuC5(H)$_2$**}] **5.1c** (0.0412 g, 0.0356 mmol) dissolved in 4 mL of anhydrous benzene was added dropwise a light lime yellow solution of $MoO_2(acac)_2$ (0.0140 g, 0.0429 mmol) in 3 mL of anhydrous benzene. The resulting brilliant orange solution was stirred for 7 hrs, then centrifuged for 10 minutes and the supernatant pumped to dryness. The red solid obtained from the supernatant was stirred with 5 mL of anhydrous pentane for 5 min, and centrifuged for 10 min. The supernatant was discarded while the solid was recovered and dried in *vacuo*, affording **6.7** as a red solid (0.0439 g, 0.0318 mmol, 89%). Mp: >220 ^oC. ^1H NMR ($CDCl_3$) δ (ppm): 9.63 (br, 1H, OH), 9.38 (d, 1H, *J* = 7.2 Hz, bipy), 9.28 (d, 1H, *J* = 6.6 Hz, bipy), 8.62 (d, 1H, *J* = 5.2 Hz, bipy), 8.50 (dd, 1H, *J* = 8.4, 6.6 Hz, bipy), 8.43 (d, 1H, *J* = 5.2 Hz, bipy), 8.08 (dd, 1H, *J* = 8.4, 7.1 Hz, bipy), 7.51 (dd, 1H, *J* = 6.9, 6.9 Hz, bipy), 7.26 (s, 1H, Ar-*H*), 7.24 (d, 1H, *J* = 2.2 Hz, Ar-*H*), 7.21 (s, 2H, Ar-*H*), 7.17 (d, 1H, *J* = 2.2 Hz, Ar-*H*), 7.13 (dd, 1H, *J* = 6.2, 6.9 Hz, bipy), 6.99 (d, 1H, *J* = 2.2 Hz, Ar-*H*), 6.80 (s, 2H, Ar-*H*), 6.68 (d, 1H, *J* = 2.5 Hz, Ar-*H*), 6.64 (d, 1H, *J* = 14.0 Hz, Ar-CH_2-Ar), 6.26 (d, 1H, *J* = 2.2 Hz, Ar-*H*), 5.22 (d, 1H, *J* = 15.4 Hz, Ar-CH_2-Ar), 5.02 (s, 1H, C*H* acac), 5.02 (d, 1H, *J* = 14.3 Hz, Ar-CH_2-Ar), 4.94 (d, 1H, *J* = 13.7 Hz, Ar-CH_2-Ar), 4.40 (d, 1H, *J* = 13.2 Hz, Ar-CH_2-Ar), 3.53 (d, 1H, *J* = 15.4 Hz, Ar-CH_2-Ar), 3.42 (d, 1H, *J* = 12.6 Hz, Ar-CH_2-Ar), 3.28 (d, 1H, *J* = 14.3 Hz, Ar-CH_2-Ar), 3.17 (d, 1H, *J* = 14.3 Hz, Ar-CH_2-Ar), 3.11 (d, 1H, *J* = 13.5 Hz, Ar-CH_2-Ar), 1.46 (s, 3H, CH_3 acac), 1.40 (s, 9H, ^{t}Bu), 1.32 (s,

21H, CH_3 acac overlapped ^{t}Bu), 1.02 (s, 9H, ^{t}Bu), 0.85 (s, 9H, ^{t}Bu). $^{13}C\{^1H\}$ NMR ($CDCl_3$) δ (ppm): 192.5 (*C*=O (acac)), 185.5, 159.8, 159.1, 157.8, 157.4, 155.6, 154.8, 150.6, 148.5, 147.1, 143.1, 142.8, 141.9, 141.3, 140.5, 139.3, 139.0, 132.9, 132.3, 132.2, 131.8, 131.6, 131.5, 129.2, 128.8, 128.7, 128.5, 128.4, 128.1, 127.8, 126.8, 126.2, 125.7, 125.4, 125.1, 124.9, 123.8 (aromatic carbons), 101.7 (*C*H (acac)), 36.8 ($C(CH_3)_3$), 36.5, 34.3, 34.2, 34.0, 33.97 (Ar-CH_2-Ar), 32.1, 31.9, 31.8, 31.7 ($C(CH_3)_3$), 30.8 ($C(CH_3)_3$), 26.7, 26.6, 22.5, 14.3 (CH_3 (acac)). FTIR (KBr, cm^{-1}): 3423b,m (OH), 3109w, 3087w, 3047m, 2958vs, 2906s, 2867s, 1604s ($C=O_{acac}$), 1523s ($C=C_{acac}$), 1477vs, 1468vs, 1458vs, 1391s, 1362s, 1297s, 1264s, 1250m, 1208s, 1126m, 1026m, 915s (Mo=O), 888s (Mo=O), 832m, 799m, 768s, 726w, 675w, 550w, 441w. UV/vis (C_6H_6) $\lambda_{max/nm}$ (ε/dm^3 mol^{-1} cm^{-1}): 278 (2.59 x 10^4), 305 (2.25 x 10^4), 431 (1.83 x 10^3).

[MoO_2(acac){Rb·^{t}**BuC5(H)**}Pd((4-Me)$_2$bipy)] **(6.8)**: ([Pd((4-Me)$_2$bipy){Rb·^{t}**BuC5(H)$_2$**}] **5.2c**: 0.0423 g, 0.0357 mmol; $MoO_2(acac)_2$: 0.0139 g, 0.0426 mmol). **6.8** was obtained as a red-orange solid (0.0433 g, 0.0307 mmol, 86%). Mp: 276 – 278 ^oC. ^1H NMR ($CDCl_3$) δ (ppm): 9.84 (s, 1H, OH), 9.60 (br, 1H, (4-Me)$_2$bipy), 9.22 (br, 1H, (4-Me)$_2$bipy), 8.58 (d, 1H, *J* = 5.8 Hz, (4-Me)$_2$bipy), 7.95 (d, 1H, *J* = 5.8 Hz, (4-Me)$_2$bipy), 7.33 (s, 1H, Ar-*H*), 7.30 (d, 1H, *J* = 2.2 Hz, Ar-*H*), 7.23 (d, 1H, *J* = 1.9 Hz, Ar-*H*), 7.23 (d, 1H, *J* = 12.9 Hz, Ar-CH_2-Ar), 7.29-7.23 (1H of (4-Me)$_2$bipy) overlapped in this area), 7.18 (d, 1H, *J* = 2.5 Hz, Ar-*H*), 7.14 (d, 1H, *J* = 2.2 Hz, Ar-*H*), 6.91 (s, 2H, Ar-*H*), 6.75 (d, 1H, *J* = 2.5 Hz, Ar-*H*), 6.71 (d, 1H, *J* = 2.5 Hz, Ar-*H*), 6.61 (br, 1H, (4-Me)$_2$bipy), 6.17 (s, 1H, Ar-*H*), 5.16 (d, 1H, *J* = 15.1 Hz, Ar-CH_2-Ar), 5.13 (d, 1H, *J* = 13.5 Hz, Ar-CH_2-Ar), 4.98 (s, 1H, C*H* acac), 4.80 (d, 1H, *J* = 12.9 Hz, Ar-CH_2-Ar), 4.60 (d, 1H, *J* = 14.0 Hz, Ar-CH_2-Ar), 3.59 (d, 1H, *J* = 14.6 Hz, Ar-CH_2-Ar), 3.46 (d, 1H, *J* = 17.0 Hz, Ar-CH_2-Ar), 3.41 (d, 1H, *J* = 17.0 Hz, Ar-CH_2-Ar), 3.11 (d, 1H, *J*

= 14.0 Hz, Ar-CH_2-Ar), 3.02 (d, 1H, J = 13.7 Hz, Ar-CH_2-Ar), 2.86 (s, 3H, CH_3 (4-Me)$_2$bipy), 2.58 (s, 3H, CH_3 (4-Me)$_2$bipy), 1.63 (s, 3H, CH_3 acac), 1.49 (s, 3H, CH_3 acac), 1.40 (s, 9H, ^{t}Bu), 1.31 (s, 9H, ^{t}Bu), 1.30 (s, 9H, ^{t}Bu), 1.07 (s, 9H, ^{t}Bu), 0.78 (s, 9H, ^{t}Bu). No integration was performed in the ^{1}H NMR spectrum of **6.8**. However, the number of protons reported is based on compound **6.11** due to similarity. No ^{13}C{^{1}H} NMR was obtained due to sample precipitation during the collection time. FTIR (KBr, cm^{-1}): 3421m (OH), 3045m, 2957vs, 2906s, 2866s, 1615s (C=O$_{acac}$), 1522s (C=C$_{acac}$), 1478vs, 1458vs, 1391s, 1362s, 1299s, 1266s, 1250m, 1208s, 1126m, 1026m, 915s (Mo=O), 886s (Mo=O), 830s, 799m, 769m, 731w, 675w, 575w, 548w, 463w. UV/vis (C_6H_6) $\lambda_{max/nm}$ (ε/dm^3 mol^{-1} cm^{-1}): 284 (2.84 x 10^4), 304 (2.61 x 10^4).

[MoO$_2$(acac){Rb·**^{t}BuC5(H)**}Pd(phen)] **(6.9):** ([Pd(phen){Rb·**^{t}BuC5(H)$_2$**}] **5.3c**: 0.0422 g, 0.0358 mmol; MoO$_2$(acac)$_2$: 0.0142 g, 0.0435 mmol). Unlike the previous synthesis, compound **6.9** precipitates from the reaction mixture as a yellow-orange solid (0.0398 g, 0.0283 mmol, 79% yield). Mp: > 270 ^{o}C. ^{1}H NMR ($CDCl_3$) δ (ppm): 9.84 (br, 1H, OH), 8.92 (d, 1H, J = 4.9 Hz, phen), 8.56 (d, 1H, J = 4.7 Hz, phen), 8.26 (d, 1H, J = 8.2 Hz, phen), 7.98 (dd, 1H, J = 4.9, 7.6 Hz, phen), 7.28-7.18 (m, 6H,* Ar-H), 6.97 (s, 1H, Ar-H), 6.87 (d, 1H, J = 14.8 Hz, Ar-CH_2-Ar), 6.85 (s, 1H, Ar-H), 6.80 (d, 1H, J = 2.2 Hz, Ar-H), 6.76 (d, 1H, J = 1.9 Hz, Ar-H), 6.25 (s, 1H, Ar-H), 5.37 (d, 1H, J = 15.1 Hz, Ar-CH_2-Ar), 5.06 (d, 1H, J = 13.7 Hz, Ar-CH_2-Ar), 5.02 (d, 1H, J = 10.7 Hz, Ar-CH_2-Ar), 4.94 (s, 1H, CH acac), 4.57 (d, 1H, J = 13.2 Hz, Ar-CH_2-Ar), 3.61 (d, 1H, J = 15.4 Hz, Ar-CH_2-Ar), 3.47 (d, 1H, J = 13.5 Hz, Ar-CH_2-Ar), 3.43 (d, 1H, J = 12.9 Hz, Ar-CH_2-Ar), 3.17 (d, 1H, J = 14.3 Hz, Ar-CH_2-Ar), 3.08 (d, 1H, J = 13.2 Hz, Ar-CH_2-Ar), 1.48 (s, 3H, CH_3 acac), 1.37 (s, 9H, ^{t}Bu), 1.33 (s, 9H, ^{t}Bu), 1.32 (s, 9H, ^{t}Bu), 1.05 (s, 9H, ^{t}Bu), 1.04 (s, 3H, CH_3 acac), 0.85 (s, 9H, ^{t}Bu). *The integral value reported for the

compound is not consistent with the value required. This disagreement in value could be due to overlapping with solvent or impurities. $^{13}C\{^1H\}$ NMR ($CDCl_3$) δ (ppm): 192.4 (*C*=O (acac)), 185.1, 160.2, 159.4, 157.3, 150.8, 148.8, 145.1, 142.9, 142.7, 140.4, 139.4, 139.2, 132.9, 132.4, 132.1, 131.7, 131.6, 131.5, 129.6, 129.2, 128.7, 128.5, 128.3, 127.4, 125.8, 124.9, 124.2, 123.7 (aromatic carbons), 109.1 (*C*H (acac)), 37.3, 36.4 ($C(CH_3)_3$), 34.3, 34.2, 34.1, 34.0 (Ar-CH_2-Ar), 32.5 ($C(CH_3)_3$), 32.0, 31.9, 31.7 ($C(CH_3)_3$), 31.1, 29.5 ($C(CH_3)_3$), 26.7, 26.1 (CH_3 (acac)). FTIR (KBr, cm^{-1}): 3434m (OH), 3051m, 2957vs, 2904s, 2866s, 1604s ($C=O_{acac}$), 1522s ($C=C_{acac}$), 1479s, 1458vs, 1433s, 1390s, 1362s, 1296s, 1267s, 1206s, 1126w, 1111w, 1025m, 916s (Mo=O), 894s (Mo=O), 844m, 829m, 799w, 768m, 748w, 727w, 716m, 676w, 550w, 448w, 417m. UV/vis (C_6H_6) $\lambda_{max/nm}$ ($\varepsilon/dm^3\ mol^{-1}\ cm^{-1}$): 278 ($3.10 \times 10^4$), 432 ($3.41 \times 10^3$), 436 ($3.41 \times 10^3$).

[MoO_2(acac){Cs·^{t}**BuC5(H)**}Pd(bipy)] **(6.10):** ([Pd(bipy){Cs·^{t}**BuC5(H)$_2$**}] **5.1d**: 0.0434 g, 0.0361 mmol; $MoO_2(acac)_2$: 0.0145 g, 0.0445 mmol). **6.10** was obtained as a red-orange solid (0.0493 g, 0.0345 mmol, 96%). Mp: >230 ^oC. ^1H NMR ($CDCl_3$) δ (ppm): 9.39 (d, 1H, *J* = 8.0 Hz, bipy), 9.33 (d, 1H, *J* = 8.0 Hz, bipy), 9.30 (s, 1H, OH), 8.64 (d, 1H, *J* = 4.7 Hz, bipy), 8.55 (dd, 1H, *J* = 7.7, 7.7 Hz, bipy), 8.44 (d, 1H, *J* = 4.9 Hz, bipy), 8.12 (dd, 1H, *J* = 7.7, 7.7 Hz, bipy), 7.52 (dd, 1H, *J* = 6.0, 6.3 Hz, bipy), 7.31 (d, 1H, *J* = 2.5 Hz, Ar-*H*), 7.26 (d, 1H, *J* = 2.2 Hz, Ar-*H*), 7.23 (d, 1H, *J* = 2.5 Hz, Ar-*H*), 7.21 (s, 2H, Ar-*H*), 7.13 (dd, 1H, *J* = 6.6, 6.6 Hz, bipy), 6.96 (d, 1H, *J* = 2.5 Hz, Ar-*H*), 6.80 (d, 1H, *J* = 2.5 Hz, Ar-*H*), 6.76 (d, 1H, *J* = 2.5 Hz, Ar-*H*), 6.70 (d, 1H, *J* = 15.9 Hz, Ar-CH_2-Ar), 6.67 (d, 1H, *J* = 2.5 Hz, Ar-*H*), 6.43 (d, 1H, *J* = 1.9 Hz, Ar-*H*), 5.26 (d, 1H, *J* = 15.1 Hz, Ar-CH_2-Ar), 5.07 (d, 1H, *J* = 13.7 Hz, Ar-CH_2-Ar), 5.00 (s, 1H, C*H* acac), 4.93 (d, 1H, *J* = 13.7 Hz, Ar-CH_2-Ar), 4.48 (d, 1H, *J* = 13.7 Hz, Ar-CH_2-Ar), 3.53

(d, 1H, J = 15.4 Hz, Ar-CH_2-Ar), 3.42 (d, 1H, J = 13.7 Hz, Ar-CH_2-Ar), 3.30 (d, 1H, J = 14.0 Hz, Ar-CH_2-Ar), 3.14 (d, 1H, J = 14.0 Hz, Ar-CH_2-Ar), 3.07 (d, 1H, J = 13.5 Hz, Ar-CH_2-Ar), 1.45 (s, 3H, CH_3 acac), 1.41 (s, 9H, ^{t}Bu), 1.34 (s, 9H, ^{t}Bu), 1.33 (s, 9H, ^{t}Bu), 1.31 (s, 3H, CH_3 acac), 0.99 (s, 9H, ^{t}Bu), 0.89 (s, 10H,* ^{t}Bu). *The integral value reported for the compound is not consistent with the value required. This disagreement in value could be due to overlapping with solvent or impurities. ^{13}C{^{1}H} NMR ($CDCl_3$) δ (ppm): 192.4 (C=O (acac)), 185.2, 160.4, 158.9, 157.2, 155.7, 154.8, 150.7, 148.4, 147.1, 142.9, 142.7, 141.9, 141.4, 140.5, 139.3, 138.7, 132.8, 132.5, 131.8, 129.1, 128.6, 127.4, 126.8, 126.0, 125.9, 125.7, 125.2, 124.8, 123.9 (aromatic carbons), 101.5 (CH (acac)), 100.2 (impurity), 36.7, 36.6 (C(CH_3)$_3$), 34.3, 34.2, 34.1, 34.0, 33.9 (Ar-CH$_2$-Ar), 32.1, 32.0, 31.8, 31.7 (C(CH$_3$)$_3$), 30.4, 29.6 (C(CH_3)$_3$), 26.7, 26.6 (CH$_3$ (acac)). FTIR (KBr, cm^{-1}): 3435m (OH), 3109w, 3084w, 3046m, 2958vs, 2904s, 2866s, 1605s (C=O$_{acac}$), 1522s (C=C$_{acac}$), 1478vs, 1458vs, 1391s, 1362s, 1297s, 1264s, 1207s, 1127w, 1026w, 916s (Mo=O), 887s (Mo=O), 832m, 799w, 767s, 726w, 674w, 550w, 439w. UV/vis (C_6H_6) $\lambda_{max/nm}$ (ε/dm^3 mol^{-1} cm^{-1}): 277 (2.22 x 10^4), 306 (1.78 x 10^4), 425 (1.12 x 10^3). E. A. for $C_{70}H_{81}CsMoN_2O_9Pd\cdot 2H_2O$ calc(found): C: 57.36 (57.06); H: 5.85 (5.76).

[MoO_2(acac){Cs·^{t}**BuC5(H)**}Pd((4-Me)$_2$bipy)] **(6.11):** ([Pd((4-Me)$_2$bipy){Cs·^{t}**BuC5(H)$_2$**}] **5.2d**: 0.0439 g, 0.0356 mmol; MoO_2(acac)$_2$: 0.0142 g, 0.0435 mmol). **6.11** was obtained as a red-orange solid (0.0446 g, 0.0306 mmol, 86%). Mp: 290 - 292 ^{o}C. ^{1}H NMR ($CDCl_3$) δ (ppm): 9.66 (br, 2H, OH, overlapped with (4-Me)$_2$bipy), 9.23 (br, 1H, (4-Me)$_2$bipy), 8.61 (d, 1H, J = 5.5 Hz, (4-Me)$_2$bipy), 7.96 (d, 1H, J = 5.5 Hz, (4-Me)$_2$bipy), 7.41 (s, 1H, (4-Me)$_2$bipy), 7.28 (s, 1H, Ar-H), 7.25 (s, 1H, Ar-H), 7.21 (d, 1H, J = 12.4 Hz, Ar-CH_2-Ar), 7.20 (s, 1H, Ar-H), 7.19 (s, 1H, Ar-H), 7.12 (d, 1H, J = 2.5 Hz, Ar-H), 6.89 (s, 2H, Ar-H),

6.68 (d, 2H, J = 2.5 Hz, Ar-H), 6.62 (br, 1H, (4-Me)$_2$bipy), 6.35 (s, 1H, Ar-H), 5.21 (d, 1H, J = 15.1 Hz, Ar-CH_2-Ar), 5.18 (d, 1H, J = 13.7 Hz, Ar-CH_2-Ar), 4.96 (s, 1H, CH acac), 4.87 (d, 1H, J = 12.6 Hz, Ar-CH_2-Ar), 4.61 (d, 1H, J = 14.0 Hz, Ar-CH_2-Ar), 3.55 (d, 1H, J = 14.0 Hz, Ar-CH_2-Ar), 3.44 (d, 2H,* J = 14.0 Hz, Ar-CH_2-Ar), 3.40 (d, 1H, J = 14.0 Hz, Ar-CH_2-Ar), 3.09 (d, 1H, J = 14.3 Hz, Ar-CH_2-Ar), 2.99 (d, 1H, J = 14.0 Hz, Ar-CH_2-Ar), 2.86 (s, 3H, CH_3 (4-Me)$_2$bipy), 2.56 (s, 3H, CH_3 (4-Me)$_2$bipy), 2.36 (s, §, toluene), 1.62 (s, 3H, CH_3 acac), 1.47 (s, 3H, CH_3 acac), 1.41 (s, 9H, ^{t}Bu), 1.32 (s, 9H, ^{t}Bu), 1.32 (s, 9H, ^{t}Bu), 1.03 (s, 9H, ^{t}Bu), 0.84 (s, 9H, ^{t}Bu). § integral value not available. *The integral value reported for the compound is not consistent with the value required. This disagreement in value could be due to overlapping with solvent or impurities. ^{13}C{^{1}H} NMR (C_6D_6) δ (ppm): 191.6, 184.6 (C=O (acac)), 162.2, 159.5, 157.4, 155.6, 154.1, 153.8, 149.5, 148.8, 146.0, 142.7, 142.2, 140.7, 139.1, 138.5, 134.1, 133.8, 132.9, 132.8, 132.4, 129.6, 129.3, 128.9, 126.6, 126.5, 126.4, 126.2, 125.7, 125.6, 125.0, 124.5 (aromatic carbons), 101.0 (CH (acac)), 38.2, 37.1 (C(CH$_3$)$_3$), 34.3, 34.2, 34.1, 33.8, 33.7 (Ar-CH$_2$-Ar), 32.2, 32.0, 31.9, 31.8, 31.6 (C(CH$_3$)$_3$), 31.0, 26.7, 26.5 (C(CH$_3$)$_3$), 22.1, 21.8 (CH$_3$ (acac)). FTIR (KBr, cm^{-1}): 3450m (OH), 3230w, 3120w, 3044m, 2958vs, 2902s, 2866s, 1615s (C=O$_{acac}$), 1522s (C=C$_{acac}$), 1479vs, 1458vs, 1392s, 1362s, 1299s, 1266s, 1208s, 1127w, 1026w, 916s (Mo=O), 886s (Mo=O), 831m, 799w, 769w, 731w, 675w, 549w. UV/vis (C_6H_6) $\lambda_{max/nm}$ (ε/dm^3 mol^{-1} cm^{-1}): 288 (2.09 x 10^4), 304 (1.96 x 10^4), 426 (1.37 x 10^3), 432 (1.37 x 10^3). E. A. for $C_{72}H_{85}CsMoN_2O_9Pd{\cdot}H_2O$ calc(found): C: 58.60 (58.44); H: 5.94 (5.97).

[MoO$_2$(acac){Cs·^{t}**BuC5(H)**}Pd(phen)] **(6.12):** ([Pd(phen){Cs·^{t}**BuC5(H)$_2$**}] **5.3d**: 0.0441 g, 0.0359 mmol; MoO$_2$(acac)$_2$: 0.0145 g, 0.0445 mmol). Unlike the previous synthesis, compound **6.12** precipitates from the reaction mixture as a yellow-orange solid (0.0475 g, 0.0327

mmol, 91%). Mp: > 280 ^{o}C decomposes. ^{1}H NMR ($CDCl_3$) δ (ppm): 9.56 (br, 1H, OH), 8.93 (d, 1H, *J* = 4.9 Hz, phen), 8.59 (d, 1H, *J* = 4.7 Hz, phen), 8.25 (d, 1H, *J* = 8.2 Hz, phen), 7.98 (dd, 1H, *J* = 4.1, 6.0 Hz, phen), 7.36-7.22 (m, 9H,* Ar-*H*), 6.95 (s, 1H, Ar-*H*), 6.93 (d, 1H, *J* = 12.9 Hz, Ar-CH_2-Ar), 6.84 (s, 1H, Ar-*H*), 6.76 (s, 1H, Ar-*H*), 6.73 (s, 1H, Ar-*H*), 6.40 (s, 1H, Ar-*H*), 5.41 (d, 1H, *J* = 14.6 Hz, Ar-CH_2-Ar), 5.11 (d, 1H, *J* = 14.0 Hz, Ar-CH_2-Ar), 5.00 (d, 1H, *J* = 14.0 Hz, Ar-CH_2-Ar), 4.90 (s, 1H, C*H* acac), 4.66 (d, 1H, *J* = 14.0 Hz, Ar-CH_2-Ar), 3.61 (d, 1H, *J* = 14.6 Hz, Ar-CH_2-Ar), 3.46 (d, 1H, *J* = 14.0 Hz, Ar-CH_2-Ar), 3.44 (d, 1H, *J* = 14.7 Hz, Ar-CH_2-Ar), 3.14 (d, 1H, *J* = 13.7 Hz, Ar-CH_2-Ar), 3.04 (d, 1H, *J* = 13.5 Hz, Ar-CH_2-Ar), 1.47 (s, 3H, CH_3 acac), 1.38 (s, 9H, ^{t}Bu), 1.35 (s, 9H, ^{t}Bu), 1.33 (s, 9H, ^{t}Bu), 1.02 (s, 12H, CH_3 acac, ^{t}Bu), 0.88 (s, 9H, ^{t}Bu). *The integral value reported for the compound is not consistent with the value required. This disagreement in value could be due to overlapping with solvent or impurities. No ^{13}C{^{1}H} NMR was performed due to sample precipitation during the collection time. FTIR (KBr, cm^{-1}): 3444m (OH), 3051m, 2957vs, 2906s, 2866s, 1605s (C=O$_{acac}$), 1521s (C=C$_{acac}$), 1479vs, 1458vs, 1431s, 1391s, 1362s, 1296s, 1268s, 1207s, 1128w, 1111w, 1025w, 917s (Mo=O), 891s (Mo=O), 842s, 799w, 769w, 746w, 716w, 676w, 550w, 425w. UV/vis (C_6H_6) $\lambda_{max/nm}$ (ε/dm^3 mol^{-1} cm^{-1}): 279 (3.89 x 10^4), 443 (1.96 x 10^3). E. A. for $C_{72}H_{81}CsMoN_2O_9Pd{\cdot}2H_2O$ calc(found): C: 58.05 (57.92); H: 5.75 (5.57).

6.4 General X-ray crystal structure information

The crystallographic data and some details of the data collection and refinement of complex **6.1**·C_6H_6 are given in Table 6.8. Absorption corrections were applied by SADABS.[155] The X-ray structure of **6.1**·C_6H_6 was solved by direct methods and subsequent difference Fourier syntheses and refined by full matrix least-squares methods against F^2 (SHELX 97).[121]The H

atoms in structures were taken in calculated positions. The programs Mercury,[157] ORTEP32[216] and POVRay[158] were used to generate the X-ray structural diagrams pictured in this Chapter.

Table 6.8 Crystallographic data for complex Ti[(bipy)Pd{Rb·^{t}**BuC5**}]$_2$·C_6H_6 **6.1**·C_6H_6.

	6.1·C_6H_6
Formula	$C_{166}H_{182}N_4O_{10}Pd_2Rb_2Ti$
FW	2824.80
cryst syst	Monoclinic
Space group	P 21/c
T, K	153(2)
a, Å	28.387(5)
b, Å	29.158(5)
c, Å	18.167(3)
α, deg	90
β, deg	107.968(2)
γ, deg	90
V, A^3	14304(4)
Z	4
d_{calcd}, g·cm^{-3}	1.312
μ, mm^{-1}	1.040
refl colected	146381
T_{min} / T_{max}	0.775
N_{measd}	26313
[R_{int}]	[0.0773]
R [I>2sigma(I)]	0.0429
R (all data)	0.0749
R_w [I>2sigma(I)]	0.1187
R_w (all data)	0.1468
GOF	0.949

6.5 Conclusions

We have reported the synthesis and characterization of the first Pd(II)/Ti(IV) and Pd(II)/Mo(VI) heterobimetallic calix[5]arene complexes by the reaction of [Pd(L){M·^{t}**BuC5(H)$_2$**}] **5.1c-d**, **5.2c-d** and **5.3c-d** (M = Rb, Cs; L = bipy, (4-Me)$_2$bipy, phen) precursors with $Ti(NEt_2)_4$ and $MoO_2(acac)_2$ in benzene. Complexes **6.1** – **6.12** can be easily isolated because they either precipitate from the reaction mixture or precipitate when pentane or hexane is added. The crystal packing for complex **6.1** shows extended π-π stacking interactions between the bipy ligands and the aromatic rings of the calix[5]arenes.

The lower rim of the calix[5]arene clearly allows enough room for both transition metals. The new heterobimetallic complexes are ideal starting points for future studies of heterobimetallic catalysts.

References

(1) Evans, D. G.; Boeyens, J. C. A. *Acta Crystallogr., Sect. B: Struct. Sci* **1988**, *44*, 663-671.

(2) Gutsche, C. D. *Calixarenes*; Stoddart, J. F. Ed.; The Royal Society of Chemistry: Cambridge, 1989.

(3) Baeyer, A. *J. Chem. Soc.* **1872**, *25*, Chem. Abstract 1906:228328.

(4) Baeyer, A. *Ber. Dtsch. Chem. Ges.* **1872**, *5*, 280-282.

(5) Baeyer, A. *Ber. Dtsch. Chem. Ges.* **1872**, *5*, 1094-1100.

(6) Gutsche, C. D.; Iqbal, M.; Watson, A. T.; Heathcock, C. H. *Org. Synth.* **1990**, *68*, 234-237.

(7) Gutsche, C. D.; Dhawan, B.; Leonis, M.; Stewart, D. *Org. Synth.* **1990**, *68*, 238-242.

(8) Munch, J. H.; Gutsche, C. D. *Org. Synth.* **1990**, *68*, 243-244.

(9) Gutsche, C. D. *Calixarenes Revisited*; Royal Society of Chemistry: Cambridge, 1998.

(10) Bell, S. E. J.; Browne, J. K.; McKee, V.; Mckervey, M. A.; Malone, J. F.; O´Leary, M.; Walker, A. *J. Org. Chem.* **1998**, *63*, 489-501.

(11) Asfari, Z.; Böhmer, V.; Harrowfield, J.; Vicens, J. *Calixarenes 2001*; Kluwer Academic Publishers: Dordrecht, 2001.

(12) Creaven, B. S.; Donlon, D. F.; McGinley, J. *Coord. Chem Rev.* **2009**, *253*, 893-962.

(13) Harvey, P. D. *Coord. Chem. Rev.* **2002**, *233-234*, 289-309.

(14) Jose, P.; Menon, S. *Bioinorg. Chem. Appl.* **2007**, *2007*, 1-16.

(15) Roundhill, D. M. *Prog. Inorg. Chem.,* **1995**, *43*, 533-592.

(16) Floriani, C.; Floriani-Moro, R. *Adv. Organomet. Chem.* **2001**, *47*, 167-233.

(17) Homden, D. M.; Redshaw, C. *Chem. Rev.* **2008**, *108*, 5086-5130.

(18) Śliwa, W. *Croat. Chem. Acta* **2002**, *1*, 131-153.

(19) Śliwa, W. *J. Inclusion Phenom. Macrocyclic Chem.* **2005**, *52*, 13-37.

(20) Śliwa, W.; Deska, M. *ARKIVOC* **2008**, *1*, 87-127.

(21) Śliwa, W.; Girek, T. *J. Inclusion Phenom. Macrocyclic Chem.* **2010**, *66*, 15-41.

(22) Wieser, C.; Dieleman, C. B.; Matt, D. *Coord. Chem. Rev.* **1997**, *165*, 93-161.

(23) Redshaw, C. *Coord. Chem. Rev.* **2003**, *244*, 45-70.

(24) Baldini, L.; Casnati, A.; Sansone, F.; Ungaro, R. *Chem. Soc. Rev.* **2007**, *36*, 254-266.

(25) Böhmer, V. *Angew. Chem., Int. Ed.* **1995**, *34*, 713-745.

(26) Leray, I.; Valeur, B. *Eur. J. Inorg. Chem.* **2009**, 3525-3535.

(27) Ikeda, A.; Shinkai, S. *Chem. Rev.* **1997**, *97*, 1713-1734.

(28) Diamond, D.; Nolan, K. *Anal. Chem.* **2001**, *73*, 22A-29A.

(29) Gutsche, C. D. *Calixarenes An Introduction 2nd Edition*; Stoddart, J. F. Ed.; The Royal Society of Chemistry: Cambridge, 2008.

(30) Stewart, D. R.; Krawiec, M.; Kashyap, R. P.; Watson, W. H.; Gutsche, C. D. *J. Am. Chem. Soc.* **1995**, *117*, 586-601.

(31) Olmstead, M. M.; Sigel, G.; Hope, H.; Xu, X.; Power, P. P. *J. Am. Chem. Soc.* **1985**, *107*, 8087-8091.

(32) Bott, S. G.; Coleman, A. W.; Atwood, J. L. *J. Chem. Soc., Chem. Commun.* **1986**, 610-611.

(33) Hofmeister, G. E.; Hahn, F. E.; Pedersen, S. F. *J. Am. Chem. Soc.* **1989**, *111*, 2318-2319.

(34) Corazza, F.; Floriani, C.; Chiesi-Villa, A.; Guastini, C. *J. Chem. Soc., Chem. Commun.* **1990**, 640-641.

(35) Corazza, F.; Floriani, C.; Chiesi-Villa, A.; Guastini, C. *J. Chem. Soc., Chem. Commun.* **1990**, 1083-1084.

(36) Corazza, F.; Floriani, C.; Chiesi-Villa, A.; Rizzoli, C. *Inorg. Chem.* **1991**, *30*, 4465-4468.

(37) Floriani, C. *Chem. Eur. J.* **1999**, *5*, 19-23.

(38) Guillemot, G.; Solari, E.; Scopelliti, R.; Floriani, C. *Organometallics* **2001**, *20*, 2446-2448.

(39) Giannini, L.; Guillemot, G.; Solari, E.; Floriani, C.; Re, N.; Chiesi-Villa, A.; Rizzoli, C. *J. Am. Chem. Soc.* **1999**, *121*, 2797-2807.

(40) Caselli, A.; Giannini, L.; Solari, E.; Floriani, C.; Re, N.; Chiesi-Villa, A.; Rizzoli, C. *Organometallics* **1997**, *16*, 5457-5469.

(41) Giannini, L.; Caselli, A.; Solari, E.; Floriani, C.; Chiesi-Villa, A.; Rizzoli, C.; Re, N.; Sgamellotti, A. *J. Am. Chem. Soc.* **1997**, *119*, 9198-9210.

(42) Giannini, L.; Caselli, A.; Solari, E.; Floriani, C.; Chiesi-Villa, A.; Rizzoli, C.; Re, N.; Sgamellotti, A. *J. Am. Chem. Soc.* **1997**, *119*, 9709-9719.

(43) Castellano, B.; Solari, E.; Floriani, C.; Re, N.; Chiesi-Villa, A.; Rizzoli, C. *Organometallics* **1998**, *17*, 2328-2336.

(44) Castellano, B.; Solari, E.; Floriani, C.; Scopelliti, R.; Re, N. *Inorg. Chem.* **1999**, *38*, 3406-3413.

(45) Castellano, B.; Zanotti-Gerosa, A.; Solari, E.; Floriani, C. *Organometallics* **1996**, *15*, 4894-4896.

(46) Giannini, L.; Solari, E.; Floriani, C.; Chiesi-Villa, A.; Rizzoli, C. *J. Am. Chem. Soc.* **1998**, *120*, 823-824.

(47) Guillemot, G.; Solari, E.; Floriani, C.; Re, N.; Rizzoli, C. *Organometallics* **2000**, *19*, 5218-5230.

(48) Acho, J. A.; Ren, T.; Yun, J. W.; Lippard, S. J. *Inorg. Chem.* **1995**, *34*, 5226-5233.

(49) Hoppe, E.; Limberg, C.; Ziemer, B. *Inorg. Chem.* **2006**, *45*, 8308-8317.

(50) Wetherby, A. E., Jr.; Goeller, L. R.; Dipasquale, A. G.; Rheingold, A. L.; Weinert, C. S. *Inorg. Chem.* **2007**, *46*, 7579-7586.

(51) Iwasa, K.; Kochi, T.; Ishii, Y. *Angew. Chem., Int. Ed.* **2003**, *42*, 3658-3660.

(52) Petrella, A. J.; Craig, D. C.; Lamb, R. N.; Raston, C. L.; Roberts, N. K. *Dalton Trans.,* **2003**, 4590-4597.

(53) Petrella, A. J.; Roberts, N. K.; Raston, C. L.; Craig, D. C.; Thornton-Pett, M.; Lamb, R. N. *Eur. J. Inorg. Chem.* **2003**, 4153-4158.

(54) Gardiner, M. G.; Lawrence, S. M.; Raston, C. L.; Skelton, B. W.; White, A. H. *Chem. Commun.,* **1996**, 2491-2492.

(55) Gottfriedsen, J.; Blaurock, S. *Z. Anorg. Allg. Chem.* **2005**, *631*, 3037-3039.

(56) Bukhaltsev, E.; Goldberg, I.; Vigalok, A. *Organometallics* **2004**, *23*, 4540-4543.

(57) Bukhaltsev, E.; Goldberg, I.; Vigalok, A. *Organometallics* **2005**, *24*, 5732-5736.

(58) Liu, L.; Zakharov, L. N.; Golen, J. A.; Rheingold, A. L.; Hanna, T. A. *Inorg. Chem.* **2008**, *47*, 11143-11153.

(59) Redshaw, C.; Elsegood, M. R. J. *Inorg. Chem.* **2000**, *39*, 5164-5168.

(60) Shang, S.; Khasnis, D. V.; Zhang, H.; Small, A. C.; Fan, M.; Lattman, M. *Inorg. Chem.* **1995**, *34*, 3610-3615.

(61) Atwood, J. L.; Gardiner, M. G.; Jones, C.; Raston, C. L.; Skelton, B. W.; White, A. H. *Chem. Commun.,* **1996**, 2487-2488.

(62) Zanotti-Gerosa, A.; Solari, E.; Giannini, L.; Floriani, C.; Chiesi-Villa, A.; Rizzoli, C. *J. Am. Chem. Soc.* **1998**, *120*, 437-438.

(63) Caselli, A.; Solari, E.; Scopelliti, R.; Floriani, C. *J. Am. Chem. Soc.* **2000**, *122*, 538-539.

(64) Giannini, L.; Solari, E.; Zanotti-Gerosa, A.; Floriani, C.; Chiesi-Villa, A.; Rizzoli, C. *Angew. Chem. Int. Ed.* **1997**, *36*, 753-754.

(65) Zanotti-Gerosa, A.; Solari, E.; Giannini, L.; Floriani, C.; Chiesi-Villa, A.; Rizzoli, C. *Chem. Commun.,* **1997**, 183-184.

(66) Giannini, L.; Solari, E.; Floriani, C.; Re, N.; Chiesi-Villa, A.; Rizzoli, C. *Inorg. Chem.* **1999**, *38*, 1438-1445.

(67) Guillemot, G.; Solari, E.; Floriani, C.; Rizzoli, C. *Organometallics* **2001**, *20*, 607-615.

(68) Clegg, W.; Elsegood, M. R. J.; Teat, S. J.; Redshaw, C.; Gibson, V. C. *J. Chem. Soc., Dalton Trans.* **1998**, 3037-3040.

(69) McBurnett, B. G.; Cowley, A. H. *Chem. Commun.,* **1999**, 17-18.

(70) Ozerov, O. V.; Brock, C. P.; Carr, S. D.; Ladipo, F. T. *Organometallics* **2000**, *19*, 5016-5025.

(71) Ozerov, O. V.; Patrick, B. O.; Ladipo, F. T. *J. Am. Chem. Soc.* **2000**, *122*, 6423-6431.

(72) Kingston, J. V.; Ozerov, O. V.; Parkin, S.; Brock, C. P.; Ladipo, F. T. *J. Am. Chem. Soc.* **2002**, *124*, 12217-12224.

(73) Kingston, J. V.; Sarveswaran, V.; Parkin, S.; Ladipo, F. T. *Organometallics* **2003**, *22*, 136-144.

(74) Anwander, R.; Eppinger, J.; Nagl, I.; Scherer, W.; Tafipolsky, M.; Sirsch, P. *Inorg. Chem.* **2000**, *39*, 4713-4720.

(75) Cotton, F. A.; Dikarev, E. V.; Murillo, C. A.; Petrukhina, M. A. *Inorg. Chim. Acta* **2002**, *332*, 41-46.

(76) Morohashi, N.; Iki, N.; Miyano, S.; Kajiwara, T.; Ito, T. *Chem. Lett.* **2001**, *1*, 66-67.

(77) Takemoto, S.; Tanaka, S.; Mizobe, Y.; Hidai, M. *Chem. Commun.,* **2004**, 838-839.

(78) Hirata, K.; Suzuki, T.; Noya, A.; Takei, I.; Hidai, M. *Chem. Commun.,* **2005**, 3718-3720.

(79) Buccella, D.; Parkin, G. *J. Am. Chem. Soc.* **2008**, *130*, 8617-8619.

(80) Bi, Y.; Li, Y.; Liao, W.; Zhang, H.; Li, D. *Inorg. Chem.* **2008**, *47*, 9733-9735.

(81) Petrella, A. J.; Roberts, N. K.; Craig, D. C.; Raston, C. L.; Lamb, R. N. *Chem. Commun.,* **2003**, 1728-1729.

(82) Fan, M.; Zhang, H.; Lattman, M. *Chem. Commun.,* **1998**, 99-100.

(83) Fan, M.; Zhang, H.; Lattman, M. *Inorg. Chem.* **2006**, *45*, 6490-6496.

(84) Salmon, L.; Thuéry, P.; Ephritikhine, M. *Eur. J. Inorg. Chem.* **2006**, 4289-4293.

(85) Mendoza-Espinosa, D.; Hanna, T. A. *Dalton. Trans.,* **2009**, 5211-5225.

(86) Mendoza-Espinosa, D.; Hanna, T. A. *Inorg. Chem.* **2009**, *48*, 10312-10325.

(87) Leverd, P. C.; Nierlich, M. *Eur. J. Inorg. Chem.* **2000**, 1733-1738.

(88) Salmon, L.; Thuéry, P.; Ephritikhine, M. *Dalton Trans.,* **2006**, *30*, 3629-3637.

(89) Leverd, P. C.; Rinaldo, D.; Nierlich, M. *Eur. J. Inorg. Chem.* **2001**, 2021-2025.

(90) Petrella, A. J.; Roberts, N. K.; Craig, D. C.; Raston, C. L.; Lamb, R. N. *Chem. Commun.,* **2003**, 1014-1015.

(91) Petrella, A. J.; Roberts, N. K.; Craig, D. C.; Raston, C. L.; Lamb, R. N. *Chem. Commun.,* **2003**, 2288-2289.

(92) Petrella, A. J.; Craig, D. C.; Lamb, R. N.; Raston, C. L.; Roberts, N. K. *Dalton Trans.,* **2004**, 327-333.

(93) Mendoza-Espinosa, D.; Rheingold, A. L.; Hanna, T. A. *Dalton Trans.,* **2009**, 5226-5238.

(94) Gibson, V. C.; Redshaw, C.; Clegg, W.; Elsegood, M. R. J. *J. Chem. Soc., Chem. Commun.* **1995**, 2371-2372.

(95) Gibson, V. C.; Redshaw, C.; Elsegood, M. R. J. *Chem. Commun.,* **2002**, 1200-1201.

(96) Bukhaltsev, E.; Frish, L.; Cohen, Y.; Vigalok, A. *Org. Lett.* **2005**, *7*, 5123-5126.

(97) Arnecke, R.; Böhmer, V.; Cacciapaglia, R.; Cort, A. D.; Mandolini, L. *Tetrahedron* **1997**, *53*, 4901-4908.

(98) Haino, T.; Yanase, M.; Fukazawa, Y. *Angew. Chem., Int. Ed.* **1997**, *36*, 259-260.

(99) Steed, J. W.; Johnson, C. P.; Barnes, C. L.; Juneja, R. K.; Atwood, J. L.; Reilly, S.; Hollis, R. L.; Smith, P. H.; Clark, D. L. *J. Am. Chem. Soc.* **1995**, *117*, 11426-11433.

(100) Bott, S. G.; Coleman, A. W.; Atwood, J. L. *J. Am. Chem. Soc.* **1988**, *110*, 610-611.

(101) Garozzo, D.; Gattuso, G.; Kohnke, F. H.; Notti, A.; Pappalardo, S.; Parisi, M. F.; Pisagatti, I.; White, A. J. P.; Williams, D. J. *Org. Lett.* **2003**, *5*, 4025-4028.

(102) Arnaud-Neu, F.; Fuangswasdi, S.; Notti, A.; Pappalardo, S.; Parisi, M. F. *Angew. Chem., Int. Ed.* **1998**, *37*, 112-114.

(103) Coleman, A. W.; Bott, S. G.; Morley, S. D.; Means, C. M.; Robinson, K. D.; Zhang, H.; Atwood, J. L. *Angew. Chem., Int. Ed.* **1988**, *27*, 1361-1362.

(104) Atwood, J. L.; Coleman, A. W.; Zhang, H.; Bott, S. G. *J. Inclusion Phenom. Mol. Recognit. Chem.* **1989**, *7*, 203-211.

(105) Izatt, R. M.; Lamb, J. D.; Hawkins, R. T.; Brown, P. R.; Izatt, S. R.; Christensen, J. J. *J. Am. Chem. Soc.* **1983**, *105*, 1782-1785.

(106) Casnati, A.; Pochini, A.; Ungaro, R.; Ugozzoli, F.; Arnaud, F.; Fanni, S.; Schwing, M.-J.; Egberink, R. J. M.; de Jong, F.; Reinhoudt, D. N. *J. Am. Chem. Soc.* **1995**, *117*, 2767-2777.

(107) Hanna, T. A.; Liu, L.; Angeles-Boza, A. M.; Kou, X.; Gutsche, C. D.; Ejsmont, K.; Watson, W. H.; Zakharov, L. N.; Incarvito, C. D.; Rheingold, A. L. *J. Am. Chem. Soc.* **2003**, *125*, 6228-6238.

(108) Hanna, T. A.; Liu, L.; Zakharov, L. N.; Rheingold, A. L.; Watson, W. H.; Gutsche, C. D. *Tetrahedron* **2002**, *58*, 9751-9757.

(109) Liu, L.; Zakharov, L. N.; Rheingold, A. L.; Hanna, T. A. *Chem. Commun.,* **2004**, 1472-1473.

(110) Liu, L.; Zakharov, L. N.; Golen, J. A.; Rheingold, A. L.; Watson, W. H.; Hanna, T. A. *Inorg. Chem.* **2006**, *45*, 4247-4260.

(111) Barrett, G.; McKervey, M. A.; Malone, J. F.; Walker, A.; Arnaud-Neu, F.; Guerra, L.; Schwing-Weill, M.-J.; Gutsche, C. D.; Stewart, D. R. *J. Chem. Soc., Perkin Trans. 2,* **1993**, 1475-1479.

(112) Charbonière, L. J.; Balsiger, C.; Schenk, K. J.; Bünzli, J.-C. G. *J. Chem. Soc., Dalton Trans.* **1998**, 505-510.

(113) Mendoza-Espinosa, D.; Martínez-Ortega, B. A.; Quiroz-Guzmán, M.; Golen, J. A.; Rheingold, A. L.; Hanna, T. A. *J. Organomet. Chem.* **2009**, *694*, 1509-1523.

(114) Friebolin, H. *Basic One- and Two-Dimensional NMR Spectroscopy*; Third Ed.; Wiley-VCH: Weinheim, 1998.

(115) Stewart, D. R.; Gutsche, C. D. *J. Am. Chem. Soc.* **1999**, *121*, 4136-4146.

(116) Kanamathareddy, S.; Gutsche, C. D. *J. Org. Chem.* **1994**, *59*, 3871-3879.

(117) Gutsche, C. D.; Bauer, L. J. *J. Am. Chem. Soc.* **1985**, *107*, 6059-6063.

(118) Thuéry, P.; Asfari, Z.; Vicens, J.; Lamare, V.; Dozol, J.-F. *Polyhedron* **2002**, *21*, 2497-2503.

(119) Harrowfield, J. M.; Ogden, M. I.; Richmond, W. R.; White, A. H. *J. Chem. Soc., Chem. Commun.* **1991**, 1159-1161.

(120) Stewart, D. R.; Gutsche, C. D. *Org. Prep. Proced. Int.* **1993**, *25*, 137-139.

(121) Sheldrick, G. M. *SHELX97, Program for Crystal Structure Solution and Refinement*; University of Göttingen: Göttingen, Germany, 1998.

(122) Matthews, S. E.; Schmitt, P.; Felix, V.; Drew, M. G. B.; Beer, P. D. *J. Am. Chem. Soc.* **2002**, *124*, 1341-1353.

(123) Guillemot, G.; Castellano, B.; Prangé, T.; Solari, E.; Floriani, C. *Inorg. Chem.* **2007**, *46*, 5152-5154.

(124) Arimori, S.; Davidson, M. G.; Fyles, T. M.; Hibbert, T. G.; James, T. D.; Kociok-Kohn, G. I. *Chem. Commun.,* **2004**, 1640-1641.

(125) Redshaw, C.; Elsegood, M. R. J. *Chem. Commun.,* **2005**, 5056-5058.

(126) Smith, J. M.; Bott, S. G. *Chem. Commun.,* **1996**, 377-378.

(127) Shang, S.; Khasnis, D. V.; Burton, J. M.; Santini, C. J.; Fan, M.; Small, A. C.; Lattman, M. *Organometallics* **1994**, *13*, 5157-5159.

(128) Fan, M.; Zhang, H.; Lattman, M. *Organometallics* **1996**, *15*, 5216-5219.

(129) Fan, M.; Shevchenko, I. V.; Voorhies, R. H.; Eckert, S. F.; Zhang, H.; Lattman, M. *Inorg. Chem.* **2000**, *39*, 4704-4712.

(130) Sood, P.; Zhang, H.; Lattman, M. *Organometallics* **2002**, *21*, 4442-4447.

(131) Hascall, T.; Rheingold, A. L.; Guzei, I.; Parkin, G. *Chem. Commun.,* **1998**, 101-102.

(132) Hascall, T.; Pang, K.; Parkin, G. *Tetrahedron* **2007**, *63*, 10826–10833.

(133) Jacoby, D.; Floriani, C.; Chiesi-Villa, A.; Rizzoli, C. *J. Chem. Soc., Dalton Trans.,* **1993**, 813-814.

(134) Matt, D.; Loeber, C.; Vicens, J.; Asfari, Z. *J. Chem. Soc., Chem. Commun.* **1993**, 604-606.

(135) Stolmàr, M.; Floriani, C.; Chiesi-Villa, A.; Rizzoli, C. *Inorg. Chem.* **1997**, *36*, 1694-1701.

(136) Parlevliet, F. J.; Zuideveld, M. A.; Kiener, C.; Kooijman, H.; Spek, A. L.; Kamer, P. C. J.; van Leeuwen, P. W. N. M. *Organometallics* **1999**, *18*, 3394-3405.

(137) Alexandratos, S. D.; Natesan, S. *Ind. Eng. Chem. Res.* **2000**, *39*, 3998-4010.

(138) Sood, P.; Koutha, M.; Fan, M.; Klichko, Y.; Zhang, H.; Lattman, M. *Inorg. Chem.* **2004**, *43*, 2975-2980.

(139) Ozerov, O. V.; Rath, N. P.; Ladipo, F. T. *J. Organomet. Chem.* **1999**, *586*, 223-233.

(140) Arbaoui, A.; Redshaw, C.; Elsegood, M. R. J.; Wright, V. E.; Yoshizawa, A.; Yamato, T. *Chem. Asian J.* **2010**, *5*, 621-633.

(141) Kotzen, N.; Goldberg, I.; Vigalok, A. *Inorg. Chem. Commun.* **2005**, *8*, 1028–1030.

(142) Trifonov, A. A.; Fedorova, E. A.; Fukin, G. K.; Dechert, S.; Schumann, H.; Bochkarev, M. N. *Russ.Chem.Bull., Int.Ed.,* **2003**, *52*, 2683-2688.

(143) Caselli, A.; Solari, E.; Scopelliti, R.; Floriani, C. *J. Am. Chem. Soc.* **1999**, *121*, 8296-8305.

(144) Caselli, A.; Solari, E.; Scopelliti, R.; Floriani, C.; Re, N.; Rizzoli, C.; Chiesi-Villa, A. *J. Am. Chem. Soc.* **2000**, *122*, 3652-3670.

(145) Acho, J. A.; Doerrer, L. H.; Lippard, S. J. *Inorg. Chem.* **1995**, *34*, 2542-2556.

(146) Gibson, V. C.; Redshaw, C.; Clegg, W.; Elsegood, M. R. J. *Chem. Commun.,* **1997**, 1605-1606.

(147) Chisholm, M. H.; Folting, K.; Streib, W. E.; Wu, D.-D. *Inorg. Chem.* **1999**, *38*, 5219-5229.

(148) Giusti, M.; Solari, E.; Giannini, L.; Floriani, C.; Chiesi-Villa, A.; Rizzoli, C. *Organometallics* **1997**, *16*, 5610-5612.

(149) Petrella, A. J.; Roberts, N. K.; Raston, C. L.; Thornton-Pett, M.; Lamb, R. N. *Chem. Commun.,* **2003**, 1238-1239.

(150) Dieleman, C. B.; Marsol, C.; Matt, D.; Kyritsakas, N.; Harriman, A.; Kintzinger, J.-P. *J. Chem. Soc., Dalton Trans.* **1999**, 4139-4148.

(151) Ishii, Y.; Onaka, K.-i.; Hirakawa, H.; Shiramizu, K. *Chem. Commun.,* **2002**, 1150-1151.

(152) Kotzen, N.; Goldberg, I.; Lipstman, S.; Vigalok, A. *Inorg. Chem.* **2006**, *45*, 5266-5268.

(153) Lide, D. R. *CRC Handbook of Chemistry and Physics*; 90 Ed.; CRC Press: Boca Raton, FL, 2009.

(154) Alcock, N. W. *Adv. Inorg. Chem. Radiochem.* **1972**, *15*, 1-58.

(155) Sheldrick, G. M. *SADABS, Program for Empirical Absorption Correction of Area Detector Data;* Göttingen, Germany, 1996.

(156) van der Sluis, P.; Spek, A. L. *Acta Crystallogr., Sect. A: Found. Crystallogr.* **1990**, *46*, 194-201.

(157) *Mercury v 2.3 - Crystal Structure Visualisation and Exploration Made Easy* Cambridge, United Kingdom, 2009. Retrieved from http://www.ccdc.cam.ac.uk/products/mercury/.

(158) *POVRAY v. 3.6.2 Persistence of Vision Ray Tracer* Williamstown, Australia, 2005. Retrieved from http://www.povray.org.

(159) Kühn, F. E.; Santos, A. M.; Abrantes, M. *Chem. Rev.* **2006**, *106*, 2455-2475.

(160) Enemark, J. H.; Cooney, J. J. A.; Wang, J.-J.; Holm, R. H. *Chem. Rev.* **2004**, *104*, 1175-1200.

(161) Hoppe, E.; Limberg, C. *Chem. Eur. J.* **2007**, *13*, 7006-7016.

(162) Giannini, L.; Solari, E.; Dovesi, S.; Floriani, C.; Re, N.; Chiesi-Villa, A.; Rizzoli, C. *J. Am. Chem. Soc.* **1999**, *121*, 2784-2796.

(163) Gibson, V. C.; Redshaw, C.; Clegg, W.; Elsegood, M. R. J. *Chem. Commun.,* **1998**, 1969-1970.

(164) Zanotti-Gerosa, A.; Solari, E.; Giannini, L.; Floriani, C.; Chiesi-Villa, A.; Rizzoli, C. *Chem. Commun.,* **1996**, 119-120.

(165) Radius, U. *Inorg. Chem.* **2001**, *40*, 6637-6642.

(166) Young, C. G. In *Comprehensive Coordination Chemistry II*; McCleverty, J. A., Meyer, T. J., Ed.; Elsevier: Amsterdam, 2004; Vol. 4, p 415-527.

(167) Cotton, F. A.; Wilkinson, G.; Murillo, C. A.; Bochmann, M. *Advanced Inorganic Chemistry*; 6th Ed.; Wiley-Interscience: New York, 1999.

(168) Abramenko, V. L.; Sergienko, V. S. *Russ. J. Inorg. Chem.* **2009**, *54*, 2031-2053.

(169) Hull, C. G.; Stiddard, M. H. B. *J. Chem. Soc. A.* **1966**, 1633-1635.

(170) Carmichael, W. M.; Edwards, D. A.; Fowles, G. W. A.; Marshall, P. R. *Inorg. Chim. Acta* **1967**, *1*, 93-96.

(171) Herrmann, W. A.; Thiel, W. R.; Herdtweck, E. *Chem. Ber.* **1990**, *123*, 271-276.

(172) Kühn, F. E.; Herdtweck, E.; Haider, J. J.; Herrmann, W. A.; Gonçalves., I. S.; Lopes, A. D.; Romão, C. C. *J. Organomet. Chem.* **1999**, *583*, 3-10.

(173) Kühn, F. E.; Groarke, M.; Bencze, É.; Herdtweck, E.; Prazeres, A.; Santos, A. M.; Calhorda, M. J.; Romão, C. C.; Gonçalves, I. S.; Lopes, A. D.; Pillinger, M. *Chem. Eur. J.* **2002**, *8*, 2370-2383.

(174) Technical Bulletin K0520 - Solvent Miscibility & Viscosity Chart. Protasis / MRM Corp. Retrieved from http://www.micronmr.com/technical_bulletins.html. Accessed date Sep 2010, **2007**.

(175) Pearson, R. G.; Dillon, R. L. *J. Am. Chem. Soc.* **1953**, *75*, 2439-2443.

(176) Berg, J. M.; Holm, R. H. *J. Am. Chem. Soc.* **1985**, *107*, 917-925.

(177) Hawkins, J. M.; Dewan, J. C.; Sharpless, K. B. *Inorg. Chem.* **1986**, *25*, 1501-1503.

(178) Huang, M.; DeKock, C. W. *Inorg. Chem.* **1993**, *32*, 2287-2291.

(179) Barbaro, P.; Bianchini, C.; Scapacci, G.; Masi, D.; Zanello, P. *Inorg. Chem.* **1994**, *31*, 3180-3186.

(180) Pedrosa, M. R.; Escribano, J.; Aguado, R.; Sanz, R.; Díez, V.; Arnáiz, F. J. *Polyhedron* **2010**, *29*, 841-849.

(181) Hanna, T. A.; Ghosh, A. K.; Ibarra, C.; Mendez-Rojas, M. A.; Rheingold, A. L.; Watson, W. H. *Inorg. Chem.* **2004**, *43*, 1511-1516.

(182) Rodrigues, C. W.; Limberg, C.; Pritzkow, H. *Eur. J. Inorg. Chem.* **2004**, *2004*, 3644-3650.

(183) Kim, G.-S.; Huffman, D.; DeKock, C. W. *Inorg. Chem.* **1989**, *28*, 1279-1283.

(184) Hanna, T. A.; Incarvito, C. D.; Rheingold, A. L. *Inorg. Chem.* **2000**, *39*, 630-631.

(185) Nakanishi, K.; Solomon, P. H. *Infrared Absorption Spectroscopy*; 2nd Ed.; Holden-Day: San Francisco, CA., 1977.

(186) Jones, M. M. *J. Am. Chem. Soc.* **1959**, *81*, 3188-3189.

(187) Šoptrajanov, B.; Trpkovska, M.; Pejov, L. *Croat. Chem. Acta* **1999**, *72*, 663-672.

(188) Cameron, B. R.; Loeb, S. J.; Yap, G. P. A. *Inorg. Chem.* **1997**, *36*, 5498-5504.

(189) Stang, P. J.; Cao, D. H.; Chen, K.; Gray, G. M.; Muddiman, D. C.; Smith, R. D. *J. Am. Chem. Soc.* **1997**, *119*, 5163-5168.

(190) Jeunesse, C.; Armspach, D.; Matt, D. *Chem. Commun.,* **2005**, 5603-5614.

(191) Steed, J. W.; Juneja, R. K.; Atwood, J. L. *Angew. Chem.* **1994**, *106*, 2571-2573.

(192) Steed, J. W.; Juneja, R. K.; Burkhalter, R. S.; Atwood, J. L. *J. Chem. Soc., Chem. Commun.,* **1994**, 2205-2206.

(193) Steed, J. W.; Johnson, C. P.; Juneja, R. K.; Atwood, J. L.; Burkhalter, R. S. *Supramol. Chem.* **1996**, *6*, 235-238.

(194) Staffilani, M.; Hancock, K. S. B.; Steed, J. W.; Holman, K. T.; Atwood, J. L.; Juneja, R. K.; Burkhalter, R. S. *J. Am. Chem. Soc.* **1997**, *119*, 6324-6335.

(195) Wimmer, F. L.; Wimmer, S.; Castan, P.; Puddephatt, R. J. *Inorg. Synth.,* **1992**, *29*, 185-187.

(196) Aleksiuk, O.; Cohen, S.; Biali, S. E. *J. Am. Chem. Soc.* **1995**, *117*, 9645-9652.

(197) Alsters, P. L.; Baesjou, P. J.; Janssen, M. D.; Kooijman, H.; Sicherer-Roetman, A.; Spek, A. L.; van Koten, G. *Organometallics* **1992**, *11*, 4124-4135.

(198) Kapteijn, G. M.; Grove, D. M.; Kooijman, H.; Smeets, W. J. J.; Spek, A. L.; van Koten, G. *Inorg. Chem.* **1996**, *35*, 526-533.

(199) Brookhart, M.; Green, M. L. H.; Parkin, G. *PNAS* **2007**, *104*, 6908-6914.

(200) Buccella, D.; Parkin, G. *J. Am. Chem. Soc.* **2006**, *128*, 16358-16364.

(201) Yao, W.; Eisenstein, O.; Crabtree, R. H. *Inorg. Chim. Acta* **1997**, *254*, 105-111.

(202) Albinati, A.; Pregosin, P. S.; Wombacher, F. *Inorg. Chem.* **1990**, *29*, 1812-1817.

(203) Kapteijn, G. M.; Dervisi, A.; Grove, D. M.; Kooijman, H.; Lakin, M. T.; Spek, A. L.; van Koten, G. *J. Am. Chem. Soc.* **1995**, *117*, 10939-10949.

(204) Kapteijn, G. M.; Grove, D. M.; van Koten, G.; Smeets, W. J. J.; Spek, A. L. *Inorg. Chim. Acta* **1993**, *207*, 131-134.

(205) Steed, J. W.; Atwood, J. L. *Supramolecular Chemistry*; 2nd Ed.; John Wiley & Sons: New York, 2009.

(206) Gutsche, C. D.; Lin, L.-g. *Tetrahedron* **1986**, *42*, 1633-1640.

(207) Note: The analytical samples used for EA and m.p. were dried in air for 24 hrs. NMR, IR, and UV/vis samples were dried under vacuum for 48 hrs in order to avoid any interference with the residual solvent. Coordinated solvent determined by EA data was included when determining molecular weights for yields. Due to chemical similarity EA studies were performed on selected samples only.

(208) Hanna, T. A. *Coord. Chem Rev.* **2004**, *248*, 429-440.

(209) Hanna, T. A.; Ghosh, A. K.; Ibarra, C.; Zakharov, L. N.; Rheingold, A. L.; Watson, W. H. *Inorg. Chem.* **2004**, *43*, 7567-7569.

(210) Hanna, T. A.; Rieger, A. L.; Rieger, P. H.; Wang, X. *Inorg. Chem.* **2002**, *41*, 3590-3592.

(211) Kou, X.; Wang, X.; Mendoza-Espinosa, D.; Zakharov, L. N.; Rheingold, A. L.; Watson, W. H.; Brien, K. A.; Jayarathna, L. K.; Hanna, T. A. *Inorg. Chem.* **2009**, *48*, 11002-11016.

(212) Charbonnière, L. J.; Balsiger, C.; Schenk, K. J.; Bünzli, J.-C. G. *J. Chem. Soc., Dalton Trans.* **1998**, 505-510.

(213) Mendoza-Espinosa, D.; Hanna, T. A. *Inorg. Chem.* **2009**, *48*, 7452-7456.

(214) Canty, A. J.; Done, M. C.; Skelton, B. W.; White, A. H. *Inorg. Chem. Commun.* **2001**, *4*, 648-650.

(215) Frisch, M. J.; Trucks, G. W.; Schlegel, H. B.; Scuseria, G. E.; Robb, M. A.; Cheeseman, J. R.; Scalmani, G.; Barone, V.; Mennucci, B.; Petersson, G. A.; Nakatsuji, H.; Caricato, M.; Li, X.; Hratchian, H. P.; Izmaylov, A. F.; Bloino, J.; Zheng, G.; Sonnenberg, J. L.; Hada, M.; Ehara, M.; Toyota, K.; Fukuda, R.; Hasegawa, J.; Ishida, M.; Nakajima, T.; Honda, Y.; Kitao, O.; Nakai, H.; Vreven, T.; Montgomery, J. A., Jr. ; Peralta, J. E.; Ogliaro, F.; Bearpark, M.; Heyd, J. J.; Brothers, E.; Kudin, K. N.; Staroverov, V. N.; Kobayashi, R.; Normand, J.; Raghavachari, K.; Rendell, A.; Burant, J. C.; Iyengar, S. S.; Tomasi, J.; Cossi, M.; Rega, N.; Millam, J. M.; Klene, M.; Knox, J. E.; Cross, J. B.; Bakken, V.; Adamo, C.; Jaramillo, J.; Gomperts, R.; Stratmann, R. E.; Yazyev, O.; Austin, A. J.; Cammi, R.; Pomelli, C.; Ochterski, J. W.; Martin, R. L.; Zakrzewski, K. M. V. G.; Voth, G. A.; Salvador, P.; Dannenberg, J. J.; Dapprich, S.; Parandekar, P. V.; Mayhall, N. J.; Daniels, A. D.; Farkas, O.; Foresman, J. B.; Ortiz, J. V.; Cioslowski, J.; Fox, D. J. *Gaussian Development Version, Revision H.07* Wallingford CT, 2009.

(216) Farrugia, L. J. *J. Appl. Cryst.* **1997**, *30*, 565.

VITA

Bernat Abeit Martínez-Ortega was born on June 18, 1979 in Pachuca de Soto, Hidalgo city, México. He is son of Prof. Elias Martínez-Guillén and Silvia Ortega-Cerritos. Before enrolling for his undergraduate studies in Chemistry he received a scholarship from the Chemistry Department of Centro de Investigación y de Estudios Avanzados del Instituto Politécnico Nacional (CINVESTAV-IPN) in 1999. After 6 months of internship at CINVESTAV-IPN in the same year, he enrolled and he received his Bachelor in Sciences degree with Major in Inorganic Chemistry from Universidad Autónoma del Estado de Hidalgo, Pachuca de Soto Hidalgo, México, *cum laude*, in 2004.

In 2004, he enrolled in graduate study at Texas Christian University, Fort Worth, TX, to pursue a Ph. D. in Inorganic Chemistry. While working on his doctorate in Chemistry, he worked as a Graduate Teaching Assistant for four semesters and was awarded the Outstanding Teaching Assistant Honorable Mention from the Department of Chemistry in fall 2006. He is member of the American Chemical Society.

He is married to Adriana Luqueño Reyes and proud father of three children, Azul, Carlos, and Oscar.

ABSTRACT

SYNTHESIS AND CHARACTERIZATION OF EARLY AND LATE TRANSITION METALLOCALIX[5]ARENE COMPLEXES

by Bernat Abeit Martinez-Ortega
Department of Chemistry
Texas Christian University

Dissertation Advisor: Tracy A. Hanna, Associate Professor

Calixarenes are macrocyclic oligomers of phenols bridged with methylenes. They have been extensively studied because of their unique structure, complexing abilities, conformational flexibility, and reactivity. Their chemistry has been applied as an oxo platform for catalyst model studies.

The coordination chemistry of the simple calix[4]arenes is now relatively well developed. By contrast, metal compounds containing the larger ring systems, for example calix[5]arene, are still quite rare. Our interest in calix[5]arene chemistry is related to our longer-term research objectives. We are interested in modeling a bifunctional oxo surface, in which two metals can react in a cooperative manner. This requires a conformation that will allow two metals, or a metal and non-metal, to interact on the calixarene "surface" (Chapter1).

We synthesized a series of deprotonated calixarenes "calix[n]anions" (including mono- to dianionic species) by the reaction of parent calix[5]arene with alkali metal bases (Chapter 2). In this context, we were able to synthesize and characterize a variety of Ti(IV) (Chapter 3), Mo(VI) (Chapter 4) and Pd(II) (Chapter 5) metallocalix[5]arene complexes using calixanions as starting materials in which the transition metal binds directly to the oxygen surface of the calix[5]arene.

Finally, the reactivity of the palladium calix[5]arene complexes was tested and successfully utilized in the synthesis and characterization of the first examples of Pd(II)/Ti(IV) and Pd(II)/Mo(VI) heterobimetallic complexes (Chapter 6).